# HIGH-RATE QUANTUM KEY DISTRIBUTION SCHEME RELYING ON CONTINUOUSLY PHASE AND AMPLITUDE-MODULATED COHERENT LIGHT PULSES

## Related Applications

**[0001]** This patent application takes priority from U.S. Provisional Application No. 60/394,330, filed on July 5, 2002, which is hereby incorporated by reference.

## Field of the Invention

**[0002]** The present invention is related to the distribution of a random bit string between two authorised parties, for use as a secret key in a secure i.e., encrypted and authenticated communication.

**[0003]** The key distribution uses quantum carriers, typically single-photon or strongly attenuated pulses, for encoding the key bits. It is supplemented with classical post-processing algorithms, namely reconciliation and privacy amplification algorithms, in order to distil the secret key.

**[0004]** The Heisenberg uncertainty principle of quantum mechanics, together with the use of a privacy amplification protocol, guarantees that an unauthorised third party (any eavesdropper) cannot gain any information on the secret key.

## State of the Art

**[0005]** Quantum key distribution (QKD), usually known as quantum cryptography, is presently the most advanced application of quantum communication. QKD has been proposed in 1984 by C. H. Bennett and G. Brassard as a technique for distributing a secret key, i.e., a random bit string, between two authorised parties that relies on quantum mechanics. This secret key, also called symmetric key, can then be used by the parties to transmit a confidential message by use of a standard cryptographic method such as the Vernam code, which is unconditionally secure. It can also be used to authenticate the communication, i.e., distinguish legitimate messages from fake ones.

[0006] Quantum key distribution requires a quantum channel supplemented with a (classical) authenticated public channel. Typically, a sequence of light pulses is sent in the quantum channel, encoding each a key bit. The quantum properties of light, in particular the Heisenberg uncertainty principle, ensure that no information can be gained on these key bits without disturbing the quantum state of the photons. Public communications over the classical channel are then used to estimate the maximum amount of information that a potential eavesdropper may have acquired, and distil a secret key out of the raw data.

[0007] Several practical schemes for quantum key distribution have been proposed and implemented over the last ten years. The present state-of-the-art quantum cryptographic schemes make use of a binary encoding of the key using ideally single-photon states, or, in practice, very faint coherent states containing on average a fraction of a photon per pulse. The secret key rate is limited due to the need for photon-counting detectors, which have a relatively low maximum repetition frequency in order to keep the detector's afterpulse probability negligible. In addition, the range over which the security is guaranteed is limited by a threshold on the quantum bit error rate, which is reached above a certain attenuation (beyond a certain range) as a consequence of the detector's dark counts. A review of quantum cryptography can be found in ref. [1].

[0008] Another potential implementation of QKD that was raised very recently consists in using quantum continuous variables (QCV)[29], such as the electric field amplitudes, to obtain possibly more efficient alternatives to usual photon-counting QKD techniques.

[0009] Many recent proposals[2-10] to use QCV for QKD have been made that are based on the use of "non-classical" light beams, namely squeezed light or entangled light beams ("EPR beams"). In contrast, embodiments of the present invention discuss the use of "quasi-classical" (coherent) light beams. U.S. Patent No. 5,515,438, hereby incorporated by reference, describes a quantum key distribution using non-orthogonal macroscopic signals.

Summary of Certain Aspects of the Invention

[0010] Embodiments of the present invention are a potential alternative to the usual single-photon quantum cryptographic techniques devised so far. Key carriers used are quasi-classical (coherent) light pulses that contain many photons and are continuously modulated in amplitude and phase[11]. The continuous raw data is then converted into a usable

binary key using a continuous reconciliation protocol[9,22]. In contrast to previous proposals, this shows that there is no need for squeezed light in the context of QCV QKD: an equivalent level of security may be obtained simply by generating and transmitting continuous distributions of coherent states, an easier task compared to generating squeezed states or single-photon states.

**[0011]** More specifically, embodiments of the present invention distribute secret keys at a high rate over long distances. A protocol uses shot-noise limited coherent (homodyne) detection, which works at much higher repetition frequencies than single-photon detectors, so that high secret-bit rates can indeed be achieved. It remains, in principle, secure for very lossy transmission lines by use of a reverse reconciliation algorithm, so it may therefore be used over long distances.

**[0012]** One further goal of the invention is to demonstrate the practicability of the QCV QKD protocol when using Gaussian-modulated coherent states that are laser pulses containing several photons. The scope of the invention is not restricted to Gaussian distributions (other continuous distributions may be used as well) but this makes the demonstration easier. Embodiments of the invention cover the security analysis of the protocol and a proof-of-principle experimental implementation, followed by the complete secret key extraction, including data reconciliation and privacy amplification. The tested set-up yields a secret key rate of approximately 1.7 Mbps for a lossless line and of 75 kbps for a 3.1 dB line.

**[0013]** Embodiments of this invention describe the distribution of a secret key between two remote parties by use of quantum coherent states, e.g., attenuated laser pulses, that are continuously modulated in phase and amplitude. Coherent (homodyne) detection is then performed by the receiver in order to measure the quadrature components of these states.

**[0014]** One protocol embodiment of the invention ensures that the information a potential eavesdropper may gain at most can be estimated from the measured parameters characterising the channel (line attenuation and error rate). Using an authenticated public (classical) channel, the resulting raw data (partly correlated continuous variables) can be converted into a secret binary key by using a (direct or reverse) reconciliation protocol supplemented with privacy amplification. The resulting key can then be used as a private key

in order to ensure the confidentiality and/or authentication of a transmission using standard cryptographic techniques.

**[0015]** Aspects of the quantum continuous-variable cryptographic scheme include the continuous distribution of coherent states. This is in contrast with all other schemes, which rely on a binary encoding. Here, the encoding of continuous variables into the quadrature components of a coherent state makes it possible to encode several key bits per coherent pulse. Also, the use of homodyne detection techniques to measure the quadrature components of the light field allows this scheme to work at high frequencies by comparison with photon-counting techniques.

**[0016]** Other aspects of the scheme include the use of a continuous reconciliation protocol in order to convert the raw key resulting from the first item into a usable binary key. A direct or reverse reconciliation protocol may be used depending on the line parameters. For lines with an attenuation that exceeds 3 dB, reverse reconciliation must be used in order to ensure the security. There is, in principle, no limit on the achievable range using reverse reconciliation, but practical considerations (noise in the apparatuses, in particular in the coherent detection system, non-unity efficiency of the reconciliation protocols) put a limit on the range over which the key can be securely distributed. For very noisy lines with low losses, direct reconciliation is preferred.

**[0017]** In one embodiment of the present invention there is a quantum cryptographic system, comprising at least one sending unit comprising an encoder and distributing a raw key in the quadrature components of quantum coherent states that are continuously modulated in phase and amplitude; at least one receiving unit comprising a homodyne detector of the quantum coherent states in order to measure the quadrature components of the states; a quantum channel for connecting the sending unit to the receiving unit; and a two-way authenticated public channel for transmitting non-secret messages between the sending unit and the receiving unit.

**[0018]** According to one embodiment, the quantum cryptographic system further comprises a continuous-variable quantum key distribution protocol ensuring that the amount of information a potential eavesdropper may gain at most on the sent and received data can be estimated from the measured parameters of the quantum channel (error rate and line attenuation).

[0019] The sent and received raw data resulting from the continuous-variable protocol are converted into a secret binary key by using a continuous reconciliation protocol supplemented with privacy amplification.

[0020] According to one embodiment, the encoder of the quadrature components with a high signal-to-noise ratio encodes several key bits per coherent light pulse.

[0021] According to another embodiment, the decoding of the quadrature components of the light field via the homodyne detector achieves high secret bit rates in comparison to photon-counting techniques.

[0022] In case of noisy quantum channels with low losses, the continuous reconciliation protocol is a direct reconciliation protocol, which allows the receiver to discretize and correct its data according to the sent values.

[0023] In case of quantum channels with an attenuation that exceeds 3 dB, the continuous reconciliation protocol is a reverse reconciliation protocol, which allows the sending unit to discretize and correct its data according to the values measured by the receiver.

[0024] The key secret can be used as a private key for ensuring confidentiality and authentication of a cryptographic transmission.

[0025] According to one embodiment, the quadrature components of the quantum coherent states are modulated with a Gaussian distribution, the coordinate values of the center of the Gaussian distribution being arbitrary.

[0026] According to another embodiment, the variance of the Gaussian distribution for the quadrature X is different from the variance of the Gaussian distribution for the conjugate quadrature P.

[0027] According to another embodiment, the Gaussian-modulated coherent sates are attenuated laser light pulses typically containing several photons.

[0028] The information, an eavesdropper may gain on the sent and received Gaussian-distributed values, can be calculated explicitly using Shannon's theory for Gaussian channels.

[0029] In another embodiment of the present invention there is a method of distributing continuous quantum key between two parties which are a sender and a receiver, the method comprising selecting, at a sender, two random numbers $x_A$ and $p_A$ from a

Gaussian distribution of mean zero and variance $V_A N_0$, where $N_0$ refers to the shot-noise variance; sending a corresponding coherent state $|x_A+ip_A>$ in the quantum channel; randomly choosing, at a receiver, to measure either quadrature x or p using homodyne detection; informing the sender about the quadrature that was measured so the sender may discard the wrong one; measuring channel parameters on a random subset of the sender's and receiver's data, in order to evaluate the maximum information acquired by an eavesdropper; and converting the resulting raw key in the form of a set of correlated Gaussian variables into a binary secret key comprising direct or reverse reconciliation in order to correct the errors and get a binary key, and privacy amplification in order to make secret the binary key.

**[0030]** The reconciliation can produce a common bit string from correlated continuous data, which comprises the following: transforming each Gaussian key element of a block of size n by the sender into a string of m bits, giving m bit strings of length n, referred to as slices; converting, by the receiver, the measured key elements into binary strings by using a set of slice estimators; and sequentially reconciliating the slices by using an implementation of a binary error correction algorithm, and communicating on the public authenticated channel.

**[0031]** The post-processing of privacy amplification can comprise distilling a secret key out of the reconciliated key by use of a random transformation taken in a universal class of hash functions.

**[0032]** Informing the sender can comprise utilizing a public authenticated channel by the receiver to inform the sender. The channel parameters can include an error rate and a line attenuation.

**[0033]** In another embodiment of the present invention there is a device for implementing a continuous-variable quantum key exchange, the device comprising a light source or a source of electromagnetic signals configured to generate short quantum coherent pulses at a high repetition rate; an optical component configured to modulate the amplitude and phase of the pulses at a high frequency; a quantum channel configured to transmit the pulses from an emitter to a receiver; a system that permits the transmission of a local oscillator from the emitter to the receiver; a homodyne detector capable of measuring, at a high acquisition frequency, any quadrature component of the electromagnetic field collected at the receiver's station; a two-way authenticated public channel that is used to

communicating non-secret messages in postprocessing protocols; and a computer at the emitter's and receiver's stations that drives or reads the optical components and runs the postprocessing protocols.

**[0034]** Alternatively, a local oscillator can be transmitted together with the signal by use of a polarization encoding system whereby each pulse comprises a strong local oscillator pulse and a weak orthogonally-polarized signal pulse with modulated amplitude and phase.

**[0035]** If polarization encoding is used, the receiving system relies on polarization-mode homodyne detection requiring a quarter-wave plate and a polarizing beam splitter.

**[0036]** In another embodiment of the present invention, there is a device for exchanging Gaussian key elements between two parties which are a sender and a receiver, the device comprising a laser diode associated with a grating-extended external cavity, the laser diode configured to send light pulses at a high repetition rate, each pulse typically containing several photons; an integrated electro-optic amplitude modulator and a piezoelectric phase modulator, configured to generate randomly-modulated light pulses, the data being organized in bursts of pulses; a beam-splitter to separate the quantum signal from a local oscillator; and a homodyne detector combining the quantum signal and local oscillator pulses in order to measure one of the two quadrature components of the light field.

**[0037]** The device may further comprise an acquisition board and a computer on the sender's and receiver's sides in order to run the post-processing protocols described here above.

**[0038]** The laser can operate at a wavelength comprised between about 700 and about 1600 nm, or the laser can operate at a wavelength comprising telecom wavelengths between about 1540 and 1580 nm.

**[0039]** The device may additionally comprise means for selecting, at the emitter, two random numbers $x_A$ and $p_A$ from a Gaussian distribution of mean zero and variance $V_A N_0$, where $N_0$ refers to the shot-noise variance; means for sending a corresponding coherent state $|x_A+ip_A\rangle$ in the quantum channel; means for randomly choosing, at the receiver, to measure either quadrature x or p using homodyne detection; means for informing the emitter about the quadrature that was measured so the emitter may discard the wrong one;

means for measuring channel parameters on a random subset of the emitter's and receiver's data, in order to evaluate the maximum information acquired by an eavesdropper; and means for converting the resulting raw key in the form of a set of correlated Gaussian variables into a binary secret key comprising direct or reverse reconciliation in order to correct the errors and get a binary key, and privacy amplification in order to make secret the binary key.

Brief Description of the Drawings

**[0040]** FIG. 1 is a diagram of one configuration of components demonstrating embodiments of the present invention.

**[0041]** FIG. 2 is a diagram representing Bob's measured values of the quadrature component as a function of Alice's sent values (in Bob's measurement basis) for a burst of 60,000 pulses exchanged between Alice and Bob in the configuration shown in Figure 1.

**[0042]** FIG. 3. is a diagram representing the channel equivalent noise $\chi$ as a function of the channel transmission G, adjusted using a variable attenuator on the signal line.

**[0043]** FIG. 4 is a diagram representing the values of $I_{BA}$ (increasing curve), $I_{AE}$ (decreasing curve), $I_{BE}$ (inverse U-shaped curve) as a function of the channel transmission G for $V \approx 40$.

Description of Certain Embodiments of the Present Invention

**[0044]** One realisation of this quantum cryptographic scheme consists in modulating the quadrature components of coherent light pulses with a Gaussian distribution. The corresponding protocol is demonstrated in what follows. Dealing with Gaussian distributions makes the security of the entire protocol easier to analyse, but the scope of the present invention is not limited to such random distributions. Alternative continuous distributions may be used as well. Other improvements of the present invention can be foreseen, such as the use of more efficient reconciliation protocols that may potentially increase the achievable range.

**[0045]** The protocol described herein works by continuously modulating the phase and amplitude of coherent light pulses and measuring the quadrature components of the received coherent states. This clearly gives very important practical advantages to such a

protocol, in view of the simplicity of the techniques needed to preparing and detecting coherent states. In particular, the high dimensionality of the phase space may be exploited by modulating the phase and amplitude quadratures with a large dynamics, allowing the encoding of several key bits per pulse. This, together with the fact that fast modulation and detection can be achieved, results in a high-rate secret key distribution.

**[0046]** This protocol, supplemented with a direct reconciliation scheme, can be shown to be secure provided that the transmission of the line is larger than 50%, i.e., the transmission loss is less than 3 dB[11]. This is in accordance with the fact that QKD fundamentally relies on the use of non-orthogonal states only and may perfectly well work with macroscopic signals instead of single photons (see patent US5515438). The security of the protocol is related to the no-cloning theorem[12-14], and non-classical features like squeezing or EPR correlations have no influence on the achievable secret key rate. The 3 dB loss limit of these protocols makes the security demonstration quite intuitive, but there may exist in principle multiple ways for two user/partners, e.g., Alice and Bob, to go beyond this limit, for instance by using QCV entanglement purification[15].

**[0047]** The concept of reverse reconciliation, detailed below, is an efficient technique to cross this 3 dB limit that does not require the generation and purification of entanglement, but only a modified classical post-processing. The corresponding coherent-state protocol can, in principle, be secure for any value of the line transmission[18,32]. There is therefore no theoretical limit on the achievable range over which security can be guaranteed. In addition, it can be shown that the cryptographic security is strongly linked with entanglement, even though the protocol does not rely on entanglement.

**[0048]** Referring to FIG. 1, a configuration of components demonstrating embodiments of the present invention will be described. The components are partitioned into exemplary use by two users, Alice and Bob. The components include the following: Laser diode 102: e.g., SDL 5412 lasing at 780nm; OI 104: e.g., optical isolator; $\lambda/2$ 106: e.g., half-wave plate; AOM 108: e.g., acousto-optic modulator; MF 110: e.g., polarization maintaining monomode fibre; OD 112: e.g., optical density (attenuator); EOM 114: e.g., integrated $LiNbO_3$ electro-optic amplitude modulator; PBS 116: e.g., polarizing beam splitter; BS 118: e.g., beam splitter inducing variable attenuation; and PZT 120: e.g., piezo-electric

transductor. The lenses are marked with a "f" followed by their focal lengths in millimeters. R and T are reflection and transmission coefficients.

**[0049]** The basic idea behind reverse reconciliation is to interchange the roles of Alice and Bob when converting the measured data into a common binary key, that is, Alice attempts to guess what was received by Bob rather than Bob guessing what was sent by Alice. Consequently, Alice always has an advantage over a potential eavesdropper, Eve, as the latter only has a noisy estimate of Alice's data at their disposal in order to guess Bob's data. This is, roughly speaking, the mechanism that ensures the security of these new protocols.

**[0050]** In the description below, the concept of coherent-state QKD supplemented with reverse reconciliation is introduced and then an individual attack using an entangling cloner is described. An explicit expression of the maximum achievable secret key rate is deduced. A table-top experiment that generates streams of data corresponding to the protocol will be described. Although Alice and Bob are not fully separated in the present implementation, the data are created by the same physical process and thus have the same structure as they would have in a real cryptographic exchange. Explicitly how to process the experimental data to extract the secret key will be demonstrated, that is, reverse reconciliation and privacy amplification protocols is performed. Finally, a quantitative evaluation of the expected performances of the scheme in a realistic key exchange is given.

Coherent-State Quantum Key Exchange and Reconciliation Protocols

**[0051]** In a QKD protocol such as BB84, Alice and Bob randomly choose one out of two complementary bases for respectively preparing and measuring a quantum signal, so their data are significant only when their bases are compatible. After this quantum exchange, they thus have to agree on a common basis and discard the wrong measurements. According to the present invention, we make use of a coherent-state protocol that extends this principle to QCV and runs as follows[11]. First, Alice draws two random numbers $x_A$ and $p_A$ from a Gaussian distribution of mean zero and variance $V_A N_0$, where $N_0$ denotes the shot-noise variance, and then she sends to Bob the coherent state $|x_A+ip_A>$. Next, Bob randomly chooses to measure either the quadrature x or p. Then, using a public authenticated channel, he informs Alice about the quadrature that he measured so she may discard the wrong one. After

running this protocol several times, Alice and Bob (and possibly the eavesdropper Eve) share a raw key, that is, a set of correlated Gaussian variables that are called key elements. After this quantum exchange, Alice and Bob must convert this raw key into a binary secret key by proceeding with the various steps described below including channel evaluation, direct or reverse reconciliation (to correct the errors and make the key binary), and privacy amplification (to make the key secret).

Channel Evaluation

**[0052]** First, Alice and Bob openly compare a sample of their key elements over the classical public channel in order to evaluate the error rate and transmission efficiency of the quantum channel. The sacrificed key elements must be chosen randomly and uniformly, so that they are representative of the whole sequence, and are unknown in advance to Eve. Knowing the correlations between their key elements, Alice and Bob can then evaluate the amount of information they share ($I_{AB}$) as well as the information that Eve can have about their values ($I_{AE}$ and $I_{BE}$).

**[0053]** The estimated amount of eavesdropped information has some significance later on, in the privacy amplification procedure, when Eve's knowledge is destroyed. Indeed, it is known that Alice and Bob can in principle distil a secret key with a size $S > \sup(I_{AB}-I_{AE}, I_{AB}-I_{BE})$ bits per key element[24]. Thus, if $S > 0$, they can extract a common key from their correlated key elements by performing one-way classical communication over a public authenticated channel, revealing as little information as possible to Eve. There are actually two main options for doing this key extraction that are closely related to the above expression for S, namely performing either direct or reverse reconciliation.

Direct Reconciliation (DR)

**[0054]** Alice publicly sends correction information, revealing R bits, so Bob corrects his key elements to have the same values as Alice. At the end of this step, Alice and Bob have a common bit string of length $I_{AB}+R$, and Eve knows $I_{AE}+R$ bits of this string (slightly more if the reconciliation protocol is not perfect). Therefore Alice and Bob get a useable secret key if $(I_{AB}-I_{AE}) > 0$ at the beginning. We call this "direct reconciliation" (DR) because the classical information flow has the same direction as the initial quantum

information flow. Direct reconciliation is quite intuitive, but it is not secure as soon as the quantum channel efficiency falls below 50%[11]. It may prove useful, however, for very noisy low-loss quantum channels.

Reverse Reconciliation (RR)

**[0055]** Alternatively, in a reverse reconciliation protocol, Bob publicly sends correction information and Alice corrects her key elements to have the same values as Bob. Since Bob gives the correction information, this reconciliation keeps ($I_{AB}$-$I_{BE}$) constant, and provides a useable key if ($I_{AB}$-$I_{BE}$) > 0. We call this "reverse reconciliation" (RR) because Alice needs to estimate what *will be* measured by Bob. Such a procedure is actually closer, in spirit, to single-photon QKD as there Bob simply communicates to Alice the time slots where he did not detect a photon (Alice thus reconciliates her data with Bob's measured values).

Privacy Amplification

**[0056]** The last step of a practical QKD protocol consists in Alice and Bob performing privacy amplification to filter out Eve's information. This can be done by properly mixing the reconciliated bits so as to spread Eve's uncertainty over the entire final key as described above. This procedure requires having an estimate of the amount of information collected by Eve on the reconciliated key, so we need to have a bound on $I_{AE}$ for DR or on $I_{BE}$ for RR. In addition, Alice and Bob must keep track of the number of bits exchanged publicly during reconciliation since Eve might have monitored them. This knowledge is destroyed at the end of the privacy amplification procedure, reducing the key length by the same amount. For a coherent state protocol, the DR bound on $I_{AE}$ given in [11] leads to a security limit for a 50% line transmission as mentioned above. The RR bound on $I_{BE}$, is now established and shown that it is *not* associated with a minimum value of the line transmission.

Eavesdropping Strategy Based on an Entangling Cloner

**[0057]** In order to eavesdrop a reverse reconciliation scheme, Eve needs to guess the result of Bob's measurement without superimposing too much noise on Bob's data. We will call "entangling cloner"[18,32] a system allowing her to do so. Such a cloner creates two

quantum-correlated copies of Alice's quantum state, so Eve simply keeps one of them and sends the other one to Bob. Let ($x_{in}$, $p_{in}$) be the input field quadratures of the entangling cloner, and ($x_B$,$p_B$), ($x_E$,$p_E$) the quadratures of Bob's and Eve's output fields. To be safe, Alice and Bob must assume Eve uses the best possible entangling cloner knowing Alice-Bob's channel quality: Eve's cloner should minimise the conditional variances[16-17] $V(x_B|x_E)$ and $V(p_B|p_E)$, i.e., the variance of Eve's estimates of Bob's field quadratures ($x_B$,$p_B$). As described above, these variances are constrained by Heisenberg-type relations, which limit what can be obtained by Eve,

$$V(x_B|x_A)V(p_B|p_E) \geq N_0^2 \quad \text{and} \quad V(p_B|p_A)V(x_B|x_E) \geq N_0^2 \qquad (1)$$

**[0058]** where $V(x_B|x_A)$ and $V(p_B|p_A)$ denote Alice's conditional variances. This means that Alice and Eve cannot jointly know more about Bob's conjugate quadratures than allowed by the Heisenberg principle, even if they conspire together. As we shall see, Alice's conditional variances can be bounded by using the measured parameters of the quantum channel, which in turn makes it possible to bound Eve's variance. Here, the channel is described by the linearized relations $x_B = \sqrt{G_x}(x_{in}+B_x)$ and $p_B = \sqrt{G_p}(p_{in}+B_p)$, with $\langle x_{in}^2\rangle = \langle p_{in}^2\rangle = VN_0 \geq N_0$, $\langle B_{x,p}^2\rangle = \chi_{x,p}N_0$, and $\langle x_{in}B_x\rangle = \langle p_{in}B_p\rangle = 0$. The quantities $\chi_x$, $\chi_p$ represent the channel noises referred to its input, also called equivalent input noises[16-17], while $G_x$, $G_p$ are the channel gains for x and p ($G_{x,p} < 1$ for a lossy transmission line), and V is the variance of Alice's field quadratures in shot-noise units ($V=V_A+1$).

**[0059]** Now comes the crucial point of the demonstration. The output-output correlations of the entangling cloner, described by $V(x_B|x_E)$ and $V(p_B|p_E)$, should only depend on the density matrix $D_{in}$ of the field ($x_{in}$,$p_{in}$) at its input, and not on the way Alice produced this field namely whether it is a Gaussian mixture of coherent states or one of two EPR-correlated beams. Inequalities (1) thus have to be fulfilled for every physically allowed values of $V(x_B|x_A)$ and $V(p_B|p_A)$ given $D_{in}$. If we look for a bound to Eve's knowledge by using (1), we have thus to use the smallest possible value for $V(x_B|x_A)$ and $V(p_B|p_A)$ given $D_{in}$. In particular, we must assume that Alice uses EPR beams to maximise her knowledge of Bob's results, even though she does not do so in practice. The two-mode squeezing (or entanglement) that Alice may use is, however, bounded by the variance of her field V, which in turn implies a limit on how well Alice can know Bob's signal as described above:

$$V(p_B|p_A) \geq G_p(\chi_p+V^{-1})N_0 \quad \text{and} \quad V(x_B|x_A) \geq G_x(\chi_x+V^{-1})N_0 \qquad (2)$$

**[0060]** These lower bounds may be compared with the actual values if Alice sends coherent states, that is, $V(x_B|x_A)_{coh} = G_x(\chi_x + 1)\, N_0$ and $V(p_B|p_A)_{coh} = G_p(\chi_p+1)\, N_0$. Nevertheless, if we look for an upper bound on Eve's knowledge by using (1), we need to use the pessimistic limits given by (2), which implies

$$V(x_B|x_E) \geq N_0/\{G_p(\chi_p+V^{-1})\} \quad \text{and} \quad V(p_B|p_E) \geq N_0/\{G_x(\chi_x+V^{-1})\} \quad (3)$$

**[0061]** It is worthwhile asking whether Eve can reach these bounds. In a practical QKD scheme, Alice and Bob will give the same roles to x and p, and Bob will randomly choose one of them, as explained above. Assuming therefore that $G_x = G_p = G$ and $\chi_x = \chi_p = \chi$, the two bounds of (3) reduce to $V(B|E) \geq N_0/\{G(\chi+V^{-1})\}$. An entangling cloner achieving this limit can be sketched as follows. Eve uses a beamsplitter with a transmission $G < 1$ to split up a part of the signal transmitted from Alice to Bob, and she injects into the other input port a field $E_m$ that will induce a noise with the appropriate variance at Bob's end. In order to fully control this field $E_m$, Eve will inject one of two EPR-correlated beams, and she will keep the second one until Alice and Bob have revealed their bases. This ensures Eve is maximally entangled with Bob's field, compatible with the noise observed by Bob (this is an "entangling" attack). A straightforward calculation[18] shows that such an entangling cloner does reach the lower limit of (3).

Security Condition and Secret Bit Rate for a Reverse Reconciliation Protocol

**[0062]** In a reverse quantum cryptography protocol, Eve's ability to infer Bob's measurement is limited by the inequalities (3) and one must assume that a "perfect" Eve is able to reach these limits. In order to estimate the limits on information rates, we use Shannon's theory for Gaussian additive-noise channels (Shannon). The information shared by Alice and Bob is given by the decrease of Bob's field entropy that comes with the knowledge of Alice's field, i.e., $I_{AB}=H(B)-H(B|A)$. For a Gaussian distribution, the entropy is given, up to a constant, by $H(B)=(1/2)\log_2(V_B)$ bits per symbol, where $V_B$ is the variance. For simplicity, we assume here that the channel gains and noises, and the signal variances are the same for x and p. In practice, deviations from this should be estimated by statistical tests). Thus, according to Shannon's formula, the information rates $I_{BA}$ and $I_{BE}$ are given by:

$$I_{BA} = (1/2)\log_2[V_B/(V_{B|A})_{coh}]=(1/2)\log_2[(V+\chi)/(1+\chi)] \quad (4a)$$

$$I_{BE} = (1/2)\log_2[V_B/(V_{B|E})_{min}]=(1/2)\log_2[G^2(V+\chi)(V^{-1}+\chi)] \quad (4b)$$

where $V_B = \langle x_B^2 \rangle = \langle p_B^2 \rangle = G(V+\chi)N_0$ is Bob's variance, $(V_{B|E})_{min} = V(x_B|x_E)_{min} = V(p_B|p_E)_{min} = N_0/\{G(\chi+V^{-1})\}$ is Eve's minimum conditional variance, and $(V_{B|A})_{coh} = V(x_B|x_A)_{coh} = V(p_B|p_A)_{coh} = G(\chi+1)N_0$ is Alice's conditional variance for a coherent-state protocol. The secret information rate for such a reverse reconciliation protocol is thus[18,32]

$$\Delta I_{RR} = I_{BA} - I_{BE} = -(1/2)\log_2[G^2(1+\chi)(V^{-1}+\chi)] \qquad (5)$$

and the security is guaranteed ($\Delta I>0$) provided that $G^2(1+\chi)\ (V^{-1}+\chi) < 1$. For a direct reconciliation protocol, a similar calculation gives $\Delta I_{DR} = I_{AB} - I_{AE} = (1/2)\log_2[(V+\chi)/(1+V\chi)]$ so the security is guaranteed if $\chi<1$. The equivalent input noise $\chi$ includes two contributions: one is the "vacuum noise" due to the losses along the line, given by $\chi_{vac} = (1-G)/G$. The noise above vacuum noise, which we call "excess noise", is defined as $\varepsilon = \chi - \chi_{vac} = \chi - (1-G)/G$. In the limit of high losses ($G << 1$) one has $\Delta I_{RR} \approx -(1/2)\log_2[1+G(2\varepsilon+V^{-1}-1)]$, and thus the protocol will be secure provided that $\varepsilon < (V-1)/(2V) \sim 1/2$. Therefore RR may indeed be secure for any value of the line transmission G provided that the amount of excess noise $\varepsilon$ is not too large. This is an important difference with DR, which may tolerate large excess noise but requires low line losses since we have the conditions $G > 1/2$ and $\varepsilon < (2G-1)/G$.

**[0063]** It should be emphasised that squeezing and entanglement do play a crucial role in the security demonstration, even though we deal with a coherent state protocol. This is because the bound on $I_{BA}$ is obtained by assuming that Alice may use squeezed or entangled beams, and the bound on $I_{BE}$ can be achieved only if Eve uses an entangling attack. Therefore, though we did not consider the most general situation of a collective and/or non-Gaussian attack on the whole key exchange between Alice and Bob, we can reasonably conjecture that the security proof encompasses all eavesdropping strategies.

Detailed Description of an Experimental Optical Set-Up

**[0064]** In order to exchange correlated sets of Gaussian variables with Bob, Alice sends randomly modulated light pulses of 120 ns duration at a 800 kHz repetition rate. Each pulse contains up to 250 photons, and Bob performs an homodyne measurement of either x or p, using local oscillator (LO) pulses, containing about $10^8$ photons, that are also transmitted to him. One configuration of an experimental set-up[32] is shown on FIG. 1. The

channel losses are simulated by inserting a variable attenuator between Alice and Bob. FIG. 2 shows a data burst of 60,000 pulses measured by Bob, as a function of the amplitude sent by Alice in Bob's measurement basis. The line transmission is 100% and the modulation variance is V = 41.7. The solid line is the theoretical prediction (slope equal to one), and the insert shows the corresponding histograms of Alice's (gray curve) and Bob's (black curve) data.

**[0065]** The laser source consists of a commercially available CW laser diode (SDL 5412) at 780nm associated with an acousto-optic modulator, that is used to chop pulses with a duration 120 ns (full width half-maximum), at a repetition rate 800 kHz. In order to reduce excess noise, a grating-extended external cavity is used, and the beam is spatially filtered using a polarisation maintaining single mode fibre. Light pulses are then split onto a 10% reflecting beam-splitter, one beam being the local oscillator (LO), the other Alice's signal beam. The data is organised in bursts of 60000 pulses, separated by time periods that are used to lock the phase of the LO and sequences of pulses to synchronise the parties. In the present experiment, there is a burst every 1.6 seconds, which corresponds to a duty cycle of about 5%, but this should be easy to improve.

**[0066]** The desired coherent state distribution is generated by Alice by modulating randomly both the amplitude and phase of the light pulses with the appropriate probability law. In the present experiment, the amplitude of each pulse is arbitrarily modulated at the nominal 800 kHz rate. However, due to the unavailability of a fast phase modulator at 780 nm, the phase is not randomly modulated but scanned continuously from 0 to $2\pi$ using a piezoelectric modulator. For such a determinist phase variation, the security of the protocol is of course not warranted and thus no genuine secret key can be distributed. However, the experiment provides realistic data, that will have exactly the awaited structure provided that random phase permutation on Bob's data are performed. The amplitude modulator is an integrated electro-optic $LiNbO_3$ Mach-Zehnder interferometer, allowing for small voltages inputs ($V_\pi = 2.5V$) at 780nm. All voltages for the electro-optic modulator or the piezoelectric transductor are generated by an acquisition board (National Instruments PCI6111E) connected to a computer. Though all discussions assume the modulation to be continuous, digitised voltages are obviously used in practice. With the experimental parameters, a resolution of 8 bits is enough to hide the amplitude or phase steps under shot

noise. Since the modulation voltage is produced using a 16 bits converter, and the data is digitised over 12 bits, we may fairly assume the modulation to be continuous. Due to an imbalance between the paths of the interferometer, the modulator extinction is not strictly zero. In the present experiment that is only aimed at a proof of principle, the offset field from the data received by Bob is subtracted. In a real cryptographic transmission, the offset field should be compensated by Alice, either by adding a zeroing field, or by using a better modulator. For each incoming pulse, either the x or p signal quadrature is measured by appropriate switching of the LO phase. The homodyne detection was checked to be shot-noise limited for LO power up to $5x10^8$ photons/pulse. The overall homodyne detection efficiency is 0.76, due to the optical transmission (0.9), the mode-matching efficiency (0.92) and the photodiode quantum efficiency (0.92).

**[0067]** The experiment is thus carried out in such a way that all useful parameters – such as photon numbers, signal to noise ratios, added noises, information rate, etc. – can be measured experimentally. Reconciliation and privacy amplification protocols can thus be performed in realistic – though not fully secret – conditions. The limitations of the present set-up are essentially due to the lack of appropriate fast amplitude and phase modulator at 780 nm. This should be easily solved by operating at telecom wavelengths (1540-1580 nm) where such equipment is readily available.

**[0068]** Referring to FIG. 3, the curve is the theoretical prediction $\chi_{vac} = (1-G)/G$. The error bars include two contributions with approximately the same size, from statistics (evaluated over bursts of 60,000 pulses) and systematics (calibration errors and drift). After the quantum exchange, Alice and Bob evaluate the total added noise by calculating the variance of the difference between their respective values. This variance has four contributions: the shot noise $N_0$, the channel noise $\chi N_0$, the electronics noise of Bob's detector ($N_{el} = 0.26N_0$), and the noise due to imperfect homodyne detection efficiency ($N_{hom} = 0.32N_0$). In the absence of line losses, the measured $\chi$ is $(0.01 \pm 0.04)$, while it is expected to be zero. This is attributed to various calibration errors and drifts in the set-up, and gives an idea of the experimental uncertainty in the evaluation of the channel noise. In presence of line losses, the measured $\chi$ increases as (1-G)/G as expected, see FIG. 3.

**[0069]** Referring to FIG. 4, the value of $I_{BE}$ is calculated by assuming that Eve cannot know the noises $N_{el}$ and $N_{hom}$, which are internal to Bob's detector. This corresponds

to a "realistic" hypothesis, where the noise of Bob's detector is not controlled by Eve. The theoretical value of $I_{AE}$ is also plotted in order to compare RR with DR.

**[0070]** The detection noises $N_{el}$ and $N_{hom}$ originate from Bob's detection system only, so one may reasonably assume that they do not contribute to Eve's knowledge. In this "realistic" approach, $I_{BE}$ is given by Eq.(4b) with $\chi$ being the channel noise (i.e., subtracting the detection noises). In FIG. 4, $I_{BE}$ is plotted together with the value of $I_{BA}$ as given by Eq. (4a), where $\chi$ is now the total equivalent noise including both transmission and detection. The difference between these two curves gives the achievable secret key rate in reverse reconciliation $\Delta I_{RR}$ as a function of the line transmission G. We also show Alice-Eve information $I_{AE} = (1/2)\log_2[(V+\chi^{-1})/(1\chi^{-1})]$, corresponding to a direct reconciliation protocol[11], with $\chi$ being the channel noise. The comparison of the DR and RR protocols is straightforward by looking at FIG. 4.

Computer Simulation of the Secret Key Distillation

**[0071]** One aspect in the protocol is to design a (direct or reverse) reconciliation algorithm that can efficiently extract a binary common key from the measured data. A computer program that performs the various steps of secret key distillation described above, namely channel evaluation, reconciliation, and privacy amplification[32] was written. Under the scope of this "proof-of-principle" experiment, Alice and Bob are simulated on the same computer, although it poses no fundamental problem to make them remotely communicate over a network. This would require the use of a classical public authenticated channel in addition to the quantum channel. The designed program accepts as input the sequences of Alice's sent values and Bob's measurement outcomes, and produces a secret key as detailed below. First, Alice's and Bob's key elements are compared in order to measure the relevant parameters of the quantum channel, namely the overall transmission G and added noise $\chi$. The estimation of Eve's knowledge is based on Eq.(4), that gives a bound on $I_{BE}$ once G and $\chi$ are known to Alice and Bob. Then, a reconciliation algorithm is performed, with as few leaked bits to Eve as possible. Protocols based on discrete quantum states such as BB84[20] can use a discrete reconciliation protocol, for example Cascade[21]. In contrast, since continuous key elements are produced here, we instead needed to develop a "sliced" reconciliation algorithm[9,22], which produces a common bit string from correlated continuous key elements

as described above. Finally, we carry out privacy amplification in such a way that, loosely speaking, every bit of the final key is a function of most if not all of the reconciliated bits. Following[23-25], we can reduce the size of the key by $(nI_{BE}+r+\Delta(n))$ bits, where r indicates the public information leaked during the reconciliation of the sequence of size n, and $\Delta(n)$ is an extra security margin as described above. This follows from the assumption that Eve can only use individual attacks, so that we can consider key elements and eavesdropping as independent repetitions of identical random processes.

Demonstration of Relevant Heisenberg Relations

**[0072]** Let us consider the situation where Alice tries to evaluate $x_B$, and Eve tries to evaluate $p_B$ in a reverse reconciliation protocol. The corresponding estimators can be de noted as $\alpha x_A$ for Alice and $\beta p_E$ for Eve, where $\alpha$ and $\beta$ can be taken as real numbers. The errors for these estimators will be $x_{B|A,\alpha} = x_B - \alpha x_A$, and $p_{B|E,\beta} = p_B - \beta p_E$. Since all operators for Alice, Bob and Eve commute, one has obviously $[x_{B|A,\alpha}, p_{B|E,\beta}] = [x_B, p_B]$ and thus we get the Heisenberg relation $\Delta x_{B|A,\alpha}^2 \, \Delta p_{B|E,\beta}^2 \geq N_0^2$. Since the conditional variances are by definition given by $V(x_B|x_A) = \min_\alpha \{\Delta x_{B|A,\alpha}^2\}$ and $V(p_B|p_E) = \min_\beta \{\Delta p_{B|E,\beta}^2\}$, we obtain the expected relation $V(x_B|x_A)\, V(p_B|p_E) \geq N_0^2$. Exchanging the roles of x and p, one gets also the symmetrical relation $V(p_B|p_A)\, V(x_B|x_E) \geq N_0^2$.

**[0073]** Alice has the estimators $(x_A, p_A)$ for the field $(x_{in}, p_{in})$ that she sends out, so that one can write $x_{in} = x_A + A_x$ and $p_{in} = p_A + A_p$ with $\langle A_x^2 \rangle = \langle A_p^2 \rangle = sN_0$ , where s is related to the amount of squeezing that may be used by Alice to generate this field, and obeys $s \geq V^{-1}$. By calculating the correlation coefficients $\langle p_A^2 \rangle = (V - s)\, N_0$ , $\langle p_B^2 \rangle = G_p\, (V + \chi_p)\, N_0$, and $\langle p_A p_B \rangle = \sqrt{G_p}\, \langle p_A^2 \rangle$, one obtains Alice's conditional variance on Bob's measurement, $V(p_B|p_A) = \langle p_B^2 \rangle - |\langle p_A p_B \rangle|^2 / \langle p_A^2 \rangle = G_p(s+\chi_p)N_0$. This equation and the constraint $s \geq V^{-1}$ gives finally $V(p_B|p_A) \geq G_p\, (V^{-1}+\chi_p)\, N_0$, and similarly $V(x_B|x_A) \geq G_x(V^{-1}+\chi_x)N_0$ by exchanging the roles of x and p.

Detailed Description of Sliced Reconciliation

**[0074]** We assume that Alice and Bob share correlated Gaussian key elements from which they wish to extract I(A; B) common bits, where A (resp. B) denotes the random

variable representing one of Alice's (resp. Bob's) Gaussian key elements, described using their binary expansion. In order to deal with realistic streams of data despite the non-random phase modulation used in the current experiment, the key elements must actually be randomly permuted before processing. The reconciliation procedure[9,22] works in the following way. Alice chooses m functions $S_1(A),...,S_m(A)$ that map her key elements onto $\{0, 1\}^m$. If Alice and Bob exchanged a block of n key elements $A_1,...,A_n$, Alice thus creates m bit strings of length n, called "slices", by applying each function $S_i$ to all her key elements: $S_i(A_1),..., S_i(A_n)$. Then Alice and Bob reconciliate each slice sequentially for i=1...n. Since this comes down to reconciliating bit strings, we used an implementation[19] of the binary error correction algorithm Cascade[21]. Bob, on his side, must also convert his key elements $B_1,...,B_n$ into binary strings. To this end, he uses another set of functions $R_i$, called "slice estimators", which estimate the bits $S_i(A)$ given Bob's current knowledge. Since the slices are corrected sequentially for i=1,...,m, Bob already knows $S_1(A),...,S_{i-1}(A)$ upon correcting slice i, so that the slice estimator $R_i$ is a function of B *and* of the previous reconciliated slices, that is $R_i(B; S_1(A),...,S_{i-1}(A))$. It remains to detail how the functions $S_i$ are created. On the one hand, we wish to extract as many bits as possible out of A and B, but, on the other hand, any bit leaked during the binary reconciliation with Cascade does not count as a secret bit since it is publicly known. The difference between these two quantities defines the net amount of (potentially secret) reconciliated bits per key element, which can be expressed as $H(S_1(A),...,S_m(A))-\Sigma_i h(e_i)$, where the first term is the entropy of the Alice's produced bits, and $e_i = Pr[R_i(B;S_1(A),...,S_{i-1}(A)) \neq S_i(A)]$. This uses the fact that, according to Shannon theory, at least n h(e) bits must be disclosed to correct a string of length n with bit error probability e, where $h(x) = - x \log_2 x - (1-x) \log_2(1-x)$. Note that in practice Cascade leaks a little bit more than Shannon's formula. In the case of the current set-up, it appeared useless to reconciliate the bits beyond some precision level, so we chose to use m = 5 slices as a trade-off between a satisfactory number of reconciliated bits and reasonable computing resources. We discretized the field amplitudes into $2^m = 32$ intervals, numbered from 0 to 31. What was found to work best[22] is to assign the least significant bit of the interval number to $S_1(A)$, the second least significant bit to $S_2(A)$, and so on, up to the most significant bit to $S_5(A)$. In other words, the reconciliation is carried out from a fine-grained level to a coarse-gained level. We then numerically optimized the interval boundaries so as to maximise the net amount of

reconciliated bits. It should be stressed that the binary error correction algorithm used in this implementation, Cascade[21], is a two-way interactive protocol, so that the information leaking to Eve should be estimated carefully. For example, in RR, Eve may gain some knowledge on Alice's value that might give her some additional information on the key (Bob's value). The same problem occurs in DR, but to a smaller extent. This additional information, which reduces the number of secret bits, must be evaluated numerically[32].

Detailed Description of Privacy Amplification

**[0075]** Privacy amplification amounts to process the reconciliated key into a random transformation taken in a universal class of hash functions[25,26]. In this case, we chose the class of truncated linear functions in a finite field. This means we considered the reconciliated bits as coefficients of a binary polynomial in a representation of the Galois field $GF(2^{110503})$ whose size allows to process up to 110503 bits at once, and hashing was achieved by first multiplying the reconciliated polynomial with a random element of the field and then extracting the desired number of least significant bits[32]. This operation can be implemented efficiently (see e.g.[27]). In practice, the explicit knowledge of a prime polynomial over GF(2) is needed to perform the modular reduction, so we used the polynomial[28] $x^{110503}+x^{519}+1$. Finally, the number of extracted bit is $n\,H(S_1(A),\ldots, S_m(A))-I(A;E)-r-\Delta(n)$, where we reduced the final key size by some extra amount $\Delta(n)$, which depends on the actual number of key elements and the desired security margin. The evaluation of $\Delta(n)$, which is basically a finite size effect, will not be described here.

Evaluation of the Proposed QKD Schemes

**[0076]** Table 1 shows the ideal and practical secret key rates of the direct-reconciliation and reverse-reconciliation QKD protocols for several values of the line transmission G. The RR scheme is in principle efficient for any value of G, provided that the reconciliation protocol achieves the limit given by $I_{BA}$. However, in practice, unavoidable deviations of the algorithm from Shannon's limit reduce the actual reconciled information shared by Alice and Bob, while $I_{BE}$ is of course assumed unaffected. For high modulation ($V\approx 40$), the reconciliation efficiency lies around 80%, which makes it possible to distribute a secret key at a rate of several hundreds of kbits per second for low losses. However, the

achievable reconciliation efficiency drops when the signal-to-noise ratio (SNR) decreases, so that no secret bits can be extracted when the channel gain G is too low. This can be improved by reducing the modulation variance, which increases the ratio $I_{BA}/I_{BE}$ so the constraint on the reconciliation efficiency is less severe. Although the ideal secret key rate is then lower, we could process the data with a reconciliation efficiency of 78% for G = 0.49 (3.1 dB) and V=27, resulting in a net key rate of 75 kbits/s. This clearly demonstrates that RR continuous-variable protocols operate efficiently at and beyond the 3dB loss limit of DR protocols. We emphasize that, although we were not able to extract a key well above 3 dB in this "proof-of-principle" experiment, an increase of the reconciliation efficiency would immediately translate into a larger achievable range.

**[0077]** The QCV protocol can be compared with single-photon protocols on two aspects: the raw repetition frequency and the secret key rate in bits per time slot. In photon-counting QKD, the key rate is intrinsically limited by the maximum repetition frequency of the single-photon detector, typically of the order of 100 kHz, due to the lifetime of trapped charges in the semiconductor. In contrast, homodyne detection may run at frequencies of up to tens of MHz. In addition, a specific advantage of the high dimensionality of the QCV phase space is that the field quadratures can be modulated with a large dynamics, allowing the encoding of several key bits per pulse. Very high secret bit rates are therefore attainable with the coherent-state protocol when using transmission lines of low losses (up to about 3 dB in the present implementation). For high-loss transmission lines, the protocol is presently limited by the reconciliation efficiency, but its intrinsic performances remain very high. Let us consider an ideal situation where the reconciliation algorithm attains Shannon's bound and the excess noise is negligible. Then, the net key rate of the protocol is slightly above that of BB84, which yields $G\, n_{ph}/2$ secret bits per time slot for a noiseless line, where $n_{ph}$ is the number of photons sent per time slot. Taking for instance a 67.1 km line (typical current distance for state-of-the-art single-photon QKD[30]) with 14.3 dB loss and a reasonable modulation V = 10, the protocol would ideally yield a secret key rate of 0.025 bits per time slot. Thus, assuming perfect reconciliation and a pulse repetition rate of a few MHz, the QCV protocol could achieve a secret key rate as high as 100 kbits/sec. Note, however, that $I_{BA}$ = 0.208 bits per time slot in this case, so that a reconciliation efficiency of about 90 % would actually be needed in a regime of very low (around -5 dB) signal-to-noise ratio. The currently

available reconciliation protocols do not reach this regime. For comparison, the secret key rate of BB84 with an ideal single-photon source and perfect detectors would be at best 0.019 bits per time slot with the same line, and even one order of magnitude smaller using attenuated light pulses with $n_{ph} = 0.1$.

**[0078]** Although the present "proof-of-principle" setup is far from reaching these numbers, there is still a considerable margin for improvement, both in the hardware and the software. For example, working at telecom wavelengths where fast modulators are available would overcome some of the technical limitations of the present set-up. Concerning the receiver's system, increasing the detection bandwidth or the homodyne efficiency, and decreasing the electronic noise would significantly enhance the achievable range. Also, significant improvement may result from further research on reconciliation algorithms[31]. This suggests that the way is open for testing the present proposal as a practical, high bit-rate, quantum key distribution scheme over moderate distances.

TABLE 1

| V | G (%) | Losses (dB) | Ideal RR rate (kb/s) | Practical RR rate (kbs/s) | Ideal DR rate (kb/s) | Practical DR rate (kb/s) |
|---|---|---|---|---|---|---|
| 41.7 | 100 | 0.0 | 1,920 | 1,690 | 1,910 | 1,660 |
| 38.6 | 79 | 1.0 | 730 | 470 | 540 | 270 |
| 32.3 | 68 | 1.7 | 510 | 185 | 190 | - |
| 27.0 | 49 | 3.1 | 370 | 75 | 0 | - |
| 43.7 | 26 | 5.9 | 85 | - | 0 | - |

**[0079]** Table 1 summarizes the parameters of the quantum key exchange for several values of the line transmission G (the corresponding losses are given in dB). The variations of Alice's field variance V are due to different experimental adjustments. The ideal secret key bit rates would be obtained from the measured data with perfect key distillation, yielding exactly $I_{BA}$-$I_{BE}$ bits (RR) or $I_{AB}$-$I_{AE}$ (DR). The practical secret key bit rates are the one achieved with the current key distillation procedure ("-" means that no secret key is generated). Both bit rates are calculated over bursts of about 60,000 pulses at 800 kHz, not taking into account the duty cycle (≈5 %) in the present setup.

References


1. For a review, see for instance: Gisin, N., Ribordy, G., Tittel, W. & Zbinden H., *Rev. Mod. Phys.* 74, 145 (2002); see also Tittel, W., Ribordy, G. & Gisin, N, Quantum cryptography, *Physics World*, 41-45 (March 1998).

2. Hillery, M., Quantum cryptography with squeezed states, *Phys. Rev. A* 61, 022309-1—022309-8 (2000).

3. Ralph, T. C., Continuous variable quantum cryptography, *Phys. Rev. A* 61, 010303(R)-1—010303-4 (2000).

4. Ralph, T. C., Security of continuous-variable quantum cryptography., *Phys. Rev. A* 62, 062306-1—062306-7 (2000).

5. Reid, M. D., Quantum cryptography with a predetermined key, using continuous-variable Einstein-Podolsky-Rosen correlations, *Phys. Rev. A* 62, 062308-1—062308-6 (2000).

6. Gottesman, D. & Preskill, J., Secure quantum key distribution using squeezed states, *Phys. Rev. A* 63, 022309-1—022309-18 (2001).

7. Cerf, N. J., Lévy, M. & Van Assche, G. Quantum distribution of gaussian keys using squeezed states, *Phys. Rev. A* 63, 052311-1—052311-5 (2001).

8. Bencheikh, K., Symul, Th., Jankovic, A. & Levenson, J.A., Quantum key distribution with continuous variables, *J. Mod. Optics* 48, 1903-1920 (2001);

9. Cerf, N.J., Iblisdir, S. & Van Assche, G., Cloning and cryptography with quantum continuous variables, *Eur. Phys. J. D* 18, 211-218 (2002).

10. Silberhorn, Ch., Korolkova, N. & Leuchs, G., Quantum key distribution with bright entangled beams, *Phys. Rev. Lett.* 88, 167902-1—167902-4 (2002).

11. Grosshans, F. & Grangier, Ph., Continuous variable quantum cryptography using coherent states, *Phys. Rev. Lett.* 88, 057902-1—057902-4 (2002).

12. Cerf, N.J., Ipe, A. & Rottenberg, X., Cloning of continuous variables, *Phys. Rev. Lett.* 85, 1754-1757 (2000).

13. Cerf, N.J. & Iblisdir, S, Optimal N-to-M cloning of conjugate quantum variables, *Phys. Rev. A* 62, 040301(R)-1—040301-3 (2000).

14. Grosshans, F. & Grangier, Ph, Quantum cloning and teleportation criteria for continuous quantum variables, *Phys. Rev. A* 64, 010301(R)-1—010301-4 (2001).

15. Duan, L.-M., Giedke, G., Cirac, J. I. & Zoller, P., Entanglement purification of gaussian continuous variable quantum states, *Phys. Rev. Lett.* 84, 4002-4005 (2000).

16. Poizat, J.Ph., Roch, J.-F. & Grangier, P., Characterization on quantum non-demolition measurements in optics, *Ann. Phys. (Paris)* 19, 265-297 (1994).

17. Grangier, Ph., Levenson, J. A. & Poizat, J.-Ph., Quantum non-demolition measurements in optics, *Nature* 396, 537-542 (1998).

18. Grosshans, F. & Grangier, Ph., Reverse reconciliation protocols for quantum cryptography with continuous variables, *E-print arXiv:quant-ph/*0204127-1—0204127-5 (April 2002).

19. Nguyen, K., *Extension des Protocoles de Réconciliation en Cryptographie Quantique,* Master Thesis, (Université Libre de Bruxelles, Bruxelles, 2002).

20. Bennett, C.H. & Brassard, G., Quantum key distribution and coin tossing, *Proceedings of the IEEE International Conference on Computers, Systems, and Signal Processing, Bangalore, India,* 175-179 (IEEE, New York, 1984).

21. Brassard, G. & Salvail, L., Secret-key reconciliation by public discussion, *Advances in Cryptology - Eurocrypt'93, Lecture Notes in Computer Science,* 411-423 (Springer-Verlag, New York, 1993).

22. Van Assche, G., Cardinal, J. & Cerf, N.J., Reconciliation of a quantum-distributed Gaussian key, *E-print arXiv:cs.CR/*0107030 (2001).

23. Maurer, U. M. & Wolf, S., Information theoretic key agreement : from weak to strong secrecy for free, *Advances in Cryptology - Eurocrypt 2000, Lecture Notes in Computer Science*, 351-368 (Springer-Verlag, New York, 2000).

24. Maurer, U.M., Secret key agreement by public discussion from common information, *IEEE Trans. Inform. Theory* 39, 733-742 (1993).

25. Bennett, C. H., Brassard, G., Crépeau, C. & Maurer, U.M., Generalized privacy amplification, *IEEE Trans. on Inform. Theory* 41, 1915-1935 (1995).

26. Carter, J.L. & Wegman, M.N., Universal Classes of Hash Functions, *J. of Comp. and Syst. Sci.* 18, 143-154 (1979).

27. Schönhage, A., Schnelle Multiplikation von Polynomen über Körpern der Charakteristik 2, *Acta Informatica* 7, 395-398 (1977).

28. Brent, R.P., Larvala, S. & Zimmermann, P., A fast algorithm for testing irreductibility of trinomials mod 2, *Tech. Rep., Oxford University Computing Laboratory*, 1-16 (2000).

29. Braunstein, S.L. & Pati, A.K., Quantum information theory with continuous variables, Kluwer Academic, Dordrecht, 2003.

30. Stucki, D., Gisin, N., Guinnard, O., Ribordy, G. & Zbinden H., Quantum Key Distribution over 67 km with a plug & play system, *E-print arXiv:quant-ph/*0203118 (2002).

31. Buttler,W.T., Lamoreaux, S.K., Torgerson, J.R., Nickel, G.H. & Peterson, C.G., Fast, efficient error reconciliation for quantum cryptography. *E-print arXiv:quant-ph/*0203096 (2002).

32. Grosshans F., Van Assche G., Wenger J., Brouri R., Cerf N. J. & Grangier Ph., Quantum key distribution using gaussian-modulated coherent states, *Nature* 421, 238-241 (2003).

# Quantum Distribution of Gaussian Keys with Squeezed States

N. J. Cerf,[1,2] M. Lévy,[1] and G. Van Assche[1]
[1] *Ecole Polytechnique, CP 165, Université Libre de Bruxelles, 1050 Brussels, Belgium*
[2] *Jet Propulsion Laboratory, California Institute of Technology, Pasadena, California 91109*
(August 2000)

A continuous key distribution scheme is proposed that relies on a pair of canonically conjugate quantum variables. It allows two remote parties to share a secret Gaussian key by encoding it into one of the two quadrature components of a single-mode electromagnetic field. The resulting quantum cryptographic information vs disturbance tradeoff is investigated for an individual attack based on the optimal continuous cloning machine. It is shown that the information gained by the eavesdropper then simply equals the information lost by the receiver.

PACS numbers: 03.67.Dd, 03.65.Bz, 42.50.-p, 89.70.+c



Quantum cryptography—or, more precisely, quantum key distribution—is a technique that allows two remote parties to share a secret chain of random bits (a secret key) that can be used for exchanging encrypted information [1–3]. The security of this process fundamentally relies on the Heisenberg uncertainty principle, or on the fact that any measurement of incompatible variables inevitably affects the state of a quantum system. Any leak of information to an eavesdropper necessarily induces a disturbance of the system, which is, in principle, detectable by the authorized receiver.

In most quantum cryptosystems proposed so far, a single photon (or, in practice, a weak coherent state with an average photon number lower than one) is used to carry each bit of the key. Mathematically, the security is based on the use of a pair of non-commuting observables such as the $x$- and $z$-projections of a spin-1/2 particle, $\sigma_x$ and $\sigma_z$, whose eigenstates are used to encode the key. The sender (Alice) randomly chooses to encode the key using either $\sigma_z$ (0 is encoded as $|\uparrow\rangle$ and 1 as $|\downarrow\rangle$) or $\sigma_x$ (0 is encoded as $2^{-1/2}(|\uparrow\rangle+|\downarrow\rangle)$ and 1 as $2^{-1/2}(|\uparrow\rangle-|\downarrow\rangle)$), the choice of the basis being disclosed only *after* the receiver (Bob) has measured the photon. This guarantees that an eavesdropper (Eve) cannot read the key without corrupting the transmission. Such a procedure, known as BB84 [1], is at the heart of most of the quantum cryptographic schemes that have been experimentally demonstrated in the past few years, which are based either on the polarization (e. g. [4,5]) or the optical phase (e. g. [6]) of single photons. An alternative scheme, realized experimentally only a year ago [7–9], can also be used based on a pair of polarization-entangled photons instead of single photons [10]. It is, however, fundamentally equivalent to BB84 (see [11]) and it again relies on the algebra of spin-1/2 particles.

Recently, it has been shown that another protocol for quantum key distribution can be devised based on continuous variables, where squeezed coherent light modes are used to carry the key [12–14]. In these techniques, one exploits a pair of (continuous) canonical variables such as the two quadratures $X_1$ and $X_2$ of the amplitude of a mode of the electromagnetic field, which behave just as position and momentum. The uncertainty relation $\Delta X_1 \Delta X_2 \geq 1/4$ then implies than Eve cannot read both quadrature components without degrading the state. Even though the experimental preparation of squeezed states is a difficult task, these schemes circumvent a main weakness of the above-mentioned cryptosystems that is the critical dependence of their security on the ability of preparing single-photon states.

In this paper, we propose an alternative squeezed-state quantum cryptographic scheme, which provides a means to distribute a *continuous* secret key. The goal of our protocol is to have Alice and Bob sharing a continuous key that consists of a random list of Gaussian-distributed variables that cannot be known to Eve. Thus, in this scenario, *both* the key and the quantum variable that carries it are continuous. This is in contrast with the schemes proposed in Ref. [12–14], which appear hybrid as a continuous quantum variable was used to carry a discrete key element (the shared key was made of bits, or, in general, discrete variables). Instead, our approach can be viewed as an *all-continuous* quantum cryptographic scheme, which is the proper continuous extension of the BB84 scheme. First, from a theoretical perspective, this provides a more satisfying continuous treatment of quantum key distribution. Remarkably, the tradeoff between Eve's information gain and the disturbance at Bob's station can be expressed in an unexpectedly simple way (if we restrict ourselves to an individual attack based on the optimal continuous cloning machine): the information gained by Eve on one quadrature is at most equal to the information lost by Bob on the other quadrature. This results in a simple information-theoretic measure of the disturbance, namely the defect of information at Bob's station. Moreover, this all-continuous scheme avoids a potential attack against the scheme proposed in Ref. [12–14] by filling in the gaps between the values used to encode the discrete key values (this will be explained later on).

Let us now detail our protocol. The uncertainty relation implies that it is impossible to measure with full accuracy *both* quadratures of a single mode, $X_1$ and $X_2$. Alice exploits this property by encoding the key elements (random Gaussian samples) as a quadrature squeezed

state either in $X_1$ or in $X_2$, in such a way that an eavesdropper ignoring which of these two "bases" is used cannot acquire information without disturbing the state. In basis 1, Alice prepares a squeezed vacuum state such that the fluctuations of $X_1$ are squeezed ($\Delta X_1^2 = \sigma_1^2 < 1/4$), and then applies a displacement of $X_1$ by an amount equal to the value of the Gaussian key ($\langle X_1 \rangle = x$, where $x$ is the encoded key element). The quantity $\sigma_1^2$ refers here to the intrinsic variance of $X_1$ in the squeezed state; the corresponding squeeze parameter is $r_1 = -\ln(2\sigma_1)$. We denote by $\Sigma_1^2$ the variance of this Gaussian key, so the mean value $\langle X_1 \rangle$ is itself distributed as a Gaussian of mean 0 and variance $\Sigma_1^2$. Conversely, in basis 2, Alice sends a squeezed state in $X_2$ ($\Delta X_2^2 = \sigma_2^2 < 1/4$), whose displacement encodes the Gaussian key ($\langle X_2 \rangle = x$). Again, $\langle X_2 \rangle$ has a Gaussian profile with mean 0 and variance $\Sigma_2^2$, while the squeeze parameter in mode 2 is $r_2 = -\ln(2\sigma_2)$. Thus, in both basis, Alice encodes the key into a displaced vacuum squeezed state, the squeezing (by $r$) and displacement (by $x$) being applied at random on $X_1$ or $X_2$.

Now, for the cryptographic setup to be secure, we require the statistical distribution of the $X_1$ measurement outcomes to be indistinguishable whether basis 1 or 2 is used by Alice. If this condition is fulfilled, Eve cannot obtain any indication on whether she is measuring a type 1 or type 2 squeezed state, whatever the statistics she accumulates. If basis 1 is used, the outcomes of $X_1$ measurements (that can be obtained in practice by homodyne detection) are distributed as a Gaussian of variance $\Sigma_1^2 + \sigma_1^2$ since each squeezed state gives an extra contribution of $\sigma_1^2$ to the variance. If, on the contrary, a type 2 squeezed state is measured, then the outcomes of $X_1$ measurements exhibit a Gaussian distribution of variance $1/(16\sigma_2^2)$ as a result of the uncertainty principle. Thus, we impose the condition

$$\Sigma_1^2 + \sigma_1^2 = 1/(16\sigma_2^2) \tag{1}$$

Similarly, the requirement that type 1 and 2 squeezed states are indistinguishable when performing $X_2$ measurements implies that $\Sigma_2^2 + \sigma_2^2 = 1/(16\sigma_1^2)$. These two relations can be summarized as

$$1 + \Sigma_1^2/\sigma_1^2 = 1 + \Sigma_2^2/\sigma_2^2 = 1/\alpha^2 \tag{2}$$

where $\alpha = 4\sigma_1\sigma_2 = e^{-(r_1+r_2)}$ is a (positive) dimensionless constant which must satisfy $\alpha \leq 1$ (or $\sigma_1\sigma_2 \leq 1/4$) for Eq. (2) to be consistent. More generally, these two conditions guarantee that the density matrices of the encoded key elements are the same in bases 1 and 2, making them indistinguishable. Thus, choosing the squeeze parameters $r_1$ and $r_2$ is sufficient to completely characterize the protocol.

Let us now analyze the transmission of the Gaussian key elements in the case where there is no eavesdropper and the transmission is perfect. We first need to recall some standard notions of Shannon theory concerning the treatment of continuous transmission channels. Consider a discrete-time continuous channel which adds a Gaussian noise of variance $\sigma^2$ on each signal. If the input $x$ of the channel is a Gaussian signal of variance $\Sigma^2$, the uncertainty on $x$ can be measured by the differential Shannon entropy $h(x) = 2^{-1}\log_2(2\pi e\,\Sigma^2)$ bits [15]. Conditionally on $x$, the output $y$ is distributed as a Gaussian of variance $\sigma^2$, so that the entropy of $y$ conditionally on $x$ becomes $h(y|x) = 2^{-1}\log_2(2\pi e\,\sigma^2)$ bits. Now, the distribution of $y$ is given by the convolution of these two Gaussians, i. e., a Gaussian of variance $\Sigma^2 + \sigma^2$. Hence, the output entropy is $h(y) = 2^{-1}\log_2(2\pi e\,(\Sigma^2 + \sigma^2))$ bits. According to Shannon theory, the information that is processed through this noisy channel can be expressed as the mutual information between $x$ and $y$ (the amount by which the uncertainty on $y$ is reduced by knowing $x$):

$$I\ (\text{bits}) = h(y) - h(y|x) = \frac{1}{2}\log_2(1+\gamma) \tag{3}$$

where $\gamma = \Sigma^2/\sigma^2$ can be viewed as the signal-to-noise ratio (SNR). This is Shannon's famous formula for the capacity of a Gaussian additive noise channel [16]. Here, the signal variance (or power) is simply $\Sigma^2$, while the noise variance is $\sigma^2$. This capacity measures the number of bits that can be transmitted asymptotically (using block coding) per use of the channel, with an arbitrary high fidelity for a given SNR. It can be shown to be attainable if the signal is Gaussian distributed (which is the case under consideration here).

Coming back to our cryptographic setup, consider the situation (with no eavesdropping) where Bob performs a measurement in the good basis after the latter is publicly announced by Alice. (It is equivalent to the more realistic procedure where Bob measures the key in a random basis, but then discards the bad outcomes after the basis is disclosed by Alice.) The SNR in basis 1 is simply $\gamma_1 = \Sigma_1^2/\sigma_1^2$, while it is $\gamma_2 = \Sigma_2^2/\sigma_2^2$ in basis 2. Using this notation, Eq. (2) becomes $1 + \gamma_1 = 1 + \gamma_2 = 1/\alpha^2$, so that we must have the same SNR in both basis, $\gamma = e^{2(r_1+r_2)} - 1$. This means that the processed information is also the same in both bases, and can be expressed, using Eq. (3), as

$$I_0\ (\text{bits}) = -\log_2(\alpha) = (r_1 + r_2)/\ln(2) \tag{4}$$

Thus, our continuous quantum cryptographic technique can be essentially characterized by a single dimensionless constant $\alpha$ (the product of the $X_1$ noise of type-1 squeezed states times the $X_2$ noise of type-2 squeezed states). It works provided that $\alpha \leq 1$, as a finite amount of information is then processed from Alice to Bob. Note that $I_0$ (expressed in natural units—nats—rather than in bits) is simply equal to the sum of the squeeze parameters in bases 1 and 2, which reflects that the processed information is zero in the absence of squeezing, and grows linearly with squeezing in bases 1 and 2. For example, if $\sigma_1^2 = \sigma_2^2 = 1/8$, i. e., if we have a squeeze factor $e^r = \sqrt{2}$ in each basis, then $\alpha = 1/2$, so we can process one bit on

average per use of the channel. This corresponds to $\gamma = 3$ in both bases. More generally, we see that the processed information in the absence of eavesdropping increases as $\alpha$ gets smaller. In some sense, the more we violate a pseudo-uncertainty relation $\sigma_1\sigma_2 \geq 1/4$, the larger this information gets. Remember that $\sigma_1$ and $\sigma_2$ are standard deviations of $X_1$ and $X_2$ measurements on type 1 and 2 states, respectively. If they referred to $X_1$ and $X_2$ measurements on a *same* state, then the above uncertainty relation would apply, and Eq. (2) could not be satisfied (except for the useless case $\alpha = 1$).

The average photon number contained in each encoded key state clearly increases with the widening of the displacement ($\Sigma^2$) needed to represent Alice's key values for a given SNR. It also increases as squeezing increases, but then the displacement distribution can be narrowed to achieve a same SNR. Let us determine the relative contribution of these two effects focusing on one basis, and assuming for simplicity that $\sigma_1 = \sigma_2 = \sigma$ so that the same squeezing is applied on both quadratures. In this case, Eq. (2) implies that $\sigma^2 = \frac{1}{4}e^{-2r}$, $\Sigma^2 = \frac{1}{2}\sinh(2r)$, and $1 + \gamma = e^{4r}$. For a given encoded key state (with a squeeze parameter $r$ and displacement $x$, where $x$ is the key value Alice wishes to transmit), the mean photon number can be written as $N = x^2 + \sinh^2 r$, where the first term reflects the displacement effect while the second characterizes vacuum squeezing [17]. For a given SNR $\gamma$ (or a given squeezing parameter $r$), we obtain the average number of photons over all possible values $x$ sent by Alice (distributed as a Gaussian of mean 0 and variance $\Sigma^2$), $\langle N \rangle = \Sigma^2 + \sinh^2 r$. Using the relation between $\gamma$ and $r$, this gives for the average number of photons per key pulse:

$$\langle N \rangle = \frac{1-\alpha}{2\alpha} = \frac{e^{2r}-1}{2} = \frac{(1+\gamma)^{1/2}-1}{2} \qquad (5)$$

Equivalently, the processed information can be expressed as a function of the average photon number,

$$I_0 \text{ (bits)} = \log_2(2\langle N \rangle + 1) \qquad (6)$$

implying that the photon number must increase exponentially with the processed information.

We shall now investigate the tradeoff between the information acquired by Bob and Eve in this continuous cryptographic protocol. First, we should emphasize that, even in the absence of eavesdropping, the key elements received by Bob are not exactly equal to those sent by Alice. This is in contrast with BB84, and is simply due to the fact that the noise due to the intrinsic fluctuations of the squeezed states always adds to the signal, giving rise to a finite SNR. This already holds at Alice's station, regardless the (possibly tapped) channel. So, an eavesdropper will be visible in this scheme by an enhanced noise variance (or a reduced SNR) at Bob's station. A protocol that Alice can follow to detect any eavesdropping can be to disclose, on a public channel, the exact values $x$ of a random subset of key elements. Then, Bob compares them to the received values $y$ and computes the distribution of the differences $y - x$. For a perfect and untapped channel, it should be a Gaussian of variance $\sigma^2$, so the SNR is unchanged. Otherwise, the SNR decreases by an amount that can be viewed as a measure of the disturbance of the Alice-to-Bob channel. Assume, for example, that Eve uses an individual "intercept-and-resend" attack, measuring each key element in basis 1 or 2, at random, and resending a squeezed state centered on the value of the measured quadrature. The variance at Bob's station is $2\sigma^2$ (twice the intrinsic variance!) if Eve used the good basis, or $1/(16\sigma^2)$ in the opposite case, so the resulting noise variance is $\sigma^2[1 + 1/(2\alpha^2)]$. Thus Bob's computed SNR is reduced by a factor $2/(3+\gamma)$.

Let us now make the assumption that the optimal individual eavesdropping strategy for Eve consists in using the optimal (Gaussian) cloning machine for continuous quantum variables [18,19]. This is a very sensible conjecture as the phase-covariant qubit cloner is known to be the best individual eavesdropping strategy for BB84 [20] (actually, the universal qubit cloner is optimal for the related six-state quantum cryptographic protocol [21,22]). We consider an attack where Eve makes two imperfect copies of the key element, and sends one of them to Bob while she keeps the other one. Bob and Eve both wait until Alice reveals the basis she used for encoding the key before measuring the received state in the appropriate basis (again, this is equivalent to Bob measuring in a random basis and then discarding the bad measurements after the basis disclosure). To analyze the information-theoretic balance between Bob and Eve, we use a general class of *asymmetric* Gaussian cloners defined in Ref. [18] that result in a different amount of noise on both quadratures and for Bob and Eve. It is proven in Ref. [18] that the inequality

$$\sigma^2_{1,B}\,\sigma^2_{2,E} \geq 1/16 \qquad (7)$$

must hold (and is saturated for this class of cloners), where $\sigma^2_{1,B}$ and $\sigma^2_{2,E}$ are the variances of the errors that affect Bob's $X_1$ measurements and Eve's $X_2$ measurements, respectively. For example, if basis 1 is used, then the outcomes of $X_1$ measurements on Bob's side will be distributed as a Gaussian of variance $\sigma_1^2 + \sigma^2_{1,B}$ since cloning-induced errors are superimposed on the intrinsic fluctuations of the squeezed states. Similarly, a second no-cloning uncertainty relation holds, connecting Bob's errors on $X_2$ and Eve's errors on $X_1$: $\sigma^2_{2,B}\,\sigma^2_{1,E} \geq 1/16$. Let us now characterize the cloners that saturate these inequalities by two parameters $\chi$ and $\gamma$: we rewrite the error variances on Bob's side as $\sigma^2_{1,B} = \chi\gamma(\sigma_1^2/\alpha)$ and $\sigma^2_{2,B} = \chi\gamma^{-1}(\sigma_2^2/\alpha)$, while the errors on Eve's side are written as $\sigma^2_{1,E} = \chi^{-1}\gamma(\sigma_1^2/\alpha)$ and $\sigma^2_{2,E} = \chi^{-1}\gamma^{-1}(\sigma_1^2/\alpha)$. Thus, $\chi$ characterizes the balance between Bob's and Eve's errors as $\sigma_{1,B}/\sigma_{1,E} = \sigma_{2,B}/\sigma_{2,E} = \chi$. The limit $\chi \to 0$ corresponds to the case where Bob has a negligible cloning-induced additional error on his measured quadratures, so he gets the entire

information $I_0$ (Eve does not get any information). The case $\chi = 1$ represents a symmetric situation where the errors induced by cloning are the same for Bob and Eve. Of course, the limit $\chi \to \infty$ is the opposite situation where Eve gets most of the information with no error. Similarly, $\gamma$ describes the quadrature 1 vs 2 balance, that is, $\sigma_{1,B}/\sigma_{2,B} = \sigma_{1,E}/\sigma_{2,E} = \gamma(\sigma_1/\sigma_2)$.

Now, we need to express the information processed from Alice to Bob (or from Alice to Eve) in basis 1 (or basis 2). In basis 1, the variance of Bob's measurement outcomes is $\sigma_1^2 + \sigma_{1,B}^2 = (1 + \chi\gamma/\alpha)\sigma_1^2$, while the distribution of the key elements has a variance $\Sigma_1^2$. Using Shannon's formula, Eq. (3), and the identity $1 + \Sigma_1^2/\sigma_1^2 = 1/\alpha^2$, we obtain the information processed from Alice to Bob in basis 1:

$$I_{1,B} = \frac{1}{2}\log_2\left(\frac{1+\alpha\chi\gamma}{\alpha^2+\alpha\chi\gamma}\right) \tag{8}$$

Similarly, using the variance of Eve's outcomes in basis 2, $\sigma_2^2 + \sigma_{2,E}^2 = [1 + 1/(\chi\gamma\alpha)]\sigma_2^2$, an analogous calculation yields for Eve's information in basis 2

$$I_{2,E} = \frac{1}{2}\log_2\left(\frac{1+\alpha/(\chi\gamma)}{\alpha^2+\alpha/(\chi\gamma)}\right) \tag{9}$$

Finally, the balance between Bob's and Eve's information can be expressed by calculating the *sum* of equations (8) and (9):

$$I_{1,B} + I_{2,E} = \frac{1}{2}\log_2(1/\alpha^2) = I_0 \tag{10}$$

Remarkably, it appears that the information acquired by Eve on the second quadrature, $I_{2,E}$, is *exactly* counterbalanced by the defect of information at Bob's side on the first quadrature, $I_0 - I_{1,B}$. Of course, the counterpart of Eq. (10) also holds when interchanging the bases, that is, $I_{2,B} + I_{1,E} = I_0$.

Thus, assuming that the use of the continuous cloner is the best possible individual attack against our continuous cryptographic protocol, Bob's information loss can be viewed as a proper disturbance measure as it simply is an upper bound on the information that might potentially have been gained by an eavesdropper. Consequently, the net amount of key bits that can be generated by this method is bounded by $I_B - I_E = I_0 - 2I_E$. This follows from [23] where it is proven that the secret key rate of $A$ and $B$ with respect to $E$ is lower bounded by the difference of mutual information $I(A;B) - I(A;E)$. Even though $A$, $B$ and $E$ here denote continuous variables, we can use this result provided that the generated key and the exchanged reconciliation messages are discrete as required in [23]. Our continuous variables $A$, $B$ and $E$ only appear at the right of the conditional bar in entropy formulas, so they can be approximated by discrete numbers (that is, they can be replaced by an integer such as $\lfloor nA \rfloor$, approximating the real variable $A$). As $n$ grows, it will soon be close to the real variable with a precision far beyond what is needed given the noise level. Thus, we conclude that our protocol can only work provided that $I_E < I_0/2$, that is, iff $\chi < 1$. Stated otherwise, the quality of the signals measured by Alice and Bob must be bounded by $I_B > I_0/2$, or in terms of signal-to-noise ratios $\gamma' > \sqrt{1+\gamma} - 1$, where $\gamma'$ is the SNR measured by Bob. This means that a 1-bit channel ($\gamma = 3$) may still be used if the noise power is almost tripled ($\gamma' > 1$). In summary, the procedure we propose here consists in the quantum distribution of a (real) Gaussian key, followed by a discretization procedure so as to apply some (discrete) reconciliation and privacy amplification protocol. Such a strategy avoids a weakness of the squeezed-state cryptosystems as presented in Refs. [12–14]. There, the key is binary (or belong to a larger finite alphabet), so there are always gaps between the discrete key values. This allows Eve to gain knowledge about the occurrences where she measured the wrong quadrature (without getting the key value). This knowledge alone is sufficient for her to attack this key distribution scheme simply by omitting to resend the corresponding key elements to Bob, thereby faking a small attenuation in the transmission. This limitation does not apply to our scheme since the continuous key values fill in an entire region in the $(X_1, X_2)$ phase space.

In conclusion, an all-continuous quantum cryptographic protocol was proposed that is based on single-mode squeezed states of the electromagnetic field. It exploits the uncertainty relation between the conjugate pair of quadrature components $X_1$ and $X_2$ by encoding a continuous Gaussian-distributed key into either $X_1$- or $X_2$-squeezed states, thereby allowing a continuous key distribution between two remote parties. It is shown that the information acquired by an eavesdropper on the key elements encoded in $X_1$ is compensated by a reduction (by a same amount) of the key information available on the $X_2$ amplitude at the receiver's station. This information-theoretic tradeoff characterizes the worst-case individual attack based on the cloning machine, so we conclude that the loss of information at the receiver's end is a good upper bound on the tapped information. A realization of this continuous protocol based on squeezed states would be very challenging, as the generation of squeezed light has been a difficult experimental target for years. Also, it would require synchronized local oscillators at Alice's and Bob's stations, in order for them to have a common phase for homodyne detecting the amplitudes $X_1$ and $X_2$. In addition, probably the main limitation in the implementation of this protocol is related to the loss of squeezing effected by attenuation in the transmission medium. This would dramatically decrease the SNR, and make the protocol less efficient (or insecure). In analogy with what is known for BB84, there probably is a threshold on the squeeze parameter that Alice should reach, below which the protocol would fail. Nevertheless, it should be stressed that the cryptographic protocol proposed here was analyzed using the conjugate pair $X_1$ and $X_2$, but other complementary variables might be exploited as

well. In particular, one could possibly imagine a continuous cryptographic scheme based on the time-frequency complementarity, where ultra-short single-photon pulses, or, alternatively, single-photon pulses that are highly resolved in frequency would be used in order to encode the Gaussian key. Such a scheme might possibly avoid some of the weaknesses of the squeezed state protocol, and be more appropriate for an experimental realization.

We are grateful to Jonathan Dowling, Nicolas Gisin, Serge Massar, and Hugo Zbinden for helpful discussions. G. V. A. acknowledges support from the Banque Nationale de Belgique.

---

[1] C. H. Bennett and G. Brassard, in *Proceedings of the IEEE International Conference on Computers, Systems, and Signal Processing, Bangalore, India* (IEEE, New York, 1984), pp. 175–179.
[2] C. H. Bennett, Phys. Rev. Lett. **68**, 3121 (1992).
[3] N. Lütkenhaus, Phys. Rev. A **59**, 3301 (1999).
[4] C. H. Bennett *et al.*, J. Cryptology **5**, 3 (1992).
[5] H. Zbinden, H. Bechmann-Pasquinucci, N. Gisin, and G. Ribordy, Appl. Phys. B **67**, 743 (1998).
[6] P. D. Townsend, Opt. Fiber Tech. **4**, 345 (1998).
[7] T. Jennewein *et al.*, Phys. Rev. Lett. **84**, 4729 (2000).
[8] D. S. Naik *et al.*, Phys. Rev. Lett. **84**, 4733 (2000).
[9] W. Tittel, J. Brendel, H. Zbinden, and N. Gisin, Phys. Rev. Lett. **84**, 4737 (2000).
[10] A. K. Ekert, Phys. Rev. Lett. **67**, 661 (1991).
[11] C. H. Bennett, G. Brassard, and N. D. Mermin, Phys. Rev. Lett. **68**, 557 (1992).
[12] T. C. Ralph, Phys. Rev. A **61**, 010303 (2000).
[13] M. Hillery, Phys. Rev. A **61**, 022309 (2000).
[14] M. D. Reid, (1999), e-print quant-ph/9909030.
[15] T. M. Cover and J. A. Thomas, *Elements of Information Theory* (Wiley & Sons, New York, 1991).
[16] C. E. Shannon, Bell Syst. Tech. J. **27**, 623 (1948).
[17] M. O. Scully and M. S. Zubairy, *Quantum Optics* (Cambridge University Press, Cambridge, 1997).
[18] N. J. Cerf, A. Ipe, and X. Rottenberg, Phys. Rev. Lett. (2000), in press; also in e-print quant-ph/9909037.
[19] N. J. Cerf and S. Iblisdir, Phys. Rev. A (2000), in press; also in e-print quant-ph/0005044.
[20] C. A. Fuchs *et al.*, Phys. Rev. A **56**, 1163 (1997).
[21] D. Bruß, Phys. Rev. Lett. **81**, 3018 (1998).
[22] H. Bechmann-Pasquinucci and N. Gisin, Phys. Rev. A **59**, 4238 (1999).
[23] U. M. Maurer, IEEE Transactions on Information Theory **39**, 733 (1993).

**EPJ manuscript No.**
(will be inserted by the editor)

# Cloning and Cryptography with Quantum Continuous Variables*

N. J. Cerf[1,2], S. Iblisdir[1], and G. Van Assche[1]

[1] Ecole Polytechnique, CP 165, Université Libre de Bruxelles, 1050 Brussels, Belgium
[2] Jet Propulsion Laboratory, California Institute of Technology, Pasadena, CA 91109, USA



July 2001

**Abstract.** The cloning of quantum variables with continuous spectra is investigated. We define a Gaussian 1-to-2 cloning machine, which copies equally well two conjugate variables such as position and momentum or the two quadrature components of a light mode. The resulting cloning fidelity for coherent states, namely $F = 2/3$, is shown to be optimal. An asymmetric version of this Gaussian cloner is then used to assess the security of a continuous-variable quantum key distribution scheme that allows two remote parties to share a Gaussian key. The information versus disturbance tradeoff underlying this continuous quantum cryptographic scheme is then analyzed for the optimal individual attack. Methods to convert the resulting Gaussian keys into secret key bits are also studied. The extension of the Gaussian cloner to optimal $N$-to-$M$ continuous cloners is then discussed, and it is shown how to implement these cloners for light modes, using a phase-insensitive optical amplifier and beam splitters. Finally, a phase-conjugated inputs $(N, N')$-to-$(M, M')$ continuous cloner is defined, yielding $M$ clones and $M'$ anticlones from $N$ replicas of a coherent state and $N'$ replicas of its phase-conjugate (with $M' - M = N' - N$). This novel kind of cloners is shown to outperform the standard $N$-to-$M$ cloners in some situations.

**PACS.** 03.67.Dd – 03.65.Bz – 42.50.-p – 89.70.+c

## 1 Introduction

Quantum information theory was originally developed for discrete quantum variables, in particular quantum bits (qubits). Recently, however, it has been discovered that several concepts that were invented for qubits extend very naturally to the domain of continuous variables (e.g., position and momentum of a particle, or the quadrature components of a mode of the electromagnetic field). The first result in this direction concerned quantum teleportation [23,7], and gave rise to a lot of interest in continuous-variable quantum information processing. In the present paper, we focus on the notions of quantum cloning and quantum key distribution, and investigate how they can be extended to continuous variables.

Cloning machines (that achieve the optimal approximate cloning transformation compatible with the so-called no-cloning theorem) have been a fundamental research topic in the last five years. In Section 2, we will define a Gaussian cloner, which achieves the optimal cloning of a continuous variable compatible with the requirement of being covariant with respect to displacements and rotations in phase space. In other words, this cloner duplicates all coherent states with a same fidelity ($F = 2/3$). The optical implementation of this cloner and its extension to $N$-to-$M$ cloners are also discussed. In Section 3, we then turn to quantum key distribution, and propose a continuous-variable cryptosystem that allows two remote parties to share a Gaussian key by exchanging continuous key elements carried by squeezed states. This scheme is the proper continuous counterpart of the protocol BB84 [2] for qubits. Our continuous cryptosystem is related to the Gaussian cloner for an asymmetric version of the latter achieves the optimal individual eavesdropping strategy. Thus, our previous results on continuous cloning can be used to analyze the information versus disturbance tradeoff, in order to assess the security of this continuous cryptosystem. We find that the information gained by the eavesdropper is exactly upper bounded by the information lost by the authorized receiver. We also investigate a protocol to convert the raw Gaussian keys into a string of secret key bits, that is, we show how to apply reconciliation and privacy amplification on continuous key elements. Finally, in Section 4, we come back to the issue of cloning continuous variables, and define a new class of "phase-conjugated inputs" cloners. These cloners produce several clones (and anticlones) from several replicas of an input coherent state *and* its phase conjugate. We show that adding these extra phase-conjugated inputs makes it possible to improve the cloning (and anticloning) fidelity with respect to the standard $N$-to-$M$ cloners.

* Submitted to the special issue of the European Physical Journal D on "Quantum interference and cryptographic keys: novel physics and advancing technologies". Proceedings of the conference QUICK 2001, Cargese, Corsica, April 7–13, 2001.

## 2 Quantum Cloning Machines

Let us first seek for a transformation which duplicates with a same fidelity all coherent states $|\psi\rangle$, with $\psi = (x+ip)/\sqrt{2}$. The fundamental requirement we put on this transformation is that it is covariant with respect to displacements in phase space. That is, if two input states are identical up to a displacement $\hat{D}(x,p) = e^{-ix\hat{p}}e^{ip\hat{x}}$, then their respective copies should be identical up to the same displacement. (In this paper, we put $\hbar = 1$). Thus, cloning can be defined as a completely positive trace-preserving linear map $\mathcal{C} : |\psi\rangle\langle\psi| \rightarrow \mathcal{C}(|\psi\rangle\langle\psi|)$ such that

$$\begin{aligned}&\hat{D}^{\otimes 2}(x,p)\mathcal{C}(|\psi\rangle\langle\psi|)\hat{D}^{\dagger\otimes 2}(x,p)\\ &= \hat{D}(x,p)\mathcal{C}(|\psi\rangle\langle\psi|)\hat{D}^{\dagger}(x,p),\end{aligned} \tag{1}$$

for all displacements $\hat{D}(x,p)$ in the phase space. A simple way to meet displacement covariance is to seek for a cloning transformation whose output clone individual states are given each by a Gaussian mixture:

$$\begin{aligned}\rho(|\psi\rangle\langle\psi|) = \frac{1}{2\pi\sigma^2}\int dx\, dp\, e^{-\frac{x^2+p^2}{2\sigma^2}}\\ \times\hat{D}(x,p)|\psi\rangle\langle\psi|\hat{D}^{\dagger}(x,p),\end{aligned} \tag{2}$$

where $\sigma^2$ is the cloning-induced error variance. In the following we will refer to such a transformation as a Gaussian cloner. Note that Eq. (2) is such that the cloning induced noise on the quadratures $\hat{x}$ or $\hat{p}$ is invariant under rotations in the phase space, which is certainly a desirable property since it is satisfied by coherent states. Consider the following unitary operator:

$$\hat{U}_{1,2,3} = e^{-i(\hat{x}_3-\hat{x}_2)\hat{p}_1}e^{-i\hat{x}_1(\hat{p}_2+\hat{p}_3)}e^{-i\hat{x}_2\hat{p}_3}, \tag{3}$$

where modes 1, 2 and 3 refer respectively to the original, the additional copy, and an auxiliary mode (also refered to as an ancilla). This operator can be used to build a Gaussian cloner if the additional copy and the ancilla are initially prepared in the vacuum state[12]. Indeed, it is readily checked that this transformation outputs two clones whose individual states are Gaussian-distributed, as in Eq.(2), with a variance $\sigma^2 = 1/2$. In particular, it copies all coherent states $|\psi\rangle$ with the same fidelity $f_{1,2} = \langle\psi|\rho(\psi)|\psi\rangle = 2/3$.

This machine is optimal in the sense that it is impossible to have $\sigma^2(1,2) < 1/2$. To prove this, let us consider the following situation. A coherent state is processed through such a cloner, the observable $\hat{x}$ being measured at one output clone while the observable $\hat{p}$ is measured at the other output. Let us denote by $\Sigma_x^2$ and $\Sigma_p^2$ the respective error variances corresponding to this joint measurement. From the general theory on the simultaneous measurement of conjugate observables [1], we know that

$$\Sigma_x^2\Sigma_p^2 \geq 1. \tag{4}$$

Using Eq. (2), we get

$$(\delta\hat{x}^2+\sigma^2)(\delta\hat{p}^2+\sigma^2) \geq 1, \tag{5}$$

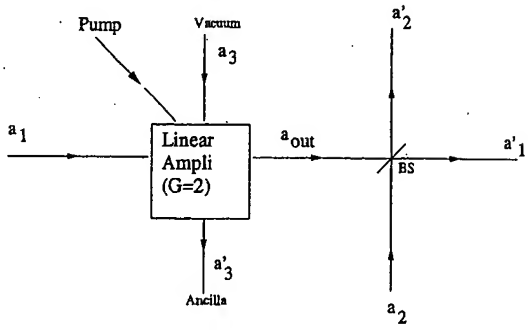


**Fig. 1.** Implementation of a $1 \rightarrow 2$ cloner using a phase-insensitive linear amplifier and a 50 : 50 beam-splitter (BS).

where $\delta\hat{x}^2(\delta\hat{p}^2)$ is the intrinsic variance of $\hat{x}$ ($\hat{p}$) of the input state and $\sigma^2$ is the cloning-induced variance. Now, using the uncertainty principle $\delta\hat{x}^2\delta\hat{p}^2 \geq 1/4$ and the inequality $a^2+b^2 \geq 2\sqrt{a^2b^2}$, we conclude that $\sigma^2 \geq 1/2$, implying that the unitary operator Eq. (3) is indeed optimal to achieve Gaussian cloning[10].

A possible implementation of this machine (see Fig. 1) consists in processing the input mode into a linear phase-insensitive amplifier [8] of gain $G = 2$:

$$\hat{a}_{out} = \sqrt{2}\hat{a}_1 + \hat{a}_3^{\dagger}, \qquad \hat{a'}_3 = \hat{a}_1^{\dagger} + \sqrt{2}\hat{a}_3, \tag{6}$$

with $a_j = (\hat{x}_j + i\hat{p}_j)/\sqrt{2}$ denoting the annihilation operator for mode $j$). Then, one produces the two output clones by processing the output signal of the amplifier through a 50 : 50 phase-free beam-splitter:

$$\hat{a'}_1 = \frac{1}{\sqrt{2}}(\hat{a}_1+\hat{a}_2), \qquad \hat{a'}_2 = \frac{1}{\sqrt{2}}(\hat{a}_1-\hat{a}_2), \tag{7}$$

It is readily checked that this scheme leads to an equal $x$-error and $p$-error variance of $1/2$ for both clones, that is, it achieves the optimal Gaussian cloner.

We will now present two generalizations of this $1 \rightarrow 2$ Gaussian quantum cloning machine. The first one consists in a transformation which from $N$ ($\geq 1$) original input states produces $M$ ($\geq 2$) output copies whose individual states are again given by an expression similar to Eq.(2), but with a different error variance $\sigma^2{}_{N,M}$. Using an argument based on the concatenation of cloners, it is possible to derive a lower bound on $\sigma^2{}_{N,M}$, that is[10]

$$\sigma^2{}_{N,M} \geq \frac{1}{N} - \frac{1}{M}, \tag{8}$$

with the corresponding fidelity for coherent states

$$f_{N,M} \leq \frac{MN}{MN+M-N}. \tag{9}$$

Again, these bounds can be attained by a transformation whose implementation necessitates only a phase-insensitive linear amplifier and beam splitters [6]. Loosely speaking, the procedure consists in concentrating the $N$ input modes into a single mode by a network of beam splitters, to amplify the resulting mode, and then to distribute the output

amplified mode into $M$ output modes through a second network of beam-splitters.

The second generalization of the $1 \rightarrow 2$ Gaussian quantum cloning machine we will briefly consider here is the case where the $\hat{x}$ and $\hat{p}$ quadratures are not treated equally, and the case where the two output clones do not have the same fidelity. Equation (2) then has to be replaced by

$$\rho(|\psi\rangle\langle\psi|) = \frac{1}{2\pi\sqrt{\sigma_{i,x}^2\sigma_{i,p}^2}} \int dx\, dp\, e^{-\left(\frac{x^2}{2\sigma_{i,x}^2}+\frac{p^2}{2\sigma_{i,p}^2}\right)} \times \hat{D}(x,p)|\psi\rangle\langle\psi|\hat{D}^\dagger(x,p), \tag{10}$$

where $\sigma_{i,x}^2$ (resp. $\sigma_{i,p}^2$) stands for the cloning-induced error variance in the quadrature $\hat{x}$ (resp. $\hat{p}$) for the $i$th clone. In this case, it is possible to prove [12] that the following cloning uncertainty relations must hold:

$$\sigma_{1,x}^2\sigma_{2,p}^2 \geq 1/4, \quad \sigma_{1,p}^2\sigma_{2,x}^2 \geq 1/4. \tag{11}$$

Asymmetries between the output clones and between the $x/p$ variables can be characterized by the following two parameters:

$$\chi = \frac{\sigma_{1,x}}{\sigma_{2,x}} = \frac{\sigma_{1,p}}{\sigma_{2,p}}, \text{ and } \lambda = \frac{\sigma_{1,x}}{\sigma_{1,p}} = \frac{\sigma_{2,x}}{\sigma_{2,p}}. \tag{12}$$

As suggested in [16], asymmetric machines (with $\chi \neq 1$) can be implemented by a scheme akin to Fig. 1 in the sense that only two beam splitters and a single linear amplifier are needed. We will see in the following section how these asymmetric quantum cloning machines can be used to assess the security of a continuous-variable quantum key distribution protocol.

## 3 Quantum Key Distribution

In this section, we introduce a quantum protocol for the distribution of Gaussian key elements, which is a continuous-variable analogue of the protocol BB84 [2] – we assume here that the reader is familiar with BB84. Our protocol, introduced in [13], works like BB84 but with binary information being replaced by continuous information that behaves essentially like in a Gaussian channel.

One exploits a pair of canonically conjugate continuous variables $x$ and $p$, which can be thought of, for instance, as the two quadratures $X_1$ and $X_2$ of the amplitude of a mode of the electromagnetic field [21]. Alice randomly chooses a random key element $r$ that follows a Gaussian distribution with mean zero and variance $\Sigma^2$, and randomly decides to encode it into either $x$ (i.e., $\langle x\rangle = r$) or $p$ (i.e., $\langle p\rangle = r$). An eavesdropper ignoring which of these two encoding rules is used cannot acquire information without disturbing the state.

Let us now describe the exact nature of the states used for encoding each key element. When encoding the value $r \sim N(0,\Sigma_x)$ in $x$, Alice creates a Gaussian state such that $\langle x\rangle = r$, $\langle p\rangle = 0$, $\Delta x^2 = \sigma_x^2$ and thus $\Delta p^2 = 1/4\sigma_x^2$. Similarly, when the value $r \sim N(0,\Sigma_p)$ is encoded in $p$, the encoding state has $\langle p\rangle = r$, $\langle x\rangle = 0$, $\Delta p^2 = \sigma_p^2$ and thus $\Delta x^2 = 1/4\sigma_p^2$.

On his side, Bob measures either $x$ or $p$ at random. Like in BB84, half of the measurements give results that are uncorrelated to Alice's values, so half of the samples must be discarded when Alice discloses the encoding variable. Unlike BB84, however, measuring the correct variable does not yield the exact value of $r$, even with a perfect apparatus, because of the intrinsic noise of the Gaussian state. The value $r$ follows a Gaussian distribution $N(0,\Sigma_{x,p})$, to which some Gaussian noise is added $N(0,\sigma_{x,p})$, thus resulting in a Gaussian distribution with variance $\Sigma_{x,p}^2 + \sigma_{x,p}^2$. We can therefore model the transmission of $r$ as a Gaussian channel with a signal-to-noise ratio (SNR) equal to $\Sigma_x^2/\sigma_x^2$ or $\Sigma_p^2/\sigma_p^2$.

An important requirement of the protocol is to make it impossible for Eve to be able to infer which encoding variable Alice used. For this, measuring the correct or incorrect variable ($x$ or $p$) must yield statistically indistinguishable results. If, in contrast, Eve was able to detect (even not perfectly) that she measured the wrong set, then she could fake an attenuation by discarding wrong key elements and retransmitting only the correctly measured ones. This indistinguishability requirement can be expressed as the equality of the density matrices resulting from the two encoding rules, or equivalently as [13]

$$1 + \frac{\Sigma_x^2}{\sigma_x^2} = 1 + \frac{\Sigma_p^2}{\sigma_p^2} = \frac{1}{4\sigma_x^2\sigma_p^2}. \tag{13}$$

A proof of this is given in Appendix A. This also means that the SNR is the same for both variables $x$ and $p$, and that the information rate is [15]

$$I = \frac{1}{2}\log_2(1+\Sigma_x^2/\sigma_x^2) = -\log_2(2\sigma_x\sigma_p). \tag{14}$$

### 3.1 Eavesdropping by cloning

Let us now discuss an individual eavesdropping of this protocol with cloning machines such as those defined in Section 2. Eve makes two clones of the state sent by Alice, one of which is transmitted to Bob, and the other is measured in the correct variable when Alice reveals the encoding rule. This happens to be the optimal individual eavesdropping strategy as shown in [13] and [20].

We use a $1 \rightarrow 2$ cloning machine, and we keep the freedom to make a better clone for Bob or Eve (parameter $\chi$) and to get more accuracy in $x$ or $p$ (parameter $\lambda$). The subscripts 1 and 2 for the two copies are replaced respectively by $B$ and $E$ for the two recipients. The added variances on the clones will be:

$$\sigma_{B,x}^2 = \tfrac{1}{2}\chi\lambda, \quad \sigma_{B,p}^2 = \frac{1}{2}\chi\lambda^{-1}, \tag{15}$$

$$\sigma_{E,x}^2 = \tfrac{1}{2}\chi^{-1}\lambda, \; \sigma_{E,p}^2 = \frac{1}{2}\chi^{-1}\lambda^{-1}. \tag{16}$$

Let us calculate the resulting information rates. When Bob measures $x$, the result is affected both by the intrinsic fluctuations of $x$ and by the noise induced by the cloning operation, thus resulting in a total variance $\sigma_x^2+\frac{1}{2}\chi\lambda$. This is the noise power in the Gaussian channel representing the communication between Alice and Bob through Eve's cloning machine. Therefore, the information rate is now

$$I_{B,x} = \frac{1}{2}\log_2(1+\frac{\Sigma_x^2}{\sigma_x^2+\frac{1}{2}\chi\lambda}). \quad (17)$$

Similarly, one can calculate the new variance on $p$ measured by Eve on her clone, namely $\sigma_p^2+\frac{1}{2}\chi^{-1}\lambda^{-1}$. This gives an information rate

$$I_{E,p} = \frac{1}{2}\log_2(1+\frac{\Sigma_p^2}{\sigma_p^2+\frac{1}{2}\chi^{-1}\lambda^{-1}}). \quad (18)$$

Adding the last two information rates indicates the balance between Bob's and Eve's information. Remarkably, the information that Eve gains by using this attack on $p$ is exactly equal to the information that Bob loses on $x$ [13],

$$I_{B,x}+I_{E,p} = \frac{1}{2}\log_2(1+\frac{\Sigma_x^2}{\sigma_x^2}) = I. \quad (19)$$

Of course, this balance also works when swapping $x$ and $p$, namely $I_{B,p}+I_{E,x}=I$.

This result is interesting because it allows Bob to bound from above the information gained by a possible eavesdropper. Assuming symmetry of the protocol in $x$ and $p$, Bob can estimate $I-I_B$ and is guaranteed that $I_E \leq I-I_B$ (in practice, a part of the information loss will be due to channel noise). From Ref. [19], it is kwown that with reconciliation and privacy amplification carried out over a public authenticated channel, one is guaranteed to generate key bits whenever $I_B > I_E$. This last condition is in turn guaranteed provided that $I_B > I/2$, so that up to a 50% information loss on Bob's side is acceptable in order to generate key bits.

### 3.2 From Gaussian key elements to secret bits

Let us now investigate the classical part of the key distribution protocol since we have to deal with reconciliation and privacy amplification based on *continuous* raw key elements here, in contrast to BB84. Shannon's formula gives us an upper limit on the number of bits one can send through a Gaussian channel with a given SNR. In our protocol, neither Alice nor Bob chooses the Gaussian random values. Yet, we want them to be able to extract a common string of bits out of their correlated Gaussian values, revealing as little information as possible on the public channel.

Our secret key distillation procedure [24] works in the following way. First, Alice and Bob are going to extract common bits out of their Gaussian-distributed values, using a binary correction algorithm such as Cascade or a variant [5,22,25,14]. They will use it several times, on several real-to-binary conversion functions. Then, the resulting bits will undergo the usual privacy amplification procedure [19,4,3], for instance using a universal class of hash functions.

Let $X$ denote the random variable representing Alice's Gaussian values, and $X'$ Bob's values. Alice uses a set of real-to-binary conversion functions $S_i(X)=0,1$, $(1\leq i\leq m)$. These are called *slices*, in the sense that instead of performing reconciliation on the real-valued string $x_{1\ldots l}$, we operate on each string $S_i(x_{1\ldots l})$ sequentially, like slices of the main, real-valued string. On his side, Bob uses another set of functions $\tilde{S}_i$, called *slice estimators*, which reflects his best guess on the bit $S_i(X)$ given his current knowledge. The slice estimator $\tilde{S}_i$ is not only a function of $X'$ but also of the previous slices, $\tilde{S}_i(X', S_1(X),\ldots,S_{i-1}(X))$. This results from the fact that the slices are corrected sequentially for $i=1,\ldots,m$, and thus upon correcting slice $i$ Bob already knows $S_1(X),\ldots S_{i-1}(X)$. By carefully choosing the functions $S_i$ and $\tilde{S}_i$, both parties can extract a common string of bits out of the correlated Gaussian values, while only disclosing a little more than $H(S_1(X),\ldots,S_m(X)|X')$ bits on the public channel. A more detailed analysis is given in [24].

Let us take an example. Assume the channel has $\Sigma^2/\sigma^2 = 15$, which means that Alice and Bob can share up to $I=\frac{1}{2}\log_2(1+\Sigma^2/\sigma^2)=2$ bits per raw key element. We assume $m=5$ slices as a trade-off between the efficiency of large $m$ and the use of reasonable computing resources. The slice functions $S_i(X)$, $1\leq i\leq 5$ are constructed in the following way. First, the Gaussian distribution of $X$ is divided into $2^m=32$ intervals. The interval labeling function $T(X)$, which associates an interval number (from 0 to 31) to each value of $x$, is chosen so as to maximize $I(T(X);X')$. Thus, Bob starts with an optimal knowledge of $T(X)$. Then, we create the slice functions by assigning bit values to each of these intervals. Stated otherwise, we create a bijection between $S_{1\ldots5}(X)$ and $T(X)$ so that each vector of the 5 slice bits represents one (and only one) interval defined by $T(X)$. Much freedom is permitted at this step, but what we found to work best is to assign the least significant bit of the interval number to $S_1(X)$, the second bit to $S_2(X)$, and so on up to the most significant bit to $S_5(X)$.

The slice estimator functions $\tilde{S}_{1\ldots5}(X',\ldots)$ are constructed from the slices $S_{1\ldots5}(X)$ and from the joint probability density $f_{X,X'}(x,x')$. Each estimator $\tilde{S}_i$ evaluates whether $S_i(X)=0$ or $S_i(X)=1$ is more likely conditionally on the arguments given to the estimator, namely $X'$ and the previous slices $S_{j<i}(X)$.

In the present example, Alice's and Bob's bits are almost uncorrelated when correcting slices 1 and 2. The binary correction algorithm does not have to be used at this point – it is enough for Alice to entirely reveal $S_1(X)$ and $S_2(X)$ for the whole string. Then, slice 3 on Alice's side and the slice estimator 3 on Bob's side produce two bit strings that match 76% of the time – it is thus possible to proceed with error correction using a binary correction algorithm. Note that the bit strings would be less correlated

if the knowledge of $S_1(X)$ and $S_2(X)$ was not brought to Bob. Then for slice 4 (resp. slice 5), Alice's and Bob's string match 98% (resp. 99.999%) of the time, for which the binary correction will disclose only a small amount of information. Again, the knowledge of slices 1-3 helped Bob accurately estimate slice 4, which in turn helped him estimate slice 5.

As a result of this 5-step correction, Alice and Bob share a string of bits whose entropy is $H(S_{1...5}) = 4.8$ bits per raw key element. Assuming a perfect binary correction algorithm, about 3 bits per raw key elements were disclosed. Roughly speaking, the net effect is thus $4.8 - 3 = 1.8$ bit of secret information per raw key element after privacy amplification (which is to be compared with the 2 bits per key element as given by Shannon's formula).

This is of course only an example. More elaborate constructions can be performed, such as gathering $d$ Gaussian key elements at once. In fact, it was shown in [24] that the disclosed information reaches the Shannon bound as $d \to \infty$, just like for instance data compression works best for asymptotically large block sizes.

Now that we showed how quantum cryptography (followed by reconciliation and privacy amplification) can work with continuous variables, let us investigate another application of continuous variables to a special kind of quantum cloning machines.

## 4 Phase-Conjugated Inputs Quantum Cloning Machines

It has been shown that an antiparallel pair of qubits is intrinsically more informative than a pair of parallel qubits if the goal is to encode a direction in space [18]. Similarly for quantum continuous variables, one can show that more information can be encoded in a pair of phase- conjugated coherent states $|\psi\rangle|\psi^*\rangle$ than in two identical replicas $|\psi\rangle|\psi\rangle$ [9]. Following on these ideas, we present here a phase-conjugated input (PCI) quantum cloning machine, that is, a transformation which taking as input $N$ replicas of a coherent state $|\psi\rangle$ and $N'$ replicas of its complex conjugate $|\psi^*\rangle$, produces $M$ optimal clones of $|\psi\rangle$ [11]. Again we will require that all the clones are treated equally, and that the cloner is covariant with respect to both displacements and rotations in phase space. As a matter of fact, it turns out that such a transformation can be implemented optimally using a sequence of beam-splitters, a single nonlinear medium, and another sequence of beam-splitters, just as in the case of standard cloning. The procedure is the following (see Fig. 2):

(i) Concentrate the $N$ replicas of $|\psi\rangle$ stored in the $N$ modes $\{c_l\}$ $(l = 0 \dots N-1)$ into a single mode $a_1$, resulting in a coherent state of amplitude $\sqrt{N}\,\psi$. This operation can be performed with a network of beam-splitters achieving a $N$-mode Discrete Fourier Transform (DFT)[6]. We get:

$$a_1 = \frac{1}{\sqrt{N}} \sum_{l=0}^{N-1} c_l, \tag{20}$$

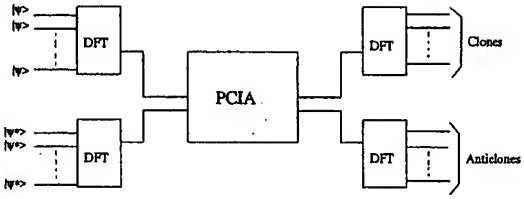


**Fig. 2.** PCI cloner that produces $M$ clones and $M'$ anti-clones from $N$ replicas of $|\psi\rangle$ and $N'$ replicas of $|\psi^*\rangle$. Modes are concentrated and distributed by Discrete Fourier Transform (DFT).

and $N-1$ vacuum modes. Similarly, with a $N'$-mode DFT, concentrate the $N'$ replicas of $|\psi^*\rangle$ stored in the $N'$ modes $\{d_l\}$ $(l = 0 \dots N'-1)$ into a single mode $a_2$. This results in a coherent state of amplitude $\sqrt{N'}\,\psi^*$. We have:

$$a_2 = \frac{1}{\sqrt{N}} \sum_{l=0}^{N'-1} d_l. \tag{21}$$

(ii) Apply the following transformation on the modes $a_1$ and $a_2$, resulting in modes $b_1$ and $b_2$ defined by

$$\begin{aligned} b_1 &= \sqrt{G}a_1 + \sqrt{G-1}a_2^\dagger, \\ b_2 &= \sqrt{G-1}a_1^\dagger + \sqrt{G}a_2, \end{aligned} \tag{22}$$

where

$$\sqrt{G} = \frac{\sqrt{N'M'} - \sqrt{NM}}{N' - N}, \tag{23}$$

with

$$M' - M = N' - N. \tag{24}$$

For obvious reasons, we call this transformation a 'phase-conjugated input amplification' (PCIA).

(iii) Distribute the output mode $b_1$ into $M$ clones $\{c_l'\}$ $(l = 0 \dots M-1)$ with a $M$-mode DFT:

$$c_l' = \frac{1}{\sqrt{M}}(b_1 + e^{i\pi kl/M} v_k), \tag{25}$$

where $\{v_k\}$ $(k = 1 \dots M-1)$ denote $M-1$ additional vacuum modes. It is readily verified that this procedure yields $M$ clones of $|\psi\rangle$. Interestingly, the amplitude $b_2$ of the other output of the PCIA has a mean value $\sqrt{M'}\psi^*$. Therefore, it can be used to produce $M'$ phase-conjugated clones (or anti-clones) of $|\psi\rangle$, $\{d_l'\}$ $(l = 0 \dots M'-1)$, using a $M'$-mode DFT:

$$d_l' = \frac{1}{\sqrt{M'}}(b_2 + e^{i\pi kl/M'} w_k) \tag{26}$$

where $\{w_k\}$ $(k = 1 \dots M'-1)$ denote $M'-1$ additional vacuum modes.

Some algebra shows that this procedure is optimal to produce $M$ clones, and that the additional $M'$ anti-clones

are also optimal[11]. Furthermore, since the step (ii) of our procedure is linear and phase-insensitive, the resulting PCI cloner is covariant with respect to translations and rotations of the state to be copied: all coherent states are copied equally well, and the cloning-induced noise is the same for all quadratures.

It is straightforward to calculate the noise of the clones and anti-clones:

$$(\Delta c_l')^2 = \frac{1}{2}\langle c_l' c_l'^{\dagger} + c_l'^{\dagger} c_l' \rangle - \langle c_l' \rangle \langle c_l' \rangle = \frac{1}{2} + \frac{G-1}{M},$$
$$(\Delta d_l')^2 = \frac{1}{2} + \frac{G-1}{M'}, \qquad (27)$$

As expected, the variance of the output clones exceeds $1/2$, reflecting that perfect cloning (anti-cloning) is indeed impossible. Instead, they suffer from a thermal noise with a mean number of photons given by $\langle n_{th} \rangle = (G-1)/M$. In other words, their $P$-function [21] is a Gaussian distribution

$$P(\xi, \xi^*) = \frac{1}{\pi \langle n_{th} \rangle} e^{-|\xi - \psi|^2 / \langle n_{th} \rangle}. \qquad (28)$$

rather than a Dirac distribution $P(\xi, \xi^*) = \delta^{(2)}(\xi - \psi)$.

### 4.1 Balanced phase-conjugated inputs cloner

Consider now the balanced case ($N = N'$, $M = M'$), for which simple expressions of the noise variance and the fidelity can be obtained. We then have $G = (M+N)^2/4MN$, giving

$$(\Delta c_l')^2 = (\Delta d_l')^2 = \frac{1}{2} + \frac{(M-N)^2}{4M^2N}. \qquad (29)$$

and

$$f_{N,M}^{N} = \frac{1}{1 + \langle n_{th} \rangle} = \frac{4M^2N}{4M^2N + (M-N)^2}. \qquad (30)$$

Let us compare these quantities to the variance and fidelity of a $2N \to M$ usual cloning machine, as obtained by replacing $N$ into $2N$ in Eqs. (8) and Eq.(9). Of course, in the trivial case where $M = 2N$, standard cloning can be achieved perfectly, while the balanced PCI cloner yields an additional variance $\langle n_{th} \rangle = 1/(16N)$. However, whenever $M \geq 2N+1$, the $\binom{N}{N} \to M$ PCI cloner outperforms the standard $2N \to M$ cloning machine. Also, comparatively more anti-clones with a higher fidelity are produced with the PCI cloner. Indeed, a standard $2N \to M$ cloning machine produces $M - 2N$ anti-clones of fidelity $2N/2N+1$, which is actually the fidelity of an optimal measurement of $2N$ replicas of $|\psi\rangle$, whereas a PCI cloner produces $M$ anti-clones with a higher fidelity, as given by Eq. (30). In particular, for $M \to \infty$, we see from Eq. (29) that the additional noise induced by a PCI cloner is $1/4N$, that is, *one half* of the noise induced by a standard $2N \to \infty$ cloner (i. e., $1/2N$). In this case, the output of the PCIA can be considered as classical and the underlying process appears to be equivalent to a measurement. This reflects that more classical information can be encoded in $N$ pairs of phase-conjugated replicas of a coherent state rather than in $2N$ identical replicas, a result which was proven for $N = 1$ in [9]. More generally, in the unbalanced case ($N \neq N'$), it is readily checked, using Eq.(23), that the optimal measurement results in a noise that is equal to that obtained by measuring $(\sqrt{N} + \sqrt{N'})^2$ identical replicas of the input, in the absence of phase-conjugated inputs.

### 4.2 Unbalanced phase-conjugated inputs cloner

As we have just shown, the balanced PCI cloner results in better cloning fidelities than a standard cloner. More generally, we may ask the following question: in order to produce $M$ clones of a coherent state $|\psi\rangle$ from a fixed total number $n$ of input modes, $N$ of which being in the coherent state $|\psi\rangle$ and $N'$ of which being in the phase-conjugated state $|\psi^*\rangle$, what is the phase-conjugate fraction $a = N'/n$ that minimizes the error variances of the clones?

From Eq. (22), we see that for fixed values of the total number of input replicas $n$ and number of output clones $M$, the gain $G$ (and thus the noise of the clones $\langle n_{th} \rangle$) only depends on $a$ and varies as

$$G(a) = \left( \frac{\sqrt{a}\sqrt{\frac{M}{n} + (2a-1)} - \sqrt{\frac{M}{n}}\sqrt{1-a}}{2a-1} \right)^2 \qquad (31)$$

In Fig. 3, the value of $\sqrt{\langle n_{th} \rangle}$ is plotted as a function of $a$ for $n = 8$ and different values of $M \geq n$. In the trivial case where $M = n = 8$, the minimum additional variance is of course zero, and is obtained for $a = 0$. The cloning transformation is then just the identity. However, when $M \geq n+1$, using phase-conjugated input modes yields lower variances than standard cloning if $a$ is correctly chosen (the lowest variance is then always attained for $a \neq 0$). Remarkably, the value of $a$ achieving the minimum variance is not equal to $1/2$ for finite $M$, that is the optimal input partition contains more replicas than anti-replicas. In the limit of large $M$, however, the number of anti-replicas achieving the lowest variances tends to $n/2$, and the curve $G(a)$ tends to a symmetric curve around $a = 1/2$. This behavior was expected, since $M = \infty$ corresponds to a measurement [17,10] and we expect that measuring the value of $\psi$ from $N$ replicas of $|\psi\rangle$ and $N'$ replicas of $|\psi^*\rangle$ is equivalent to a cloning transformation starting from $N'$ replicas of $|\psi\rangle$ and $N$ replicas of $|\psi^*\rangle$. So, we conclude that the optimal measurement is achieved with balanced inputs ($N = N'$), as previously mentioned. Finally, in the case where $a = 1$, the transformation consists in producing $M$ clones of $|\psi\rangle$ from $n$ replicas of $|\psi^*\rangle$. This is just phase-conjugation, for which we know that the best strategy is to perform a measurement [9]. The additional variance is therefore given by $1/n$, which does not depend on $M$. This explains why the curves converge all to the same point at $a = 1$.

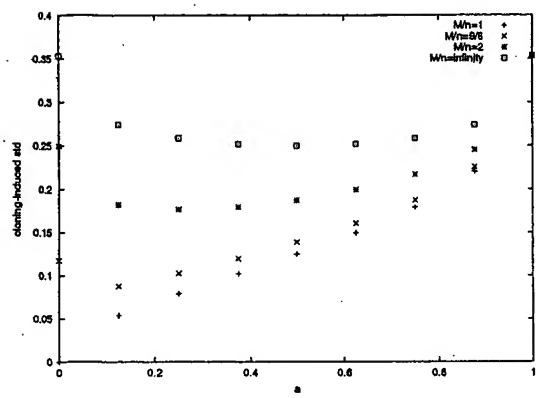


**Fig. 3.** Cloning-induced noise standard deviation $\sqrt{\langle n_{th}\rangle}$ as a function of the phase-conjugate fraction $a = N'/n$, for $n = 8$ and several values of $M/n$.

## 5 Conclusions

In summary, we have studied continuous-variable cloning machines, which produce several copies from one or more replicas of an arbitrary coherent state. We have derived the optimal fidelity of such cloners, as well as the actual cloning transformations and the potential methods to implement them. We have then proposed a quantum key distribution protocol relying on continuous variables, and shown how to apply reconcilation and privacy amplification to the generated continuous key elements. We have investigated the balance between the information gained by the eavesdropper and that received by the authorized receiver, using cloning as an optimal individual eavesdropping strategy. Finally, we have analyzed a new class of continuous-variable cloning machines, which admit phase-conjugated inputs in addition to the normal inputs. By exploiting the antiunitarity of phase-conjugation, these new cloners can beat the standard cloners in some cases. There is in general some non-zero optimal phase-conjugate input fraction in order to maximize the cloning fidelity. As a conclusion, it should be emphasized that these phase-conjugated inputs cloners do not extend on a qubit-based concept, in contrast with all previously developed information-theoretic processes for continuous quantum variables. Such a qubit cloner, admitting additional flipped qubits as inputs, has yet to be found.

N. J. C. is funded in part by the project EQUIP under the IST-FET-QJPC European programme. S. I. acknowledges support from the Belgian FRIA foundation. G. V. A. acknowledges support from the *Communauté Française de Belgique* under an *Action de Recherche Concertée*.

## A Density Matrices of Encoding Rules

In this Appendix, we would like to give further details regarding the protocol defined in section 3. In particular, we will prove the equality of the density matrices $\rho_x$ and $\rho_p$ corresponding to Alice's two encoding rules provided that eq. (13) is verified.

Define the Gaussian states $|\psi_x(r,\sigma_x)\rangle$ such that $\langle x\rangle = r$, $\langle p\rangle = 0$, $\Delta x^2 = \sigma_x^2$ and $\Delta p^2 = 1/4\sigma_x^2$. Similarly, let $|\psi_p(r,\sigma_p)\rangle$ be such that $\langle x\rangle = 0$, $\langle p\rangle = r$, $\Delta x^2 = 1/4\sigma_p^2$ and $\Delta p^2 = \sigma_p^2$. With the eigenstates $|x\rangle$ of $x$, our states have the following scalar products:

$$\langle x|\psi_x(r,\sigma_x)\rangle = \frac{1}{\sqrt{\sigma_x\sqrt[4]{2\pi}}} e^{-(x-r)^2/4\sigma_x^2} \tag{32}$$

$$\langle x|\psi_p(r,\sigma_p)\rangle = \frac{\sqrt{2\sigma_p}}{\sqrt[4]{2\pi}} e^{-\sigma_p^2 x^2} e^{irx} \tag{33}$$

The density matrices $\rho_x$ and $\rho_p$ are defined as:

$$\rho_x = \int_{-\infty}^{+\infty} dr \frac{e^{-r^2/2\Sigma_x^2}}{\Sigma_x\sqrt{2\pi}} |\psi_x(r,\sigma_x)\rangle\langle\psi_x(r,\sigma_x)| \tag{34}$$

and

$$\rho_p = \int_{-\infty}^{+\infty} dr \frac{e^{-r^2/2\Sigma_p^2}}{\Sigma_p\sqrt{2\pi}} |\psi_p(r,\sigma_p)\rangle\langle\psi_p(r,\sigma_p)| \tag{35}$$

Let us now calculate $\langle x|\rho_x|x'\rangle$ and $\langle x|\rho_p|x'\rangle$ in order to show that $\rho_x = \rho_p$.

$$\langle x|\rho_x|x'\rangle = \int_{-\infty}^{+\infty} dr \frac{e^{-r^2/2\Sigma_x^2 - (x-r)^2/4\sigma_x^2 - (x'-r)^2/4\sigma_x^2}}{\sigma_x\Sigma_x 2\pi} \tag{36}$$

The exponent of $e$ in the above equation can be rewritten as

$$-\frac{(r-\frac{\Sigma_x^2(x+x')}{2(\sigma_x^2+\Sigma_x^2)})^2}{2\Sigma_x^2\sigma_x^2/(\sigma_x^2+\Sigma_x^2)} - \frac{x^2+x'^2}{4(\sigma_x^2+\Sigma_x^2)} - \frac{\Sigma_x^2(x-x')^2}{8\sigma_x^2(\sigma_x^2+\Sigma_x^2)}. \tag{37}$$

After integration, this yields

$$\langle x|\rho_x|x'\rangle = \frac{e^{-\frac{x^2+x'^2}{4(\sigma_x^2+\Sigma_x^2)}} e^{-\frac{\Sigma_x^2(x-x')^2}{8\sigma_x^2(\sigma_x^2+\Sigma_x^2)}}}{\sqrt{2\pi}\sqrt{\sigma_x^2+\Sigma_x^2}}. \tag{38}$$

For $\rho_p$, we have

$$\begin{aligned}\langle x|\rho_p|x'\rangle &= \int_{-\infty}^{+\infty} dr \frac{2\sigma_p}{2\pi\Sigma_p} e^{-r^2/2\Sigma_p^2} \\ &\quad \times e^{ir(x'-x)} e^{-\sigma_p^2(x^2+x'^2)} \\ &= \frac{2\sigma_p}{\sqrt{2\pi}} e^{-\sigma_p^2(x^2+x'^2)} e^{-\frac{\Sigma_p^2}{2}(x-x')^2}.\end{aligned} \tag{39}$$

Taking (13) into account, we have $\langle x|\rho_x|x'\rangle = \langle x|\rho_p|x'\rangle$ for all $x$, $x'$. Therefore, $\rho_x = \rho_p$.

## References

1. E. Arthurs and J. L. Kelly, Jr, Bell Syst. Tech. J. 44 (1965), 725.

2. C. H. Bennett and G. Brassard, *Public-key distribution and coin tossing*, Proceedings of the IEEE International Conference on Computers, Systems, and Signal Processing, Bangalore, India (New York), IEEE, 1984, pp. 175–179.
3. C. H. Bennett, G. Brassard, C. Crépau, and U. M. Maurer, *Generalized privacy amplification*, IEEE Trans. on Inform. Theory **41** (1995), no. 6, 1915–1923.
4. C. H. Bennett, G. Brassard, and J.-M. Robert, *Privacy amplification by public discussion*, SIAM Journal on Computing **17** (1988), no. 2, 210–229.
5. G. Brassard and L. Salvail, *Secret-key reconciliation by public discussion*, Advances in Cryptology – Eurocrypt'93 (New York) (T. Helleseth, ed.), Lecture Notes in Computer Science, Springer-Verlag, 1993, pp. 411–423.
6. S. L. Braunstein, N. J. Cerf, S. Iblisdir, P. van Loock, and S. Massar, *Optimal cloning of coherent states with a linear amplifier and beam splitters*, Phys. Rev. Lett. **86** (2001), no. 21, 4438–4941.
7. S. L. Braunstein and H. J. Kimble, *Teleportation of continuous quantum variables*, Phys. Rev. Lett. **80** (1998), 869.
8. C. M. Caves, *Quantum limits on noise in linear amplifiers*, Phys. Rev. D **26** (1982), no. 8, 1817–1839.
9. N. Cerf and S. Iblisdir, *Phase conjugation of continuous quantum variables*, e-print quant-ph/0012020, to appear in Phys. Rev. A.
10. N. J. Cerf and S. Iblisdir, *Optimal n-to-m cloning of conjugate quantum variables*, Phys. Rev. A **62** (2000), 040301.
11. ———, *Phase-conjugated input quantum cloning machines*, (2001), e-print quant-ph/0102077.
12. N. J. Cerf, A. Ipe, and X. Rottenberg, *Cloning of continuous quantum variables*, Phys. Rev. Lett. **85** (2000), no. 8, 1754–1757.
13. N. J. Cerf, M. Lévy, and G. Van Assche, *Quantum distribution of gaussian keys using squeezed states*, Phys. Rev. A **63** (2001), 052311.
14. K. Chen, *Reconciliation by public discussion: Throughput and residue error rate*, unpublished, 2001.
15. T. M. Cover and J. A. Thomas, *Elements of information theory*, Wiley & Sons, New York, 1991.
16. J. Fiurasek, *Optical implementation of continuous-variable quantum cloning machines*, Phys. Rev. Lett. **86** (2001), no. 21, 4942–4945.
17. N. Gisin and S. Massar, *Optimal quantum cloning machines*, Phys. Rev. Lett. **79** (1997), 2153.
18. N. Gisin and S. Popescu, Phys. Rev. Lett. **83** (1999), 432.
19. U. M. Maurer, *Secret key agreement by public discussion from common information*, IEEE Trans. Inform. Theory **39** (1993), no. 3, 733–742.
20. T. C. Ralph, *Security of continuous-variable quantum cryptography*, Phys. Rev. A **62** (2000), 062306.
21. M. O. Scully and M. S. Zubairy, *Quantum optics*, Cambridge University Press, Cambridge, 1997.
22. T. Sugimoto and K. Yamazaki, *A study on secret key reconciliation protocol cascade*, IEICE Trans. Fundamentals **E83-A** (2000), no. 10, 1987–1991.
23. L. Vaidman, *Teleportation of quantum states*, Phys. Rev. A **49** (1994), 1473.
24. G. Van Assche, J. Cardinal, and N. J. Cerf, *Reconciliation of a quantum-distributed gaussian key*, submitted for publication, 2001.
25. K. Yamazaki and T. Sugimoto, *On secret key reconciliation protocol*, Int. Symp. on Inf. Th. and Its App., 2000.

# Reconciliation of a Quantum-Distributed Gaussian Key

Gilles Van Assche, Jean Cardinal and Nicolas J. Cerf



*Abstract*— **Two parties, Alice and Bob, wish to distill a binary secret key out of a list of Gaussian variables that were distributed with the help of quantum cryptography. We present a novel construction that allows the legitimate parties to get equal strings out of correlated variables, using a classical channel, with as few leaked information as possible. This opens the way to securely correcting non-binary key elements. In particular, the construction is refined to the case of Gaussian-distributed variables as it applies directly to a quantum cryptography protocol developed recently.**

*Keywords*— **Cryptography, secret-key agreement, privacy amplification, quantum secret key distribution.**

## I. Introduction

With the advent of quantum cryptography, it is possible for two parties, Alice and Bob, to securely agree on secret information that shall later be used as a key to encrypt messages [1], [2], [3], [4]. The quantum channel, which Alice and Bob use to create a secret key, is not deemed to be perfect. Noise will necessarily make Alice's and Bob's values different. Furthermore, laws of quantum mechanics imply that eavesdropping also causes extra discrepancies. To overcome this, one can correct errors by using some interactive *reconciliation* protocol, carried out over a public authenticated channel [5], [6]. Yet, this does not entirely solve the problem as an eavesdropper can gain some information about the key while Alice and Bob exchange their public reconciliation messages. Fortunately, such gained information can then be wiped out, at the cost of a reduction in the secret key length, using another protocol called *privacy amplification* [7], [8]. This paper focuses on a specific extention of reconciliation protocols in the case of Gaussian-distributed key elements.

Current reconciliation and privacy amplification protocols are aimed at correcting and distillating strings of bits. Their purpose is to complement existing quantum key distribution schemes, which enable Alice and Bob to share a common random string of elements from a binary alphabet. However, a recently proposed crypto-scheme shows how to distribute a secret key composed of Gaussian-distributed elements instead of bits [9]. Not surprisingly, the existing reconciliation and privacy amplification protocols are not well suited for this kind of application. There is thus a need for extending such protocols to be able to process continuous keys.

The core material presented in this paper assumes that Alice and Bob initially share some correlated list of continuous values. Our strategy is as follows. First, Alice and Bob exchange public reconciliation messages over an authenticated channel. Our extended protocol is designed to turn Alice's and Bob's values into identical strings of bits. Notice that the input is a list of continuous variables, whereas its output has a discrete nature – our reconciliation protocol mixes error correction and continuous-to-discrete conversion purposes. Then, Alice and Bob perform privacy amplification. Since both the input and the output of the privacy amplification step are discrete, existing protocols can be used without any change.

The outline of this paper is as follows. First, we give an overview of the Gaussian key quantum distribution scheme [9]. Then, we discuss our choices in terms of continuous vs discrete components at various stages of the present protocol. In the subsequent section, we introduce the concept of *sliced error correction* as a framework on which our reconciliation protocol is based. We then analyze this protocol in terms of leaked information. Finally, we display specific results when the protocol is used to extract secret information out of correlated Gaussian values.

## II. Quantum Distribution of a Gaussian Key

Quantum cryptography—or, more precisely, quantum key distribution—is a technique that allows two remote parties to share secret random information (a secret key) that can be used for exchanging encrypted information [1], [2], [3], [4]. The security of such a process fundamentally relies on the fact that the measurement of incompatible variables inevitably affects the state of a quantum system.

The basic idea is the following. A legitimate user (Alice) sends random key elements to another user (Bob) using either one of two sets of quantum carriers of information. Alice randomly chooses one of the two sets of carriers, encodes a random key element using this set, and sends it to Bob. On his side, Bob measures the received quantum state by guessing which set of carriers Alice chose. The sets of information carriers are designed in such a way that measuring the wrong set yields random uncorrelated results. Therefore, Bob will measure correctly only half of the key elements Alice sent him, not knowing which ones are wrong. After the process, Alice will reveal which set of carriers she chose for each key element, and Bob will be



G. Van Assche is with the École Polytechnique, CP 165, Université Libre de Bruxelles, 1050 Brussels, Belgium (e-mail: gvanassc@ulb.ac.be).

J. Cardinal is with the Faculté des Sciences, CP 212, Université Libre de Bruxelles, 1050 Brussels, Belgium (e-mail: jcardin@ulb.ac.be).

N. Cerf is with the Ecole Polytechnique. He is also with the Information and Computing Technologies Research Section, Jet Propulsion Laboratory, California Institute of Technology, Pasadena, CA 91109 (e-mail: ncerf@ulb.ac.be).

able to discard all the wrong measurements.

An eavesdropper (Eve) can of course intercept quantum carriers and try to measure them. However, like Bob, Eve does not know which set of carriers Alice chose for each key element. A measurement will yield irrelevant results about half of the time, and thereby disturb the sate of the carrier. Not knowing if she has a correct value, Eve can decide to retransmit or not a quantum carrier with the key element she obtained. Discarding the element is useless for Eve since this sample will not be used by Alice and Bob. However, if she does retransmit the state (even though it is wrong half of the time), Alice and Bob can detect her presence by an unusually high error rate between their key elements.

The quantum key distribution works because of the advantage Bob has over Eve of being able to talk to Alice over a classical authenticated channel. This allows the legitimate users to compare some key elements to detect eavesdropping, agree on a secret key using a reconciliation protocol, and apply privacy amplification techniques to reduce Eve's partial knowledge on the final key.

As an example, some quantum key distribution protocols use as carriers single photons whose polarization encodes the key element. In one set of carriers, a binary 0 is encoded as a vertical polarization of the emitted photon, whereas a binary 1 is sent with horizontal polarization. The other set of carriers uses 45-degree and 135-degree polarization. Of course, measuring a photon using the wrong set of polarization yields random uncorrelated results and disturbs the quantum carrier.

Unlike the above example, which is based on binary information, the protocol proposed in [9] uses two sets of carriers that behave essentially like Gaussian channels. One exploits a pair of canonically conjugate continuous variables such as the two quadratures $X_1$ and $X_2$ of the amplitude of a mode of the electromagnetic field [10], which behave just like position $x$ and momentum $p$. The uncertainty relation $\Delta X_1 \Delta X_2 \geq 1/4$ then states that it is impossible to measure with full accuracy *both* quadratures of a single mode, $X_1$ and $X_2$. Alice exploits this property by encoding the key elements (random Gaussian samples) as a quadrature squeezed state either in $X_1$ or in $X_2$, in such a way that an eavesdropper ignoring which of these two sets is used cannot acquire information without disturbing the state.

Simply stated, such states behave like 2D Gaussian distributions in the $X_1, X_2$ plane. In set 1, the carriers are shaped as $N(x, \sigma_1) \times N(0, 1/4\sigma_1)$ in the $X_1, X_2$ plane, where $x$ is the key element Alice wishes to send, and $x$ is itself distributed as a Gaussian: $x \sim N(0, \Sigma_1)$. In set 2, the carriers are similar but $X_1$ and $X_2$ are interchanged, $N(0, 1/4\sigma_2) \times N(x, \sigma_2)$.

More formally, creating a state from set 1 requires Alice to prepare a squeezed vacuum state such that the fluctuations of $X_1$ are squeezed ($\Delta X_1^2 = \sigma_1^2 < 1/4$), and to apply a displacement of $X_1$ by an amount equal to the key element $x$ such that $\langle X_1 \rangle = x$. The quantity $\sigma_1^2$ refers here to the intrinsic variance of $X_1$. Conversely, in set 2, Alice sends a squeezed state in $X_2$ ($\Delta X_2^2 = \sigma_2^2 < 1/4$), whose displacement encodes the Gaussian key $\langle X_2 \rangle = x$. Again, $\langle X_2 \rangle$ has a zero mean and a variance $\Sigma_2^2$.

The intrinsic fluctuations of the transmitted states are such that Bob's measurement will not give him the exact value $x$ chosen by Alice, even in absence of eavesdropping and with a perfect measurement apparatus. If set $i = 1, 2$ is used, the outcomes of $X_i$ measurements (that can be obtained by homodyne detection) are distributed as a Gaussian of variance $\Sigma_i^2 + \sigma_i^2$, since each squeezed state gives an extra contribution of $\sigma_i^2$ to the key variance $\Sigma_i^2$. Therefore, we can model the transmission as a Gaussian channel with a signal-to-noise ratio (SNR) equal to $\Sigma_i^2/\sigma_i^2$.

An important requirement of the protocol is to make impossible for Eve to be able to infer which set Alice used. For this, measuring the correct or the wrong set must yield statistically indistinguishable results. If, in contrast, Eve was able to detect (even not perfectly) that she measured the wrong set, then she could fake an attenuation by discarding wrong key elements and retransmitting the correct ones. This requirement can be expressed [9] as $1 + \Sigma_1^2/\sigma_1^2 = 1 + \Sigma_2^2/\sigma_2^2$. This means that the SNR is the same for both set 1 and set 2, and the information rate is $I = \frac{1}{2}\log(1 + \Sigma_1^2/\sigma_1^2)$. We proved in [9] that, in case of eavesdropping, the optimal strategy on individual carriers (using cloning machines) will give Eve an expected information rate equal to the expected information rate Bob will lose on his side. The sum of Bob's and Eve's information rate is thereby a constant: $I_B + I_E = I$.

The requirement of equal distributions is strong in the sense that Alice must strictly respect $x \sim N(0, \Sigma_{1 \text{ or } 2})$. She may not choose a mapping $x(k)$ from some discrete alphabet to $\mathbb{R}$ that satisfies $\Delta x = \Sigma_{1 \text{ or } 2}$. The resulting distribution would not be Gaussian, and Eve would be able to infer whether she measured the correct set of carriers. It is therfore essential for Alice and Bob to exchange a fully continuous raw key through the quantum channel. Extracting discrete information, which is the scope of this paper, can only appear in a later stage, namely during reconciliation and privacy amplification.

## III. Discrete vs Continuous Variables

It is shown in [9] that working with continuous quantum states as carriers of information naturally leads to expressing information in a continuous form as well. It was thus tempting to generalize the whole key distribution process with continuous variables, including reconciliation and privacy amplification, to get a continuous secret key. However, encrypting a message with a continuous Vernam-like cipher would probably suffer from incompatibilities or inefficiencies with regard to current technologies and applications. Furthermore, it is much more convenient to rely on the equality of Alice's and Bob's values in the discrete case, rather than dealing with bounded errors on real numbers.

Because modern communication technologies are designed to carry zeroes and ones, we decided to transform the sifted Gaussian key values into a discrete key. With the choice of a discrete final key as starting point, we de-

duce that, at the very end of the privacy amplification step, the two communicating parties must get discrete variables. Yet, we have to show why we chose discrete reconciliation messages and a discrete output after reconciliation.

Because of the finiteness of the (public authenticated) reconciliation channel capacity, exchanged reconciliation messages are either discrete or noisy continuous values. The latter case introduces additional noise into the protocol. This quite contradicts our requirements, as we would precisely expect from an error correction protocol to reduce differences between Alice's and Bob's raw key elements. Furthermore, a noisy continuous reconciliation message would not be able to benefit from the authentication feature of the reconciliation channel. Hence, discrete reconciliation messages are preferred.

The choice of a discrete final key also induces discrete effects in the protocols, which makes natural the choice of a continuous-to-discrete conversion during reconciliation. Call $x$ the original Gaussian value that Alice sent, $x'$ the Gaussian value as received by Bob and $k$ the resulting discrete key element. The process of reconciliation and privacy amplification can be summarized as functions $k = f_A(x, C_1, C_2, \ldots, C_m)$ and $k = f_B(x', C_1, C_2, \ldots, C_m)$, where the $(C_i)$ indicate the exchanged messages. As both $k$ and $(C_i)$ are to be taken in some finite set, these two functions define each a finite family of subsets of values that give the same result: $S_{kC_1 \ldots C_m} = \{x : f_A(x, C_1, \ldots, C_m) = k\}$ and $S'_{kC_1 \ldots C_m} = \{x' : f_B(x', C_1, \ldots, C_m) = k\}$. The identification of the subset in which $x$ (or $x'$) lies is the only data of interest – and can be expressed using discrete variables – whereas the value within that subset does not affect the result and can merely be considered as noise.

For all the reasons stated above, our extended reconciliation protocol mainly consists of exchanging discrete information between the two communicating parties so that they can deduce the same discrete representation from the real values they share.

## IV. Sliced Error Correction

Sliced error correction is a generic reconciliation protocol that corrects strings of non-binary elements. It gives, with high probability, two communicating parties (Alice and Bob) equal binary digits from a list of correlated values. Just like other error correction protocols, it makes use of a public authenticated channel. The underlying idea is to convert Alice's and Bob's values into strings of bits, apply a bitwise correction algorithm as a primitive (e.g., Cascade [5]) and take advantage of all available information to minimize the number of exchanged reconciliation messages.

The key feature of this generic protocol is that it enables Alice and Bob to correct errors that are not modeled using a binary symmetric channel. Instead, by carefully supplying slice and slice estimator functions described below, one can deal with errors whose severity is intermediate between perfect equality (a correct bit) and full error (a flipped bit). An example for an intermediately severe error would be a 5 becoming either a 4 or a 6 in a decimal alphabet. And of course, an error on a Gaussian key element can have a degree of severity depending on the difference between the original and the noisy value.

Let us now assume that Alice and Bob both have a list of values, namely $x_1 \ldots x_l$ for Alice and $x'_1 \ldots x'_l$ for Bob. Any distribution $p(x, x')$ is acceptable, as long as $I(X; X') > 0$ (where $X$ is the random variable associated to Alice's key element and $X'$ to Bob's). To be general, it is possible for Alice and Bob to process multi-dimensional key values rather than individual ones. To this end, Alice and Bob may agree on a number $d$ of dimensions and group their values into $d$-dimensional vectors. In the subsequent paragraphs, $x$ denotes one of Alice's (possibly vectorial) values while $x'$ denotes one of Bob's. Alice's (resp. Bob's) raw key space is defined as the set of possible $d$-dimensional values $x$ (resp. $x'$). In the case of Gaussian-distributed values the raw key space is $\mathbb{R}^d$.

The first ingredients we need to define are the slices. A slice $S(x)$ is a function from Alice's raw key space to the set $\{0, 1\}$. A set of slices $S_1(x) \ldots S_m(x)$ is chosen so that the vector $\mathbf{S}(x) = (S_1(x), \ldots S_m(x))$ implicitly defines a mapping from Alice's raw key space to a discrete alphabet of size $2^m$ (or less if some combinations are left out). Without describing the entire protocol yet, let us say that Alice will convert her values into binary digits using the defined slices.

On his side, Bob has a set of slice estimators $\tilde{S}_1(x')$, $\tilde{S}_2(x', S_1(x)) \ldots \tilde{S}_m(x', S_1(x), \ldots, S_{m-1}(x))$. Each slice estimator defines a mapping from Bob's raw key space and Alice's slices of lower indexes to the set $\{0, 1\}$. As explained below, an estimator $\tilde{S}_i(x', S_1(x), \ldots S_{i-1}(x))$ will be used by Bob as his best guess on the value of $S_i(x)$ given the (already corrected, therefore known) previous binary values $S_1(x) \ldots S_{i-1}(x)$.

The construction of slices $S_i(x)$ depends on the nature of the raw key space. These aspects are covered in a following section, where we apply the sliced error correction to our Gaussian key elements.

Let us now describe our generic protocol.

- From her list of $l$ (possibly vectorial) values $x_1 \ldots x_l$, Alice creates $m$ strings of bits using the defined slices $(S_1(x_1), \ldots, S_1(x_l)) \ldots (S_m(x_1), \ldots, S_m(x_l))$.
- Bob constructs a string of bits from his values $x'_1 \ldots x'_l$ using his slice estimator $\tilde{S}_1$: $(\tilde{S}_1(x'_1), \ldots, \tilde{S}_1(x'_l))$.
- Alice and Bob make use of a chosen bitwise correction protocol (e.g., Cascade [5]) so that Bob aligns his bit values on Alice's.
- For each subsequent slice $i$, $2 \leq i \leq m$, Bob constructs a new string of bits using his slice estimator $\tilde{S}_i$ applied to his values $x'_1 \ldots x'_l$ and taking into account the correct bit values of the previous slices $S_1(x_1), \ldots, S_2(x_1), \ldots, S_{i-1}(x_l)$. Again, Alice and Bob align their bit values using the chosen bitwise correction protocol.
- For Alice, the resulting bitstring is simply the concatenation of the $m \times l$ slice values $(S_1(x_1), \ldots, S_2(x_1), \ldots, S_m(x_l))$ as in step 1. For Bob, the shared bitstring is the same as Alice's, obtained from the previous steps.

### A. Underlying Idea

The algorithms proposed in [11], [5], [12], [13], [14] make use of parity check bits to perform a dichotomy, find an error and correct it. The nice thing about binary digits is the obvious fact that when a wrong bit is found, flipping it is correcting it. The same is not true for other alphabets. For an alphabet $\mathcal{A}$ of size $n$, it may be tempting to find errors by using mod $n$ parity checks, the most direct generalization of its binary counterpart. This would require that Alice sends $\log n$ bits for each parity check, reducing the secrecy by the same amount. However, the error may be less severe than a completely wrong symbol: A symbol $a$ may simply be changed to a neighboring symbol $b$ as for instance the joint probability $p(a,b)$ may contain significant mass only when $a-1 \leq b \leq a+1$. The exchanged information needed to correct an error should be of order $H(A|B)$, the entropy of Alice's symbol knowing that of Bob. Rather than disclosing $\log n$ bits for every parity check, we need to be finer-grained. By using slices, an error that was benign enough to be corrected in one slice, will not induce errors in subsequent slices. We thus avoid disclosing excessive information because of that particular error in subsequent slices.

### B. Sliced Error Correction as a Universal Tool

A natural target goal of sliced error correction is to correct errors by disclosing as few information as possible on the key shared by Alice and Bob. However, one does not expect a protocol running with strings of finite length and using finite computing resources to achieve the Shannon bound exactly. Yet, we show in the subsequent paragraphs that sliced error correction is indeed asymptotically efficient, that is, it reaches the Shannon bound in terms of leaked information when the number of dimensions $d$ (i.e., the input alphabet size) goes to infinity. This result makes use of the asymptotic equipartition property [15] and is pretty much in line with similar information theory results.

For simplicity, and without loss of generality, we now consider discrete raw key spaces. The outline of the proof is as follows. Assume that the number of dimensions $d$ is very large. Stated otherwise, Alice and Bob create a string whose elements are vectors of raw key values with high dimensionality. The number of slices $m$ needed to encode $X^d$ grows about linearly with $d$, as $m \approx dH(X)$. Conversely, the length $l$ of the string does not matter, and can remain finite. By the asymptotic equipartition property (AEP), one can only consider the typical values of $d$-dimensional sequences $x^d$, which are almost uniformly distributed – the density of non-typical cases vanishes. There are about $2^{dH(X)}$ such typical values. When Bob receives a value $x'^d$, he must guess among about $2^{dH(X|X')}$ possible values from Alice in the set $\{X^d|x'^d\}$. This results from the AEP applied to the jointly typical values $(X, X')$. Bringing the knowledge of a slice $S_i(X)$ to Bob cuts approximately in half the number of remaining possibilities. Hence, after revealing about $dH(X|X')$ slices, Bob should know Alice's value with almost certainty.

*Lemma 1:* Let $Z = (Z_1 \dots Z_N)$ a list of $N$ random bit strings of arbitrary length, independently and uniformly distributed. The probability that a given string from the list, say $Z_j$, can be uniquely identified in $Z$ by specifying only the first $r$ bits is $(1-2^{-r})^{N-1}$.

*Proof:* The probability of $Z_j$ being uniquely identifiable from its first $r$ bits is the probability that no string among the $N-1$ other ones in the list starts with the same pattern. Hence, this probability is $(1-2^{-r})^{N-1}$. ∎

*Lemma 2:* Let $X$ and $X'$ be random variables distributed as $p(x,x')$ and $A_\epsilon^{(d)}(X,X')$ be the set of jointly typical sequences $(X^d, X'^d)$ of length $d$ [15]. Let $x'^d$ be some fixed sequence in the set $A_\epsilon^{(d)}(X')$ of typical sequences in the marginal distribution of $X'$. Define $A_\epsilon^{(d)}(X|x'^d) = \{x^d : (x^d, x'^d) \in A_\epsilon^{(d)}(X,X')\}$. Then, $|A_\epsilon^{(d)}(X|x'^d)| \leq 2^{d(H(X|X')+2\epsilon)}$.

*Proof:*

$$
\begin{aligned}
1 &= \sum_{x^d} p(x^d|x'^d) \\
&\geq \sum_{x^d \in A_\epsilon^{(d)}(X|x'^d)} p(x^d|x'^d) \\
&= \frac{1}{p(x'^d)} \sum_{x^d \in A_\epsilon^{(d)}(X|x'^d)} p(x^d, x'^d) \\
&\geq \frac{1}{2^{-d(H(X')-\epsilon)}} |A_\epsilon^{(d)}(X|x'^d)| 2^{-d(H(X,X')+\epsilon)}
\end{aligned}
$$

Hence, $|A_\epsilon^{(d)}(X|x'^d)| \leq 2^{d(H(X|X')+2\epsilon)}$. ∎

*Lemma 3:* Suppose that Alice sends a random sequence $X^d$ of length $d$ and Bob receives a correlated sequence $X'^d$, which are jointly typical $(x^d, x'^d) \in A_\epsilon^{(d)}(X,X')$. Let $m = \lceil dH(X) + \epsilon \rceil$. Let the $m$ slices $\mathbf{S}(X)$ be chosen randomly using a uniform distribution independently for all input values. Let $r = \lceil dH(X|X') + 2\epsilon - \log\epsilon + 1 \rceil$. Then $\forall \epsilon > 0$ $\exists D$ such that $\forall d > D$, Bob can recover $X^d$ given $X'^d$ and $S_1(X) \dots S_r(X)$ with a probability of identification failure $P_i < \epsilon$.

*Proof:* Alice and Bob agree on a random $\mathbf{S}(X)$. Assume that they draw sequences $x^d$ and $x'^d$ that fulfill the typicality conditions above. For the value received, Bob prepares a list of guesses: $\{x^d \in A_\epsilon^{(d)}(X|x'^d)\}$. From Lemma 2, this list contains no more than $N \leq 2^{dH(X|X')+2\epsilon}$ elements. Alice reveals $r$ slice values, with $r \geq dH(X|X') + 2\epsilon - \log\epsilon + 1$. From Lemma 1, the probability that Bob is unable to correctly identify the correct string is bounded as $P_i \leq 1-(1-2^{-dH(X|X')-2\epsilon+\log\epsilon-1})^{2^{dH(X|X')+2\epsilon}-1}$. This quantity goes to $1-e^{-\epsilon/2}$ when $d \to \infty$, and $1-e^{-\epsilon/2} < \epsilon/2$ for $\epsilon > 0$. Therefore, $\exists D$ such that $P_i < \epsilon$ for all $d > D$. ∎

The above discussion determines the underlying error correction protocol. Alice and Bob use a trivial all-or-nothing correction protocol: Alice entirely reveals slices $S_i(X)$ for $1 \leq i \leq r$ and does not reveal anything for other slices. (In practice, however, $d$ is finite and the all-or-nothing correction is not appropriate: One must thus make use of a more elaborate binary correction protocol.)

*Theorem 1:* Sliced error correction, together with an all-or-nothing correction protocol, leaks an amount of information that is asymptotically close to $H(X|X')$ as $d \to \infty$, with a probability of failure that can be made as small as desired.

*Proof:* Lemma 3 states that $\lim_{d\to\infty} \frac{r}{dH(X|X')} = 1$. Regarding the probability of failure, there are two sources of possible failure: the failure of identification $P_i$ and the fact that $(x^d, x'^d) \notin A_\epsilon^{(d)}(X, X')$. From Lemma 3 and from the AEP, both probabilities are upper bounded by $\epsilon$. Therefore, the total failure probability behaves as $O(\epsilon)$ when $\epsilon \to 0$. ■

## V. Analysis of Sliced Error Correction

The net amount of secret information that Alice and Bob can rely on after correction and privacy amplification is determined by both the entropy of the slices and the leaked information in the reconciliation messages. We now analyze these quantities and derive an explicit construction for slice estimators.

### A. Net Amount of Secret Information

The amount of information shared by Alice and Bob at the end of the reconciliation protocol is $H(\mathbf{S}(X))$. This is simply because Alice and Bob end up with identical binary values. This entropy can be made arbitrarily large simply by cutting the raw key space in an arbitrarily large number $m$ of slices. However, when $H(\mathbf{S}(X)) > I(X;X')$, not all slices are significant and further error correction is required, resulting in additional leaked information. A trade off must thus be found.

The error correction is based on a chosen binary error correction protocol. In [5], the optimality criterion states, among other things, that the disclosed information $I_E$ should be comparable to $lH(A|B)$, where $l$ is the length of the string and where $H(A|B)$ is the per-symbol conditional entropy. In the special case of a binary symmetric channel with error probability $e$, it reads $H(A|B) = h(e)$, with $h(e) = -e\log e - (1-e)\log(1-e)$. For the algorithm Cascade [5], we can expect that $\lim_{k\to\infty} \frac{I_E}{kh(e)} = 1 + \xi$ for some small overhead factor $\xi$.

We will consider that running the binary correction protocol reveals a $H(S_i(X)|S_i(X', S_1(X), \ldots, S_{i-1}(X)))$-bit function of $\mathbf{S}(X)$. In the subsequent paragraphs, we drop the $\xi$ factor because our interest is mainly focused on the slicing construction rather than on the underlying primitive.

*Definition 1:* The total disclosed information $I_D = I(\mathbf{S}(X); M)$ is the expected information that an eavesdropper acquires about $\mathbf{S}(X)$ from the exchanged reconciliation messages, collectively denoted $M$.

*Proposition 1:* In case of one-way communication (Alice to Bob), the total disclosed information is lower bounded as $I_D \geq H(\mathbf{S}(X)|X')$.

*Proof:* $M(\mathbf{S}(X))$ depends only on Alice's slices and therefore, $H(M|\mathbf{S}(X)) = 0$. Using the messages $M$ and his own value $X'$, Bob can reconstruct $\mathbf{S}(X)$; hence $H(\mathbf{S}(X)|MX') = 0$. Therefore,

$$\begin{aligned} I_D - H(\mathbf{S}(X)|X') &= H(M) + H(X') - H(\mathbf{S}(X), X') \\ &\geq H(M, X') - H(\mathbf{S}(X), X') \\ &= H(\mathbf{S}(X), M, X') - H(\mathbf{S}(X), X') \geq 0. \end{aligned}$$

■

*Proposition 2:* For sliced error correction, the total disclosed information is upper bounded as

$$I_D \leq \sum_i H(S_i(X) \mid \tilde{S}_i(X', S_1(X), \ldots, S_{i-1}(X))). \quad (1)$$

*Proof:* Each use of the underlying binary correction protocol leaks $H(S_i(X)|S_i(X', S_1(X), \ldots, S_{i-1}(X)))$ bits of information about $\mathbf{S}(X)$. In the worst case, the leaked information is uniformly distributed and independent from slice to slice, and must thus be summed up. ■

One of the main results of [8] states that if Eve gains a $t$-bit eavesdropping function $V$ from a $n$-bit string shared by Alice and Bob, privacy amplification using a universal class of hash functions can give the legitimate parties a $r$-bit secret key $K$ (where $r = n - t - s$, with $0 \leq s < n - t$ a security parameter) through the use of the randomly chosen function $G$, such that Eve's expected information is upper bounded as $I(K; GV) \leq 2^{-s}/\ln 2$.

In our case, the $m \times l$ binary values generated by Alice's slices can in average be converted to a $lH(\mathbf{S}(X))$-bit string, thus $E[n] = lH(\mathbf{S}(X))$. On the other hand, Eve gets a $lI_D$-bit eavesdropping function about the key, giving $E[t] = lI_D$. Therefore, the expected number of bits Alice and Bob can distill per raw key element is equal to $H(\mathbf{S}(X)) - I_D - \frac{s}{l}$. For this reason, the design criteria of slices will be to maximize the expression $H(\mathbf{S}(X)) - I_D$.

### B. Information Leakage in Terms of Binary Error Rates

The amount of leaked information in each use of the underlying protocol can be expressed in an easier way than equation (1) by simply using $e_i$, the probability of error when correcting slice $i$.

*Proposition 3:* The total disclosed information is upper bounded as $I_D \leq I_\epsilon = \sum_i h(e_i)$.

*Proof:* For a binary alphabet, Fano's inequality [15] states that

$$H(S_i(X) \mid \tilde{S}_i(X', S_1(X), \ldots, S_{i-1}(X))) \leq h(e_i).$$

The conclusion follows from Prop. 2. ■

In order to give an explicit expression for $e_i$, we must first define subsets of Alice's and Bob's raw key spaces.

*Definition 2:* Let us define a subset of the joint domain $(X, X')$:

$$\mathcal{D}^{ab}_{S_i\tilde{S}_i} = \{(x, x') \ : \ S_i(x) = a \ \wedge \ \tilde{S}_i(x', x) = b\},$$

where $\tilde{S}_i(x', x)$ summarizes $\tilde{S}_i(x', S_1(x), \ldots, S_{i-1}(x))$. With such a set, we define the associated probability:

$$P^{ab}_{S_i\tilde{S}_i} = \int_{\mathcal{D}^{ab}_{S_i\tilde{S}_i}} p(x, x')dxdx'.$$

Other symbols, such as $\mathcal{D}^{\beta_1\beta_2 1}_{S_1S_2\tilde{S}_2}$ and the associated probability $P^{\beta_1\beta_2 1}_{S_1S_2\tilde{S}_2}$, are constructed using the same pattern.

The error probability in slice $i$ can then be expressed as the probability that Bob's slice estimator yields a result different from Alice's slice:

$$e_i = P^{01}_{S_i\tilde{S}_i} + P^{10}_{S_i\tilde{S}_i}.$$

### C. Maximum Likelihood Slice Estimators

We now give an explicit construction for slice estimators by minimizing the binary error rates. It turns out that this construction reduces to the maximum likelihood estimator.

Maximizing the global efficiency of the slice estimators is not a simple task because the efficiency of a slice estimator $\tilde{S}_i$ recursively depends on all previous estimators $\tilde{S}_{j<i}$. For this reason, our goal here is simply to minimize each $e_i$, of which $h(e_i)$ is an increasing function for $0 \leq e_i < \frac{1}{2}$, by acting only on $\tilde{S}_i$. This results in an explicit expression for $\tilde{S}_i(x', S_1(x), \ldots, S_{i-1}(x))$.

*Definition 3:* Subsets of Alice's raw key space are defined using the following pattern: $\mathcal{A}^{\beta_i}_{S_i} = \{x : S_i(x) = \beta_i\}$. The associated probability measure becomes a function of $x'$:

$$P^{\beta_1\ldots\beta_{i-1}a}_{S_1\ldots S_{i-1}S_i}(x') = \int_{\mathcal{A}^{\beta_1\ldots\beta_{i-1}a}_{S_1\ldots S_{i-1}S_i}} p(x, x')dx$$

*Definition 4:* Symmetrically, we define subsets of Bob's received values using the same kind of pattern. For instance, $\mathcal{B}^{\beta_1 b}_{S_1\tilde{S}_1}$ is defined as $\{x' : \tilde{S}_1(x', \beta_1) = b\}$.

*Lemma 4:* An individual probability $P^{ab}_{S_i\tilde{S}_i}$ can be expanded as a sum of smaller probabilities over all possible values $\beta_{j<i}$ of the previous slices:

$$P^{ab}_{S_i\tilde{S}_i} = \sum_{\beta_1\ldots i-1} P^{\beta_1\beta_2\ldots\beta_{i-1}ab}_{S_1S_2\ldots S_{i-1}S_i\tilde{S}_i} \quad (2)$$

*Lemma 5:* Each of these smaller terms can be expanded as

$$P^{\beta_1\ldots ab}_{S_1\ldots S_i\tilde{S}_i} = \int_{\mathcal{B}^{\beta_1\ldots\beta_{i-1}b}_{S_1\ldots S_{i-1}\tilde{S}_i}} P^{\beta_1\ldots a}_{S_1\ldots S_i}(x')dx'. \quad (3)$$

*Theorem 2:* A slice estimator $\tilde{S}_i$ minimizes $e_i$ if it has the form

$$\tilde{S}_i(x', \beta_1, \ldots) = \begin{cases} 0 & \text{if } P^{\beta_1\ldots 0}_{S_1\ldots S_i}(x') > P^{\beta_1\ldots 1}_{S_1\ldots S_i}(x'), \\ 1 & \text{otherwise,} \end{cases} \quad (4)$$

except for cases where the probabilities are equal or over some zero-measure set.

*Proof:* A slice estimator can make its decision to output a zero or a one as a function of the previously known slices. Therefore, it can be designed to do its best guess over a restricted set $\mathcal{A}^{\beta_1\ldots\beta_{i-1}}_{S_1\ldots S_{i-1}}$, independently of the others. To minimize $e_i = P^{01}_{S_i\tilde{S}_i} + P^{10}_{S_i\tilde{S}_i}$, one can thus take advantage of the independence of smaller terms in (2) and minimize them individually.

From equation (3), the terms $P^{\beta_1\ldots aa}_{S_1\ldots S_i\tilde{S}_i}$, for a correct guess, and $P^{\beta_1\ldots a\bar{a}}_{S_1\ldots S_i\tilde{S}_i}$, for a wrong guess, result from the integration of the same function over two different sets, namely $\mathcal{B}^{\beta_1\ldots\beta_{i-1}a}_{S_1\ldots S_{i-1}\tilde{S}_i}$ and $\mathcal{B}^{\beta_1\ldots\beta_{i-1}\bar{a}}_{S_1\ldots S_{i-1}\tilde{S}_i}$. Therefore, the domain of correct guesses should simply cover all subsets in which the integrand is larger, and leave the smaller parts to the domain of wrong guesses. ■

Equation (4) is simply the maximum likelihood principle, expressed for slice estimators.

## VI. Correction of Gaussian Key Elements

We must now deal with the reconciliation of information from Gaussian-distributed variables $X \sim N(0, \Sigma)$ and $X' = X + \epsilon, \epsilon \sim N(0, \sigma)$. Let us first compare this problem with known transmission schemes, namely quantization and coded modulation. We temporarily leave out the slice estimation problem and assume that Bob wants to have most information (in ths Shannon sense) about a discrete value $T(X)$, computed by Alice, given its noisy value $X'$.

In a vector quantization (VQ) system, a random input vector $X$ is transmitted over a noiseless discrete channel using the index of the closest code-vector in a given codebook. The codebook design issue has been extensively studied in the VQ literature [16]. The criterion to optimize in that case is the average distortion between $X$ and the set of reproduction vectors. In a coded modulation system, a binary key $k$ is sent over a continuous noisy channel using a vector $X$ belonging to a codebook in a Euclidean space. Trellis-coded modulation and lattice-based coded modulation are instances of this scheme. This latter scheme is probably the closest in spirit to our problem, in that a continuous channel is used to transmit a binary key. In these two well-studied problems, however, the information sent on the channel is chosen by Alice in a codebook, which is not true in our case. The block diagrams of these methods are shown on Fig. 1.

It is conjectured that the analyzes of the quantization noise in lattices and their channel coding properties [17] might be useful in our problem, but we will restrict ourselves to the one-dimensional case. The partitioning and slice assignment issues for $d = 1$ are examined next.

### A. Design

In this section, we present how we designed slices and slice estimators for specifically correcting Gaussian raw keys. We now assume $d = 1$, that is, Alice and Bob use Gaussian key elements individually. The idea is to divide the set of real numbers into intervals and to assign slice values to each of these intervals. The slice estimators are then derived as most likelihood estimators as explained above.

For simplicity, the design of the slices was divided into two smaller independent problems. First, we cut the set of real numbers (Alice's raw key space) into a chosen number of intervals – call this process $T(X)$. For the chosen number of intervals, we try to maximize $I(T(X); X')$. Second, we assign $m$ binary values to these intervals in such a way that slices can be corrected with as few leaked information as possible.

The process $T(X)$ of dividing the real numbers into $t$ intervals is defined by $t-1$ variables $\tau_1 \ldots \tau_{t-1}$. (Note that $\mathbf{S}(X)$ will be an invertible function of $T(X)$ but for the moment we do not yet care about assigning bit values to the intervals.) The interval $a$ with $1 \leq a \leq t$ is then defined by the set $\{x : \tau_{a-1} \leq x < \tau_a\}$ where $\tau_0 = -\infty$ and $\tau_t = +\infty$. The function $I(T(X); X')$ was numerically maximized under the symmetry constrains $\tau_a = \tau_{t-a}$ to reduce the number of variables to process.

We chose to maximize $I(T(X); X') = H(T(X)) - H(T(X)|X')$ because this allows Bob to get most of the information about $T(X)$ in $X'$. Note that this formula is closely related to $H(\mathbf{S}(X)) - I_D$, as $H(\mathbf{S}(X)) = H(T(X))$ and $I_D \geq H(T(X)|X')$. The quantity $H(T(X)|X')$ mixes discrete and continuous components. Its intuitive interpretation is the following. For a given $X'$, Bob derives a distribution of possible values $T(X)$ and calculates its entropy, roughly equal to the number of bits Alice has to provide him with to recover $T(X)$. Then $H(T(X)|X')$ is simply such an entropy averaged over all possible $X'$.

The results are displayed in Fig. 2 below. $I(T(X); X')$ is bounded from above by $\log t$ and goes to $\frac{1}{2}\log(1+\mathrm{SNR})$ as $t \to \infty$.

Let us detail the expressions we evaluated. The random variable $X$ is Gaussian-distributed with variance $\Sigma^2$. $X'$ is the result of adding a random noise $\epsilon$ of variance $\sigma^2$ to $X$. Hence, the random variables $X$ and $X'$ follow the joint density function

$$f_{X,X'}(x,x') = \frac{1}{2\pi\Sigma\sigma} e^{-x^2/2\Sigma^2} e^{-(x-x')^2/2\sigma^2}.$$

Since $I(T(X); X') = H(T(X)) + H(X') - H(T(X), X')$, we need to evaluate all these terms.

$$H(T(X)) = -\sum_a P_a \log P_a, \text{ with}$$

$$P_a = \frac{1}{2}\left(\mathrm{erf}\left(\frac{\tau_a}{\sqrt{2}\Sigma}\right) - \mathrm{erf}\left(\frac{\tau_{a-1}}{\sqrt{2}\Sigma}\right)\right),$$

$$H(X') = \frac{1}{2}\log 2\pi e(\Sigma^2 + \sigma^2), \text{ and}$$

$$H(A, X') = -\sum_a \int_{-\infty}^{+\infty} dx' f_a(x') \log f_a(x'), \text{ with}$$

$$f_a(x') = \int_{\tau_{a-1}}^{\tau_a} dx f_{X,X'}(x,x').$$

From the above procedure, we get intervals that are bounded by the thresholds $\tau_a$. The next step is to construct $m$ slices that return binary values for each of these intervals. Let us restrict ourselves to the case where $t$ is a power of two, namely $t = 2^m$. We investigated several assignment methods, and it turned out that the best bit assignment method consists of mimicking Lemma 3, with the first slices containing noisy values that helps Bob narrow down his guess as quickly as possible. It is further illustrated by the fact that $h(\frac{1}{2}) + h(0) < h(\frac{1}{4}) + h(\frac{1}{4})$, whose interpretation is that it is more efficient to correct most

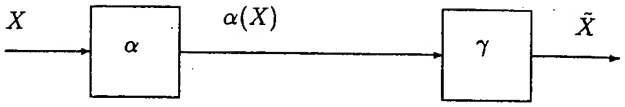


(a) Quantization (discrete noiseless channel) – min. $E \| X - \hat{X} \|^2$

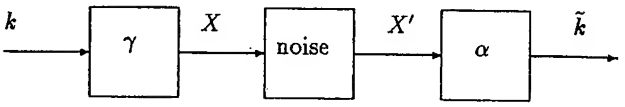


(b) Channel coding – min. $Ed_H(k, \tilde{k})$

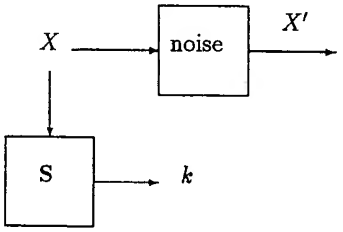


(c) Proposed scheme – max. $I(k; X')$

Fig. 1

COMPARISON WITH OTHER CODING SCHEMES. $\alpha$ DENOTES A MAPPING FROM $\mathbb{R}^d$ TO A CODEBOOK OF BINARY STRINGS AND $\gamma$ A MAPPING FROM THE SET OF BINARY STRINGS TO A CODEBOOK OF VECTORS IN $\mathbb{R}^d$. $X$, $X'$ AND $\tilde{X}$ ARE VECTORS IN $\mathbb{R}^d$, $k$ AND $\tilde{k}$ ARE BINARY STRINGS. WE INDICATE THE PERFORMANCE CRITERION TO OPTIMIZE IN EACH CASE.

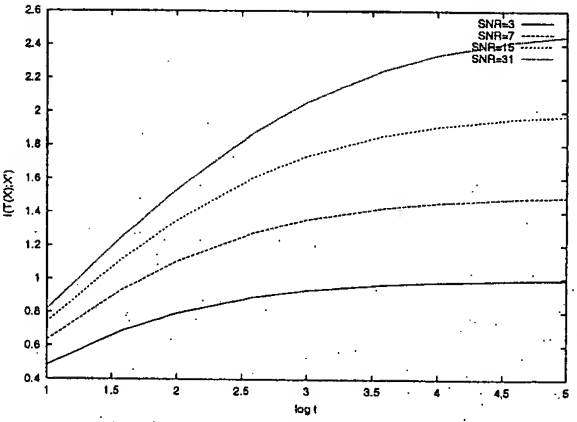


Fig. 2

OPTIMIZED $I(T(X); X')$ AS A FUNCTION OF $\log t$ FOR VARIOUS SIGNAL-TO-NOISE RATIOS

errors all at once, preferably in the beginning so that the subsequent slices can benefit from the gained knowledge.

The chosen method consists thus of assigning the least significant bit of the binary representation of $a-1$ ($0 \leq a-1 \leq 2^m-1$) to the first slice $S_1(x)$ when $\tau_{a-1} \leq x < \tau_a$. Then, each bit of $a-1$ is subsequently assigned up to the most significant bit, which is assigned to the last slice $S_m(x)$. More explicitly,

$$S_i(x) = \begin{cases} 0 & \text{if } \tau_{2^i n} \leq x < \tau_{2^i n + 2^{i-1}}, \\ 1 & \text{otherwise.} \end{cases} \quad (5)$$

*B. Numerical Results*

We evaluated $H(\mathbf{S}(X))$ and $I_e = \sum_i h(e_i)$ for several $(m, \Sigma/\sigma)$ pairs. Let us now give some numerical examples. Assume that the Gaussian channel has a signal-to-noise ratio of 3. According to Shannon's formula, a maximum of 1 bit can thus be transmitted over such a channel. These cases are plotted in Fig. 3. First, consider the case $m=1$, that is only one bit is extracted and corrected per Gaussian value. From our construction, equation (5) reduces to simply dividing the real line into two parts: $S_1(x)=1$ when $x \geq 0$ and $S_1(x)=0$ otherwise. Accordingly, Bob's most likelihood estimator (4) is essentially equivalent to Alice's slice, $\tilde{S}_1(x') = S_1(x')$. In this case, the probability that Alice's and Bob's values differ in sign is $e_1 \approx 0.167$ and hence $I_e = h(e_1) \approx 0.65$ bits. The net amount of information is thus approximately $1 - 0.65 = 0.35$ bit per raw key value when the security parameter $s$ is chosen to be zero.

The last result is not very efficient and is more useful for illustration purposes than for practical ones. Let us now investigate the case of $m=4$ slices, still with a signal-to-noise ratio of 3. The division of the raw key space into intervals that maximizes $I(T(X);X')$ is given in the table below. Note that the generated intervals blend evenly distributed intervals and equal-width intervals (except the first and the last ones of course). Evenly distributed intervals maximize entropy, whereas equal-width intervals best deal with additive Gaussian noise.

| | | | |
|---|---|---|---|
| $\tau_8$ | 0 | $\tau_{12} = -\tau_4$ | 1.081 |
| $\tau_9 = -\tau_7$ | 0.254 | $\tau_{13} = -\tau_3$ | 1.411 |
| $\tau_{10} = -\tau_6$ | 0.514 | $\tau_{14} = -\tau_2$ | 1.808 |
| $\tau_{11} = -\tau_5$ | 0.768 | $\tau_{15} = -\tau_1$ | 2.347 |

Alice's slices follow equation (5), and Bob's slice estimators are defined as usual using equation (4). The correction of the first two slices (i.e., the least two significant bits of the interval number) have an error rate that make them almost uncorrelated, namely $e_1 \approx 0.496$ and $e_2 \approx 0.468$. Correcting those slices reduces to Alice revealing them. These slices distinguish values that are pretty close from one another as compared to the standard deviation of the noise ($\sigma/\Sigma \approx 0.577$, whereas e.g., $\tau_9 - \tau_8 \approx 0.254$). However, information about the first two slices is now known to Bob, which helps him in estimating slices 3 and 4. As of slice 3, Alice's value $x$ is known to Bob to be in some interval $\tau_{4n+\beta} \leq x < \tau_{4n+\beta+1}$ for which he knows $\beta$ but not $n$. The distance between such two intervals is now larger than the standard deviation of the noise and slice 3 can thus be corrected with a reasonable error rate, $e_3 \approx 0.25$. The knowledge of slices 1 and 2 contributes in reducing the leaked information in slice 3. Correction of slice 4 takes even more advantage of the past information, and $e_4 \approx 0.02$. Globally, Alice and Bob share $H(\mathbf{S}(X)) \approx 3.78$ bits after correction, out of which $I_e \approx 2.95$ bits were necessary for running the reconciliation protocol, leaving $H(\mathbf{S}(X)) - I_e \approx 0.83$ bit of net information per raw key element.

We also investigated other signal-to-noise ratios. When $\Sigma^2/\sigma^2 = 15$, Alice and Bob can share up to 2 bits per raw key element. Such cases are plotted in Fig. 4. We recommend to use from 2 to 4 slices more than the number of bits that can be transmitted by the Gaussian channel. In the case $m=5$, we get a net amount of information of about 1.81 bits per raw key element. Evaluating the error rates gives again high error rates in the first two slices ($e_1 \approx 0.497$, $e_2 \approx 0.466$). The third one is still affected by noise ($e_3 \approx 0.242$) and then the error rate drops dramatically ($e_4 \approx 0.024$ and $e_5 \approx 6 \cdot 10^{-6}$).

As one can notice, the first few error rates (e.g., $e_1$ and $e_2$) are high and then the next ones fall dramatically. A first interpretation is related to the all-or-nothing binary reconciliation protocol used in Th. 1. The first slices are used as a way to narrow down the search among the most likely possibilities Bob can think of, and then the last slices compose the shared secret information.

A second interpretation is that slices with high error rates play the role of sketching a hypothetical codebook to which Alice's value belongs. After revealing the first few slices, Bob knows that her value lies in a certain number of narrow intervals with wide spaces between them. If Alice had the possibility of choosing a codebook, she would pick up a value from a discrete list of values – a situation similar to the one just mentioned except for the interval width. Using more slices $m > 4$ would simply make these codebook-like intervals narrower.

In figure 5, we show these error rates for $m=4$ when the noise level varies. From the role of sketching a codebook, slices gradually gain the role of really extracting information as their error rates decrease with the noise level.

## VII. Conclusions

Current reconciliation procedures are aimed at correcting strings of bits. A new construction for reconciliation was proposed, which can be implemented for correcting any kind of shared variables, either discrete or continuous. This construction is then applied to the special case of Gaussian-distributed key elements, in order to complement a new kind of quantum key distribution scheme [9]. This could also be applied to other quantum key distribution schemes [18], [19], [20], [21] that deal with continuous variables as well. We showed theoretical results on the optimality of our construction when applied to asymptotically large bloc sizes. Practical results about reconciliation of Gaussian key elements show that such a construction does not leak much more information than the theoretical bound.

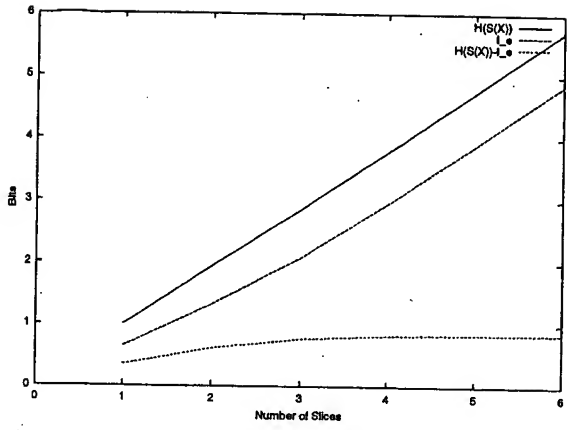


Fig. 3

$H(\mathbf{S}(\mathbf{X}))$, $I_e$ AND THEIR DIFFERENCE AS A FUNCTION OF THE NUMBER OF SLICES WHEN $\Sigma^2/\sigma^2 = 3$

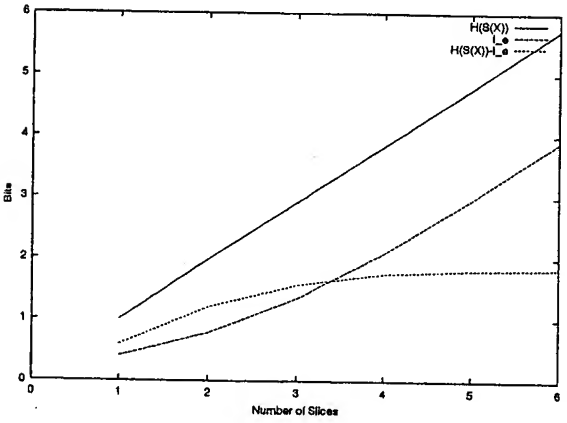


Fig. 4

$H(\mathbf{S}(\mathbf{X}))$, $I_e$ AND THEIR DIFFERENCE AS A FUNCTION OF THE NUMBER OF SLICES WHEN $\Sigma^2/\sigma^2 = 15$

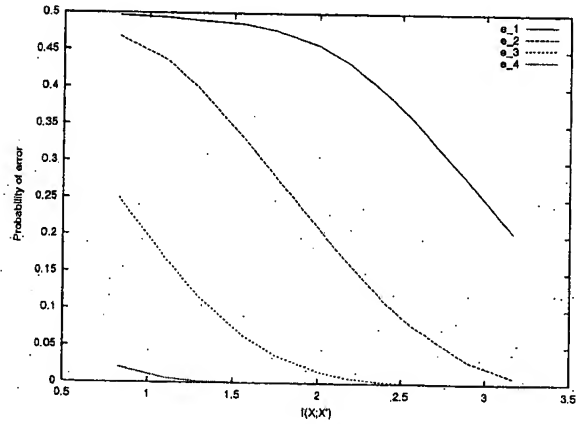


Fig. 5

ERROR RATES $e_{1,2,3,4}$ AS A FUNCTION OF THE CHANNEL CAPACITY $I(X;X')$.

## REFERENCES


[1] C. H. Bennett and G. Brassard, "Public-key distribution and coin tossing," in *Proceedings of the IEEE International Conference on Computers, Systems, and Signal Processing, Bangalore, India*, New York, 1984, pp. 175–179, IEEE.

[2] C. H. Bennett, "Quantum cryptography using any two nonorthogonal states," *Phys. Rev. Lett.*, vol. 68, pp. 3121, 1992.

[3] C. H. Bennett, G. Brassard, and A. K. Ekert, "Quantum cryptography," *Scientific American*, vol. 267, pp. 50–57, October 1992.

[4] N. Lütkenhaus, "Estimates for practical quantum cryptography," *Phys. Rev. A*, vol. 59, no. 5, pp. 3301–3319, May 1999.

[5] G. Brassard and L. Salvail, "Secret-key reconciliation by public discussion," in *Advances in Cryptology - Eurocrypt'93*, T. Helleseth, Ed., New York, 1993, Lecture Notes in Computer Science, pp. 411–423, Springer-Verlag.

[6] U. M. Maurer, "Secret key agreement by public discussion from common information," *IEEE Trans. Inform. Theory*, vol. 39, no. 3, pp. 733–742, May 1993.

[7] C. H. Bennett, G. Brassard, and J.-M. Robert, "Privacy amplification by public discussion," *SIAM Journal on Computing*, vol. 17, no. 2, pp. 210–229, 1988.

[8] C. H. Bennett, G. Brassard, C. Crépau, and U. M. Maurer, "Generalized privacy amplification," *IEEE Trans. on Inform. Theory*, vol. 41, no. 6, pp. 1915–1923, November 1995.

[9] N. J. Cerf, M. Lévy, and G. Van Assche, "Quantum distribution of gaussian keys using squeezed states," *Phys. Rev. A*, vol. 63, pp. 052311, May 2001.

[10] M. O. Scully and M. S. Zubairy, *Quantum Optics*, Cambridge University Press, Cambridge, 1997.

[11] C. H. Bennett, F. Bessette, G. Brassard, L. Salvail, and J. Smolin, "Experimental quantum cryptography," *J. Cryptology*, vol. 5, pp. 3–28, 1992.

[12] K. Chen, "Reconciliation by public discussion: Throughput and residue error rate," unpublished, 2001.

[13] T. Sugimoto and K. Yamazaki, "A study on secret key reconciliation protocol cascade," *IEICE Trans. Fundamentals*, vol. E83-A, no. 10, pp. 1987–1991, October 2000.

[14] K. Yamazaki and T. Sugimoto, "On secret key reconciliation protocol," in *Int. Symp. on Inf. Th. and Its App.*, 2000.

[15] T. M. Cover and J. A. Thomas, *Elements of Information Theory*, Wiley & Sons, New York, 1991.

[16] R. M. Gray and D. L. Neuhoff, "Quantization," *IEEE Trans. Inform. Theory*, vol. 44, 1998.

[17] V. Tarokh, A. Vardy, and K. Zeger, "Universal bound on the performance of lattice codes," *IEEE Trans. Inform. Theory*, vol. 45, no. 2, pp. 670–681, Mar. 1999.

[18] M. D. Reid, "Quantum cryptography using continuous variable einstein-podolsky-rosen correlations and quadrature phase amplitude measurements," 2000, e-print quant-ph/9909030.

[19] T. C. Ralph, "Continuous variable quantum cryptography," *Phys. Rev. A*, vol. 61, pp. 010303, 2000.

[20] M. Hillery, "Quantum cryptography with squeezed states," *Phys. Rev. A*, vol. 61, pp. 022309, 2000.

[21] Ch. Silberhorn, N. Korolkova, and G. Leuchs, "Quantum cryptography with bright entangled beams," in *IQEC'2000 Conference Digest, QMB6*, September 2000, p. 8.

# Continuous variable quantum cryptography using coherent states

Frédéric Grosshans and Philippe Grangier
*Laboratoire Charles Fabry de l'Institut d'Optique (CNRS UMR 8501) F-91403 Orsay, France*

We propose several methods for quantum key distribution (QKD) based upon the generation and transmission of random distributions of coherent or squeezed states, and we show that they are are secure against individual eavesdropping attacks. These protocols require that the transmission of the optical line between Alice and Bob is larger than 50 %, but they do not rely on "non-classical" features such as squeezing. Their security is a direct consequence of the no-cloning theorem, that limits the signal to noise ratio of possible quantum measurements on the transmission line. Our approach can also be used for evaluating various QKD protocols using light with gaussian statistics.

PACS numbers: 03.67.Dd, 42.50.Dv, 89.70.+c

Since the experimental demonstration of quantum teleportation of coherent states [1], a lot of interest has arisen in continuous variable quantum information processing. In particular, a stimulating question is whether quantum continuous variables (QCV) may provide a valid alternative to the usual "single photon" quantum key distribution schemes [2]. Most present proposals to use QCV for QKD [3–15]. are based upon the use of "non-classical" light beams, such as squeezed light, or pairs of light beams that are correlated for two different quadratures components (the so-called "EPR" beams, by analogy with the historical paper by Einstein, Podolski and Rosen [16]). But recent work on this subject [17] underlined the crucial importance of the continuous variable version of the no-cloning theorem [18], as soon as security is concerned in any exchange using QCV.

In this letter, we show that there is actually no need for squeezed light : an equivalent level of security may be obtained by simply generating and transmitting random distributions of coherent states. The security of this novel protocols is related to the no-cloning theorem, that limits its possible eavesdropping even though the transmitted light has no "non-classical" feature such as squeezing. We show that our analysis can be also applied to other protocols using light with gaussian statistics, *i.e.* squeezed or EPR beams, making thus the comparison easier. The basic tools for this analysis are the ones that have been extensively used for linearized quantum optics, including in particular optical quantum non-demolition (QND) measurements [19]. Before presenting our protocol, we will briefly review the current literature on continuous variables QKD.

Here we consider security against individual attacks only, and we do not address the issue of unconditionnal security, that was demonstrated by Gottesman and Preskill [3] for squeezed states protocols (unconditional security of coherent states protocols remains an open question). Security against individual attacks was previously considered by many authors. Hillery proposed a QKD scheme based on binary modulated squeezed light [4]. Cerf *et al* showed it could be improved considering gaussian modulation [5,6] and described a reconciliation protocol [6,7] to implement this improved protocol. In the present work we will generalize this approach to the various single beam protocols of the litterature [4–12]. The protocol described in [5,6] is then a particular member of the family of protocols described here. EPR beams were also considered for QKD schemes. Some schemes need the propagation of one beam only from Alice to Bob [9–14], the other half of the EPR pair being measured by Alice, whereas others need the propagation of two modes (or more) of the electromagnetical field [8,13–15]. In the first family, Reid [10] and Ralph [9] consider "binary" modulated EPR beams, created by a parametric amplifier with a modulated seed [10] or interfering modulated squeezed beams [9], whereas Silberhorn *et al* [11,13] and Navez *et al* [12] extract their key from correlated measurement sequences. As we will show below, these schemes can be viewed as the transmission of a modulated sub-shotnoise beam. Bencheikh *et al* [14] extract the binary key directly from the gaussian correlations. This extraction can be optimized using the reconciliation protocol described in [6,7]. The protocols transmitting several quantum-correlated modes of the electromagnetic field, using two beams [8,13–15] are beyond the scope of this letter, because their security analysis should take into account simultaneous attack on both modes. However, similar gaussian extension of these protocols seem possible. Finally, Ralph examined a binary modulated coherent beam protocol [8,9], and showed its need for privacy amplification [20]. Here we will introduce a family of gaussian protocols, and we will show that the coherent state version is secure and as efficient as the corresponding squeezed light or EPR protocols.

*General principle of the protocols.* The QKD protocols we study here are single gaussian beam protocols. Alice modulate randomly a gaussian beam and send it to Bob through a gaussian noisy channel. Both phase and amplitude are modulated with gaussian random numbers, since it allows an optimal information rate [21]. Bob then measures either the phase or the amplitude of this beam and informs Alice which measurement he made. Bob and Alice have then two correlated sets of gaussian variables, from which they can extract a common secret string of bits as explained below.

The basic tool that we will use is the Shannon formula giving the optimum information rate $I$ of a noisy transmission channel, in units of bits/symbol [21]. If the noise is white and gaussian and the signal to noise ratio (SNR) is $\Sigma$, this optimum information rate is

$$I_{AB} = 1/2 \log_2(1+\Sigma). \quad (1)$$

Since this optimum can be closely approached only if the signal has a gaussian statistics [21], we will consider only gaussian modulation protocols, and use (1) to calculate the amount of private information that Alice and Bob may exchange in presence of the eavesdropper Eve.

The sliced reconciliation protocol described in detail in [6,7] and briefly sketched in the Appendix allows us to get arbitrarly close to the value given by (1). For security purposes, one must assume that Eve has an arbitrary powerful computer, and thus she is able to reach this limit. In case Alice and Bob are not, they will have to allow for an extra security margin (see *Discussion* below). We note that it is not required to specify a "digitizing step" to connect the continuous variable and a bit value: the bits will appear at the end of the reconciliation protocol [6,7]. At this stage, Alice and Bob share a string of bits which is partly known by Eve. They can then use standard privacy amplification protocol [23] to agree on a secret key. The rate at which this secret key can be constructed is

$$\Delta I = I_{AB} - I_{AE}, \quad (2)$$

where $I_{AB}$ ($I_{AE}$) is the information rate between Alice and Bob (Eve).

*Eavesdropping.* The $I_{AB}$ term of (2) is easy to compute for a given scheme, the signal to noise ratio $\Sigma_B$ being known. We have to assume $I_{AE}$ being the maximum possible given the laws of physics (considering only individual attacks, coherent attacks are beyond the scope of this letter). If the protocols are globally invariant under the exchange of the two quadratures $X$ and $P$, the best tactic for Eve is to keep this property in her attacks. Therefore, we can restrict us to attacks that treat equally both quadrature without loss of generality.

Given these hypothesis, we will use a general result, that is demonstrated in [17] : if the added noise on Bob's side is $\chi N_0$, where $N_0$ is the vacuum noise variance, then the minimum added noise on Eve's side is $\chi^{-1} N_0$. This applies to both quadratures, and the added noise may be due to line losses, eavesdropping, or any other reason [17]. Since the demonstration of ref. [17] is just another form of the no-cloning theorem, it also adresses any individual attack by Eve using a cloning machine [18]. When the line has a transmission $\eta$ with no Eve present, one has $\chi = (1-\eta)/\eta$. The best attack for Eve is then to take a fraction $1-\eta$ of the beam at Alice's site, and to send the fraction $\eta$ to Bob through her own lossless line (that may be a perfect teleporter). Eve is then totally undetected, and she gets the maximum possible information according to the no-cloning theorem.

Equation (2) shows that these protocols are secure as long as Bob has a more in formation on Alice's key element than Eve, *i.e.* as long as $I_{AB} > I_{AE}$. Since the Shannon formula (1) is valid for both Bob and Eve, the security condition is just a condition on the signal to noise ratios, which turns to be a condition on the added noises, since the signal and the noise added at Alice's side (quantum noise, Alice's technical noises) are the same.

$$\Delta I > 0 \Leftrightarrow \Sigma_B > \Sigma_E \Leftrightarrow \chi < 1 \quad (3)$$

Since $\chi = (1-\eta)/\eta$ for a line with transmission $\eta$, the condition $\chi < 1$ requires that $\eta > 1/2$. Therefore, a usable key can be obtained in principle as soon as the transmission losses are less 3dB. Taking into account the standard loss of 0.2dB/km in optical fibers at 1550 nm, the typical range would be around 10 km.

In this security evaluation, the noise added in Alice's side cancels out because it disturbs equally Eve and Bob. This 'cancelled' noise includes the quantum noise of the beam. As a consequence, the security of these protocols relies of the quantum aspects of measuring or copying, but not on any quantum feature of the beam, like squeezing or entanglement. We can do quantum cryptography with coherent beams, as mentionned by Ralph [8,9] or even with highly noisy beams. Quantum features of the beams might influence some characteristics of the protocol like the secret key rate or the amount of classical communication needed to agree on the secret key, but not its security.

*Coherent Beam protocol.* Let us now explicitly describe the coherent beam protocols of this family:

1. Alice draws two random numbers $x_A$ and $p_A$ from a gaussian law with variance $V_A N_0$
2. She sends to Bob the coherent state $|x_A + ip_A\rangle$
3. Bob randomly chooses to measure either $X$ or $P$. This measurement can be done perfectly.
4. Using a classical public channel he informs Alice about the observable that he measured (like in the BB84 protocol, half of the key generated by Alice is unused)
5. Alice and Bob share two correlated gaussian variables. Then they may use the "sliced reconciliation" protocol [7,6] to transform it into errorless bit strings. Finally, they have to use a standard protocol for privacy amplification [23] in order to distill the private key.

According to eq. (1), the channel rate $\Delta I$ for the private key will be:

$$\Delta I = \tfrac{1}{2}\log_2(1+\Sigma_B) - \tfrac{1}{2}\log_2(1+\Sigma_E) \quad (4)$$

The total variance of any quadrature of the beam when it leaves Alice's realm is $VN_0 = V_A N_0 + N_0$. Using the expressions $1+\Sigma_B = \frac{V+\chi}{1+\chi}$, and $1+\Sigma_E = \frac{V+1/\chi}{1+1/\chi}$, the useful secret information rate is :

$$\Delta I = \tfrac{1}{2}\log_2 \tfrac{V+\chi}{1+V\chi} \quad (5)$$

If $\chi < 1$, $\Delta I$ will increase as a function of the signal modulation $V_A$. For large modulation ($\chi V \gg 1$), the asymptotic value of $\Delta I$ is :

$$\Delta I_{asymp} = -\tfrac{1}{2}\log_2 \chi = \tfrac{1}{2}\log_2 \tfrac{\eta}{1-\eta} \quad (6)$$

while the raw channel rate between Alice and Bob is $I_{AB} = \frac{1}{2}\log_2(V/(1+\chi))$.

*Squeezed state protocol.* This protocol can straightforwardly be generalized to modulated squeezed beam, with a squeezing factor $s < 1$. The protocol becomes :

1. Alice chooses randomly if the beam is squeezed in $X$ or $P$ (for instance we will later assume the beam being $X$-squeezed). Let denote $|\psi\rangle$ this squeezed state.

2. Alice draws two random numbers $x_A$ and $p_A$ from two gaussian laws with variances $V_{x_A}N_0$ and $V_{p_A}N_0$. The two squeezed direction are indistinguishable for Eve iff

$$V_{x_A}N_0 + sN_0 = V_{p_A}N_0 + \tfrac{1}{s}N_0 \equiv VN_0 \quad (7)$$

3. Alice sends to Bob the displaced squeezed state $D(x_A + ip_a)\,|\psi\rangle$

4. Bob randomly chooses to measure either $X$ or $P$.

5. Using a public channel, Alice and Bob inform each other about the squeezing direction and the measured observable.

6. Like with coherent states Alice and Bob share correlated gaussian variables, from which they can extract a private binary key.

This protocol obviously reduces to the protocol described above if $s = 1$. Another limit, where $V_{p_A} = 0$ or $V = 1/s$, is the protocol described by Cerf *et al* in [5,6]. In this case, information is gathered for the key only when Bob makes the right guess.

To compute the private rate $\Delta I$, we will average between the right guesses and the wrong guesses :

$$\Delta I = \tfrac{1}{2}[(I_{ABX} - I_{AEX}) + (I_{ABP} - I_{AEP})] \quad (8)$$

$$= \tfrac{1}{4}\log_2 \tfrac{(1+\Sigma_{BX})(1+\Sigma_{BP})}{(1+\Sigma_{EX})(1+\Sigma_{EP})} \quad (9)$$

We have $\Sigma_{BX} = \frac{V_{x_A}}{s+\chi} = \frac{V-s}{s+\chi}$ and $1 + \Sigma_{BX} = \frac{V+\chi}{s+\chi}$. The three other signal to noise ratios are obtained by replacing $\chi$ or/and $s$ by $\chi^{-1}$ or $s^{-1}$. Therefore,

$$I_{AB} = \tfrac{1}{4}\log_2 \tfrac{(V+\chi)^2}{\chi} - \tfrac{1}{4}\log_2(\chi + \tfrac{1}{\chi} + s + \tfrac{1}{s}) \quad (10)$$

$$I_{AE} = \tfrac{1}{4}\log_2 \tfrac{(V+1/\chi)^2}{1/\chi} - \tfrac{1}{4}\log_2(\chi + \tfrac{1}{\chi} + s + \tfrac{1}{s}) \quad (11)$$

Since the $s$-dependent term of these information rates are the same, they cancel each other in $\Delta I$. The secret information rate is thus again given by eq. (5), and does not depend on the degree of squeezing.

*Extension to EPR case.* The previous description does not apply directly on EPR protocols. However, an EPR QKD protocol where Alice keeps one of the beams and sends the other to Bob is logically equivalent to a randomly modulated beam with a sub-shot noise quantum variance. Let note $X_A$ the quadrature Alice measures and $X_{out}$ the same quadrature of the beam sent to Bob when it leaves Alice's lab. For a standard non-modulated EPR scheme [11] we have the following relations :

$$\langle X_A^2 \rangle = \langle X_{out}^2 \rangle \equiv V = (s + 1/s)/2 \quad (12)$$

$$\langle (X_A - X_{out})^2 \rangle = 2s \quad (13)$$

$$\langle X_A X_{out} \rangle = V - s \quad (14)$$

We can separate Bob's beams in two parts, that are respectively correlated and uncorrelated with Alice's measurement, by writing $X_{out} = gX_A + N$ where $\langle X_A N \rangle = 0$. Bob's beam is then equivalent to a beam with quantum noise $\langle N^2 \rangle$ on quadrature $X$, which is randomly modulated with the variable $gX_A$. Using eqs (12,14) one gets:

$$g = 1 - s/V = (1 - s^2)/(1 + s^2) \quad (15)$$

$$\langle N^2 \rangle = s(2 - s/V) = 2s/(1 + s^2). \quad (16)$$

These equations describe the case where Alice and Bob measure the same quadrature. When Alice changes her quadrature, while Bob keeps the same measurement, the initial wave packet is reduced onto a noisy quadrature, and no useful correlation is generated. On the average, the information rate is therefore half of the "equivalent" modulation scheme. Using (12), we have then:

$$1 + \Sigma_B = 1 + \tfrac{g^2 V}{\langle N^2 \rangle + \chi} = \tfrac{V(V+\chi)}{1+\chi V} \quad (17)$$

$$\Delta I = \tfrac{1}{4}\log_2(\tfrac{V+\chi}{1+\chi V}\tfrac{1+V/\chi}{V+1/\chi}) = \tfrac{1}{2}\log_2(\tfrac{V+\chi}{1+\chi V}) \quad (18)$$

This value of $\Delta I$ is again just the same as the coherent state result (5) for given $\chi$ and $V$, so that $s$ is defined by (12). Adding excess noise or a modulation on the outgoing beam brings no further improvement.

*Discussion.* Various comments are in order. First, it appears that non classical features like squeezing or EPR correlations have no influence on the achievable secret key rate for the family of protocols that were described here. This result may not apply to all possible protocols, *e.g.* , we did not consider using a continuous quantum memory. On the other hand, since the raw information rate are different for the same secret key rate, squeezed beams can be used to save classical communications during the privacy amplification procedure. The EPR beams have also the advantage of directly providing quantum-generated gaussian noise, rather than having it externally generated by Alice. More importantly, entanglement, that is not directly used in the present protocols, can be useful to beat the 3 dB limit by using more than one beam. Though the 3 dB loss limit of our cryptography protocols makes their security demonstration quite intuitive, there exist multiples ways for Alice and Bob to go beyond this limit. The most radical way is to send many EPR beams through the noisy channel, then to use entanglement purification [22] to build stored entanglement between Alice and Bob, and finally to implement a high fidelity teleporter. For any finite value of the losses and EPR entanglement, an arbitrarily high fidelity can be achieved [22]. The no-cloning theorem ensures the security of these schemes as soon as the fidelity of the teleporter is above 2/3 [17], which is equivalent to the 3 dB loss limit discussed above.

In some sense, a "lossless" line is re-created by using entanglement purification. There may exist more realistic ways to cross the 3 dB barrier. For instance, Alice and Bob may "invert" the reconciliation procedure, with Alice guessing Bob's measurement instead of Bob guessing Alice's value [23]. This inverted procedure may be more efficient, but its complete security analysis is beyond the scope of this letter.

On the practical side, one should note that Bob's detectors are not ideal, but have a non-zero electronic noise $B_0$, that should be much smaller than $N_0$, and a maximum (saturation) input power $\sigma B_0 \gg N_0$, where $\sigma \gg 1$ is the detector's dynamics. Taking into account these characteristics in the simplest coherent state protocol gives an optimum value of the signal variance, $V_A \sim \sqrt{\sigma}$. Another point is that Alice and Bob may not be able to achieve the Shannon limit (1), due to limited computing power (no such limitation is relevant for Eve). Assuming that the effective information rate between Alice and Bob is reduced by a factor $\alpha < 1$, the net secret rate becomes $\Delta I_{eff} = \alpha I_{AB} - I_{AE}$, and remains positive if $\alpha > I_{AE}/I_{AB}$. The quantity $\Delta I_{eff}$ is plotted on Fig.1 for $\alpha = 1$ (full lines), and for various values of $\alpha$ that are arbitrarily associated with various values of the SNR (dashed lines). It is clear from that figure that low values of $\alpha$ reduce the transmission range in which the protocol is secure. We note that according to [6,7], the sliced reconciliation protocol should yield $\alpha \sim 1$ (see also Appendix), but this may be costly in terms of calculation time and public channel transmissions. All these constraints should eventually be taken into account to choose the most appropriate value of $V_A$.

As a conclusion, it is possible to design a QKD scheme with coherent states, secure against any individual attack, by using optimized reconciliation protocols and privacy amplification. Since the protocol does not require squeezing, it can be implemented by sending light pulses in a low-loss optical fiber, like in a coherent optical telecommunication scheme. In that case, all pulses will be useful, but half of the random numbers generated by Alice will not be used. We demonstrated that the protocol is asymptotically secure [7] for losses smaller than 3dB (or a teleportation fidelity larger than 2/3 [17]), and the net information rate for the private key with a large signal modulation is $1/2 \log_2(1/\chi) = 1/2 \log_2(\eta/(1-\eta))$.

### Appendix : Sliced reconciliation protocol

In the n-slice version of the reconciliation protocol proposed in ref. [7], the real axis representing the amplitude of the signal is split in $2^n$ intervals $s_1 = ]-\infty, -t_1]$, $s_2 = ]-t_1, -t_2]$, ... $s_{2^n} = ]t_{2^n-1}, +\infty[$, where $t_p = -t_{2^n-p}$, and $t_{2^{n-1}} = 0$. Alice assigns an amount of $n$ bits to an amplitude that lies in the interval $s_p$, by using the parity of $p$ for bit 1, of $Floor(p/2)$ for bit 2, ... , and of $Floor(p/2^{n-1})$ for bit $n$. After receiving the data, Bob makes an optimized guess of the first bit value using appropriate weighting functions, that are computed by optimizing the choice of the $\{t_p\}$ (this optimization is made only once, before exchanging the data). After a first correction round by exchanging public data between Alice and Bob, Bob knows the correct value of the first bit. Then he tries to guess the second bit, with a much higher probability of success, because he already knows the first one. By increasing both the SNR $\Sigma$ and the number of slices, the process gets more and more efficient, keeping the same main idea : after each correction round, Bob can guess the next bit with a higher probability. For the 5-slice protocol with $\Sigma = 15$ presented in [7], the probabilities of guessing right for slices 4 and 5 are respectively 0.976 and 0.999994, and the efficiency is more than 90% of the Shannon limit $\frac{1}{2}\log_2(16) = 2$.

*Acknowledgments.* This work was carried out in the framework of the European IST/FET/QIPC project "QuICoV". We are grateful to N.J. Cerf and G. Van Assche for helpful discussions.

[1] A. Furusawa *et al* , Science **282**, 706 (1998).
[2] For a review see *e.g.* W. Tittel, G. Ribordy, and N. Gisin, Physics World, p. 41 (march 1998)
[3] D. Gottesman and J. Preskill, Phys. Rev. A **63**, 022309 (2001), e-print quant-ph/0008046
[4] M. Hillery, Phys. Rev. A **61**, 022309 (2000), e-print quant-ph/9909006
[5] N.J. Cerf, M. Lévy and G. Van Assche, Phys. Rev. A **63**, 052311 (2000), e-print quant-ph/0008058
[6] N.J. Cerf, S. Iblisdir and G. Van Assche, e-print quant-ph/0107077, submitted to Eur. Phys. J. D (2001)
[7] G. Van Assche, J. Cardinal and N.J. Cerf, e-print cs.CR/0107030, submitted to IEEE (2001)
[8] T.C. Ralph, Phys. Rev. A **61**, 010303(R) (2000), e-print quant-ph/9907073
[9] T.C. Ralph, Phys. Rev. A **62**, 062306 (2000), e-print quant-ph/0007024
[10] M.D. Reid, Phys. Rev. A **62**, 062308 (2000), e-print quant-ph/9909030
[11] Ch. Silberhorn, N. Korolkova and G. Leuchs, e-print quant-ph/0109009 (2001)
[12] P. Navez, A. Gatti and L.A. Lugiato, e-print quant-ph/010113 (2001)
[13] S. Lorenz *et al* , e-print quant-ph/0109018 (2001), submitted to Appl. Phys. B
[14] K. Bencheikh, Th. Symul, A. Jankovic and J.A. Levenson, to appear in J. Mod. Optics (2001)
[15] S.F. Pereira, Z.Y. Ou and H.J. Kimble, Phys. Rev. A **62**, 042311 (2000), e-print quant-ph/0003094
[16] A. Einstein, B. Podolsky and N. Rosen, Phys. Rev. **47**, 777 (1935)
[17] F. Grosshans and Ph. Grangier, Phys. Rev. A **64** 010301(R) (2001), e-print quant-ph/0012121

[18] N.J. Cerf and S. Iblisdir, Phys. Rev. A **62**, 040301(R) (2000), e-print quant-ph/0005044
[19] Ph. Grangier, J.A. Levenson and J.Ph. Poizat, Nature **396**, 537 (1998)
[20] T.C.Ralph, to appear in "Quantum information theory with continuous variables", ed. S.L. Braustein and S.L. Paki, e-print quant-ph/0109096
[21] C.E. Shannon, Bell Syst. Tech. J. **27** 623-656(1948)
[22] L.-M. Duan, G. Giedke, J.I. Cirac and P. Zoller, Phys. Rev. Lett. 84, 4002 (2000), e-print quant-ph/9912017
[23] U. Maurer and S. Wolf, *Advances in Cryptology-EUROCRYPT'00*, Lecture Notes in Computer Science **1807**, 351-368, Springer Verlag (2000)

FIG. 1. Private channel information rate $\Delta I$ as a function of the channel noise $\chi$. The three curves in full lines correspond to $V_A = 1, 5, 50$ from the bottom to the top, assuming that the reconciliation protocol between Alice and Bob reaches the Shannon limit. The three curves in dashed lines correspond to the effective $\Delta I$ with the sames values of $V_A$, with (arbitrarily chosen) reconciliation efficiencies $\alpha$ that are respectively 0.6, 0.8 and 0.95 of the Shannon limit.

REVIEWS OF MODERN PHYSICS, VOLUME 74, JANUARY 2002

# Quantum cryptography

Nicolas Gisin, Grégoir Ribordy, Wolfgang Tittel, and Hugo Zbinden

*Group of Applied Physics, University of Geneva, 1211 Geneva 4, Switzerland*

(Published 8 March 2002)

Quantum cryptography could well be the first application of quantum mechanics at the single-quantum level. The rapid progress in both theory and experiment in recent years is reviewed, with emphasis on open questions and technological issues.

## CONTENTS



## I. INTRODUCTION

Electrodynamics was discovered and formalized in the 19th century. The 20th century was then profoundly affected by its applications. A similar adventure may be underway for quantum mechanics, discovered and formalized during the last century. Indeed, although the laser and semiconductor are already common, applications of the most radical predictions of quantum mechanics have only recently been conceived, and their full potential remains to be explored by the physicists and engineers of the 21st century.

The most peculiar characteristics of quantum mechanics are the existence of indivisible quanta and of entangled systems. Both of these lie at the root of quantum cryptography (QC), which could very well be the first commercial application of quantum physics at the single-quantum level. In addition to quantum mechanics, the 20th century has been marked by two other major scientific revolutions: information theory and relativity. The status of the latter is well recognized. It is less well known that the concept of information, nowadays measured in bits, and the formalization of probabilities are

0034-6861/2002/74(1)/145(51)/$35.00

quite recent,[1] although they have a tremendous impact on our daily life. It is fascinating to realize that QC lies at the intersection of quantum mechanics and information theory and that, moreover, the tension between quantum mechanics and relativity—the famous Einstein-Rosen-Podolsky (EPR) paradox (Einstein *et al.*, 1935)—is closely connected to the security of QC. Let us add a further point for young physicists. Unlike laser and semiconductor physics, which are manifestations of quantum physics at the ensemble level and can thus be described by semiclassical models, QC, and to an even greater extent quantum computers, require a full quantum-mechanical description (this may offer an interesting challenge for physicists well trained in the subtleties of their science).

This review article has several objectives. First, we present the basic intuition behind QC. Indeed, the basic idea is so beautiful and simple that every physicist and student should be given the pleasure of learning it. The general principle is then set in the broader context of modern cryptology (Sec. II.B) and made more precise (Sec. II.C). Section III discusses the main technological challenges. Then, Secs. IV and V present the most common implementations of QC: the use of weak laser pulses and photon pairs, respectively. Finally, the important and difficult problems of eavesdropping and security proofs are discussed in Sec. VI, where the emphasis is more on the diversity of the issues than on formal details. We have tried to write the different parts of this review in such a way that they can be read independently.

## II. A BEAUTIFUL IDEA

The idea of quantum cryptography was first proposed in the 1970s by Stephen Wiesner[2] (1983) and by Charles H. Bennett of IBM and Gilles Brassard of The University of Montréal (1984, 1985).[3] However, this idea is so simple that any first-year student since the infancy of quantum mechanics could actually have discovered it! Nevertheless, it is only now that the field is mature enough and information security important enough that physicists are ready to consider quantum mechanics, not only as a strange theory good for paradoxes, but also as a tool for new engineering. Apparently, information theory, classical cryptography, quantum physics, and quantum optics first had to develop into mature sciences. It is certainly not a coincidence that QC and, more generally, quantum information were developed by a community including many computer scientists and more mathematically oriented young physicists: broader interests than traditional physics were needed.

### A. The intuition

Quantum physics is well known for being counterintuitive or even bizarre. We teach students that quantum physics establishes a set of negative rules stating things that cannot be done. For example,

(1) One cannot take a measurement without perturbing the system.
(2) One cannot determine simultaneously the position and the momentum of a particle with arbitrarily high accuracy.
(3) One cannot simultaneously measure the polarization of a photon in the vertical-horizontal basis and simultaneously in the diagonal basis.
(4) One cannot draw pictures of individual quantum processes.
(5) One cannot duplicate an unknown quantum state.

This negative viewpoint of quantum physics, due to its contrast with classical physics, has only recently been turned positive, and QC is one of the best illustrations of this *psychological revolution.* Indeed, one could characterize quantum information processing as the science of turning quantum conundrums into potentially useful applications.

Let us illustrate this point for QC. One of the basic negative statements of quantum physics reads

One cannot take a measurement without perturbing the system (1)

(unless the quantum state is compatible with the measurement). The positive side of this axiom can be seen when applied to a communication between Alice and Bob (the conventional names of the sender and receiver, respectively), provided the communication is quantum, that is, quantum systems, for example, individual photons, carry the information. When this is the case, axiom (1) also applies to eavesdroppers, i.e., to a malicious Eve (the conventional name given to the adversary in cryptology). Hence Eve cannot get any information about the communication without introducing perturbations that would reveal her presence.

To make this intuition more precise, imagine that Alice codes information in individual photons, which she sends to Bob. If Bob receives the photons unperturbed, then, according to the basic axiom (1), the photons were not measured. No measurement implies that Eve did not get any information about the photons (note that acquiring information is synonymous with carrying out measurements). Consequently, after exchanging the photons,

[1]The Russian mathematician A. N. Kolmogorov (1956) is credited with being the first to have formulated a consistent mathematical theory of probabilities in the 1940s.

[2]S. Wiesner, then at Columbia University, was the first to propose ideas closely related to QC in the 1970s. However, his revolutionary paper did not appear until a decade later. Since it is difficult to find, we reproduce his abstract here: *The uncertainty principle imposes restrictions on the capacity of certain types of communication channels. This paper will show that in compensation for this "quantum noise," quantum mechanics allows us novel forms of coding without analogue in communication channels adequately described by classical physics.*

[3]Artur Ekert (1991) of Oxford University discovered QC independently, though from a different perspective (see Sec. II.D.3).

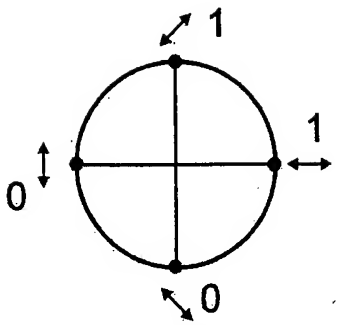


FIG. 1. Implementation of the Bennett and Brassard (BB84) protocol. The four states lie on the equator of the Poincaré sphere.

Alice and Bob can check whether someone "was listening": they simply compare a randomly chosen subset of their data using a public channel. If Bob received this subset unperturbed, then the logic goes as follows:

① No perturbation⇒No measurement

⇒No eavesdropping. (2)

Actually, there are two more points to add. First, in order to ensure that axiom (1) applies, Alice encodes her information in nonorthogonal states (we shall illustrate this in Secs. II.C and II.D). Second, as we have presented it so far, Alice and Bob could discover any eavesdropper, but only after they have exchanged their message. It would of course be much better to ensure their privacy in advance and not afterwards. To achieve this, Alice and Bob complement the above idea with a ② second idea, again a very simple one, and one which is entirely classical. Alice and Bob do not use the quantum channel to transmit information, but only to transmit a random sequence of bits, i.e., a key. Now, if the key is unperturbed, then quantum physics guarantees that no one has gotten any information about this key by eavesdropping, i.e., measuring, the quantum communication channel. In this case, Alice and Bob can safely use this key to encode messages. If, on the other hand, the key turns out to be perturbed, then Alice and Bob simply disregard it; since the key does not contain any information, they have not lost any.

Let us make this general idea somewhat more precise, in anticipation of Sec. II.C. In practice, the individual quanta used by Alice and Bob, often called *qubits* (for quantum bits), are encoded in individual photons; for example, vertical and horizontal polarization code for bit values 0 and 1, respectively. The second basis can then be the diagonal one (±45° linear polarization), with +45° coding for bit 1 and −45° for bit 0, respectively (see Fig. 1). Alternatively, the circular polarization basis could be used as second basis. For photons the quantum communication channel can be either free space (see Sec. IV.E) or optical fibers—special fibers or the ones used in standard telecommunications (Sec. III.B). The communication channel is thus not really quantum. What is quantum are the information carriers.

Before continuing, we need to see how QC could fit into existing cryptosystems. For this purpose the next section briefly surveys some of the main aspects of modern cryptology.

### B. Classical cryptography

Cryptography is the art of rendering a message unintelligible to any unauthorized party. It is part of the broader field of cryptology, which also includes cryptoanalysis, the art of code breaking (for a historical perspective, see Singh, 1999). To achieve this goal, an algorithm (also called a *cryptosystem* or cipher) is used to combine a message with some additional information—known as the key—and produce a *cryptogram*. This technique is known as *encryption*. For a cryptosystem to be secure, it should be impossible to unlock the cryptogram without the key. In practice, this requirement is often weakened so that the system is just extremely difficult to crack. The idea is that the message should remain protected at least as long as the information it contains is valuable. Although confidentiality is the traditional application of cryptography, it is used nowadays to achieve broader objectives, such as authentication, digital signatures, and nonrepudiation (Brassard, 1988).

#### 1. Asymmetrical (public-key) cryptosystems

Cryptosytems come in two main classes—depending on whether Alice and Bob use the same key. Asymmetrical systems involve the use of different keys for encryption and decryption. They are commonly known as *public-key cryptosystems*. Their principle was first proposed in 1976 by Whitfield Diffie and Martin Hellman, who were then at Stanford University. The first actual implementation was then developed by Ronald Rivest, Adi Shamir, and Leonard Adleman of the Massachusetts Institute of Technology in 1978.[4] It is known as RSA and is still widely used. If Bob wants to be able to receive messages encrypted with a public-key cryptosystem, he must first choose a private key, which he keeps secret. Then he computes from this private key a public key, which he discloses to any interested party. Alice uses this public key to encrypt her message. She transmits the encrypted message to Bob, who decrypts it with the private key. Public-key cryptosystems are convenient and have thus become very popular over the last 20 years. The security of the Internet, for example, is partially based on such systems. They can be thought of as a mailbox in which anybody can insert a letter. Only the legitimate owner can then recover it, by opening it with his private key.

[4]According to the British Government, public-key cryptography was originally invented at the Government Communications Headquarters in Cheltenham as early as 1973. For an historical account, see, for example, the book by Simon Singh (1999).

The security of public-key cryptosystems is based on computational complexity. The idea is to use mathematical objects called one-way functions. By definition, it is easy to compute the function $f(x)$ given the variable $x$, but difficult to reverse the calculation and deduce $x$ from $f(x)$. In the context of computational complexity, the word "difficult" means that the time required to perform a task grows exponentially with the number of bits in the input, while "easy" means that it grows polynomially. Intuitively, it is easy to understand that it takes only a few seconds to work out $67\times71$, but it takes much longer to find the prime factors of 4757. However, factoring has a "trapdoor," which means that it is easy to do the calculation in the difficult direction provided that you have some additional information. For example, if you were told that 67 was one of the prime factors of 4757, the calculation would be relatively simple. The security of RSA is actually based on the factorization of large integers.

In spite of its elegance, this technique suffers from a major flaw. It has not been possible yet to prove whether factoring is "difficult" or not. This implies that the existence of a fast algorithm for factorization cannot be ruled out. In addition, the discovery in 1994 by Peter Shor of a polynomial algorithm allowing fast factorization of integers with a quantum computer casts additional doubt on the nonexistence of a polynomial algorithm for classical computers.

Similarly, all public-key cryptosystems rely for their security on unproven assumptions, which could themselves be weakened or suppressed by theoretical or practical advances. So far, no one has proved the existence of any one-way function with a trapdoor. In other words, the existence of secure asymmetric cryptosystems is not proven. This poses a serious threat to these cryptosystems.

In a society like ours, where information and secure communication are of the utmost importance, one cannot tolerate such a threat. For instance, an overnight breakthrough in mathematics could make electronic money instantly worthless. To limit such economic and social risks, there is no alternative but to turn to symmetrical cryptosystems. QC has a role to play in such alternative systems.

### 2. Symmetrical (secret-key) cryptosystems

Symmetrical ciphers require the use of a single key for both encryption and decryption. These systems can be thought of as a safe in which the message is locked by Alice with a key. Bob in turns uses a copy of this key to unlock the safe. The *one-time pad*, first proposed by Gilbert Vernam of AT&T in 1926, belongs to this category. In this scheme, Alice encrypts her message, a string of bits denoted by the binary number $m_1$, using a randomly generated key $k$. She simply adds each bit of the message to the corresponding bit of the key to obtain the scrambled text ($s=m_1\oplus k$, where $\oplus$ denotes the binary addition modulo 2 without carry). It is then sent to Bob, who decrypts the message by subtracting the key ($s\ominus k=m_1\oplus k\ominus k=m_1$). Because the bits of the scrambled text are as random as those of the key, they do not contain any information. This cryptosystem is thus provably secure according to information theory (Shannon, 1949). In fact, it is the only provably secure cryptosystem known today.

Although perfectly secure, this system has a problem—it is essential for Alice and Bob to possess a common secret key, which must be at least as long as the message itself. They can only use the key for a single encryption—hence the name "one-time pad." If they used the key more than once, Eve could record all of the scrambled messages and start to build up a picture of the plain texts and thus also of the key. (If Eve recorded two different messages encrypted with the same key, she could add the scrambled texts to obtain the sum of the plain texts: $s_1\oplus s_2=m_1\oplus k\oplus m_2\oplus k=m_1\oplus m_2\oplus k\oplus k=m_1\oplus m_2$, where we use the fact that $\oplus$ is commutative.) Furthermore, the key has to be transmitted by some trusted means, such as a courier, or through a personal meeting between Alice and Bob. This procedure can be complex and expensive, and may even amount to a loophole in the system.

Because of the problem of distributing long sequences of key bits, the one-time pad is currently used only for the most critical applications. The symmetrical cryptosystems in use for routine applications such as e-commerce employ rather short keys. In the case of the Data Encryption Standard (also known as DES, promoted by the United States' National Institute of Standards and Technology), a 56-bit key is combined with the plain text divided into blocks in a rather complicated way, involving permutations and nonlinear functions to produce the cipher text blocks (see Stallings, 1999 for a didactic presentation). Other cryptosystems (e.g., IDEA, The International Data Encryption System, or AES, the Advanced Encryption Standard) follow similar principles. Like asymmetrical cryptosystems, they offer only computational security. However, for a given key length, symmetrical systems are more secure than their asymmetrical counterparts.

In practical implementations, asymmetrical algorithms are used not so much for encryption, because of their slowness, but rather for distribution of session keys for symmetrical cryptosystems such as DES. Because the security of those algorithms is not proven (see Sec. II.B.1), the security of the whole implementation can be compromised. If these algorithms were broken by mathematical advances, QC would constitute the only way to solve the key distribution problem.

### 3. The one-time pad as "classical teleportation"

The one-time pad has an interesting characteristic. Assume that Alice wants to transfer to Bob a faithful copy of a classical system, without giving any information to Eve about this system. For this purpose Alice and Bob have access only to an insecure classical channel. The operation is possible provided they share an arbitrarily long secret key. Indeed, in principle, Alice

can measure the state of her classical system with arbitrarily high precision and then use the one-time pad to securely communicate this information to Bob, who can then, in principle, reconstruct (a copy of) the classical system. This somewhat artificial use of the one-time pad has an interesting quantum relative (see Sec. II.E).

### C. The BB84 protocol

#### 1. Principle

The first protocol for QC was proposed in 1984 by Charles H. Bennett, of IBM and Gilles Brassard, of the University of Montreal, hence the name BB84, as this protocol is now known. They presented their work at an IEEE conference in India, quite unnoticed by the physics community at the term. This underscores the need for collaboration in QC between different communities, with different jargons, habits, and conventions.[5] The interdisciplinary character of QC is the probable reason for its relatively slow start, but it certainly has contributed to the rapid expansion of the field in recent years.

We shall explain the BB84 protocol using the language of spin $\frac{1}{2}$, but clearly any two-level quantum system would do. The protocol uses four quantum states that constitute two bases, for example, the states up $|\uparrow\rangle$, down $|\downarrow\rangle$, left $|\leftarrow\rangle$, and right $|\rightarrow\rangle$. The bases are maximally conjugate in the sense that any pair of vectors, one from each basis, has the same overlap, e.g., $|\langle\uparrow|\leftarrow\rangle|^2 = \frac{1}{2}$. Conventionally, one attributes the binary value 0 to states $|\uparrow\rangle$ and $|\rightarrow\rangle$ and the value 1 to the other two states, and calls the states qubits (for quantum bits). In the first step, Alice sends individual spins to Bob in states chosen at random among the four states (in Fig. 1 the spin states $|\uparrow\rangle$, $|\downarrow\rangle$, $|\rightarrow\rangle$, and $|\leftarrow\rangle$ are identified as the polarization states "horizontal," "vertical," "+45°," and "−45°," respectively). How she "chooses at random" is a delicate problem in practice (see Sec. III.D), but in principle she could use her free will. The individual spins could be sent all at once or one after the other (much more practical), the only restriction being that Alice and Bob be able to establish a one-to-one correspondence between the transmitted and the received spins. Next, Bob measures the incoming spins in one of the two bases, chosen at random (using a random-number generator independent from that of Alice). At this point, whenever they use the same basis, they get perfectly correlated results. However, whenever they use different bases, they get uncorrelated results. Hence, on average, Bob obtains a string of bits with a 25% error rate; called the *raw key*. This error rate is so high that standard error correction schemes would fail. But in this protocol, as we shall see, Alice and Bob know which bits are perfectly correlated (the ones for which Alice and Bob used the same basis) and which ones are completely uncorrelated (all the other ones). Hence a straightforward error correction scheme is possible: For each bit Bob announces publicly in which basis he measured the corresponding qubit (but he does not tell the result he obtained). Alice then reveals only whether or not the state in which she encoded that qubit is compatible with the basis announced by Bob. If the state is compatible, they keep the bit; if not, they disregard it. In this way about 50% of the bit string is discarded. This shorter key obtained after basis reconciliation is called the *sifted key*.[6] The fact that Alice and Bob use a public channel at some stage of their protocol is very common in cryptoprotocols. This channel does not have to be confidential, only authentic. Hence any adversary Eve can listen to all the communication on the public channel, but she cannot modify it. In practice Alice and Bob may use the same transmission channel to implement both the quantum and the classical channels.

Note that neither Alice nor Bob can decide which key results from the protocol.[7] Indeed, it is the conjunction of both of their random choices that produces the key.

Let us now consider the security of the above ideal protocol (ideal because so far we have not taken into account unavoidable noise in practice, due to technical imperfections). Assume that some adversary Eve intercepts a qubit propagating from Alice to Bob. This is very easy, but if Bob does not receive an expected qubit, he will simply tell Alice to disregard it. Hence Eve only lowers the bit rate (possibly down to zero), but she does not gain any useful information. For real eavesdropping Eve must send a qubit to Bob. Ideally she would like to send this qubit in its original state, keeping a copy for herself.

#### 2. No-cloning theorem

Following Wootters and Zurek (1982) one can easily prove that perfect copying is impossible in the quantum world (see also the anticipatory intuition of Wigner in 1961, as well as Dieks, 1982 and Milonni and Hardies, 1982). Let $\psi$ denote the original state of the qubit, $|b\rangle$ the blank copy,[8] and $|0\rangle \in \mathcal{H}_{QCM}$ the initial state of Eve's "quantum copy machine," where the Hilbert space $\mathcal{H}_{QCM}$ of the quantum cloning machine is arbitrary. The ideal machine would produce

[5]For instance, it is amusing to note that physicists strive to publish in reputable journals, while conference proceedings are of secondary importance. For computer scientists, in contrast, appearance in the proceedings of the best conferences is considered more important, while journal publication is secondary.

[6]This terminology was introduced by Ekert and Huttner in 1994.

[7]Alice and Bob can, however, determine the statistics of the key.

[8]$|b\rangle$ corresponds to the stock of white paper in an everyday photocopy machine. We shall assume that the machine is not empty, a purely theoretical assumption, as is well known.

$$\psi\otimes|b\rangle\otimes|0\rangle\rightarrow\psi\otimes\psi\otimes|f_\psi\rangle, \tag{3}$$

where $|f_\psi\rangle$ denotes the final state of Eve's machine, which might depend on $\psi$. Accordingly, using obvious notations,

$$|\uparrow,b,0\rangle\rightarrow|\uparrow,\uparrow,f_\uparrow\rangle, \tag{4}$$

and

$$|\downarrow,b,0\rangle\rightarrow|\downarrow,\downarrow,f_\downarrow\rangle. \tag{5}$$

By linearity of quantum dynamics it follows that

$$|\rightarrow,b,0\rangle=\frac{1}{\sqrt{2}}(|\uparrow\rangle+|\downarrow\rangle)\otimes|b,0\rangle \tag{6}$$

$$\rightarrow\frac{1}{\sqrt{2}}(|\uparrow,\uparrow,f_\uparrow\rangle+|\downarrow,\downarrow,f_\downarrow\rangle). \tag{7}$$

But the latter state differs from the ideal copy $|\rightarrow,\rightarrow,f_\rightarrow\rangle$, whatever the states $|f_\psi\rangle$ are.

Consequently, Eve cannot keep a perfect quantum copy, because perfect quantum copy machines cannot exist. The possibility of copying classical information is probably one of the most characteristic features of information in the everyday sense. The fact that quantum states, nowadays often called quantum information, cannot be copied is certainly one of the most specific attributes that make this new kind of information so different and hence so attractive. Actually, this negative capability clearly has its positive side, since it prevents Eve from perfect eavesdropping and hence makes QC potentially secure.

### 3. Intercept-resend strategy

We have seen that the eavesdropper needs to send a qubit to Bob while keeping a necessarily imperfect copy for herself. How imperfect the copy has to be, according to quantum theory, is a delicate problem that we shall address in Sec. VI. Here, let us develop a simple eavesdropping strategy, called intercept-resend. This simple and even practical attack consists of Eve's measuring each qubit in one of the two bases, precisely as Bob does. Then, she resends to Bob another qubit in the state corresponding to her measurement result. In about half of the cases, Eve will be lucky and choose the basis compatible with the state prepared by Alice. In these cases she resends to Bob a qubit in the correct state, and Alice and Bob will not notice her intervention. However, in the other half of the cases, Eve unluckily uses the basis incompatible with the state prepared by Alice. This necessarily happens, since Eve has no information about Alice's random-number generator (hence the importance of this generator's being truly random). In these cases the qubits sent out by Eve are in states with an overlap of $\frac{1}{2}$ with the correct states. Alice and Bob thus discover her intervention in about half of these cases, since they get uncorrelated results. Altogether, if Eve uses this intercept-resend strategy, she gets 50% information, while Alice and Bob have about a 25% error rate in their sifted key, i.e., after they eliminate the cases in which they used incompatible states, there is still about 25% error. They can thus easily detect the presence of Eve. If, however, Eve applies this strategy to only a fraction of the communication, say 10%, then the error rate will be only ≈2.5%, while Eve's information will be ≈5%. The next section explains how Alice and Bob can counter such attacks.

### 4. Error correction, privacy amplification, and quantum secret growing

At this point in the BB84 protocol, Alice and Bob share a so-called sifted key. But this key contains errors. The errors are caused by technical imperfections, as well as possibly by Eve's intervention. Realistic error rates in the sifted key using today's technology are of the order of a few percent. This contrasts strongly with the $10^{-9}$ error rate typical in optical communication. Of course, the few-percent error rate will be corrected down to the standard $10^{-9}$ during the (classical) error correction step of the protocol. In order to avoid confusion, especially among optical communication specialists, Beat Perny from Swisscom and Paul Townsend, then with British Telecommunications (BT), proposed naming the error rate in the sifted key QBER, for quantum bit error rate, to clearly distinguish it from the bit error rate (BER) used in standard communications.

Such a situation, in which legitimate partners share classical information with high but not 100% correlation and with possibly some correlation to a third party, is common to all quantum cryptosystems. Actually, it is also a standard starting point for classical information-based cryptosystems in which one assumes that somehow Alice, Bob, and Eve have random variables $\alpha$, $\beta$, and $\epsilon$, respectively, with a joint probability distribution $P(\alpha,\beta,\epsilon)$. Consequently, the last step in a QC protocol uses classical algorithms, first to correct the errors, and then reduce to Eve's information on the final key, a process called *privacy amplification*.

The first mention of privacy amplification appeared in Bennett, Brassard, and Robert (1988). It was then extended in collaboration with C. Crépeau from the University of Montreal and U. Maurer of ETH, Zürich, respectively (Bennett, Brassard, *et al.* 1995; see also Bennett, Bessette, *et al.*, 1992). Interestingly, this work motivated by QC found applications in standard information-based cryptography (Maurer, 1993; Maurer and Wolf, 1999).

Assume that a joint probability distribution $P(\alpha,\beta,\epsilon)$ exists. Near the end of this section, we shall comment on this assumption. Alice and Bob have access only to the marginal distribution $P(\alpha,\beta)$. From this and from the laws of quantum mechanics, they have to deduce constraints on the complete scenario $P(\alpha,\beta,\epsilon)$; in particular they have to bound Eve's information (see Secs. VI.E and VI.G). Given $P(\alpha,\beta,\epsilon)$, necessary and sufficient

conditions for a positive secret-key rate between Alice and Bob, $S(\alpha,\beta\|\epsilon)$, are not yet known. However, a useful lower bound is given by the difference between Alice and Bob's mutual Shannon information $I(\alpha,\beta)$ and Eve's mutual information (Csiszár and Körner, 1978, and Theorem 1 in Sec. VI.G):

$$S(\alpha,\beta\|\epsilon)\geq\max\{I(\alpha,\beta)-I(\alpha,\epsilon),I(\alpha,\beta)-I(\beta,\epsilon)\}. \quad (8)$$

Intuitively, this result states that secure-key distillation (Bennett, Bessette, *et al.*, 1992) is possible whenever Bob has more information than Eve.

The bound (8) is tight if Alice and Bob are restricted to one-way communication, but for two-way communication, secret-key agreement might be possible even when condition (8) is not satisfied (see Sec. II.C.5).

Without discussing any algorithm in detail, let us offer some idea of how Alice and Bob can establish a secret key when condition (8) is satisfied. First, once the sifted key is obtained (i.e., after the bases have been announced), Alice and Bob publicly compare a randomly chosen subset of it. In this way they estimate the error rate [more generally, they estimate their marginal probability distribution $P(\alpha,\beta)$]. These publicly disclosed bits are then discarded. Next, either condition (8) is not satisfied and they stop the protocol or condition (8) is satisfied and they use some standard error correction protocol to get a shorter key without errors.

With the simplest error correction protocol, Alice randomly chooses pairs of bits and announces their XOR value (i.e., their sum modulo 2). Bob replies either "accept" if he has the same XOR value for his corresponding bits, or "reject" if not. In the first case, Alice and Bob keep the first bit of the pair and discard the second one, while in the second case they discard both bits. In reality, more complex and efficient algorithms are used.

After error correction, Alice and Bob have identical copies of a key, but Eve may still have some information about it [compatible with condition (8)]. Alice and Bob thus need to reduce Eve's information to an arbitrarily low value using some privacy amplification protocols. These classical protocols typically work as follows. Alice again randomly chooses pairs of bits and computes their XOR value. But, in contrast to error correction, she does not announce this XOR value. She only announces which bits she chose (e.g., bits number 103 and 537). Alice and Bob then replace the two bits by their XOR value. In this way they shorten their key while keeping it error free, but if Eve has only partial information on the two bits, her information on the XOR value is even less. Assume, for example, that Eve knows only the value of the first bit and nothing about the second one. Then she has no information at all about the XOR value. Also, if Eve knows the value of both bits with 60% probability, then the probability that she correctly guesses the XOR value is only $0.6^2+0.4^2=52\%$. This process would have to be repeated several times; more efficient algorithms use larger blocks (Brassard and Salvail, 1994).

The error correction and privacy amplification algorithms sketched above are purely classical algorithms. This illustrates that QC is a truly interdisciplinary field.

Actually, the above scenario is incomplete. In this presentation, we have assumed that Eve measures her probe before Alice and Bob run the error correction and privacy amplification algorithms, hence that $P(\alpha,\beta,\epsilon)$ exists. In practice this is a reasonable assumption, but in principle Eve could wait until the end of all the protocols and then optimize her measurements accordingly. Such "delayed-choice eavesdropping strategies"[9] are discussed in Sec. VI.

It should by now be clear that QC does not provide a complete solution for all cryptographic purposes.[10] Actually, quite the contrary, QC can only be used as a complement to standard symmetrical cryptosystems. Accordingly, a more precise name for QC is *quantum key distribution*, since this is all QC does. Nevertheless, we prefer to keep the well-known terminology, which lends its name to the title of this review.

Finally, let us emphasize that every key distribution system must incorporate some authentication scheme: the two parties must identify themselves. If not, Alice could actually be communicating directly with Eve. A straightforward approach is for Alice and Bob initially to share a short secret. Then QC provides them with a longer one and they each keep a small portion for authentication at the next session (Bennett, Bessette, *et al.*, 1992). From this perspective, QC is a *quantum secret-growing* protocol.

### 5. Advantage distillation

QC has motivated and still motivates research in classical information theory. The best-known example is probably the development of privacy amplification algorithms (Bennett *et al.*, 1988, 1995). This in turn led to the development of new cryptosystems based on weak but classical signals, emitted for instance by satellites (Maurer, 1993).[11] These new developments required secret-key agreement protocols that could be used even when condition (8) did not apply. Such protocols, called *advantage distillation*, necessarily use two-way communication and are much less efficient than privacy amplification. Usually, they are not considered in the literature on QC, but conceptually they are remarkable from at least two points of view. First, it is somewhat surprising that secret-key agreement is possible even if Alice and Bob start with less mutual (Shannon) information than Eve. They can take advantage of the authenticated public

[9]Note, however, that Eve has to choose the interaction between her probe and the qubits before the public discussion phase of the protocol.

[10]For a while it was thought that *bit commitment* (see, for example, Brassard, 1988), a powerful primitive in cryptology, could be realized using quantum principles. However, Dominic Mayers (1996a, 1997) and Lo and Chau (1998) proved it to be impossible (see also Brassard *et al.*, 1998).

[11]Note that here confidentiality is not guaranteed by the laws of physics, but relies on the assumption that Eve's technology is limited, e.g., her antenna is finite, and her detectors have limited efficiencies.

channel to decide which series of realizations to keep, whereas Eve cannot influence this process[12] (Maurer, 1993; Maurer and Wolf, 1999).

Recently, a second remarkable feature of advantage distillation, connecting quantum and classical secret-key agreement, has been discovered (assuming one uses the Ekert protocol described in Sec. II.D.3): If Eve follows a strategy that optimizes her Shannon information, under the assumption that she attacks the qubits one at a time (the so-called individual attack; see Sec. VI.E), then Alice and Bob can use advantage distillation if and only if Alice and Bob's qubits are still entangled (they can thus use quantum privacy amplification; Deutsch *et al.*, 1996; Gisin and Wolf, 1999). This connection between the concept of *entanglement*, central to quantum information theory, and the concept of *intrinsic classical information*, central to classical information-based cryptography (Maurer and Wolf, 1999), has been shown to be general (Gisin and Wolf, 2000). The connection seems to extend even to *bound entanglement* (Gisin *et al.*, 2000).

### D. Other protocols

#### 1. Two-state protocol

In 1992 Bennett noticed that four states are more than are really necessary for QC: only two nonorthogonal states are needed. Indeed the security of QC relies on the inability of an adversary to distinguish unambiguously and without perturbation between the different states that Alice may send to Bob; hence two states are necessary, and if they are incompatible (i.e., not mutually orthogonal), then two states are also sufficient (Bennett, 1992). This is a conceptually important clarification. It also made several of the first experimental demonstrations easier (as is discussed further in Sec. IV.D). But in practice, it is not a good solution. Indeed, although two nonorthogonal states cannot be distinguished unambiguously without perturbation, one can unambiguously distinguish between them at the cost of some losses (Ivanovic, 1987; Peres, 1988). This possibility has been demonstrated in practice (Huttner, Gautier, *et al.*, 1996; Clarke *et al.*, 2000). Alice and Bob would have to monitor the attenuation of the quantum channel (and even this would not be entirely safe if Eve were able to replace the channel by a more transparent one; see Sec. VI.H). The two-state protocol can also be implemented using interference between a macroscopic bright pulse and a dim pulse with less than one photon on average (Bennett, 1992). The presence of the bright pulse makes this protocol especially resistant to eavesdropping, even in settings with high attenuation. Bob can monitor the bright pulses to make sure that Eve does not remove any. In this case, Eve cannot eliminate the dim pulse without revealing her presence, because the interference of the bright pulse with vacuum would introduce errors. A practical implementation of this so-called 892 protocol is discussed in Sec. IV.D. Huttner *et al.* extended this reference-beam monitoring to the four-state protocol in 1995.

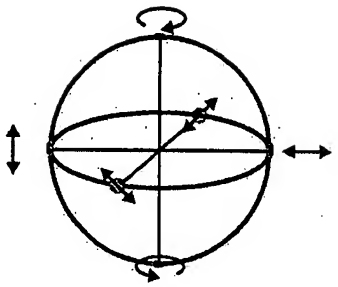

FIG. 2. Poincaré sphere with a representation of six states that can be used to implement the generalization of the BB84 protocol.

#### 2. Six-state protocol

While two states are enough and four states are standard, a six-state protocol better respects the symmetry of the qubit state space; see Fig. 2 (Bruss, 1998; Bechmann-Pasquinucci and Gisin, 1999). The six states constitute three bases, hence the probability that Alice and Bob choose the same basis is only $\frac{1}{3}$, but the symmetry of this protocol greatly simplifies the security analysis and reduces Eve's optimal information gain for a given error rate QBER. If Eve measures every photon, the QBER is 33%, compared to 25% in the case of the BB84 protocol.

#### 3. Einstein-Podolsky-Rosen protocol

This variation of the BB84 protocol is of special conceptual, historical, and practical interest. The idea is due to Artur Ekert (1991) of Oxford University, who, while elaborating on a suggestion of David Deutsch (1985), discovered QC independently of the BB84 paper. Intellectually, it is very satisfying to see this direct connection to the famous EPR paradox (Einstein, Podolski, and Rosen, 1935): the initially philosophical debate turned to theoretical physics with Bell's inequality (1964), then to experimental physics (Freedmann and Clauser, 1972; Fry and Thompson, 1976; Aspect *et al.*, 1982), and is now—thanks to Ekert's ingenious idea—part of applied physics.

The idea consists in replacing the quantum channel carrying two qubits from Alice to Bob by a channel carrying two qubits from a common source, one qubit to

[12]The idea is that Alice picks out several instances in which she got the same bit and communicates the instances—but not the bit—to Bob. Bob replies yes only if it happens that for all these instances he also has the same bit value. For high error rates this is unlikely, but when it does happen there is a high probability that both have the same bit. Eve cannot influence the choice of the instances. All she can do is use a majority vote for the cases accepted by Bob. The probability that Eve makes an error can be much higher than the probability that Bob makes an error (i.e., that all his instances are wrong), even if Eve has more initial information than Bob.

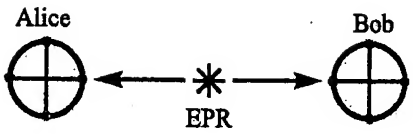


FIG. 3. Einstein-Podolsky-Rosen (EPR) protocol, with the source and a Poincaré representation of the four possible states measured independently by Alice and Bob.

Alice and one to Bob. A first possibility would be that the source always emits the two qubits in the same state chosen randomly among the four states of the BB84 protocol. Alice and Bob would then both measure their qubit in one of the two bases, again chosen independently and randomly. The source then announces the bases, and Alice and Bob keep the data only when they happen to have made their measurements in the compatible basis. If the source is reliable, this protocol is equivalent to that of BB84: It is as if the qubit propagates backwards in time from Alice to the source, and then forward to Bob. But better than trusting the source, which could be in Eve's hand, the Ekert protocol assumes that the two qubits are emitted in a maximally entangled state like

$$\phi^+=\frac{1}{\sqrt{2}}(|\uparrow,\uparrow\rangle+|\downarrow,\downarrow\rangle). \tag{9}$$

Then, when Alice and Bob happen to use the same basis, either the $x$ basis or the $y$ basis, i.e., in about half of the cases, their results are identical, providing them with a common key. Note the similarity between the one-qubit BB84 protocol illustrated in Fig. 1 and the two-qubit Ekert protocol of Fig. 3. The analogy can be made even stronger by noting that for all unitary evolutions $U_1$ and $U_2$, the following equality holds:

$$U_1\otimes U_2\Phi^{(+)}=1\otimes U_2U_1^t\Phi^{(+)}, \tag{10}$$

where $U_1^t$ denotes the transpose.

In his 1991 paper Ekert suggested basing the security of this two-qubit protocol on Bell's inequality, an inequality which demonstrates that some correlations predicted by quantum mechanics cannot be reproduced by any local theory (Bell, 1964). To do this, Alice and Bob can use a third basis (see Fig. 4). In this way the probability that they might happen to choose the same basis is reduced from $\frac{1}{2}$ to $\frac{2}{9}$, but at the same time as they establish a key, they collect enough data to test Bell's inequality.[13] They can thus check that the source really emits the entangled state (9) and not merely product states. The following year Bennett, Brassard, and Mermin (1992) criticized Ekert's letter, arguing that the violation of Bell's inequality is not necessary for the security of QC and emphasizing the close connection between the Ekert and the BB84 schemes. This criticism might be missing an important point. Although the exact relation between security and Bell's inequality is not yet fully known, there are clear results establishing fascinating connections (see Sec. VI.F). In October 1992, an article by Bennett, Brassard, and Ekert demonstrated that the founding fathers of QC were able to join forces to develop the field in a pleasant atmosphere (Bennett, Brassard, and Ekert, 1992).

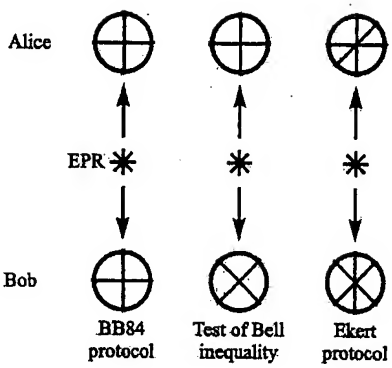


FIG. 4. Illustration of protocols exploiting EPR quantum systems. To implement the BB84 quantum cryptographic protocol, Alice and Bob use the same bases to prepare and measure their particles. A representation of their states on the Poincaré sphere is shown. A similar setup, but with Bob's bases rotated by 45°, can be used to test the violation of Bell's inequality. Finally, in the Ekert protocol, Alice and Bob may use the violation of Bell's inequality to test for eavesdropping.

### 4. Other variations

There is a large collection of variations on the BB84 protocol. Let us mention a few, chosen somewhat arbitrarily. First, one can assume that the two bases are not chosen with equal probability (Ardehali *et al.*, 1998). This has the nice consequence that the probability that Alice and Bob choose the same basis is greater than $\frac{1}{2}$, thus increasing the transmission rate of the sifted key. However, this protocol makes Eve's job easier, as she is more likely to guess correctly the basis that was used. Consequently, it is not clear whether the final key rate, after error correction and privacy amplification, is higher or not.

Another variation consists in using quantum systems of dimension greater than 2 (Bechmann-Pasquinucci and Peres, 2000; Bechmann-Pasquinucci and Tittel, 2000; Bourennane, Karlsson, and Björn, 2001). Again, the practical value of this idea has not yet been fully determined.

A third variation worth mentioning is due to Goldenberg and Vaidman of Tel Aviv University (1995). They suggested preparing the qubits in a superposition of two spatially separated states, then sending one component of this superposition and waiting until Bob receives it before sending the second component. This does not

[13] A maximal violation of Bell's inequality is necessary to rule out tampering by Eve. In this case, the QBER must necessarily be equal to zero. With a nonmaximal violation, as typically obtained in experimental systems, Alice and Bob can distill a secure key using error correction and privacy amplification.

sound of great practical value, but has the nice conceptual feature that the minimal two states do not need to be mutually orthogonal.

### E. Quantum teleportation as a "quantum one-time pad"

Since its discovery in 1993 by a surprisingly large group of physicists, quantum teleportation (Bennett *et al.*, 1993) has received much attention from both the scientific community and the general public. The dream of beaming travelers through the universe is exciting, but completely out of the realm of any foreseeable technology. However, quantum teleportation can be seen as the fully quantum version of the one-time pad (see Sec. II.B.3), hence as the ultimate form of QC. As in "classical teleportation," let us assume that Alice aims to transfer a faithful copy of a quantum system to Bob. If Alice has full knowledge of the quantum state, the problem is not really a quantum one (Alice's information is classical). If, on the other hand, Alice does not know the quantum state, she cannot send a copy, since quantum copying is impossible according to quantum physics (see Sec. II.C.2). Nor can she send classical instructions, since this would allow the production of many copies. However, if Alice and Bob share arbitrarily many entangled qubits, sometimes called a quantum key, and share a classical communication channel, then the quantum teleportation protocol provides them with a means of transferring the quantum state of the system from Alice to Bob. In the course of running this protocol, Alice's quantum system is destroyed without Alice's having learned anything about the quantum state, while Bob's qubit ends in a state isomorphic to the state of the original system (but Bob does not learn anything about the quantum state). If the initial quantum system is a quantum message coded in the form of a sequence of qubits, then this quantum message is faithfully and securely transferred to Bob, without any information leaking to the outside world (i.e., to anyone not sharing the prior entanglement with Alice and Bob). Finally, the quantum message could be formed of a four-letter quantum alphabet consisting of the four states of the BB84 protocol. With futuristic but not impossible technology, Alice and Bob could keep their entangled qubits in their respective wallets and could enjoy totally secure communication at any time, without even having to know where the other is located (provided they can communicate classically).

### F. Optical amplification, quantum nondemolition measurements, and optimal quantum cloning

After almost every general talk on QC, two questions arise: What about optical amplifiers? and What about quantum nondemolition measurements? In this section we briefly address these questions.

Let us start with the second one, as it is the easiest. The term "quantum nondemolition measurement" is simply confusing. There is nothing like a quantum measurement that does not perturb (i.e., modify) the quantum state, except if the state happens to be an eigenstate of the observable. Hence, if for some reason one conjectures that a quantum system is in some state (or in a state among a set of mutually orthogonal ones), one can in principle test this conjecture repeatedly (Braginsky and Khalili, 1992). However, if the state is only restricted to be in a finite set containing nonorthogonal states, as in QC, then there is no way to perform a measurement without "demolishing" (perturbing) the state. Now, in QC the term "nondemolition measurement" is also used with a different meaning: one measures the number of photons in a pulse without affecting the degree of freedom coding the qubit (e.g., the polarization; see Sec. VI.H), or one detects the presence of a photon without destroying it (Nogues *et al.*, 1999). Such measurements are usually called *ideal measurements*, or *projective measurements*, because they produce the least possible perturbation (Piron, 1990) and because they can be represented by projectors. It is important to stress that these "ideal measurements" do not invalidate the security of QC.

Let us now consider optical amplifiers (a laser medium, but without mirrors, so that amplification takes place in a single pass; see Desurvire, 1994). They are widely used in today's optical communication networks. However, they are of no use for quantum communication. Indeed, as seen in Sec. II.C, the copying of quantum information is impossible. Here we illustrate this characteristic of quantum information by the example of optical amplifiers: the necessary presence of spontaneous emission whenever there is stimulated emission prevents perfect copying. Let us clarify this important and often confusing point, following the work of Simon *et al.* (1999, 2000; see also De Martini *et al.*, 2000 and Kempe *et al.*, 2000). Let the two basic qubit states $|0\rangle$ and $|1\rangle$ be physically implemented by two optical modes: $|0\rangle \equiv |1,0\rangle$ and $|1\rangle \equiv |0,1\rangle$. Thus $|n,m\rangle_{ph} \otimes |k,l\rangle_a$ denotes the state of $n$ photons in mode 1 and $m$ photons in mode 2, while $k,l = 0(1)$ denotes the ground (or excited) state of two-level atoms coupled to mode 1 or 2, respectively. Hence spontaneous emission corresponds to

$$|0,0\rangle_{ph} \otimes |1,0\rangle_a \rightarrow |1,0\rangle_{ph} \otimes |0,0\rangle_a , \tag{11}$$

$$|0,0\rangle_{ph} \otimes |0,1\rangle_a \rightarrow |0,1\rangle_{ph} \otimes |0,0\rangle_a , \tag{12}$$

and stimulated emission to

$$|1,0\rangle_{ph} \otimes |1,0\rangle_a \rightarrow \sqrt{2}|2,0\rangle_{ph} \otimes |0,0\rangle_a , \tag{13}$$

$$|0,1\rangle_{ph} \otimes |0,1\rangle_a \rightarrow \sqrt{2}|0,2\rangle_{ph} \otimes |0,0\rangle_a , \tag{14}$$

where the factor of $\sqrt{2}$ takes into account the ratio of stimulated to spontaneous emission. Let the initial state of the atom be a mixture of the following two states, each with equal (50%) weight:

$$|0,1\rangle_a \text{ and } |1,0\rangle_a . \tag{15}$$

By symmetry, it suffices to consider one possible initial state of the qubit, e.g., one photon in the first mode $|1,0\rangle_{ph}$. The initial state of the photon+atom system is thus a mixture:

$$|1,0\rangle_{ph}\otimes|1,0\rangle_a \quad \text{or} \quad |1,0\rangle_{ph}\otimes|0,1\rangle_a. \tag{16}$$

This corresponds to the first-order term in an evolution with a Hamiltonian (in the interaction picture): $H=\chi(a_1^\dagger\sigma_1^- + a_1\sigma_1^\dagger + a_2^\dagger\sigma_2^- + a_2\sigma_2^\dagger)$. After some time the two-photon component of the evolved states becomes

$$\sqrt{2}|2,0\rangle_{ph}\otimes|0,0\rangle_a \quad \text{or} \quad |1,1\rangle_{ph}\otimes|0,0\rangle_a. \tag{17}$$

The correspondence with a pair of spin $\frac{1}{2}$ goes as follows:

$$|2,0\rangle=|\uparrow\uparrow\rangle, \quad |0,2\rangle=|\downarrow\downarrow\rangle, \tag{18}$$

$$|1,1\rangle_{ph}=\psi^{(+)}=\frac{1}{\sqrt{2}}(|\uparrow\downarrow\rangle+|\downarrow\uparrow\rangle). \tag{19}$$

Tracing over the amplifier (i.e., the two-level atom), an (ideal) amplifier achieves the following transformation:

$$P_\uparrow \rightarrow 2P_{\uparrow\uparrow}+P_{\psi^{(+)}}, \tag{20}$$

where the $P$'s indicate projectors (i.e., pure-state density matrices) and the lack of normalization results from the first-order expansion used in Eqs. (11)–(14). Accordingly, after normalization, each photon is in the state

$$\mathrm{Tr}_{1-ph\ mode}\left(\frac{2P_{\uparrow\uparrow}+P_{\psi^{(+)}}}{3}\right)=\frac{2P_\uparrow+\frac{1}{2}1}{3}. \tag{21}$$

The corresponding fidelity is

$$F=\frac{2+\frac{1}{2}}{3}=\frac{5}{6}, \tag{22}$$

which is precisely the optimal fidelity compatible with quantum mechanics (Buzek and Hillery, 1996; Gisin and Massar, 1997; Bruss *et al.*, 1998). In other words, if we start with a single photon in an arbitrary state and pass it through an amplifier, then due to the effect of spontaneous emission the fidelity of the state exiting the amplifier, when it consists of exactly two photons, with the initial state will be equal to at most 5/6. Note that if it were possible to make better copies, then signaling at arbitrarily fast speed, using EPR correlations between spatially separated systems, would also be possible (Gisin, 1998).

## III. TECHNOLOGICAL CHALLENGES

The very first demonstration of QC was a table-top experiment performed at the IBM laboratory in the early 1990s over a distance of 30 cm (Bennett, Bessette, *et al.*, 1992), marking the start of a series of impressive experimental improvements over the past few years. The 30-cm distance is of little practical interest. Either the distance should be even shorter [think of a credit card and an ATM machine (Huttner, Imoto, and Barnett, 1996), in which case all of Alice's components should fit on the credit card—a nice idea, but still impractical with present technology] or the distance should be much longer, at least in the kilometer range. Most of the research so far uses optical fibers to guide the photons from Alice to Bob, and we shall mainly concentrate on such systems here. There is also, however, some very significant research on free-space systems (see Sec. IV.E).

Once the medium has been chosen, there remain the questions of the source and detectors. Since they have to be compatible, the crucial choice is that of the wavelength. There are two main possibilities. Either one chooses a wavelength around 800 nm, for which efficient photon counters are commercially available, or one chooses a wavelength compatible with today's telecommunications optical fibers, i.e., near 1300 or 1550 nm. The first choice requires free-space transmission or the use of special fibers, hence the installed telecommunications networks cannot be used. The second choice requires the improvement or development of new detectors, not based on silicon semiconductors, which are transparent above a wavelength of 1000 nm.

In the case of transmission using optical fibers, it is still unclear which of the two alternatives will turn out to be the best choice. If QC finds niche markets, it is conceivable that special fibers will be installed for that purpose. But it is equally conceivable that new commercial detectors will soon make it much easier to detect single photons at telecommunications wavelengths. Actually, the latter possibility is very likely, as several research groups and industries are already working on it. There is another good reason to bet on this solution: the quality of telecommunications fibers is much higher than that of any special fiber; in particular, the attenuation is much lower (this is why the telecommunications industry chose these wavelengths): at 800 nm, the attenuation is about 2 dB/km (i.e., half the photons are lost after 1.5 km), while it is only of the order of 0.35 and 0.20 dB/km at 1300 and 1550 nm, respectively (50% loss after about 9 and 15 km).[14]

In the case of free-space transmission, the choice of wavelength is straightforward, since the region where good photon detectors exist—around 800 nm—coincides with that where absorption is low. However, free-space transmission is restricted to line-of-sight links and is very weather dependent.

In the next sections we successively consider the questions of how to produce single photons (Sec. III.A), how to transmit them (Sec. III.B), how to detect single photons (Sec. III.C), and finally how to exploit the intrinsic randomness of quantum processes to build random generators (Sec. III.D).

### A. Photon sources

Optical quantum cryptography is based on the use of single-photon Fock states. Unfortunately, these states are difficult to realize experimentally. Nowadays, practical implementations rely on faint laser pulses or entangled photon pairs, in which both the photon and the photon-pair number distribution obey Poisson statistics.

[14]The losses in dB ($l_{db}$) can be calculated from the losses in percent ($l_{\%}$): $l_{dB}=-10\log_{10}[1-(l_{\%}/100)]$.

Hence both possibilities suffer from a small probability of generating more than one photon or photon pair at the same time. For large losses in the quantum channel, even small fractions of these multiphotons can have important consequences on the security of the key (see Sec. VI.H), leading to interest in "photon guns"; see Sec. III.A.3). In this section we briefly comment on sources based on faint pulses as well as on entangled photon pairs, and we compare their advantages and drawbacks.

### 1. Faint laser pulses

There is a very simple solution to approximate single-photon Fock states: coherent states with an ultralow mean photon number $\mu$. They can easily be realized using only standard semiconductor lasers and calibrated attenuators. The probability of finding $n$ photons in such a coherent state follows the Poisson statistics:

$$P(n,\mu)=\frac{\mu^n}{n!}e-\mu. \tag{23}$$

Accordingly, the probability that a nonempty weak coherent pulse contains more than one photon,

$$P(n>1|n>0,\mu)=\frac{1-P(0,\mu)-P(1,\mu)}{1-P(0,\mu)}$$

$$=\frac{1-e^{-\mu}(1+\mu)}{1-e^{-\mu}}\cong\frac{\mu}{2}, \tag{24}$$

can be made arbitrarily small. Weak pulses are thus extremely practical and have indeed been used in the vast majority of experiments. However, they have one major drawback. When $\mu$ is small, most pulses are empty: $P(n=0)\approx 1-\mu$. In principle, the resulting decrease in bit rate could be compensated for thanks to the achievable gigahertz modulation rates of telecommunications lasers. But in practice, the problem comes from the detectors' dark counts (i.e., a click without a photon's arriving). Indeed, the detectors must be active for all pulses, including the empty ones. Hence the total dark counts increase with the laser's modulation rate, and the ratio of detected photons to dark counts (i.e., the signal-to-noise ratio) decreases with $\mu$ (see Sec. IV.A). The problem is especially severe for longer wavelengths, at which photon detectors based on indium gallium arsenide semiconductors (InGaAs) are needed (see Sec. III.C), since the noise of these detectors explodes if they are opened too frequently (in practice with a rate larger than a few megahertz). This prevents the use of really low photon numbers, smaller than approximately 1%. Most experiments to date have relied on $\mu=0.1$, meaning that 5% of the nonempty pulses contain more than one photon. However, it is important to stress that, as pointed out by Lütkenhaus (2000), there is an optimal $\mu$ depending on the transmission losses.[15] After key distillation, the security is just as good with faint laser pulses as with Fock states. The price to pay for using such states is a reduction of the bit rate.

### 2. Photon pairs generated by parametric downconversion

Another way to create pseudo-single-photon states is the generation of photon pairs and the use of one photon as a trigger for the other one (Hong and Mandel, 1986). In contrast to the sources discussed earlier, the second detector must be activated only whenever the first one has detected a photon, hence when $\mu=1$, and not whenever a pump pulse has been emitted, therefore circumventing the problem of empty pulses.

The photon pairs are generated by spontaneous parametric downconversion in a $\chi^{(2)}$ nonlinear crystal.[16] In this process, the inverse of the well-known frequency doubling, one photon spontaneously splits into two daughter photons—traditionally called signal and idler photons—conserving total energy and momentum. In this context, momentum conservation is called phase matching and can be achieved despite chromatic dispersion by exploiting the birefringence of the nonlinear crystal. Phase matching allows one to choose the wavelength and determines the bandwidth of the downconverted photons. The latter is in general rather large and varies from a few nanometers up to some tens of nanometers. For the nondegenerate case one typically gets a bandwith of 5–10 nm, whereas in the degenerate case (where the central frequency of both photons is equal), the bandwidth can be as large as 70 nm.

This photon-pair creation process is very inefficient; typically it takes some $10^{10}$ pump photons to create one pair in a given mode.[17] The number of photon pairs per mode is thermally distributed within the coherence time of the photons and follows a Poissonian distribution for larger time windows (Walls and Milburn, 1995). With a pump power of 1 mW, about $10^6$ pairs per second can be collected in single-mode fibers. Accordingly, in a time window of roughly 1 ns, the conditional probability of finding a second pair, having already detected one, is $10^6\times 10^{-9}\approx 0.1\%$. In the case of continuous pumping, this time window is given by the detector resolution. Tolerating, for example, 1% of these multipair events, one can generate $10^7$ pairs per second using a realistic

[15]Contrary to a frequent misconception, there is nothing special about a $\mu$ value of 0.1, even though it has been selected by most experimentalists. The optimal value—i.e., the value that yields the highest key exchange rate after distillation—depends on the optical losses in the channel and on assumptions about Eve's technology (see Secs. VI.H and VI.I).

[16]For a review see Rarity and Tapster (1988), and for more recent developments see Kwiat *et al.* (1999), Tittel *et al.* (1999), Jennewein, Simon, *et al.* (2000), and Tanzilli *et al.* (2001).

[17]Recently we achieved a conversion rate of $10^{-6}$ using an optical waveguide in a periodically poled $LiNbO_3$ crystal (Tanzilli *et al.*, 2001).

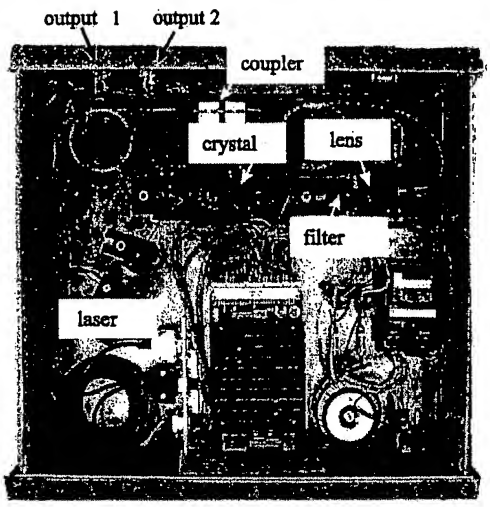


FIG. 5. Photo of our entangled photon-pair source as used in the first long-distance test of Bell's inequalities (Tittel *et al.*, 1998). Note that the whole source fits into a box only 40×45 ×15 $cm^3$ in size and that neither a special power supply nor water cooling is necessary.

10-mW pump. To detect, for example, 10% of the trigger photons, the second detector has to be activated $10^6$ times per second. In comparison, the example of 1% of multiphoton events corresponds in the case of faint laser pulses to a mean photon number of $\mu=0.02$. In order to get the same number ($10^6$) of nonempty pulses per second, a pulse rate of 50 MHz is needed. For a given photon statistics, photon pairs thus allow one to work with lower pulse rates (e.g., 50 times lower) and hence reduced detector-induced errors. However, due to limited coupling efficiency in optical fibers, the probability of finding the sister photon after detection of the trigger photon in the respective fiber is in practice less than 1. This means that the effective photon number is not 1 but rather $\mu\approx 2/3$ (Ribordy *et al.*, 2001), still well above $\mu=0.02$.

Photon pairs generated by parametric downconversion offer a further major advantage if they are not merely used as a pseudo-single-photon source, but if their entanglement is exploited. Entanglement leads to quantum correlations that can be used for key generation (see Secs. II.D.3 and V). In this case, if two photon pairs are emitted within the same time window but their measurement basis is chosen independently, they produce completely uncorrelated results. Hence, depending on the realization, the problem of multiple photons can be avoided; see Sec. VI.J.

Figure 5 shows one of our sources creating entangled photon pairs at a wavelength of 1310 nm, as used in tests of Bell's inequalities over 10 kilometers (Tittel *et al.*, 1998). Although not as simple as faint laser sources, diode-pumped photon-pair sources emitting in the near infrared can be made compact, robust, and rather handy.

### 3. Photon guns

The ideal single-photon source is a device that, when one pulls the trigger, and only then, emits one and only one photon. Hence the name *photon gun*. Although photon antibunching was first demonstrated years ago (Kimble *et al.*, 1977), a practical and handy device is still awaited. At present, there are essentially three different experimental approaches that more or less come close to this ideal.

A first idea is to work with a single two-level quantum system that obviously cannot emit two photons at a time. The manipulation of single trapped atoms or ions requires a much too involved technical effort. Single organic dye molecules in solvents (Kitson *et al.*, 1998) or solids (Brunel *et al.*, 1999; Fleury *et al.*, 2000) are easier to handle but offer only limited stability at room temperature. A promising candidate, however, is the nitrogen-vacancy center in diamond, a substitutional nitrogen atom with a vacancy trapped at an adjacent lattice position (Brouri *et al.*, 2000; Kurtsiefer *et al.*, 2000). It is possible to excite individual nitrogen atoms with a 532-nm laser beam, which will subsequently emit a fluorescence photon around 700 nm (12-ns decay time). The fluorescence exhibits strong photon antibunching, and the samples are stable at room temperature. However, the big remaining experimental challenge is to increase the collection efficiency (currently about 0.1%) in order to obtain mean photon numbers close to 1. To obtain this efficiency, an optical cavity or a photonic band-gap structure must suppress emission in all spatial modes but one. In addition, the spectral bandwidth of this type of source is broad (on the order of 100 nm), enhancing the effect of perturbations in a quantum channel.

A second approach is to generate photons by single electrons in a mesoscopic *p-n* junction. The idea is to profit from the fact that thermal electrons show antibunching (the Pauli exclusion principle) in contrast to photons (Imamoglu and Yamamoto, 1994). The first experimental results have been presented (Kim *et al.*, 1999), but with extremely low efficiencies and only at a temperature of 50 mK!

Finally, another approach is to use the photon emission of electron-hole pairs in a semiconductor quantum dot. The frequency of the emitted photon depends on the number of electron-hole pairs present in the dot. After one creates several such pairs by optical pumping, they will sequentially recombine and hence emit photons at different frequencies. Therefore, a single-photon pulse can be obtained by spectral filtering (Gérard *et al.*, 1999; Michler *et al.*, 2000; Santori *et al.*, 2000). These dots can be integrated in solid-state microcavities with strong enhancements of spontaneous emission (Gérard *et al.*, 1998).

In summary, today's photon guns are still too complicated to be used in a QC prototype. Moreover, due to their low quantum efficiencies, they do not offer an advantage over faint laser pulses with extremely low mean photon numbers $\mu$.

### B. Quantum channels

The single-photon source and the detectors must be connected by a "quantum channel." Such a channel is not especially quantum, except that it is intended to carry information encoded in individual quantum systems. Here "individual" does not mean "nondecomposible," but only the opposite of "ensemble." The idea is that the information is coded in a physical system only once, in contrast to classical communication, in which many photons carry the same information. Note that the present-day limit for fiber-based classical optical communication is already down to a few tens of photons, although in practice one usually uses many more. With increasing bit rate and limited mean power—imposed to avoid nonlinear effects in silica fibers—these figures are likely to get closer and closer to the quantum domain.

Individual quantum systems are usually two-level systems, called qubits. During their propagation they must be protected from environmental noise. Here "environment" refers to everything outside the degree of freedom used for the encoding, which is not necessarily outside the physical system. If, for example, the information is encoded in the polarization state, then the optical frequencies of the photon are part of the environment. Hence coupling between the polarization and the optical frequency has to be mastered[18] (e.g., by avoiding wavelength-sensitive polarizers and birefringence). Moreover, the sender of the qubits should avoid any correlation between the polarization and the spectrum of the photons.

Another difficulty is that the bases used by Alice to code the qubits and the bases used by Bob for his measurements must be related by a known and stable unitary transformation. Once this unitary transformation is known, Alice and Bob can compensate for it and get the expected correlation between their preparations and measurements. If it changes with time, they need active feedback to track it, and if the changes are too fast, the communication must be interrupted.

#### 1. Single-mode fibers

Light is guided in optical fibers thanks to the refractive index profile $n(x,y)$ across the section of the fibers (traditionally, the $z$ axis is along the propagation direction). Over the last 25 years, a lot of effort has gone into reducing transmission losses—initially several dB per km—and today the attenuation is as low as 2 dB/km at 800-nm wavelength, 0.35 dB/km at 1310 nm, and 0.2 dB/km at 1550 nm (see Fig. 6). It is amusing to note that the dynamical equation describing optical pulse propagation (in the usual slowly varying envelope aproximation) is identical to the Schrödinger equation, with $V(x,y)=-n(x,y)$ (Snyder, 1983). Hence a positive bump in the refractive index corresponds to a potential well. The region of the well is called the fiber core. If the core is large, many bound modes exist, corresponding to many guided modes in the fiber. Such fibers are called multimode fibers, They usually have cores 50 $\mu$m in diameter. The modes couple easily, acting on the qubit like a nonisolated environment. Hence multimode fibers are not appropriate as quantum channels (see, however, Townsend, 1998a, 1998b). If, however, the core is small enough (diameter of the order of a few wavelengths), then a single spatial mode is guided. Such fibers are called single-mode fibers. For telecommunications wavelengths (i.e., 1.3 and 1.5 $\mu$m), their core is typically 8 $\mu$m in diameter. Single-mode fibers are very well suited to carry single quanta. For example, the optical phase at the output of a fiber is in a stable relation with the phase at the input, provided the fiber does not become elongated. Hence fiber interferometers are very stable, a fact exploited in many instruments and sensors (see, for example, Cancellieri, 1993).

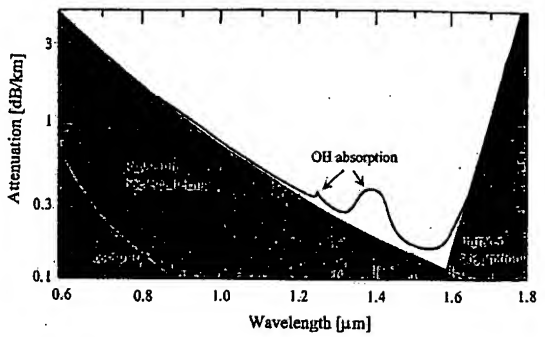


FIG. 6. Transmission losses vs wavelength in optical fibers. Electronic transitions in $SiO_2$ lead to absorption at lower wavelengths, and excitation of vibrational modes leads to losses at higher wavelengths. Superposed is the absorption due to Rayleigh backscattering and to transitions in OH groups. Modern telecommunications are based on wavelengths around 1.3 $\mu$m (the second telecommunications window) and 1.5 $\mu$m (the third telecommunications window).

Accordingly, a single-mode fiber with perfect cylindric symmetry would provide an ideal quantum channel. But all real fibers have some asymmetries, so that the two polarization modes are no longer degenerate, but rather each has its own propagation constant. A similar effect is caused by chromatic dispersion, in which the group delay depends on the wavelength. Both dispersion effects are the subject of the next subsections.

#### 2. Polarization effects in single-mode fibers

Polarization effects in single-mode fibers are a common source of problems in all optical communication schemes, classical as well as quantum ones. In recent years these effects have been the subject of a major research effort in classical optical communication (Gisin *et al.*, 1995). As a result, today's fibers are much better than the fibers of a decade ago. Today, the remaining birefringence is small enough for the telecommunications industry, but for quantum communication any

[18]Note that, as we shall see in Sec. V, using entangled photons prevents such information leakage.

birefringence, even extremely small, will always remain a concern. All fiber-based implementations of QC have to face this problem. This is clearly true for polarization-based systems, but it is equally a concern for phase-based systems, since interference visibility depends on the polarization states. Hence, although polarization effects are not the only source of difficulties, we shall describe them in some detail, distinguishing among four effects: the geometric phase, birefringence, polarization mode dispersion, and polarization-dependent losses.

The *geometric phase* as encountered when guiding light in an optical fiber is a special case of the Berry phase,[19] which results when any parameter describing a property of the system under concern, here the $k$ vector characterizing the propagation of the light field, undergoes an adiabatic change. Think first of a linear polarization state, let us say vertical at the input. Will it still be vertical at the output? Vertical with respect to what? Certainly not the gravitational field! One can follow that linear polarization by hand along the fiber and see how it may change even along a closed loop. If the loop stays in a plane, the state after a loop coincides with the input state, but if the loop explores the three dimensions of our space, then the final state will differ from the initial one by an angle. Similar reasoning holds for the axes of elliptical polarization states. The two circular polarization states are the eigenstates. During parallel transport they acquire opposite phases, called the Berry phases. The presence of a geometrical phase is not fatal for quantum communication. It simply means that initially Alice and Bob have to align their systems by defining, for instance, the vertical and diagonal directions (i.e., performing the unitary transformation mentioned before). If these vary slowly, they can be tracked, though this requires active feedback. However, if the variations are too fast, the communication might be interrupted. Hence aerial cables that swing in the wind are not appropriate (except with self-compensating configurations; see Sec. IV.C.2).

*Birefringence* is the presence of two different phase velocities for two orthogonal polarization states. It is caused by asymmetries in the fiber geometry and in the residual stress distribution inside and around the core. Some fibers are made birefringent on purpose. Such fibers are called polarization-maintaining fibers because the birefringence is large enough to effectively uncouple the two polarization eigenmodes. Note that only these two orthogonal polarization modes are maintained; all other modes, in contrast, evolve very quickly, making this kind of fiber completely unsuitable for polarization-based QC systems.[20] The global effect of the birefringence is equivalent to an arbitrary combination of two waveplates; that is, it corresponds to a unitary transformation. If this transformation is stable, Alice and Bob can compensate for it. The effect of birefringence is thus similar to the effect of the geometric phase, though, in addition to causing a rotation, it may also affect the ellipticity. Stability of birefringence requires slow thermal and mechanical variations.

*Polarization mode dispersion* (PMD) is the presence of two different group velocities for two orthogonal polarization modes. It is due to a delicate combination of two causes. First, birefringence produces locally two group velocities. For optical fibers, this local dispersion is in good approximation equal to the phase dispersion, of the order of a few picoseconds per kilometer. Hence, an optical pulse tends to split locally into a fast mode and a slow mode. But because the birefringence is small, the two modes couple easily. Hence any small imperfection along the fiber produces polarization mode coupling: some energy of the fast mode couples into the slow mode and vice versa. PMD is thus similar to a random walk[21] and grows only with the square root of the fiber length. It is expressed in $\mathrm{ps\,km^{-1/2}}$, with values as low as 0.1 $\mathrm{ps\,km^{-1/2}}$ for modern fibers and possibly as high as 0.5 or even $1\,\mathrm{ps\,km^{-1/2}}$ for older ones.

Typical lengths for polarization mode coupling vary from a few meters up to hundreds of meters. The stronger the coupling, the weaker the PMD (the two modes do not have time to move apart between the couplings). In modern fibers, the couplings are even artificially increased during the drawing process of the fibers (Hart *et al.*, 1994; Li and Nolan, 1998). Since the couplings are exceedingly sensitive, the only reasonable description is a statistical one, hence PMD is described as a statistical distribution of delays $\delta\tau$. For sufficiently long fibers, the statistics are Maxwellian, and PMD is related to the fiber length $\ell$, the mean coupling length $h$, the mean modal birefringence $B$, and the rms delay as follows (Gisin *et al.*, 1995): $\mathrm{PMD} \equiv \sqrt{\langle\langle \delta\tau^2 \rangle\rangle} = Bh\sqrt{\ell/h}$. Polarization mode dispersion could cause depolarization, which would be devastating for quantum communication, similar to any decoherence in quantum information processing. Fortunately, for quantum communication the remedy is easy; it suffices to use a source with a coherence time longer than the largest delay $\delta\tau$. Hence, when laser pulses are used (with typical spectral widths $\Delta\lambda \leq 1$ nm, corresponding to a coherence time $\geq 3$ ps; see Sec. III.A.1), PMD is no real problem. For photons cre-

[19]The Berry phase was introduced by Michael Berry in 1984, and was then observed in optical fiber by Tomita and Chiao (1986) and on the single-photon level by Hariharan *et al.* (1993). It was studied in connection with photon pairs by Brendel *et al.* (1995).

[20]Polarization-maintaining fibers may be of use for phase-based QC systems. However, this requires that the whole setup—transmission lines as well as interferometers at each end—be made of polarization-maintaining fibers. While this is possible in principle, the need to install a completely new fiber network makes this solution not very practical.

[21]In contrast to Brownian motion, which describes particle diffusion in space as time passes, here photons diffuse over time as they propagate along the fiber.

ated by parametric downconversion, however, PMD can impose severe limitations, since $\Delta\lambda \geqslant 10$ nm (coherence time $\leqslant 300$ fs) is not unusual.

*Polarization-dependent loss* is a differential attenuation between two orthogonal polarization modes. This effect is negligible in fibers, but can be significant in components like phase modulators. In particular, some integrated optics waveguides actually guide only one mode and thus behave almost like polarizers (e.g., proton exchange waveguides in $LiNbO_3$). Polarization-dependent losses are usually stable, but if connected to a fiber with some birefringence, the relation between the polarization state and the loss may fluctuate, producing random outcomes (Elamari *et al.*, 1998). Polarization-dependent loss cannot be described by a unitary operator acting in the polarization state space (but it is of course unitary in a larger space (Huttner, Gautier, *et al.*, 1996). Thus it does not preserve the scalar product. In particular, it can turn nonorthogonal states into orthogonal ones, which can then be distinguished unambiguously (at the cost of some loss; Huttner, Gautier, *et al.*, 1996; Clarke *et al.*, 2000). Note that this attenuation could be used by Eve, especially to eavesdrop on the two-state protocol (Sec. II.D.1).

Let us conclude this section on polarization effects in fibers by mentioning that they can be passively compensated for, provided one uses a go-and-return configuration, with Faraday mirrors, as described in Sec. IV.C.2.

### 3. Chromatic dispersion effects in single-mode fibers

In addition to polarization effects, chromatic dispersion can also cause problems for quantum cryptography. For instance, as explained in Secs. IV.C and V.B, schemes implementing phase or phase-and-time coding rely on photons arriving at well-defined times, that is, on photons well localized in space. However, in dispersive media like optical fibers, different group velocities act as a noisy environment on the localization of the photon as well as on the phase acquired in an interferometer. Hence the broadening of photons featuring nonzero bandwidth, or, in other words, the coupling between frequency and position, must be circumvented or controlled. This implies working with photons of small bandwidth, or, as long as the bandwidth is not too large, operating close to the wavelength $\lambda_0$ at which chromatic dispersion is zero, i.e., for standard fibers around 1310 nm. Fortunately, fiber losses are relatively small at this wavelength and amount to $\approx 0.35$ dB/km. This region is called the second telecommunications window.[22] There are also special fibers, called dispersion-shifted fibers, with a refractive index profile such that the chromatic dispersion goes to zero around 1550 nm, where the attenuation is minimal (Neumann, 1988).[23]

Chromatic dispersion does not constitute a problem in the case of faint laser pulses, for which the bandwidth is small. However, it becomes a serious issue when utilizing photon pairs created by parametric downconversion. For instance, sending photons of 70-nm bandwidth (as used in our long-distance tests of Bell's inequality; Tittel *et al.*, 1998) down 10 km of optical fibers leads to a temporal spread of around 500 ps (assuming photons centered at $\lambda_0$ and a typical dispersion slope of $0.086\ \mathrm{ps\,nm^{-2}\,km^{-1}}$). However, this can be compensated for when using energy-time-entangled photons (Franson, 1992; Steinberg *et al.*, 1992a, 1992b, Larchuk *et al.*, 1995). In contrast to polarization coding, in which frequency and the physical property used to implement the qubit are not conjugate variables, frequency and time (thus position) constitute a Fourier pair. The strict energy anticorrelation of signal and idler photons enables one to achieve a dispersion for one photon that is equal in magnitude but opposite in sign to that of the sister photon, thus corresponding to the same delay[24] (see Fig. 7). The effect of broadening of the two wave packets then cancels out, and two simultaneously emitted photons stay coincident. However, note that the arrival time of the pair varies with respect to its emission time. The frequency anticorrelation also provides the basis for avoiding a decrease in visibility due to different wave packet broadening in the two arms of an interferometer. Since the choromatic dispersion properties of optical fibers do not change with time—in contrast to birefringence—no active tracking and compensation are required. It thus turns out that phase and phase-time coding are particularly suited to transmission over long distances in optical fibers: nonlinear effects decohering the qubit "energy" are completely negligible, and chromatic dispersion effects acting on the localization can be avoided or compensated for in many cases.

### 4. Free-space links

Although today's telecommunications based on optical fibers are very advanced, such channels may not always be available. Hence there is also some effort in developing free-space line-of-sight communication sys-

[22]The first one, around 800 nm, is almost no longer used. It was motivated by the early existence of sources and detectors at this wavelength. The third window is around 1550 nm, where the attenuation reaches an absolute minimum (Thomas *et al.*, 2000) and where erbium-doped fibers provide convenient amplifiers (Desurvire, 1994).

[23]Chromatic dispersion in fibers is mainly due to the material, essentially silicon, but also to the refractive index profile. Indeed, longer wavelengths feel regions farther away from the core where the refractive index is lower. Dispersion-shifted fibers have, however, been abandoned by today's industry, because it has turned out to be simpler to compensate for the global chromatic dispersion by adding an extra fiber with high negative dispersion. The additional loss is then compensated for by an erbium-doped fiber amplifier.

[24]Here we assume a predominantly linear dependence of chromatic dispersion as a function of the optical frequency, a realistic assumption.

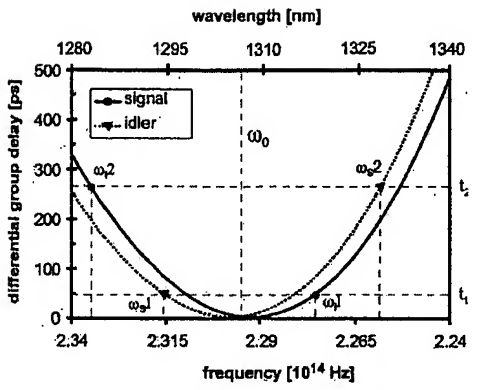


FIG. 7. Illustration of cancellation of chromatic dispersion effects in the fibers connecting an entangled-particle source and two detectors. The figure shows differential group delay curves for two slightly different fibers approximately 10 km long. Using frequency-correlated photons with central frequency $\omega_0$—determined by the properties of the fibers—the difference in propagation times $t_2-t_1$ between the signal (at $\omega_s 1,\omega_s 2$) and idler (at $\omega_i 1,\omega_i 2$) photon is the same for all $\omega_s,\omega_i$. Note that this cancellation scheme is not restricted to signal and idler photons at nearly equal wavelengths. It also applies to asymmetrical setups in which the signal photon (generating the trigger to indicate the presence of the idler photon) is at a short wavelength of around 800 nm and travels only a short distance. Using a fiber with appropriate zero dispersion wavelength $\lambda_0$, it is still possible to achieve equal differential group delay with respect to the energy-correlated idler photon sent through a long fiber at a telecommunications wavelength.

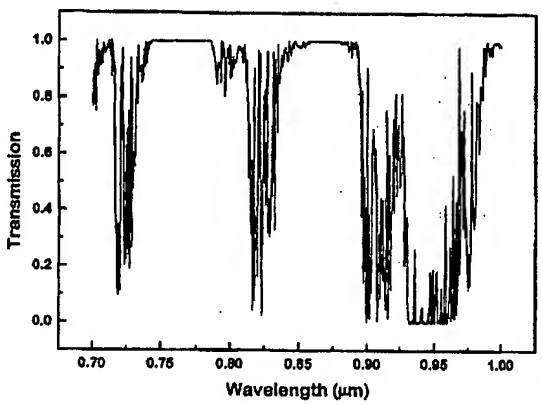


FIG. 8. Transmission losses in free space as calculated using the LOWTRAN code for earth-to-space transmission at the elevation and location of Los Alamos, USA. Note that there is a low-loss window at around 770 nm—a wavelength at which high-efficiency silicon APD's can be used for single-photon detection (see also Fig. 9 and compare to Fig. 6). Figure courtesy of Richard Hughes.

tems, not only for classical data transmission but also for quantum cryptography (see Hughes, Buttler, *et al.*, 2000 and Gorman *et al.*, 2000).

Transmission over free space features some advantages compared to the use of optical fibers. The atmosphere has a high transmission window at a wavelength of around 770 nm (see Fig. 8), where photons can easily be detected using commercial, high-efficiency photon-counting modules (see Sec. III.C.1). Furthermore, the atmosphere is only weakly dispersive and essentially nonbirefringent[25] at these wavelengths. It will thus not alter the polarization state of a photon.

However, there are some drawbacks concerning free-space links as well. In contrast to the signal transmitted in a guiding medium where the energy is "protected" and remains localized in a small region of space, the energy transmitted via a free-space link spreads out, leading to higher and varying transmission losses. In addition to loss of energy, ambient daylight, or even moonlight at night, can couple into the receiver, leading to a higher error rate. However, such errors can be kept to a reasonable level by using a combination of spectral filtering (interference filters $\leq 1$ nm), spatial filtering at the receiver, and timing discrimination using a coincidence window of typically a few nanoseconds. Finally, it is clear that the performance of free-space systems depends dramatically on atmospheric conditions and is possible only in clear weather.

Finally, let us briefly comment on the different sources leading to coupling losses. A first concern is the transmission of the signals through a turbulent medium, leading to *arrival-time jitter* and *beam wander* (hence problems with *beam pointing*). However, as the time scales for atmospheric turbulences involved are rather small—around 0.1–0.01 s—the time jitter due to a variation of the effective refractive index can be compensated for by sending a reference pulse at a different wavelength a short time (around 100 ns) before each signal pulse. Since this reference pulse experiences the same atmospheric conditions as the subsequent one, the signal will arrive essentially without jitter in the time window defined by the arrival of the reference pulse. In addition, the reference pulse can be reflected back to the transmitter and used to correct the direction of the laser beam by means of adaptive optics, hence compensating for beam wander and ensuring good beam pointing.

Another issue is beam divergence, hence increase of spot size at the receiver end caused by diffraction at the transmitter aperture. Using, for example, 20-cm-diameter optics, one obtains a diffraction-limited spot size after 300 km of $\approx 1$ m. This effect can in principle be kept small by taking advantage of larger optics. However, it can also be advantageous to have a spot size that is large compared to the receiver's aperture in order to ensure constant coupling in case of remaining beam wander. In their 2000 paper, Gilbert and Hamrick provide a comprehensive discussion of free-space channels in the context of QC.

### C. Single-photon detection

With the availability of pseudo-single-photon and photon-pair sources, the success of quantum cryptogra-

[25]In contrast to an optical fiber, air is not subject to stress and is hence isotropic.

phy essentially depends on the ability to detect single photons. In principle, this can be achieved using a variety of techniques, for instance, photomultipliers, avalanche photodiodes, multichannel plates, and superconducting Josephson junctions. The ideal detector should fulfill the following requirements:

- the quantum detection efficiency should be high over a large spectral range,
- the probability of generating noise, that is, a signal without an arriving photon, should be small,
- the time between detection of a photon and generation of an electrical signal should be as constant as possible, i.e., the time jitter should be small, to ensure good timing resolution,
- the recovery time (i.e., the dead time) should be short to allow high data rates.

In addition, it is important to keep the detectors practical. For instance, a detector that needs liquid helium or even nitrogen cooling would certainly render commercial development difficult.

Unfortunately, it turns out that it is impossible to fulfill all the above criteria at the same time. Today, the best choice is avalanche photodiodes (APD's). Three different semiconductor materials are used: either silicon, germanium, or indium gallium arsenide, depending on the wavelengths.

APDs are usually operated in the so-called *Geiger mode.* In this mode, the applied voltage exceeds the breakdown voltage, leading an absorbed photon to trigger an electron avalanche consisting of thousands of carriers. To reset the diode, this macroscopic current must be quenched—the emission of charges must be stopped and the diode recharged (Cova *et al.*, 1996). Three main possibilities exist:

- In *passive-quenching* circuits, a large (50–500 kΩ) resistor is connected in series with the APD (see, for example, Brown *et al.*, 1986). This causes a decrease in the voltage across the APD as soon as an avalanche starts. When it drops below breakdown voltage, the avalanche stops and the diode recharges. The recovery time of the diode is given by its capacitance and by the value of the quench resistor. The maximum count rate varies from a few hundred kilohertz to a few megahertz.
- In *active-quenching* circuits, the bias voltage is actively lowered below the breakdown voltage as soon as the leading edge of the avalanche current is detected (see, for example, Brown *et al.*, 1987). This mode makes possible higher count rates than those in passive quenching (up to tens of megahertz), since the dead time can be as short as tens of nanoseconds. However, the fast electronic feedback system makes active-quenching circuits much more complicated than passive ones.
- Finally, in *gated-mode* operation, the bias voltage is kept below the breakdown voltage and is raised above it only for a short time, typically a few nanosecods when a photon is expected to arrive. Maximum count rates similar to those in active-quenching circuits can be obtained using less complicated electronics. Gated-mode operation is commonly used in quantum cryptography based on faint laser pulses, for which the arrival times of the photons are well known. However, it only applies if prior timing information is available. For two-photon schemes, it is most often combined with a passive-quenched detector, generating the trigger signal for the gated detector.

In addition to Geiger mode, Brown and Daniels (1989) have investigated the performance of silicon APD's operated in *sub-Geiger mode.* In this mode, the bias voltage is kept slightly smaller than the breakdown voltage such that the multiplication factor—around 100—is sufficient to detect an avalanche, yet, is still small enough to prevent real breakdowns. Unfortunately, the single-photon counting performance in this mode is rather poor, and thus efforts have not been continued, the major problem being the need for extremely low-noise amplifiers.

An avalanche engendered by carriers created in the conduction band of the diode can be set off not only by an impinging photon, but also by unwanted causes. These might be thermal or band-to-band tunneling processes, or emissions from trapping levels populated while a current transits through the diode. The first two produce avalanches not due to photons and are referred to as *dark counts.* The third process depends on previous avalanches and its effects are called *afterpulses.* Since the number of trapped charges decreases exponentially with time, these afterpulses can be limited by applying large dead times. Thus there is a tradeoff between high count rates and low afterpulses. The time constant of the exponential decrease of afterpulses shortens for higher temperatures of the diode. Unfortunately, operating APD's at higher temperatures leads to a higher fraction of thermal noise, that is, higher dark counts. Thus there is again a tradeoff to be optimized. Finally, increasing the bias voltage leads to a higher quantum efficiency and a smaller time jitter, at the cost of an increase in noise.

We thus see that the optimal operating parameters—voltage, temperature, and dead time (i.e., maximum count rate)—depend on the specific application. Moreover, since the relative magnitudes of efficiency, thermal noise, and afterpulses vary with the type of semiconductor material used, no general solution exists. In the next two sections we briefly discuss the different types of APD's. The first section focuses on silicon APD's for the detection of photons at wavelengths below 1 $\mu$m; the second comments on germanium and on indium gallium arsenide APD's for photon counting at telecommunications wavelengths. The different behavior of the three types is shown in Fig. 9. Although the best figure of merit for quantum cryptography is the ratio of dark-count rate $R$ to detection efficiency $\eta$, we show here the better-known noise equivalent power (NEP), which shows similar behavior. The noise equivalent power is defined as the optical power required to measure a unity signal-to-noise ratio and is given by

$$NEP = \frac{h\nu}{\eta}\sqrt{2R}. \tag{25}$$

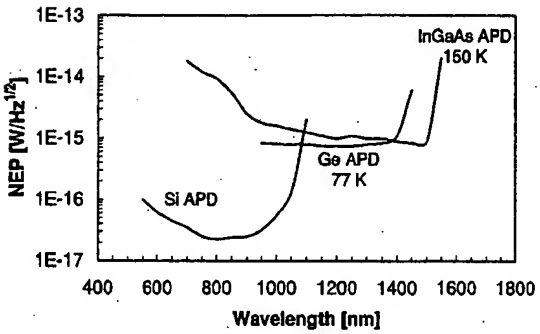


FIG. 9. Noise equivalent power as a function of wavelength for silicon, germanium, and InGaAs/InP APD's.

Here, $h$ is Planck's constant and $\nu$ is the frequency of the impinging photons.

1. Photon counting at wavelengths below 1.1 $\mu$m

Since the beginning of the 1980s much work has been done to characterize silicon APD's for single-photon counting (Ingerson 1983; Brown *et al.*, 1986, 1987; Brown and Daniels, 1989; Spinelli, 1996), and the performance of Si APD's has continuously been improved. Since the first test of Bell's inequality using Si APD's by Shih and Alley in 1988, they have completely replaced the photomultipliers used until then in the domain of fundamental quantum optics, now known as quantum communication. Today, quantum efficiencies of up to 76% (Kwiat *et al.*, 1993) and time jitter as low as 28 ps (Cova *et al.*, 1989) have been reported. Commercial single-photon counting modules are available (for example, EG&G SPCM-AQ-151), featuring quantum efficiencies of 70% at a wavelength of 700 nm, a time jitter of around 300 ps, and maximum count rates higher than 5 MHz. Temperatures of $-20\,^{\circ}$C—sufficient to keep thermally generated dark counts as low as 50 Hz—can easily be achieved using Peltier cooling. Single-photon counters based on silicon APD's thus offer an almost perfect solution for all applications in which photons of wavelengths below 1 $\mu$m can be used. Apart from fundamental quantum optics, these applications include quantum cryptography in free space and in optical fibers; however, due to high losses, the latter works only over short distances.

2. Photon counting at telecommunications wavelengths

When working in the second telecommunications window (1.3 $\mu$m), one can take advantage of APD's made from germanium or InGaAs/InP semiconductor materials. In the third window (1.55 $\mu$m), the only option is InGaAs/InP.

Photon counting with germanium APD's, although known for 30 years (Haecker *et al.*, 1971), began to be used in quantum communication as the need arose to transmit single photons over long distances using optical fibers, which necessitated working at telecommunications wavelengths. In 1993, Townsend, Rarity, and Tapster (1993a) implemented a single-photon interference scheme for quantum cryptography over a distance of 10 km, and in 1994, Tapster, Rarity, and Owens demonstrated a violation of Bell's inequalities over 4 km. These experiments were the first to take advantage of Ge APD's operated in passively quenched Geiger mode. At a temperature of 77 K, which can be achieved using either liquid nitrogen or Stirling engine cooling, typical quantum efficiencies of about 15% at dark-count rates of 25 kHz can be achieved (Owens *et al.*, 1994), and time jitter down to 100 ps has been observed (Lacaita *et al.*, 1994) a normal value being 200–300 ps.

Traditionally, germanium APD's have been implemented in the domain of long-distance quantum communication. However, this type of diode is currently being replaced by InGaAs APD's, and it has become more and more difficult to find germanium APD's on the market. Motivated by pioneering research reported in 1985 (Levine *et al.*, 1985), the latest research focuses on InGaAs APD's, which allow single-photon detection in both telecommunications windows. Starting with work by Zappa *et al.* (1994), InGaAs APD's as single-photon counters have meanwhile been thoroughly characterized (Lacaita *et al.*, 1996; Ribordy *et al.*, 1998; Karlsson *et al.*, 1999; Hiskett *et al.*, 2000; Rarity *et al.*, 2000; Stucki *et al.*, 2001), and the first implementations for quantum cryptography have been reported (Ribordy, 1998; Bourennane *et al.*, 1999; Bethune and Risk, 2000; Hughes, Morgan, and Peterson, 2000; Ribordy *et al.*, 2000). However, if operating Ge APD's is already more inconvenient than using silicon APD's, the practicality of InGaAs APD's is even worse, the problem being an extremely high afterpulse fraction. Therefore operation in passive-quenching mode is impossible for applications in which low noise is crucial. In gated mode, InGaAs APD's are better for single-photon counting at 1.3 $\mu$m than Ge APD's. For instance, at a temperature of 77 K and a dark-count probability of $10^{-5}$ per 2.6-ns gate, quantum efficiencies of around 30% and 17% have been reported for InGaAs and Ge APD's, respectively (Ribordy *et al.*, 1998), while the time jitter of both devices is comparable. If working at a wavelength of 1.55 $\mu$m, the temperature has to be increased for single-photon detection. At 173 K and a dark-count rate of $10^{-4}$, a quantum efficiency of 6% can still be observed using InGaAs/InP devices, while the same figure for germanium APD's is close to zero.

To date, no industrial effort has been made to optimize APD's operating at telecommunications wavelengths for photon counting, and their performance still lags far behind that one of silicon APD's.[26] However, there is no fundamental reason why photon counting at wavelengths above 1 $\mu$m should be more difficult than at wavelengths below 1 $\mu$m except that the high-

[26]The first commercial photon counter at telecommunications wavelengths came out only this year (the Hamamatsu photomultiplier R5509-72). However, its efficiency is not yet sufficient for use in quantum cryptography.

wavelength photons are less energetic. The real reasons for the lack of commercial products are, first, that silicon, the most common semiconductor material, is not sensitive enough (the band gap is too large), and second that the market for photon counting is not yet mature. But, without great risk, one can predict that good commercial photon counters will become available in the near future and that they will have a major impact on quantum cryptography.

### D. Quantum random-number generators

The key used in the one-time pad must be secret and used only once. Consequently it must be as long as the message, and it must be perfectly random. The latter point proves to be a delicate and interesting one. Computers are deterministic systems that cannot create truly random numbers. However, all secure cryptosystems, both classical and quantum ones, require truly random numbers.[27] Hence the random numbers must be created by a random physical process. Moreover, to make sure that the process does not merely appear random while having some hidden deterministic pattern, the process needs to be completely understood. It is thus of interest to implement a simple process in order to gain confidence in the randomness of its proper operation.

A natural solution is to rely on the random choice of a single photon at a beamsplitter[28] (Rarity *et al.*, 1994). In this case the randomness is in principle guaranteed by the laws of quantum mechanics, though one still has to be very careful not to introduce any experimental artifact that could correlate adjacent bits. Different experimental realizations have been demonstrated (Jennewein, Achleitner, *et al.*, 2000; Stefanov *et al.*, 2000; Hildebrand, 2001), and prototypes are commercially available (www.gap-optique.unige.ch). One particular problem is the dead time of the detectors, which may introduce a strong anticorrelation between neighboring bits. Similarly, afterpulses may provoke a correlation. These detector-related effects increase with higher pulse rates, limiting the bit rate of a quantum number generator to a few megahertz.

In the BB84 protocol Alice has to choose randomly among four different states and Bob between two bases. The limited random-number generation rate may force Alice to produce her numbers in advance and store them, creating a security risk. On Bob's side the random-bit creation rate can be lower, since, in principle, the basis need be changed only after a photon has been detected, which normally happens at rates below 1 MHz. However, one must make sure that this does not give a spy an opportunity for a Trojan horse attack (see Sec. VI.K).

An elegant configuration integrating the random-number generator into the QC system consists in using a passive choice of bases, as discussed in Sec. V (Muller *et al.*, 1993). However, the problem of detector-induced correlation remains.

### E. Quantum repeaters

Today's fiber-based QC systems are limited to operation over tens of kilometers due to the combination of fiber losses and detector noise. The losses by themselves only reduce the bit rate (exponentially with distance). With perfect detectors the distance would not be limited. However, because of the dark counts, each time a photon is lost there is a chance that a dark count produces an error. Hence, when the probability of a dark count becomes comparable to the probability that a photon is correctly detected, the signal-to-noise ratio tends to 0 [more precisely, the mutual information $I(\alpha,\beta)$ tends to a lower bound[29]]. In this section we briefly explain how the use of entangled photons and of entanglement swapping (Zukowski *et al.*, 1993) could offer ways to extend the achievable distances in the foreseeable future (some prior knowledge of entanglement swapping is assumed). Let $t_{link}$ denote the transmission coefficient (i.e., the probability that a photon sent by Alice gets to one of Bob's detectors), $\eta$ the detector efficiency, and $p_{dark}$ the dark-count probability per time bin. With a perfect single-photon source, the probability $P_{raw}$ of a correct qubit detection is $P_{raw}=t_{link}\eta$, while the probability $P_{det}$ of an error is $P_{det}=(1-t_{link}\eta)p_{dark}$. Accordingly, the QBER$=P_{det}/(P_{raw}+P_{det})$, and the normalized net rate is $\rho_{net}=(P_{raw}+P_{det})\cdot fct(\text{QBER})$, where the function $fct$ denotes the fraction of bits remaining after error correction and privacy amplification. For the sake of illustration, we simply assume a linear dependence dropping to zero for QBER$\geq$15% (this simplification does not affect the qualitative results of this section; for a more precise calculation, see Lütkenhaus 2000): $fct(\text{QBER})=1-\text{QBER}/15\%$. The corresponding net rate $\rho_{net}$ is displayed in Fig. 10. Note that it drops to zero near 90 km.

Let us now assume that instead of a perfect single-photon source, Alice and Bob use a perfect two-photon source set in the middle of their quantum channel. Each photon then has a probability $\sqrt{t_{link}}$ of reaching a detector. The probability of a correct joined detection is thus $P_{raw}=t_{link}\eta^2$, while an error occurs with probability $P_{det}=(1-\sqrt{t_{link}}\eta)^2p_{dark}^2+2\sqrt{t_{link}}\eta(1-\sqrt{t_{link}}\eta)p_{dark}$ (both photons lost and two dark counts, or one photon lost and one dark count). This can be conveniently rewritten as $P_{raw}=t_{link}\eta^n$ and $P_{det}=[t_{link}^{1/n}\eta+(1-t_{link}^{1/n}\eta)p_{dark}]^n-t_{link}\eta^n$, valid for any division of the

[27]The PIN number that the bank assigns to your ATM card must be random. If not, someone else knows it.

[28]Strictly speaking, the choice is made only once the photons are detected at one of the outports.

[29]The absolute lower bound is 0, but depending on the assumed eavesdropping strategy, Eve could take advantage of the losses. In the latter case, the lower bound is given by her mutual information $I(\alpha,\epsilon)$.

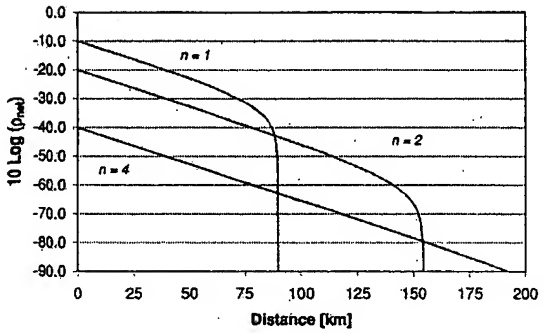


FIG. 10. Normalized net key creation rate $\rho_{net}$ as a function of distance in optical fibers. For $n=1$, Alice uses a perfect single-photon source. For $n>1$, the link is divided into $n$ equal-length sections, and $n/2$ two-photon sources are distributed between Alice and Bob. Parameters: detection efficiency $\eta=10\%$, dark-count probability $p_{dark}=10^{-4}$, and fiber attenuation $\alpha=0.25$ dB/km.

link into $n$ equal-length sections and $n$ detectors. Note that the measurements performed at the nodes between Alice and Bob transmit (swap) the entanglement to the twin photons without revealing any information about the qubit (these measurements are called Bell measurements and are at the core of entanglement swapping and of quantum teleportation). The corresponding net rates are displayed in Fig. 10. Clearly, the rates for short distances are smaller when several detectors are used, because of their limited efficiencies (here we assume $\eta=10\%$), but the distance before the net rate drops to zero is extended to longer distances! Intuitively, this can be understood as follows. Let us assume that a logical qubit propagates from Alice to Bob (although some photons propagate in the opposite direction). Then, each two-photon source and each Bell measurement acts on this logical qubit as a kind of quantum nondemolition measurement, testing whether the logical qubit is still there. In this way, Bob activates his detectors only when there is a large chance $t_{link}^{1/n}$ that the photon gets to his detectors.

Note that if in addition to detector noise there is noise due to decoherence, then the above idea can be extended, using entanglement purification. This is essentially the idea behind quantum repeaters (Briegel *et al.*, 1998; Dur *et al.*, 1999).

## IV. EXPERIMENTAL QUANTUM CRYPTOGRAPHY WITH FAINT LASER PULSES

Experimental quantum key distribution was demonstrated for the first time in 1989 (the results were published only in 1992 by Bennett, Bessette, *et al.*). Since then, tremendous progress has been made. Today, several groups have shown that quantum key distribution is possible, even outside the laboratory. In principle, any two-level quantum system could be used to implement QC. In practice, all implementations have relied on photons. The reason is that their interaction with the environment, also called decoherence, can be controlled and moderated. In addition, researchers can benefit from all the tools developed in the past two decades for optical telecommunications. It is unlikely that other carriers will be employed in the foreseeable future.

Comparing different QC setups is a difficult task, since several criteria must be taken into account. What matters in the end, of course, is the rate of corrected secret bits (the distilled bit rate $R_{dist}$) that can be transmitted and the transmission distance. One can already note that with present and near-future technology it will probably not be possible to achieve rates of the order of gigahertz, which are now common with conventional optical communication systems (in their comprehensive paper published in 2000, Gilbert and Hamrick discuss practical methods for achieving high-bit-rate QC). This implies that encryption with a key exchanged through QC will be limited to highly confidential information. While the determination of the transmission distance and rate of detection (the raw bit rate $R_{raw}$) is straightforward, estimating the net rate is rather difficult. Although, in principle, errors in the bit sequence follow only from tampering by a malevolent eavesdropper, the situation is rather different in reality. Discrepancies between the keys of Alice and Bob also happen because of experimental imperfections. The error rate QBER can be easily determined. Similarly, the error correction procedure is rather simple. Error correction leads to a reduction of the key rate that depends strongly on the QBER. The real problem is to estimate the information obtained by Eve, a quantity necessary for privacy amplification. This depends not only on the QBER, but also on other factors, such as the photon number statistics of the source or the way the choice of the measurement basis is made. Moreover in a pragmatic approach, one might also accept restrictions on Eve's technology, limiting her strategies and therefore also the information she can obtain per error she introduces. Since the efficiency of privacy amplification rapidly decreases when the QBER increases, the distilled bit rate depends dramatically on Eve's information and hence on the assumptions made. One can define as the maximum transmission distance the distance at which the distilled rate reaches zero. This distance can give one an idea of the difficulty of evaluating a QC system from a physical point of view.

Technological aspects must also be taken into account. In this article we do not focus on all the published performances (in particular not on the key rates), which strongly depend on current technology and the financial resources of the research teams who carried out the experiments. Rather, we try to weigh the intrinsic technological difficulties associated with each setup and to anticipate certain technological advances. Last but not least, the cost of realizing a prototype should also be considered.

In this section, we first deduce a general formula for the QBER and consider its impact on the distilled rate. We then review faint-pulse implementations. We class them according to the property used to encode the qubits value and follow a rough chronological order. Fi-

nally, we assess the possibility of adopting the various setups for the realization of an industrial prototype. Systems based on entangled photon pairs are presented in the next section.

### A. Quantum bit error rate

The QBER is defined as the ratio of wrong bits to the total number of bits received[30] and is normally on the order of a few percent. We can express it as a function of rates,

$$\mathrm{QBER}=\frac{N_{wrong}}{N_{right}+N_{wrong}}=\frac{R_{error}}{R_{sift}+R_{error}}\approx\frac{R_{error}}{R_{sift}}. \quad (26)$$

Here the sifted key corresponds to the cases in which Alice and Bob made compatible choices of bases, hence its rate is half that of the raw key.

The raw rate is essentially the product of the pulse rate $f_{rep}$, the mean number of photons per pulse $\mu$, the probability $t_{link}$ of a photons arriving at the analyzer, and the probability $\eta$ of the photon's being detected:

$$R_{sift}=\frac{1}{2}R_{raw}=\frac{1}{2}qf_{rep}\mu t_{link}\eta. \quad (27)$$

The factor $q$ ($q\leqslant 1$, typically 1 or $\frac{1}{2}$) must be introduced for some phase-coding setups in order to correct for noninterfering path combinations (see, for example, Secs. IV.C and V.B).

One can identify three different contributions to $R_{error}$. The first arises from photons that end up in the wrong detector due to imperfect interference or polarization contrast. The rate $R_{opt}$ is given by the product of the sifted-key rate and the probability $p_{opt}$ of a photon's going to the wrong detector:

$$R_{opt}=R_{sift}p_{opt}=\frac{1}{2}qf_{rep}\mu t_{link}p_{opt}\eta. \quad (28)$$

For a given setup, this contribution can be considered as an intrinsic error rate indicating its suitability for use in QC. We shall discuss it below in the case of each particular system.

The second contribution, $R_{det}$, arises from the detector dark counts (or from remaining environmental stray light in free-space setups). This rate is independent of the bit rate.[31] Of course, only dark counts falling within the short time window when a photon is expected give rise to errors,

$$R_{det}=\frac{1}{2}\frac{1}{2}f_{rep}p_{dark}n, \quad (29)$$

where $p_{dark}$ is the probability of registering a dark count per time window and per detector, and $n$ is the number of detectors. The two factors of $\frac{1}{2}$ are related to the fact that a dark count has a 50% chance of happening when Alice and Bob have chosen incompatible bases (and is thus eliminated during sifting) and a 50% chance of occurring in the correct detector.

Finally, error counts can arise from uncorrelated photons due to imperfect photon sources:

$$R_{acc}=\frac{1}{2}\frac{1}{2}p_{acc}f_{rep}t_{link}n\eta. \quad (30)$$

This factor appears only in systems based on entangled photons, where the photons belonging to different pairs but arriving in the same time window are not necessarily in the same state. The quantity $p_{acc}$ is the probability of finding a second pair within the time window, knowing that a first one was created.[32]

The QBER can now be expressed as follows:

$$\mathrm{QBER}=\frac{R_{opt}+R_{det}+R_{acc}}{R_{sift}} \quad (31)$$

$$=p_{opt}+\frac{p_{dark}n}{t_{link}\eta 2q\mu}+\frac{p_{acc}}{2q\mu} \quad (32)$$

$$=\mathrm{QBER}_{opt}+\mathrm{QBER}_{det}+\mathrm{QBER}_{acc}. \quad (33)$$

We now analyze these three contributions. The first one, $\mathrm{QBER}_{opt}$, is independent of the transmission distance (it is independent of $t_{link}$). It can be considered as a measure of the optical quality of the setup, depending only on the polarization or interference fringe contrast. The technical effort needed to obtain and, more importantly, to maintain a given $\mathrm{QBER}_{opt}$ is an important criterion for evaluating different QC setups. In polarization-based systems, it is rather simple to achieve a polarization contrast of 100:1, corresponding to a $\mathrm{QBER}_{opt}$ of 1%. In fiber-based QC, the problem is to maintain this value in spite of polarization fluctuations and depolarization in the fiber link. For phase-coding setups, $\mathrm{QBER}_{opt}$ and the interference visibility are related by

$$\mathrm{QBER}_{opt}=\frac{1-V}{2}. \quad (34)$$

A visibility of 98% thus translates into an optical error rate of 1%. Such a value implies the use of well-aligned and stable interferometers. In bulk optics, perfect mode overlap is difficult to achieve, but the polarization is stable. In single-mode fiber interferometers, on in contrast, perfect mode overlap is automatically achieved, but the polarization must be controlled, and chromatic dispersion can constitute a problem.

The second contribution, $\mathrm{QBER}_{det}$, increases with distance, since the dark-count rate remains constant while the bit rate goes down like $t_{link}$. It depends en-

[30]In the following section we consider systems implementing the BB84 protocol. For other protocols, some of the formulas have to be slightly adapted.

[31]This is true provided that afterpulses (see Sec. III.C) do not contribute to the dark counts.

[32]Note that a passive choice of measurement basis implies that four detectors (or two detectors during two time windows) are activated for every pulse, thus leading to a doubling of $R_{det}$ and $R_{acc}$.

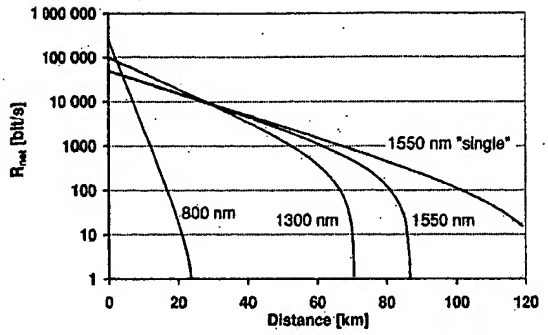


FIG. 11. Bit rate, after error correction and privacy amplification, vs fiber length. The chosen parameters are as follows: pulse rates of 10 MHz for faint laser pulses ($\mu$=0.1) and 1 MHz for the case of ideal single photons (1550-nm "single"); losses of 2, 0.35, and 0.25 dB/km; detector efficiencies of 50, 20, and 10; dark-count probabilities of $10^{-7}$, and $10^{-5}$, and $10^{-5}$ for 800, 1300, and 1550 nm, respectively. Losses at Bob's end and $QBER_{opt}$ are neglected.

tirely on the ratio of the dark-count rate to the quantum efficiency. At present, good single-photon detectors are not commercially available for telecommunications wavelengths. The span of QC is not limited by decoherence. As $QBER_{opt}$ is essentially independent of the fiber length, it is detector noise that limits the transmission distance.

Finally, the $QBER_{acc}$ contribution is present only in some two-photon schemes in which multiphoton pulses are processed in such a way that they do not necessarily encode the same bit value (see, for example, Secs. V.B.1 and V.B.2). Although all systems have some probability of multiphoton pulses, in most these contribute only to the information available to Eve (see Sec. VI.H) and not to the QBER. However, for implementations featuring passive choice by each photon, the multiphoton pulses do not contribute to Eve's information but only to the error rate (see Sec. VI.J).

Now, let us calculate the useful bit rate as a function of the distance. $R_{sift}$ and QBER are given as a function of $t_{link}$ in Eqs. (27) and (32), respectively. The fiber link transmission decreases exponentially with length. The fraction of bits lost due to error correction and privacy amplification is a function of QBER and depends on Eve's strategy. The number of remaining bits $R_{net}$ is given by the sifted-key rate multiplied by the difference between the Alice-Bob mutual Shannon information $I(\alpha,\beta)$ and Eve's maximal Shannon information $I^{\max}(\alpha,\epsilon)$:

$$R_{net}=R_{sift}[I(\alpha,\beta)-I^{\max}(\alpha,\epsilon)]. \quad (35)$$

The difference between $I(\alpha,\beta)$ and $I^{\max}(\alpha,\epsilon)$ is calculated here according to Eqs. (63) and (65) (Sec. VI.E), considering only individual attacks and no multiphoton pulses. We obtain $R_{net}$ (the useful bit rate after error correction and privacy amplification) for different wavelengths as shown in Fig. 11. There is first an exponential decrease, then, due to error correction and privacy amplification, the bit rates fall rapidly down to zero. This is most evident when comparing the curves 1550 and 1550 nm "single," since the latter features a QBER that is 10 times lower. One can see that the maximum range is about 100 km. In practice it is closer to 50 km, due to nonideal error correction and privacy amplification, multiphoton pulses, and other optical losses not considered here. Finally, let us mention that typical key creation rates on the order of a thousand bits per second over distances of a few tens of kilometers have been demonstrated experimentally (see, for example, Townsend, 1998b or Ribordy *et al.*, 2000).

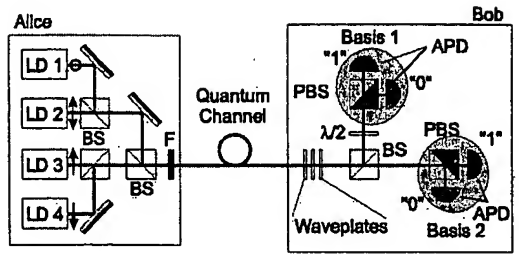


FIG. 12. Typical system for quantum cryptography using polarization coding: LD, laser diode; BS, beamsplitter; F, neutral density filter; PBS, polarizing beamsplitter; λ/2, half waveplate; APD, avalanche photodiode.

### B. Polarization coding

Encoding the qubits in the polarization of photons is a natural solution. The first demonstration of QC by Bennett and co-workers (Bennett, Bessette, *et al.*, 1992) made use of this choice. They realized a system in which Alice and Bob exchanged faint light pulses produced by a light-emitting diode and containing less than one photon on average over a distance of 30 cm in air. In spite of the small scale of this experiment, it had an important impact on the community, as it showed that it was not unreasonable to use single photons instead of classical pulses for encoding bits.

A typical QC system with the BB84 four-state protocol using the polarization of photons is shown in Fig. 12. Alice's system consists of four laser diodes. They emit short classical photon pulses (≈1 ns) polarized at −45°, 0°, +45°, and 90°. For a given qubit, a single diode is triggered. The pulses are then attenuated by a set of filters to reduce the average number of photons to well below 1, and sent along the quantum channel to Alice.

It is essential that the pulses remain polarized for Bob to be able to extract the information encoded by Alice. As discussed in Sec. III.B.2, polarization mode dispersion may depolarize the photons, provided the delay it introduces between polarization modes is longer than the coherence time. This sets a constraint on the type of lasers used by Alice.

Upon reaching Bob, the pulses are extracted from the fiber. They travel through a set of waveplates used to recover the initial polarization states by compensating for the transformation induced by the optical fiber (Sec. III.B.2). The pulses then reach a symmetric beamsplit-

ter, implementing the basis choice. Transmitted photons are analyzed in the vertical-horizontal basis with a polarizing beamsplitter and two photon-counting detectors. The polarization state of the reflected photons is first rotated with a waveplate by 45° (−45°→0°). The photons are then analyzed with a second set of polarizing beamsplitters and photon-counting detectors. This implements the diagonal basis. For illustration, let us follow a photon polarized at +45°. We see that its state of polarization is arbitrarily transformed in the optical fiber. At Bob's end, the polarization controller must be set to bring it back to +45°. If it chooses the output of the beamsplitter corresponding to the vertical-horizontal basis, it will experience an equal probability of reflection or transmission at the polarizing beamsplittter, yielding a random outcome. On the other hand, if it chooses the diagonal basis, its state will be rotated to 90°. The polarizing beamsplitter will then reflect it with unit probability, yielding a deterministic outcome.

Instead of having Alice use four lasers and Bob two polarizing beamsplitters, one can also implement this system with active polarization modulators such as Pockels cells. For emission, the modulator is randomly activated for each pulse to rotate the state of polarization to one of the four states, while, at the receiver, it randomly rotates half of the incoming pulses by 45°. It is also possible to realize the whole system with fiber optics components.

Antoine Muller and co-workers at the University of Geneva have used such a system to perform QC experiments over optical fibers (1993; see also Bréguet *et al.*, 1994). They created a key over a distance of 1100 meters with photons at 800 nm. In order to increase the transmission distance, they repeated the experiment with photons at 1300 nm (Muller *et al.*, 1995, 1996) and created a key over a distance of 23 km. An interesting feature of this experiment is that the quantum channel connecting Alice and Bob consisted of an optical fiber part of an installed cable used by the telecommunications company Swisscom for carrying phone conversations. It runs between the Swiss cities of Geneva and Nyon, under Lake Geneva (Fig. 13). This was the first time QC was performed outside of a physics laboratory. These experiments had a strong impact on the interest of the wider public in the new field of quantum communication.

These two experiments highlighted the fact that the polarization transformation induced by a long optical fiber was unstable over time. Indeed, when monitoring the QBER of their system, Muller noticed that, although it remained stable and low for some time (on the order of several minutes), it would suddenly increase after a while, indicating a modification of the polarization transformation in the fiber. This implies that a real fiber-based QC system would require active alignment to compensate for this evolution. Although not impossible, such a procedure is certainly difficult. James Franson did indeed implement an active-feedback alignment system (Franson and Jacobs, 1995), but did not pursue this line of research. It is interesting to note that replacing standard fibers with polarization-maintaining fibers does not solve the problem. The reason is that, in spite of their name, these fibers do not maintain polarization, as explained in Sec. III.B.2.

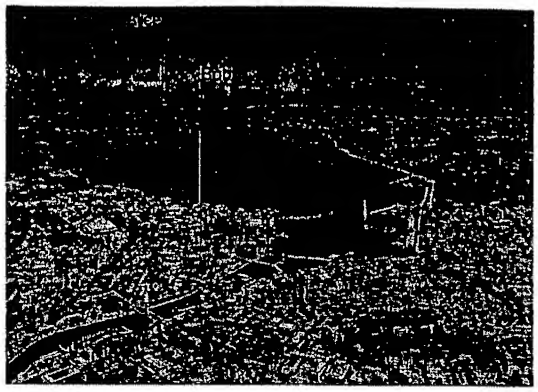

FIG. 13. Geneva and Lake Geneva. The Swisscom optical fiber cable used for quantum cryptography experiments runs under the lake between the town of Nyon, about 23 km north of Geneva, and the center of the city.

Recently, Townsend has also investigated such polarization-encoding systems for QC on short-span links up to 10 kilometers (1998a, 1998b) with photons at 800 nm. It is interesting to note that, although he used standard telecommunications fibers which could support more than one spatial mode at this wavelength, he was able to ensure single-mode propagation by carefully controlling the launching conditions. Because of the problem discussed above, polarization coding does not seem to be the best choice for QC in optical fibers. Nevertheless, this problem is drastically reduced when considering free-space key exchange, as air has essentially no birefringence at all (see Sec. IV.E).

### C. Phase coding

The idea of encoding the value of qubits in the phase of photons was first mentioned by Bennett in the paper in which he introduced the two-state protocol (1992). It is indeed a very natural choice for optics specialists. State preparation and analysis are then performed with interferometers, which can be realized with single-mode optical fiber components.

Figure 14 presents an optical fiber version of a Mach-Zehnder interferometer. It is made out of two symmetric couplers—the equivalent of beamsplitters—connected to each other, with one phase modulator in each arm. One can inject light into the setup, using a continuous and classical source, and monitor the intensity at the output ports. Provided that the coherence length of the light used is larger than the path mismatch in the interferometers, interference fringes can be recorded. Taking into account the $\pi/2$ phase shift experienced upon reflection at a beamsplitter, the effect of the phase modu-

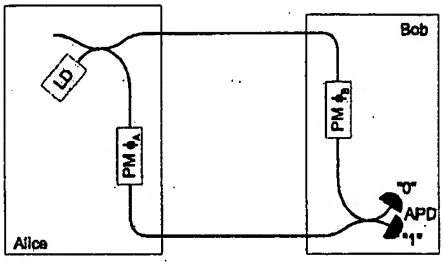


FIG. 14. Conceptual interferometric setup for quantum cryptography using an optical fiber Mach-Zehnder interferometer: LD, laser diode; PM, phase modulator; APD, avalanche photodiode.

lators ($\phi_A$ and $\phi_B$), and the path-length difference ($\Delta L$), the intensity in the output port labeled "0" is given by

$$I_0 = \bar{I} \cdot \cos^2\left(\frac{\phi_A - \phi_B + k\Delta L}{2}\right), \tag{36}$$

where $k$ is the wave number and $\bar{I}$ the intensity of the source. If the phase term is equal to $\pi/2 + n\pi$, where $n$ is an integer, destructive interference is obtained. Therefore the intensity registered in port 0 reaches a minimum, and all the light exits from port 1. When the phase term is equal to $n\pi$, the situation is reversed: constructive interference is obtained in port 0, while the intensity in port 1 goes to a minimum. With intermediate phase settings, light can be recorded in both ports. This device acts like an optical switch. It is essential to keep the path difference stable in order to record stationary interferences.

Although we have discussed the behavior of this interferometer for classical light, it works exactly the same when a single photon is injected. The probability of detecting the photon in one output port can be varied by changing the phase. It is the fiber optic version of Young's double-slit experiment, in which the arms of the interferometer replace the apertures.

This interferometer combined with a single-photon source and photon-counting detectors can be used for QC. Alice's setup consists of the source, the first coupler, and the first phase modulator, while Bob takes the second modulator and coupler, as well as the detectors. Let us consider the implementation of the four-state BB84 protocol. On the one hand, Alice can apply one of four phase shifts $(0,\pi/2,\pi,3\pi/2)$ to encode a bit value. She associates 0 and $\pi/2$ with bit 0, and $\pi$ and $3\pi/2$ with bit 1. On the other hand, Bob performs a basis choice by randomly applying a phase shift of either 0 or $\pi/2$. He associates the detector connected to the output port 0 with a bit value of 0, and the detector connected to port 1 with bit 1. When the difference of their phase is equal to 0 or $\pi$, Alice and Bob are using compatible bases and they obtain deterministic results. In such cases, Alice can infer from the phase shift she applied the output port chosen by the photon at Bob's end and hence the bit value he registered. Bob, on his side, deduces from the output port chosen by the photon the phase that Alice selected. When the phase difference equals $\pi/2$ or $3\pi/2$, the bases are incompatible and the photon randomly chooses which port it takes at Bob's coupler. This scheme is summarized in Table I. We must stress that it is essential with this scheme to keep the path difference stable during a key exchange session. It should not change by more than a fraction of a wavelength of the photons. A drift of the length of one arm would indeed change the phase relation between Alice and Bob and induce errors in their bit sequence.

TABLE I. Implementation of the BB84 four-state protocol with phase encoding.

| Alice | | | Bob | |
|---|---|---|---|---|
| Bit value | $\phi_A$ | $\phi_B$ | $\phi_A - \phi_B$ | Bit value |
| 0 | 0 | 0 | 0 | 0 |
| 0 | 0 | $\pi/2$ | $3\pi/2$ | ? |
| 1 | $\pi$ | 0 | $\pi$ | 1 |
| 1 | $\pi$ | $\pi/2$ | $\pi/2$ | ? |
| 0 | $\pi/2$ | 0 | $\pi/2$ | ? |
| 0 | $\pi/2$ | $\pi/2$ | 0 | 0 |
| 1 | $3\pi/2$ | 0 | $3\pi/2$ | ? |
| 1 | $3\pi/2$ | $\pi/2$ | $\pi$ | 1 |

It is interesting to note that encoding qubits with two-path interferometers is formally isomorphic to polarization encoding. The two arms correspond to a natural basis, and the weights $c_j$ of each qubit state $\psi = (c_1 e^{-i\phi/2}, c_2 e^{i\phi/2})$ are determined by the coupling ratio of the first beamsplitter, while the relative phase $\phi$ is introduced in the interferometer. The Poincaré sphere representation, which applies to all two-level quantum systems, can also be used to represent phase-coding states. In this case, the azimuth angle represents the relative phase between the light that has propagated along the two arms. The elevation corresponds to the coupling ratio of the first beamsplitter. States produced by a switch are on the poles, while those resulting from the use of a 50/50 beamsplitter lie on the equator. Figure 15 illustrates this analogy. Consequently, all polarization schemes can also be implemented using phase coding.

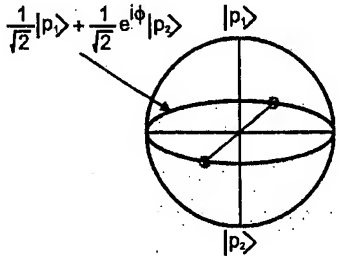


FIG. 15. Poincaré sphere representation of two-level quantum states generated by two-path interferometers. The poles correspond to the states generated by an interferometer in which the first coupler is replaced by a switch. The states generated with a symmetrical beamsplitter are on the equator. The azimuth indicates the phase between the two paths.

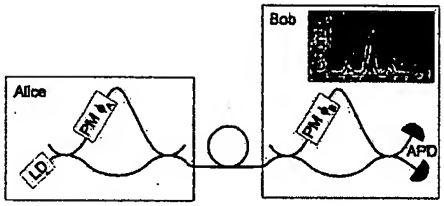


FIG. 16. Double Mach-Zehnder implementation of an interferometric system for quantum cryptography: LD, laser diode; PM, phase modulator; APD, avalanche photodiode. The inset represents the temporal count distribution recorded as a function of the time passed since the emission of the pulse by Alice. Interference is observed in the central peak.

Similarly, every coding using two-path interferometers can be realized using polarization. However, in practice one choice is often more convenient than the other, depending on circumstances like the nature of the quantum channel.[33]

### 1. The double Mach-Zehnder implementation

Although the scheme presented in the previous section works perfectly well on an optical table, it is impossible to keep the path difference stable when Alice and Bob are separated by more than a few meters. As mentioned above, the relative length of the arms should not change by more than a fraction of a wavelength. If Alice and Bob are separated by 1 kilometer, for example, it is clearly impossible to prevent path difference changes smaller than 1 $\mu$m caused by environmental variations. In his 1992 letter, Bennett also showed how to circumvent this problem. He suggested using two unbalanced Mach-Zehnder interferometers, one for Alice and one for Bob, connected in series by a single optical fiber (see Fig. 16). When monitoring counts as a function of the time since the emission of the photons, Bob obtains three peaks (see the inset in Fig. 16). The first one corresponds to the photons that chose the short path in both Alice's and Bob's interferometers, while the last one corresponds to photons that chose both the long paths. Finally, the central peak corresponds to photons that chose the short path in Alice's interferometer and the long one in Bob's, and vice versa. If these two processes are indistinguishable, they produce interference. A timing window can be used to discriminate between interfering and noninterfering events. If the latter are disregarded, it is then possible for Alice and Bob to exchange a key.

The advantage of this setup is that both "halves" of the photon travel in the same optical fiber. They thus experience the same optical length in the environmentally sensitive part of the system, provided that the variations in the fiber are slower than their temporal separations, determined by the interferometer's imbalance ($\approx$5 ns). This condition is much less difficult to fulfill. In order to obtain good fringe visibility, and hence a low error rate, the imbalances of the interferometers must be equal to within a fraction of the coherence time of the photons. This implies that the path differences must be matched to within a few millimeters, which does not constitute a problem. The imbalance must be chosen so that it is possible to distinguish the three temporal peaks clearly and thus discriminate interfering from noninterfering events. It must typically be larger than the pulse length and the timing jitter of the photon-counting detectors. In practice, the second condition is the more stringent one. Assuming a time jitter of the order of 500 ps, an imbalance of at least 1.5 ns keeps the overlap between the peaks low.

The main difficulty associated with this QC scheme is that the imbalances of Alice's and Bob's interferometers must be kept stable to within a fraction of the wavelength of the photons during a key exchange to maintain correct phase relations. This implies that the interferometers must lie in containers whose temperature is stabilized. In addition, for long key exchanges an active system is necessary to compensate for drift.[34] Finally, in order to ensure the indistinguishability of both interfering processes, one must make sure that in each interferometer the polarization transformation induced by the short path is the same as that induced by the long path. Both Alice and Bob must then use a polarization controller to fulfill this condition. However, the polarization transformation is rather stable in short optical fibers whose temperature is kept stable and which do not experience strains. Thus this adjustment does not need to be repeated frequently.

Paul Tapster and John Rarity of DERA, the Defence Evalution and Research Agency (Malvern, England), working with Paul Townsend, were the first to test this system over a fiber optic spool of 10 km (Townsend *et al.*, 1993a, 1993b). Townsend later improved the interferometer by replacing Bob's input coupler with a polarization splitter to suppress the lateral noninterfering peaks (1994). In this case, it is again unfortunately necessary to align the polarization state of the photons at Bob's end, in addition to stabilizing the imbalance in the interferometers. He later thoroughly investigated key exchange with phase coding and improved the transmission distance (Marand and Townsend, 1995; Townsend, 1998b). He also tested the possibility of multiplexing a

[33]Note, in addition, that using many-path interferometers opens up the possibility of coding quantum systems of dimensions larger than 2, like qutrits, ququarts, etc. (Bechmann-Pasquinucci and Peres, 2000; Bechmann-Pasquinucci and Tittel, 2000; Bourennane, Karlsson, and Bjorn, 2001).

[34]Polarization coding requires the optimization of three parameters (three parameters are necessary for unitary polarization control). In comparison, phase coding requires optimization of only one parameter. This is possible because the coupling ratios of the beamsplitters are fixed. Both solutions would be equivalent if one could limit the polarization evolution to rotations of the elliptic states without changes in the ellipticity.

quantum channel using two different wavelengths with conventional data transmission over a single optical fiber (Townsend, 1997a). Richard Hughes and co-workers from Los Alamos National Laboratory have also extensively tested such an interferometer (1996; Hughes, Morgan, and Peterson, 2000) up to distances of 48 km of installed optical fiber.[35]

### 2. "Plug-and-play" systems

As discussed in the two previous sections, both polarization and phase coding require active compensation of optical path fluctuations. A simple approach would be to alternate between adjustment periods—when pulses containing large numbers of photons are exchanged between Alice and Bob to adjust the compensating system correcting for slow drifts in phase or polarization—and qubits transmission periods, when the number of photons is reduced to a quantum level.

An approach invented in 1989 by Martinelli, then at CISE Tecnologie Innovative in Milano, allows one to automatically and passively compensate for all polarization fluctuations in an optical fiber (see also Martinelli, 1992). Let us first consider what happens to the polarization state of a light pulse traveling through an optical fiber, before being reflected by a Faraday mirror—a mirror with a $\lambda/4$ Faraday rotator[36] in front. We must first define a convenient description of the change in polarization of light reflected by a mirror at normal incidence. Let the mirror be in the $x$-$y$ plane and $z$ be the optical axis. Clearly, all linear polarization states are unchanged by a reflection. However, right-handed circular polarization is changed into left-handed and vice versa. Actually, after a reflection the rotation continues in the same sense, but since the propagation direction is reversed, right-handed and left-handed polarizations are swapped. The same holds for elliptic polarization states: the axes of the ellipse are unchanged, but right and left are exchanged. Accordingly, on a Poincaré sphere the polarization transformation upon reflection is described by a

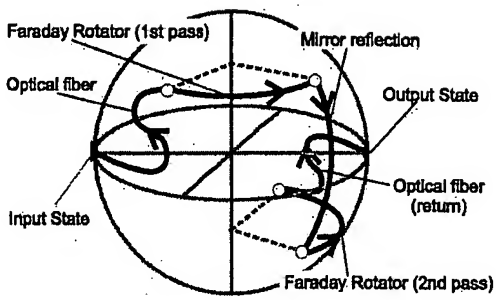


FIG. 17. Evolution of the polarization state of a light pulse represented on the Poincaré sphere over a round-trip propagation along an optical fiber terminated by a Faraday mirror.

symmetry through the equatorial plane: the north and south hemispheres are exchanged $[\vec{m}\rightarrow(m_1,m_2,-m_3)]$, or in terms of the qubit state vector,

$$T:\ \begin{pmatrix}\psi_1\\ \psi_2\end{pmatrix}\rightarrow\begin{pmatrix}\psi_2^*\\ \psi_1^*\end{pmatrix}. \tag{37}$$

This is a simple representation, but some attention has to be paid. This transformation is not unitary. Indeed, the above description switches from a right-handed reference frame $XYZ$ to a left-handed one $XY\bar{Z}$, where $\bar{Z}=-Z$. There is nothing wrong in doing this, and this explains the nonunitary polarization transformation.[37] Note that other descriptions are possible, but they require artificially breaking the $XY$ symmetry. The main reason for choosing this particular transformation is that the description of the polarization evolution in the optical fiber before and after the reflection is then straightforward. Indeed, let $U=e^{-i\omega\vec{B}\vec{\sigma}\ell/2}$ describe this evolution under the effect of some modal birefringence $\vec{B}$ in a fiber section of length $\ell$ (where $\vec{\sigma}$ is the vector whose components are the Pauli matrices). Then the evolution after reflection is simply described by the inverse operator $U^{-1}=e^{i\omega\vec{B}\vec{\sigma}\ell/2}$. Now that we have a description of the mirror, let us add the Faraday rotator. It produces a $\pi/2$ rotation of the Poincaré sphere around the north-south axis: $F=e^{-i\pi\sigma_z/4}$ (see Fig. 17). Because the Faraday effect is nonreciprocal (remember that it is due to a magnetic field, which can be thought of as produced by a spiraling electric current), the direction of rotation around the north-south axis is independent of the light propagation direction. Accordingly, after reflection on the mirror, the second passage through the Faraday rotator rotates the polarization in the same direction (see again Fig. 17) and is described by the same operator $F$. Consequently, the total effect of a Faraday mirror is to

[35]Note that in this experiment, Hughes and co-workers used an unusually high mean number of photons per pulse. They used a mean photon number of approximately 0.6 in the central interference peak, corresponding to a $\mu\approx1.2$ in the pulses leaving Alice. The latter value is the relevant one for eavesdropping analysis, since Eve could use an interferometer—conceivable with present technology—in which the first coupler was replaced by an optical switch and that allowed her to exploit all the photons sent by Alice. In light of this high $\mu$ and optical losses (22.8 dB), one may argue that this implementation was not secure, even when taking into account only so-called realistic eavesdropping strategies (see Sec. VI.I). Finally, it is possible to estimate the results that other groups would have obtained if they had used a similar value of $\mu$. One then finds that key distribution distances of the same order could have been achieved. This illustrates that the distance is a somewhat arbitrary figure of merit for a QC system.

[36]These commercially available components are extremely compact and convenient when using telecommunications wavelengths, which is not true for other wavelengths.

[37]Note that this transformation is positive, but not completely positive. It is thus closely connected to the partial transposition map (Peres, 1996). If several photons are entangled, then it is crucial to describe all of them in frames with the same chirality. Actually that this is necessary is the content of the Peres-Horodecki entanglement witness (Horodecki *et al.*, 1996).

change any incoming polarization state into its orthogonal state: $\vec{m} \rightarrow -\vec{m}$. This is best seen in Fig. 17 but can also be expressed mathematically:

$$FTF: \begin{pmatrix} \psi_1 \\ \psi_2 \end{pmatrix} \rightarrow \begin{pmatrix} \psi_2^* \\ -\psi_1^* \end{pmatrix}. \tag{38}$$

Finally, the whole optical fiber can be modeled as consisting of a discrete number of birefringent elements. If there are $N$ such elements in front of the Faraday mirror, the change in polarization during a round trip can be expressed (recall that the operator $FTF$ only changes the sign of the corresponding Bloch vector $\vec{m} = \langle \psi | \vec{\sigma} | \psi \rangle$) as

$$U_1^{-1} \cdots U_N^{-1} FTF U_N \cdots U_1 = FTF. \tag{39}$$

The output polarization state is thus orthogonal to the input one, regardless of any birefringence in the fibers. This approach can thus correct for time-varying birefringence changes, provided that they are slow compared to the time required for the light to make a round trip (a few hundred microseconds).

By combining this approach with time multiplexing in a long-path interferometer, it is possible to implement a quantum cryptography system based on phase coding in which all optical and mechanical fluctuations are automatically and passively compensated for (Muller *et al.*, 1997). We performed the first experiment on such a system in early 1997 (Zbinden *et al.*, 1997), and a key was exchanged over a 23-km installed optical fiber cable (the same one as was used in the polarization coding experiments mentioned above). This setup featured a high interference contrast (fringe visibility of 99.8%) and excellent long-term stability and clearly established the value of the approach for QC. The fact that no optical adjustments were necessary earned it the nickname of "plug-and-play" setup. It is interesting to note that the idea of combining time multiplexing with Faraday mirrors was first used to implement an "optical microphone" (Bréguet and Gisin, 1995).[38]

However, our first realization still suffered from certain optical inefficiencies, and it has been improved since then. Like the setup tested in 1997, the new system is based on time multiplexing, in which the interfering pulses travel along the same optical path, but now, in different time ordering. A schematic is shown in Fig. 18. Briefly, the general idea is that pulses emitted at Bob's end can travel along one of two paths: they can go via the short arm, be reflected at the Faraday mirror (FM) at Alice's end, and finally, back at Bob's, setup travel via the long arm. Or, they travel first via the long arm at Bob's end, get reflected at Alice's end, and return via the short arm of Bob's setup. These two possibilities then superpose on beamsplitter $C_1$. We shall now explain the

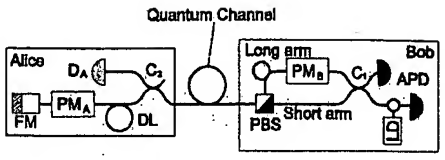


FIG. 18. Self-aligned plug-and-play system: LD, laser diode; APD, avalanche photodiode; $C_l$, fiber coupler; $PM_f$, phase modulator; PBS, polarizing beamsplitter; DL, optical delay line; FM, Faraday mirror; $D_A$, classical detector.

realization of this scheme in greater detail: A short and bright laser pulse is injected into the system through a circulator. It splits at a coupler. One of the half pulses, labeled $P_1$, propagates through the short arm of Bob's setup directly to a polarizing beamsplitter. The polarization transformation in this arm is set so that it is fully transmitted. $P_1$ is then sent through the fiber optic link. The second half pulse, labeled $P_2$, takes the long arm to the polarizing beamsplitter. The polarization evolution is such that $P_2$ is reflected. A phase modulator present in this long arm is left inactive so that it imparts no phase shift to the outgoing pulse. $P_2$ is also sent through the link, with a delay on the order of 200 ns. Both half pulses travel to Alice. $P_1$ goes through a coupler. The diverted light is detected with a classical detector to provide a timing signal. This detector is also important in preventing so-called Trojan horse attacks, which are discussed in Sec. VI.K. The nondiverted light then propagates through an attenuator and an optical delay line—consisting simply of an optical fiber spool—whose role will be explained later. Finally, it passes a phase modulator before being reflected by the Faraday mirror. $P_2$ follows the same path. Alice briefly activates her modulator to apply a phase shift on $P_1$ only, in order to encode a bit value exactly as in the traditional phase-coding scheme. The attenuator is set so that when the pulses leave Alice, they contain no more than a fraction of a photon. When they reach the polarizing beamsplitter after their return trip through the link, the polarization state of the pulses is exactly orthogonal to what it was when they left, thanks to the effect of the Faraday mirror. $P_1$ is then reflected instead of being transmitted. It takes the long arm to the coupler. When it passes, Bob activates his modulator to apply a phase shift used to implement his basis choice. Similarly, $P_2$ is transmitted and takes the short arm. Both pulses reach the coupler at the same time and they interfere. Single-photon detectors are then used to record the output port chosen by the photon.

We implemented the four full-state BB84 protocol with this setup. The system was tested once again on the same installed optical fiber cable linking Geneva and Nyon (23 km; see Fig. 13) at 1300 nm, and we observed a very low $QBER_{opt} \approx 1.4\%$ (Ribordy *et al.*, 1998, 2000). Proprietary electronics and software were developed to allow for fully automated and user-friendly operation of the system. Because of the intrinsically bidirectional nature of this system, great attention had to be paid to Rayleigh backscattering. Light traveling in an optical fi-

[38]Note that since then, we have used this interferometer for various other applications: a nonlinear index-of-refraction measurement in fibers (Vinegoni, Wegmuller, and Gisin, 2000) and an optical switch (Vinegoni, Wegmüller, Hüttner, and Gisin, 2000).

ber undergoes scattering by inhomogeneities. A small fraction ($\simeq 1\%$) of this light is recaptured by the fiber in the backward direction. When the repetition rate is high enough, pulses traveling to and from Alice must intersect at some point along the line. Their intensity, however, is strongly different. The pulses are more than a thousand times brighter before than after reflection from Alice. Backscattered photons can accompany a quantum pulse propagating back to Bob and induce false counts. We avoided this problem by making sure that pulses traveling to and from Bob are not present in the line simultaneously. They are emitted by Bob in the form of trains. Alice stores these trains in her optical delay line, which consists of an optical fiber spool. Bob waits until all the pulses of a train have reached him before sending the next one. Although it completely solves the problem of Rayleigh backscattering-induced errors, this configuration has the disadvantage of reducing the effective repetition frequency. A storage line half as long as the transmission line amounts to a reduction of the bit rate by a factor of approximately 3.

Researchers at IBM simultaneously and independently developed a similar system at 1300 nm (Bethune and Risk, 2000). However, they avoided the problems associated with Rayleigh backscattering by reducing the intensity of the pulses emitted by Bob. Since these could not be used for synchronization purposes any longer, they added a wavelength-multiplexed classical channel (1550 nm) in the line to allow Bob and Alice to synchronize their systems. They tested their setup on a 10-km optical fiber spool. Both of these systems are equivalent and exhibit similar performances. In addition, the group of Anders Karlsson at the Royal Institute of Technology in Stockholm verified in 1999 that this technique also works at a wavelength of 1550 nm (Bourennane *et al.*, 1999, 2000). These experiments demonstrate the potential of plug-and-play-like systems for real-world quantum key distribution. They certainly constitute a good candidate for the realization of prototypes.

Their main disadvantage with respect to the other systems discussed in this section is that they are more sensitive to Trojan horse strategies (see Sec. VI.K). Indeed, Eve could send a probe beam and recover it through the strong reflection by the mirror at the end of Alice's system. To prevent such an attack, Alice adds an attenuator to reduce the amount of light propagating through her system. In addition, she must monitor the incoming intensity using a classical linear detector. Systems based on this approach cannot be operated with a true single-photon source and thus will not benefit from the progress in this field.[39]

### D. Frequency coding

Phase-based systems for QC require phase synchronization and stabilization. Because of the high frequency of optical waves (approximately 200 THz at 1550 nm), this condition is difficult to fulfill. One solution is to use self-aligned systems like the plug-and-play setups discussed in the previous section. Goedgebuer and his team from the University of Besançon, in France, introduced an alternative solution (Sun *et al.*, 1995; Mazurenko *et al.*, 1997; Mérolla *et al.*, 1999; see also Molotkov, 1998). Note that the title of this section is not completely accurate, since the value of the qubits is coded not in the frequency of the light, but in the relative phase between sidebands of a central optical frequency.

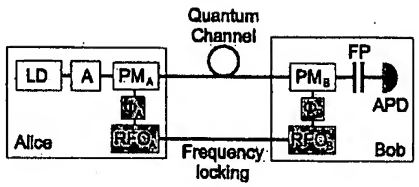


FIG. 19. Implementation of sideband modulation: LD, laser diode; A, attenuator; $PM_i$, optical phase modulator; $\Phi_i$, electronic phase controller; $RFO_k$, radio frequency oscillator; FP, Fabry-Perot filter; APD, avalanche photodiode.

Their system is depicted in Fig. 19. A source emits short pulses of classical monochromatic light with angular frequency $\omega_S$. A first phase modulator $PM_A$ modulates the phase of this beam with a frequency $\Omega \ll \omega_S$ and a small modulation depth. Two sidebands are thus generated at frequencies $\omega_S \pm \Omega$. The phase modulator is driven by a radio-frequency oscillator $RFO_A$ whose phase $\Phi_A$ can be varied. Finally, the beam is attenuated so that the sidebands contain much less than one photon per pulse, while the central peak remains classical. After the transmission link, the beam experiences a second phase modulation applied by $PM_B$. This phase modulator is driven by a second radio-frequency oscillator $RFO_B$ with the same frequency $\Omega$ and phase $\Phi_B$. These oscillators must be synchronized. After passing through this device, the beam contains the original central frequency $\omega_S$, the sidebands created by Alice, and the sidebands created by Bob. The sidebands at frequencies $\omega_S \pm \Omega$ are mutually coherent and thus yield interference. Bob can then record the interference pattern in these sidebands after removal of the central frequency and the higher-order sidebands with a spectral filter.

To implement the B92 protocol (see Sec. II.D.1), Alice randomly chooses the value of the phase $\Phi_A$ for each pulse. She associates a bit value of 0 with phase 0 and a bit value of 1 with phase $\pi$. Bob also randomly chooses whether to apply a phase $\Phi_B$ of 0 or $\pi$. One can see that if $|\Phi_A - \Phi_B| = 0$, the interference is constructive and Bob's single-photon detector has a nonzero probability of recording a count. This probability depends on the number of photons initially present in the sideband, as well as on the losses induced by the channel. On the other hand, if $|\Phi_A - \Phi_B| = \pi$, interference is destructive, and no count will ever be recorded. Consequently, Bob can infer, every time he records a count, that he applied the same phase as Alice. When a given pulse does not yield a detection, the reason can be that the phases ap-

[39]The fact that the pulses make a round trip implies that losses are doubled, yielding a reduced counting rate.

plied were different and destructive interference took place. It can also mean that the phases were actually equal, but the pulse was empty or the photon got lost. Bob cannot decide between these two possibilities. From a conceptual point of view, Alice sends one of two nonorthogonal states. There is then no way for Bob to distinguish between them deterministically. However, he can perform a generalized measurement, also known as a *positive operator value measurement*, which will sometimes fail to give an answer, but at all other times gives the correct one.

Eve could perform the same measurement as Bob. When she obtains an inconclusive result, she could just block both the sideband and the central frequency so that she does not have to guess a value and does not risk introducing an error. To prevent her from doing that, Bob verifies the presence of this central frequency. Now if Eve tries to conceal her presence by blocking only the sideband, the reference central frequency will still have a certain probability of introducing an error. It is thus possible to catch Eve in both cases. The monitoring of the reference beam is essential in all two-state protocols to reveal eavesdropping. In addition, it was shown that this reference-beam monitoring can be extended to the four-state protocol (Huttner *et al.*, 1995).

The advantage of this setup is that the interference is controlled by the phase of the radio-frequency oscillators. Their frequency is six orders of magnitude smaller than the optical frequency and thus considerably easier to stabilize and synchronize. It is indeed a relatively simple task, which can be achieved by electronic means. The Besançon group performed key distribution with such a system. The source they used was a distributed Bragg reflector (DBR) laser diode at a wavelength of 1540 nm and a bandwidth of 1 MHz. It was externally modulated to obtain 50-ns pulses, thus increasing the bandwidth to about 20 MHz. They used two identical $LiNbO_3$ phase modulators operating at a frequency $\Omega/2\pi=300$ MHz. Their spectral filter was a Fabry-Perot cavity with a finesse of 55. Its resolution was 36 MHz. They performed key distribution over a 20-km single-mode optical fiber spool, recording a $QBER_{opt}$ contribution of approximately 4%. They estimated that 2% could be attributed to the transmission of the central frequency by the Fabry-Perot cavity. Note also that the detector noise was relatively high due to the long pulse durations. Both these errors could be lowered by increasing the separation between the central peak and the sidebands, allowing reduced pulse widths and hence shorter detection times and lower dark counts. Nevertheless, a compromise must be found since, in addition to the technical drawbacks of high-speed modulation, the polarization transformation in an optical fiber depends on the wavelength. The remaining 2% of the $QBER_{opt}$ is due to polarization effects in the setup.

This system is another possible candidate. Its main advantage is that it could be used with a true single-photon source if it existed. On the other hand, the contribution of imperfect interference visibility to the error rate is significantly higher than that measured with plug-and-play systems. In addition, if this system is to be truly independent of polarization, it is essential to ensure that the phase modulators have very low polarization dependency. In addition, the stability of the frequency filter may constitute a practical difficulty.

### E. Free-space line-of-sight applications

Since optical fiber channels may not always be available, several groups are trying to develop free-space line-of-sight QC systems capable, for example, of distributing a key between building rooftops in an urban setting.

Of course it may sound difficult to detect single photons amidst background light, but the first experiments have already demonstrated the feasibility of free-space QC. Sending photons through the atmosphere also has advantages, since this medium is essentially nonbirefringent (see Sec. III.B.4). It is then possible to use plain polarization coding. In addition, one can ensure very high channel transmission over long distances by carefully choosing the wavelength of the photons (see again Sec. III.B.4). The atmosphere has, for example, a high transmission "window" in the vicinity of 770 nm (transmission as high as 80% can occur between a ground station and a satellite), which happens to be compatible with commercial silicon APD photon-counting modules (detection efficiency can be as high as 65% with low noise).

The systems developed for free-space applications are actually very similar to that shown in Fig. 12. The main difference is that the emitter and receiver are connected by telescopes pointing at each other, instead of by an optical fiber. The contribution of background light to errors can be maintained at a reasonable level by using a combination of timing discrimination (coincidence windows of typically a few nanoseconds), spectral filtering (interference filters $\leq 1$ nm), and spatial filtering (coupling into an optical fiber). This can be illustrated by the following simple calculation. Let us suppose that the isotropic spectral background radiance is $10^{-2}\ \mathrm{W\,m^{-2}\,nm^{-1}\,sr^{-1}}$ at 800 nm. This corresponds to the spectral radiance of a clear zenith sky with a sun elevation of 77° (Zissis and Larocca, 1978). The divergence $\theta$ of a Gaussian beam with radius $w_0$ is given by $\theta=\lambda/w_0\pi$. The product of beam (telescope) cross section and solid angle, which is a constant, is therefore $\pi w_0^2 \pi\theta^2=\lambda^2$. By multiplying the radiance by $\lambda^2$, one obtains the spectral power density. With an interference filter of 1-nm width, the power incident on the detector is $6\times10^{-15}$ W, corresponding to $2\times10^4$ photons per second or $2\times10^{-5}$ photons per nanosecond. This quantity is approximately two orders of magnitude larger than the dark-count probability of Si APD's, but still compatible with the requirements of QC. The performance of free-space QC systems depends dramatically on atmospheric conditions and air quality. This is problematic for urban applications where pollution and aerosols degrade the transparency of air.

The first free-space QC experiment over a distance of more than a few centimeters[40] was performed by Jacobs and Franson in 1996. They exchanged a key over a distance of 150 m in a hallway illuminated with standard fluorescent lighting and over 75 m outdoors in bright daylight without excessive QBER. Hughes and his team were the first to exchange a key over more than one kilometer under outdoor nighttime conditions (Buttler *et al.*, 1998; Hughes, Buttler, *et al.*, 2000). More recently, they even improved their system to reach a distance of 1.6 km under daylight conditions (Buttler *et al.*, 2000). Finally, Rarity and co-workers performed a similar experiment, in which they exchanged a key over a distance of 1.9 km under nighttime conditions (Gorman *et al.*, 2001).

Until quantum repeaters become available and allow us to overcome the distance limitation of fiber-based QC, free-space systems seem to offer the only possibility for QC over distances of more than a few dozen kilometers. A QC link could be established between ground-based stations and a low-orbit (300–1200 km) satellite. The idea is for Alice and Bob to each exchange a key ($k_A$ and $k_B$, respectively) with the same satellite, using QC. Then the satellite publicly announces the value $K = k_A \oplus k_B$, where $\oplus$ represents the XOR operator or, equivalently, the binary addition modulo 2 without carry. Bob subtracts his key from this value to recover Alice's key ($k_A = K \ominus k_B$).[41] The fact that the key is known to the satellite operator may at first be seen as a disadvantage. But this point might actually be conducive to the development of QC, since governments always like to control communications. Although it has not yet been demonstrated, Hughes as well as Rarity have estimated—in view of their free-space experiments—that the difficulty can be overcome. The main difficulty would come from beam pointing—do not forget that the satellites will move with respect to the ground—and wandering induced by turbulence. In order to minimize the latter problem, the photons would in practice probably be sent down from the satellite. Atmospheric turbulence is concentrated almost entirely in the first kilometer above the earth's surface. Another possibile way to compensate for beam wander is to use adaptative optics. Free-space QC experiments over distances of about 2 km constitute a major step towards key exchange with a satellite. According to Buttler *et al.* (2000), the optical depth is indeed similar to the effective atmospheric thickness that would be encountered in a surface-to-satellite application.

### F. Multi-user implementations

Paul Townsend and colleagues have investigated the application of QC over multi-user optical fiber networks (Townsend *et al.*, 1994; Phoenix *et al.*, 1995; Townsend, 1997b). They used a passive optical fiber network architecture in which one Alice, the network manager, is connected to multiple network users (i.e., many Bobs; see Fig. 20). The goal is for Alice to establish a verifiably secure and unique key with each Bob. In the classical limit, the information transmitted by Alice is gathered by all Bobs. However, because of their quantum behavior, the photons are effectively routed at the beamsplitter to one, and only one, of the users. Using the double Mach-Zehnder configuration discussed above, they tested such an arrangement with three Bobs. Nevertheless, because of the fact that QC requires a direct and low-attenuation optical channel between Alice and Bob, the ability to implement it over large and complex networks appears limited.

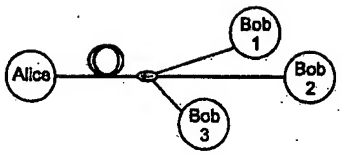


FIG. 20. Multi-user implementation of quantum cryptography with one Alice connected to three Bobs by optical fibers. The photons sent by Alice randomly choose to go to one or the other Bob at a coupler.

## V. EXPERIMENTAL QUANTUM CRYPTOGRAPHY WITH PHOTON PAIRS

The possibility of using entangled photon pairs for quantum cryptography was first proposed by Ekert in 1991. In a subsequent paper, he investigated, with other researchers, the feasibility of a practical system (Ekert *et al.*, 1992). Although all tests of Bell's inequalities (for a review see, for example, Zeilinger, 1999) can be seen as experiments in quantum cryptography, systems specifically designed to meet the special requirements of QC, like quick changes of basis, have been implemented only recently.[42] In 1999, three groups demonstrated quantum cryptography based on the properties of entangled photons. Their results were reported in the same issue of Phys. Rev. Lett. (Jennewein, Simon, *et al.*, 2000; Naik *et al.*, 2000; Tittel *et al.*, 2000), illustrating the rapid progress in the still new field of quantum communication.

One advantage of using photon pairs for QC is the fact that one can remove empty pulses, since the detec-

[40]Remember that Bennett and co-workers performed the first demonstration of QC over 30 cm in air (Bennett, Bessette, *et al.*, 1992).

[41]This scheme could also be used with optical fiber implementation provided that secure nodes existed. In the case of a satellite, one tacitly assumes that it constitutes such a secure node.

[42]This definition of quantum cryptography applies to the famous experiment by Aspect and co-workers testing Bell's inequalities with time-varying analyzers (Aspect *et al.*, 1982). QC had, however, not yet been invented. It also applies to the more recent experiments closing *locality loopholes*, like the one performed in Innsbruck using fast polarization modulators (Weihs *et al.*, 1998) or the one performed in Geneva using two analyzers on each side (Tittel *et al.*, 1999; Gisin and Zbinden, 1999).

tion of one photon of a pair reveals the presence of a companion. In principle, it is thus possible to have a probability of emitting a nonempty pulse equal to one.[43] It is beneficial only because currently available single-photon detectors feature a high dark-count probability. The difficulty of always collecting both photons of a pair somewhat reduces this advantage. One frequently hears that photon pairs have the advantage of avoiding multiphoton pulses, but this is not correct. For a given mean photon number, the probability that a nonempty pulse contains more than one photon is essentially the same for weak pulses as for photon pairs (see Sec. III.A.2).

A second advantage is that using entangled photons pair prevents unintended information leakage in unused degrees of freedom (Mayers and Yao, 1998). Observing a QBER lower than approximately 15%, or equivalently observing that Bell's inequality is violated, indeed guarantees that the photons are entangled, so that the different states are not fully distinguishable through other degrees of freedom. A third advantage was indicated recently by new and elaborate eavesdropping analyses. The fact that passive state preparation can be implemented prevents multiphoton splitting attacks (see Sec. VI.J).

The coupling between the optical frequency and the property used to encode the qubit, i.e., decoherence, is rather easy to master when using faint laser pulses. However, this issue is more serious when using photon pairs, because of the larger spectral width. For example, for a spectral width of 5 nm full width at half maximum (FWHM)—a typical value, equivalent to a coherence time of 1 ps—and a fiber with a typical polarization mode dispersion of 0.2 ps/$\sqrt{\text{km}}$, transmission over a few kilometers induces significant depolarization, as discussed in Sec. III.B.2. In the case of polarization-entangled photons, this effect gradually destroys their correlation. Although it is in principle possible to compensate for this effect, the statistical nature of the polarization mode dispersion makes this impractical.[44] Although perfectly fine for free-space QC (see Sec. IV.E), polarization entanglement is thus not adequate for QC over long optical fibers. A similar effect arises when dealing with energy-time-entangled photons. Here, the chromatic dispersion destroys the strong time correlations between the photons forming a pair. However, as discussed in Sec. III.B.3, it is possible to compensate passively for this effect either using additional fibers with opposite dispersion, or exploiting the inherent energy correlation of photon pairs.

[43]Photon-pair sources are often, though not always, pumped continuously. In these cases, the time window determined by a trigger detector and electronics defines an effective pulse.

[44]In the case of weak pulses, we saw that a full round trip together with the use of Faraday mirrors circumvents the problem (see Sec. IV.C.2). However, since the channel loss on the way from the source to the Faraday mirror inevitably increases the fraction of empty pulses, the main advantage of photon pairs vanishes in such a configuration.

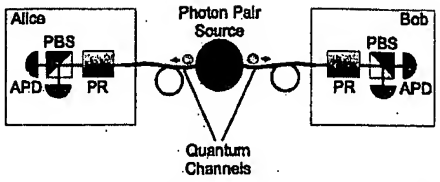


FIG. 21. Typical system for quantum cryptography exploiting photon pairs entangled in polarization: PR, active polarization rotator; PBS, polarizing beamsplitter; APD, avalanche photodiode.

Generally speaking, entanglement-based systems are far more complex than setups based on faint laser pulses. They will most certainly not be used in the near future for the realization of industrial prototypes. In addition, the current experimental key creation rates obtained with these systems are at least two orders of magnitude smaller than those obtained with faint laser pulse setups (net rate on the order of a few tens of bits per second, in contrast to a few thousand bits per second for a 10-km distance). Nevertheless, they offer interesting possibilities in the context of cryptographic optical networks. The photon-pair source can indeed be operated by a key provider and situated somewhere in between potential QC customers. In this case, the operator of the source has no way of getting any information about the key obtained by Alice and Bob.

It is interesting to emphasize the close analogy between one- and two-photon schemes, which was first noted by Bennett, Brassard, and Mermin (1992). In a two-photon scheme, when Alice detects her photon, she effectively prepares Bob's photon in a given state. In the one-photon analog, Alice's detectors are replaced by sources, while the photon-pair source between Alice and Bob is bypassed. The difference between these schemes lies only in practical issues, like the spectral widths of the light. Alternatively, one can look at this analogy from a different point of view: in two-photon schemes, it is as if Alice's photon propagates backwards in time from Alice to the source and then forward in time from the source to Bob.

### A. Polarization entanglement

A first class of experiments takes advantage of polarization-entangled photon pairs. The setup, depicted in Fig. 21, is similar to the scheme used for polarization coding based on faint pulses. A two-photon source emits pairs of entangled photons flying back to back towards Alice and Bob. Each photon is analyzed with a polarizing beamsplitter whose orientation with respect to a common reference system can be changed rapidly. The results of two experiments were reported in the spring of 2000 (Jennewein, Simon, *et al.*, 2000; Naik *et al.*, 2000). Both used photon pairs at a wavelength of 700 nm, which were detected with commercial single-photon detectors based on silicon APD's. To create the photon pairs, both groups took advantage of parametric down-conversion in one or two $\beta$-$BaB_2O_4$ (BBO) crystals

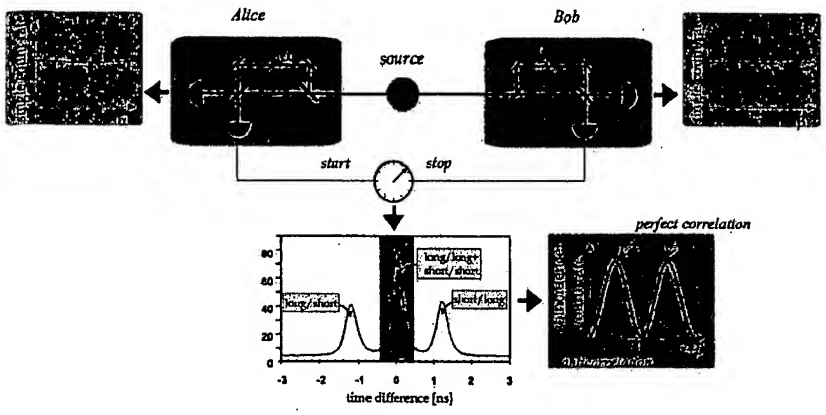


FIG. 22. Principle of phase-coding quantum cryptography using energy-time-entangled photon pairs.

pumped by an argon-ion laser. The analyzers consisted of fast modulators that were used to rotate the polarization state of the photons, in front of polarizing beam-splitters.

The group of Anton Zeilinger, then at the University of Innsbruck, demonstrated such a cryptosystem, including error correction, over a distance of 360 m (Jennewein, Simon, *et al.*, 2000). Inspired by a test of Bell's inequalities performed with the same setup a year earlier (Weihs *et al.*, 1998), they positioned the two-photon source near the center between the two analyzers. Special optical fibers, designed for guiding only a single mode at 700 nm, were used to transmit the photons to the two analyzers. The results of the remote measurements were recorded locally, and the processes of key sifting and error correction were implemented at a later stage, long after the distribution of the qubits. Two different protocols were implemented: one based on Wigner's inequality (a special form of Bell's inequalities) and the other based on BB84.

The group of Paul Kwiat, then at Los Alamos National Laboratory, demonstrated the Ekert protocol (Naik *et al.*, 2000). This experiment was a table-top realization in which the source and the analyzers were separated by only a few meters. The quantum channel consisted of a short free-space distance. In addition to performing QC, the researchers simulated different eavesdropping strategies. As predicted by theory, they observed a rise in the QBER with an increase of the information obtained by the eavesdropper. Moreover, they have also recently implemented the six-state protocol described in Sec. II.D.2 and observed the predicted QBER increase to 33% (Enzer *et al.*, 2001).

The main advantage of polarization entanglement is that analyzers are simple and efficient. It is therefore relatively easy to obtain high contrast. Naik and coworkers, for example, measured a polarization extinction of 97%, mainly limited by electronic imperfections of the fast modulators. This amounts to a $QBER_{opt}$ contribution of only 1.5%. In addition, the constraint on the coherence length of the pump laser is not very stringent (note that, if it is shorter than the length of the crystal, some difficulties can arise, but we will not go into these here).

In spite of their qualities, it would be difficult to reproduce these experiments over distances of more than a few kilometers of optical fiber. As mentioned in the introduction to this section, polarization is indeed not robust enough to avoid decoherence in optical fibers. In addition, the polarization state transformation induced by an installed fiber frequently fluctuates, making an active alignment system absolutely necessary. Nevertheless, these experiments are very interesting in the context of free-space QC.

### B. Energy-time entanglement

#### 1. Phase coding

Another class of experiments takes advantage of energy-time-entangled photon pairs. The idea originates from an arrangement proposed by Franson in 1989 to test Bell's inequalities. As we shall see below, it is comparable to the double Mach-Zehnder configuration discussed in Sec. IV.C.1. A source emits pairs of energy-correlated photons, that were created at exactly the same (unknown) time (see Fig. 22). This can be achieved by pumping a nonlinear crystal with a pump of long coherence time. The pairs of downconverted photons are then split, and one photon is sent to each party down quantum channels. Both Alice and Bob possess a widely but identically unbalanced Mach-Zehnder interferometer, with photon-counting detectors connected to the outputs. Locally, if Alice or Bob change the phase of their interferometer, no effect on the count rates is observed, since the imbalance prevents any single-photon interference. Looking at the detection time at Bob's end with respect to the arrival time at Alice's end, three different values are possible for each combination of detectors. The different possibilities in a time spectrum are shown in Fig. 22. First, both photons can propagate through the short arms of the interferometers. Second, one can take the long arm at Alice's end, while the other one takes the short one at Bob's, or vice versa. Finally, both photons can propagate through the long arms. When the path differences of the interferometers are matched to within a fraction of the coherence length of the downconverted photons, the short-short and the

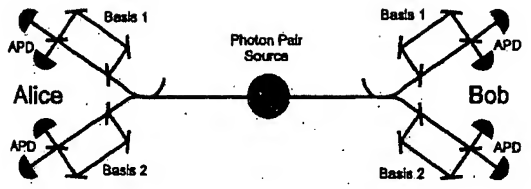


FIG. 23. System for quantum cryptography based on phase-coding entanglement: APD, avalanche photodiode. The photons choose their bases randomly at Alice and Bob's couplers.

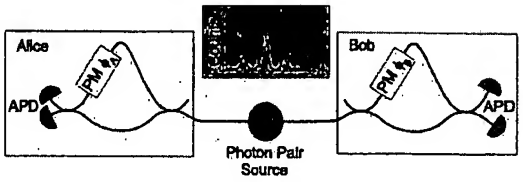


FIG. 24. Quantum cryptography system exploiting photons entangled in energy-time and active basis choice. Note the similarity to the faint-laser double Mach-Zehnder implementation depicted in Fig. 16.

long-long processes are indistinguishable, provided that the coherence length of the pump photon is larger than the path-length difference. Conditioning detection only on the central time peak, one observes two-photon interferences—nonlocal quantum correlations (Franson, 1989)[45]—that depend on the sum of the relative phases in Alice's and Bob's interferometers (see Fig. 22). The phases of Alice's and Bob's interferometers can, for example, be adjusted so that both photons always emerge from the same output port. It is then possible to exchange bits by associating values with the two ports. This, however, is insufficient. A second measurement basis must be implemented to ensure security against eavesdropping attempts. This measurement can be made, for example, by adding a second interferometer to the systems (see Fig. 23). In this case, when reaching an analyzer, a photon chooses randomly to go to one or the other interferometer. The second set of interferometers can also be adjusted to yield perfect correlations between output ports. The relative phases between their arms should, however, be chosen so that when the photons go to interferometers that are not associated with each other, the outcomes are completely uncorrelated.

Such a system features passive state preparation by Alice, yielding security against multiphoton splitting attacks (see Sec. VI.J). In addition, it also features a passive basis choice by Bob, which constitutes an elegant solution: neither a random-number generator nor an active modulator are necessary. It is nevertheless clear that $\mathrm{QBER}_{det}$ and $\mathrm{QBER}_{acc}$ [defined in Eq. (33)] are doubled, since the number of activated detectors is twice as high. This disadvantage is not as important as it first appears, since the alternative, a fast modulator, introduces losses close to 3 dB, also resulting in an increase of these error contributions. The striking similarity between this scheme and the double Mach-Zehnder arrangement discussed in the context of faint laser pulses in Sec. IV.C.1 is obvious when one compares Figs. 24 and 16.

This scheme was realized in the first half of 2000 by our group at the University of Geneva (Ribordy *et al.*, 2001). It was the first experiment in which an asymmetric setup optimized for QC was used instead of a system designed for tests of Bell's inequality, with a source located midway between Alice and Bob (see Fig. 25). The two-photon source (a $KNbO_3$ crystal pumped by a doubled Nd-YAG laser) provided energy-time-entangled photons at nondegenerate wavelengths—one at around 810 nm, the other centered at 1550 nm. This choice allowed the use of high-efficiency silicon-based single-photon counters featuring low noise to detect the photons of the lower wavelength. To avoid the high transmission losses at this wavelength in optical fibers, the distance between the source and the corresponding analyzer was very short, of the order of a few meters. The other photon, at the wavelength where fiber losses are minimal, was sent via an optical fiber to Bob's interferometer and then detected by InGaAs APD's. The decoherence induced by chromatic dispersion was limited by the use of dispersion-shifted optical fibers (see Sec. III.B.3).

Implementing the BB84 protocol in the manner discussed above, with a total of four interferometers, is difficult. Indeed, they must be aligned and their relative phase kept accurately stable during the whole key distribution session. To simplify this problem, we devised birefringent interferometers with polarization multiplexing of the two bases. Consequently the constraint on the stability of the interferometers was equivalent to that encountered in the faint-pulse double Mach-Zehnder system. We obtained interference visibilities typically of 92%, yielding in turn a $\mathrm{QBER}_{opt}$ contribution of about 4%. We demonstrated QC over a transmission distance of 8.5 km in a laboratory setting using a fiber on a spool and generated several megabits of key in hour-long ses-

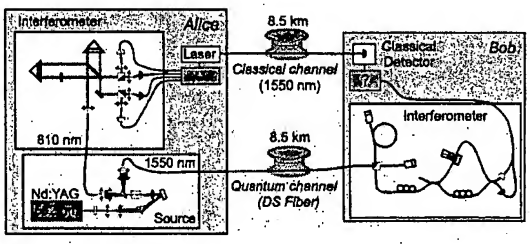


FIG. 25. Schematic diagram of the first system designed and optimized for long-distance quantum cryptography and exploiting phase coding of entangled photons.

[45]The imbalance of the interferometers must be large enough so that the middle peak can easily be distinguished from the satellite ones. This minimal imbalance is determined by the convolution of the detector's jitter (tens of picoseconds), the electronic jitter (from tens to hundreds of picoseconds), and the single-photon coherence time (<1 ps).

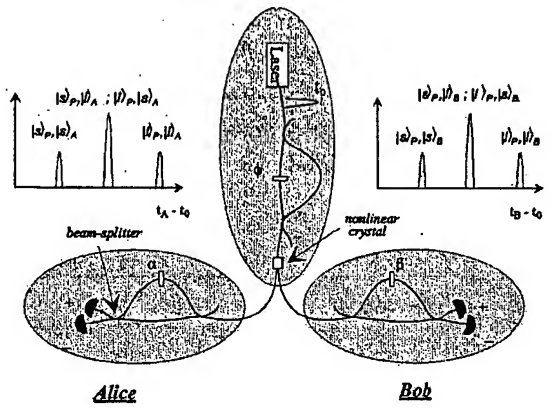


FIG. 26. Schematics of quantum cryptography using entangled-photon phase-time coding.

sions. This is the longest span realized to date for QC with photon pairs.

As already mentioned, it is essential for this scheme to have a pump laser whose coherence length is longer than the path imbalance of the interferometers. In addition, its wavelength must remain stable during a key exchange session. These requirements imply that the pump laser must be somewhat more elaborate than in the case of polarization entanglement.

### 2. Phase-time coding

We have mentioned in Sec. IV.C that states generated by two-path interferometers are two-level quantum systems. They can also be represented on a Poincaré sphere. The four states used for phase coding in the previous section would lie equally distributed on the equator of the sphere. The coupling ratio of the beamsplitter is 50%, and a phase difference is introduced between the components propagating through either arm. In principle, the four-state protocol can be equally well implemented with only two states on the equator and two others on the poles. In this section, we present a system exploiting such a set of states. Proposed by our group in 1999 (Brendel *et al.*, 1999), the scheme follows in principle the Franson configuration described in the context of phase coding. However, it is based on a pulsed source emitting entangled photons in so-called energy-time Bell states (Tittel *et al.*, 2000). The emission time of the photon pair is therefore given by a superposition of only two discrete terms, instead of by a wide and continuous range bounded only by the long coherence length of the pump laser (see Sec. V.B.1).

Consider Fig. 26. If Alice registers the arrival times of the photons with respect to the emission time of the pump pulse $t_0$, she finds the photons in one of three time slots (note that she has two detectors to take into account). For instance, detection of a photon in the first slot corresponds to the pump photon's having traveled via the short arm and the downconverted photon's having traveled via the short arm. To keep it simple, we refer to this process as $|s\rangle_P,|s\rangle_A$, where $P$ stands for the pump and $A$ for Alice's photon.[46] However, the characterization of the complete photon pair is still ambiguous, since, at this point, the path of the photon that has traveled to Bob (short or long in his interferometer) is unknown to Alice. Figure 26 illustrates all processes leading to a detection in the different time slots both at Alice's and at Bob's detector. Obviously, this reasoning holds for any combination of two detectors. In order to build up the secret key, Alice and Bob now publicly agree about the events when both detected a photon in one of the satellite peaks—without revealing in which one—or both in the central peak—without revealing in which detector. This procedure corresponds to key sifting. For instance, in the example discussed above, if Bob tells Alice that he has detected his photon in a satellite peak, she knows that it must have been the left peak. This is because the pump photon has traveled via the short arm, hence Bob can detect his photon either in the left satellite or in the central peak. The same holds for Bob, who now knows that Alice's photon traveled via the short arm in her interferometer. Therefore, in the case of joint detection in a satellite peak, Alice and Bob must have correlated detection times. Assigning a bit value to each side peak, Alice and Bob can exchange a sequence of correlated bits.

The cases where both find the photon in the central time slot are used to implement the second basis. They correspond to the $|s\rangle_P,|l\rangle_A|l\rangle_B$ and $|l\rangle_P,|s\rangle_A|s\rangle_B$ possibilities. If these are indistinguishable, one obtains two-photon interferences, exactly as in the case discussed in the previous section on phase coding. Adjusting the phases and keeping them stable, one can use the perfect correlations between output ports chosen by the photons at Alice's and Bob's interferometers to establish the key bits in this second basis.

Phase-time coding has recently been implemented in a laboratory experiment by our group (Tittel *et al.*, 2000) and was reported at the same time as the two polarization entanglement-based schemes mentioned above. A contrast of approximately 93% was obtained, yielding a $\mathrm{QBER}_{opt}$ contribution of 3.5%, similar to that obtained with the phase-coding scheme. This experiment will be repeated over long distances, since losses in optical fibers are low at the downconverted photon wavelength (1300 nm).

An advantage of this setup is that coding in the time basis is particularly stable. In addition, the coherence length of the pump laser is no longer critical. However, it is necessary to use relatively short pulses ($\approx$500 ps) powerful enough to induce a significant downconversion probability.

Phase-time coding, as discussed in this section, can also be realized with faint laser pulses (Bechmann-Pasquinucci and Tittel, 2000). The one-photon configuration has so far never been realized. It would be similar to the double Mach-Zehnder setup discussed in Sec. IV.C.1, but with the first coupler replaced by an active

[46]Note that it does not constitute a product state.

switch. For the time basis, Alice would set the switch either to full transmission or to full reflection, while for the energy basis she would set it at 50%. This illustrates how research on photon pairs can yield advances on faint-pulse systems.

#### 3. Quantum secret sharing

In addition to QC using phase-time coding, we used the setup depicted in Fig. 26 for the first proof-of-principle demonstration of quantum secret sharing—the generalization of quantum key distribution to more than two parties (Tittel *et al.*, 2001). In this new application of quantum communication, Alice distributes a secret key to two other users, Bob and Charlie, in such a way that neither Bob nor Charlie alone has any information about the key, but together they have full information. As in traditional QC, an eavesdropper trying to get some information about the key creates errors in the transmission data and thus reveals her presence. The motivation behind quantum secret sharing is to guarantee that Bob and Charlie cooperate—one of them might be dishonest—in order to obtain a given piece of information. In contrast with previous proposals using three-particle Greenberger-Horne-Zeilinger states (Zukowski *et al.*, 1998; Hillery *et al.*, 1999), pairs of entangled photons in so-called energy-time Bell states were used to mimic the necessary quantum correlation of three entangled qubits, although only two photons exist at the same time. This is possible because of the symmetry between the preparation device acting on the pump pulse and the devices analyzing the downconverted photons. Therefore the emission of a pump pulse can be considered as the detection of a photon with 100% efficiency, and the scheme features a much higher coincidence rate than that expected with the initially proposed "triple-photon" schemes.

## VI. EAVESDROPPING

### A. Problems and objectives

After the qubit exchange and basis reconciliation, Alice and Bob each have a sifted key. Ideally, these keys are identical. But in real life, there are always some errors, and Alice and Bob must apply some classical information processing protocols, like error correction and privacy amplification to their data (see Sec. II.C.4). The first protocol is necessary to obtain identical keys and the second to obtain a secret key. Essentially, the problem of eavesdropping is to find protocols which, given that Alice and Bob can only measure the QBER, either provide Alice and Bob with a verifiably secure key or stop the protocol and inform the users that the key distribution has failed. This is a delicate problem at the intersection of quantum physics and information theory. Actually, it comprises several eavesdropping problems, depending on the precise protocol, the degree of idealization one admits, the technological power one assumes Eve has, and the assumed fidelity of Alice and Bob's equipment. Let us immediately stress that a complete analysis of eavesdropping on a quantum channel has yet to be achieved. In this section we review some of the problems and solutions, without any claim for mathematical rigor or complete coverage of the huge and rapidly evolving literature.

The general objective of eavesdropping analysis is to find ultimate and practical proofs of security for some quantum cryptosystems. "Ultimate proofs" guarantee security against entire classes of eavesdropping attacks, even if Eve uses not only the best of today's technology, but any conceivable future technology. These proofs take the form of theorems, with clearly stated assumptions expressed in mathematical terms. In contrast, practical proofs deal with some actual pieces of hardware and software. There is thus a tension between "ultimate" and "practical" proofs. Indeed, the former favor general abstract assumptions, whereas the latter concentrate on physical implementations. Nevertheless, it is worth finding such proofs. In addition to the security issue, they provide illuminating lessons for our general understanding of quantum information.

In the ideal game Eve has perfect technology: she is limited only by the laws of quantum mechanics, but not at all by current technology.[47] In particular, Eve cannot clone qubits, as this is incompatible with quantum dynamics (see Sec. II.C.2), but she is free to use any unitary interaction between one or several qubits and an auxiliary system of her choice. Moreover, after the interaction, Eve may keep her auxiliary system unperturbed, in complete isolation from the environment, for an arbitrarily long time. Finally, after listening to all the public discussion between Alice and Bob, she can perform the measurement of her choice on her system, being again limited only by the laws of quantum mechanics. One assumes further that all errors are due to Eve. It is tempting to assume that some errors are due to Alice's and Bob's instruments, and this probably makes sense in practice. However, there is the danger of Eve's replacing them with higher-quality instruments (see the next section).

In the next section we elaborate on the most relevant differences between the above ideal game (ideal especially from Eve's point of view) and real systems. Next, we return to the idealized situation and present several eavesdropping strategies, starting from the simplest, in which explicit formulas can be written down, and ending with a general abstract security proof. Finally, we discuss practical eavesdropping attacks and comment on the complexity of a real system's security.

### B. Idealized versus real implementation

Alice and Bob use the technology available today. This trivial remark has several implications. First, all

[47]The question of whether QC would survive the discovery of the currently unknown validity limits of quantum mechanics is interesting. Let us argue that it is likely that quantum mechanics will always adequately describe photons at telecommunications and visible wavelengths, just as classical mechanics will always adequately describe the fall of apples, whatever the future of physics may be.

real components are imperfect, so that the qubits are not prepared and detected in the exact basis described by the theory. Moreover, a real source always has a finite probability of producing more than one photon. Depending on the details of the encoding device, all photons carry the same qubit (see Sec. VI.J). Hence, in principle, Eve could measure the photon number without perturbing the qubit. This scenario is discussed in Sec. VI.H. Recall that, ideally, Alice should emit single-qubit photons, i.e., each logical qubit should be encoded in a single degree of freedom of a single photon.

On Bob's side the efficiency of his detectors is quite limited and the dark counts (spontaneous counts not produced by photons) are non-negligible. The limited efficiency is analogous to the losses in the quantum channel. The analysis of the dark counts is more delicate, and no complete solution is known. Conservatively, Lütkenhaus (2000) assumes in his analysis that all dark counts provide information to Eve. He also advises that, whenever two detectors fire simultaneously (generally due to a real photon and a dark count), Bob should not disregard such events but should choose a value at random. Note also that the different contributions of dark counts to the total QBER depend on whether Bob's choice of basis is implemented using an active or a passive switch (see Sec. IV.A).

Next, one usually assumes that Alice and Bob have thoroughly checked their equipment and that it is functioning according to specifications. This assumption is not unique to quantum cryptography but is critical, as Eve could be the actual manufacturer of the equipment. Classical cryptosystems must also be carefully tested, like any commercial apparatus. Testing a cryptosystem is tricky, however, because in cryptography the client buys confidence and security, two qualities difficult to quantify. Mayers and Yao (1998) proposed using Bell's inequality to test whether the equipment really obeys quantum mechanics, but even this is not entirely satisfactory. Interestingly, one of the most subtle loopholes in all present-day tests of Bell's inequality, the detection loophole, can be exploited to produce purely classical software mimicking all quantum correlations (Gisin and Gisin, 1999). This illustrates once again the close connection between practical issues in QC and philosophical debates about the foundations of quantum physics.

Finally, one must assume that Alice and Bob are perfectly isolated from Eve. Without such an assumption the entire game would be meaningless: clearly, Eve is not allowed to look over Alice's shoulder. However, this elementary assumption is again nontrivial. What if Eve uses the quantum channel connecting Alice to the outside world? Ideally, the channel should incorporate an isolator[48] to keep Eve from shining light into Alice's output port to examine the interior of her laboratory. Since all isolators operate only on a finite bandwidth, there should also be a filter, but filters have only a finite efficiency, and so on. Except for Sec. VI.K, in which this assumption is discussed, we shall henceforth assume that Alice and Bob are isolated from Eve.

### C. Individual, joint, and collective attacks

In order to simplify the problem, several eavesdropping strategies of limited generality have been defined (Lütkenhaus, 1996; Biham and Mor, 1997a, 1997b) and analyzed. Of particular interest is the assumption that Eve attaches independent probes to each qubit and measures her probes one after the other. This class of attack is called the *individual attack*, or *incoherent attack*. This important class is analyzed in Secs. VI.D and VI.E. Two other classes of eavesdropping strategies let Eve process several qubits coherently, hence the name *coherent attacks*. The most general coherent attacks are called *joint attacks*, while an intermediate class assumes that Eve attaches one probe per qubit, as in individual attacks, but can measure several probes coherently, as in coherent attacks. This intermediate class is called the *collective attack*. It is not known whether this class is less efficient than the most general class, that of joint attacks. It is also not known whether it is more efficient than the simpler individual attacks. Actually, it is not even known whether joint attacks are more efficient than individual ones.

For joint and collective attacks, the usual assumption is that Eve measures her probe only after Alice and Bob have completed all public discussion about basis reconciliation, error correction, and privacy amplification. For the more realistic individual attacks, one assumes that Eve waits only until the basis reconciliation phase of the public discussion.[49] The motivation for this assumption is that one hardly sees what Eve could gain by waiting until after the public discussion on error correction and privacy amplification before measuring her probes, since she is going to measure them independently anyway.

Individual attacks have the nice feature that the problem can be entirely translated into a classical one: Alice, Bob, and Eve all have classical information in the form of random variables $\alpha$, $\beta$, and $\epsilon$, respectively, and the laws of quantum mechanics impose constraints on the joint probability distribution $P(\alpha,\beta,\epsilon)$. Such classical scenarios have been widely studied by the classical cryptology community, and many of their results can thus be directly applied.

### D. Simple individual attacks: Intercept-resend and measurement in the intermediate basis

The simplest attack for Eve consists in intercepting all photons individually, measuring them in a basis chosen randomly between the two bases used by Alice, and sending new photons to Bob prepared according to her

[48]Optical isolators, based on the Faraday effect, let light pass through in only one direction.

[49]With today's technology, it might even be fair to assume that in individual attacks Eve must measure her probe before the basis reconciliation.

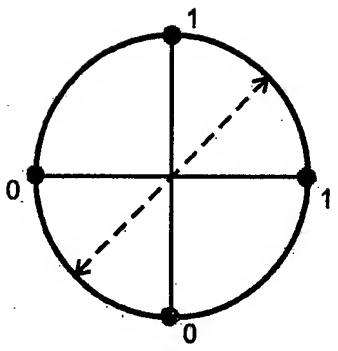


FIG. 27. Poincaré representation of the BB84 states and the intermediate basis, also known as the Breidbart basis, that can be used by Eve.

result. As presented in Sec. II.C.3 and assuming that the BB84 protocol is used, Eve thus gets 0.5 bits of information per bit in the sifted key, for an induced QBER of 25%. Let us illustrate the general formalism with this simple example. Eve's mean information gain on Alice's bit, $I(\alpha,\epsilon)$, equals their relative entropy decrease:

$$I(\alpha,\epsilon)=H_{a\ priori}-H_{a\ posteriori}, \tag{40}$$

i.e., $I(\alpha,\beta)$ is the number of bits one can save by writing $\alpha$ when knowing $\beta$. Since the *a priori* probability for Alice's bit is uniform, $H_{a\ priori}=1$. The *a posteriori* entropy has to be averaged over all possible results $r$ that Eve might get:

$$H_{a\ posteriori}=\sum_r P(r)H(i|r), \tag{41}$$

$$H(i|r)=-\sum_i P(i|r)\log_2[P(i|r)], \tag{42}$$

where the *a posteriori* probability of bit $i$, given Eve's result $r$, is given by Bayes's theorem:

$$P(i|r)=\frac{P(r|i)P(i)}{P(r)}, \tag{43}$$

with $P(r)=\Sigma_i P(r|i)P(i)$. In the case of intercept resend, Eve gets one out of four possible results: $r\in\{\uparrow,\downarrow,\leftarrow,\rightarrow\}$. After the basis has been revealed, Alice's input assumes one of two values: $i\in\{\uparrow,\downarrow\}$ (assuming the $\uparrow\downarrow$ basis was used, the other case is completely analogous). One gets $P(i=\uparrow|r=\uparrow)=1$, $P(i=\uparrow|r=\rightarrow)=\frac{1}{2}$, and $P(r)=\frac{1}{2}$. Hence, $I(\alpha,\epsilon)=1-\frac{1}{2}h(1)-\frac{1}{2}h(\frac{1}{2})=1-\frac{1}{2}=\frac{1}{2}$ [with $h(p)=p\log_2(p)+(1-p)\log_2(1-p)$].

Another strategy for Eve, no more difficult to implement, consists in measuring the photons in the intermediate basis (see Fig. 27), also known as the Breidbart basis (Bennett, Bessette, *et al.*, 1992). In this case the probability that Eve guesses the correct bit value is $p=\cos(\pi/8)^2=\frac{1}{2}+\sqrt{2}/4\approx 0.854$, corresponding to a QBER$=2p(1-p)=25\%$ and a Shannon information gain per bit of

$$I=1-H(p)\approx 0.399. \tag{44}$$

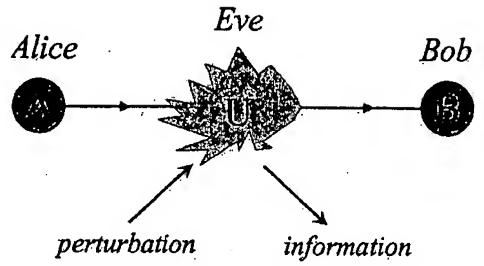


FIG. 28. Eavesdropping on a quantum channel. Eve extracts information from the quantum channel between Alice and Bob at the cost of introducing noise into that channel.

Consequently, this strategy is less advantageous for Eve than the intercept-resend strategy. Note however, that with this strategy Eve's probability of guessing the correct bit value is 85%, compared to only 75% in the intercept-resend case. This is possible because in the latter case, Eve's information is deterministic in half the cases, while in the former Eve's information is always probabilistic (formally, this results from the convexity of the entropy function).

### E. Symmetric individual attacks

In this section we present in some detail how Eve could get the maximum Shannon information for a fixed QBER, assuming a perfect single-qubit source and restricting Eve to attacks on one qubit after the other (i.e., individual attacks). The motivation is that this idealized situation is rather simple to treat and nicely illustrates several of the subtleties of the subject. Here we concentrate on the BB84 four-state protocol; for related results on the two-state and six-state protocols, see Fuchs and Peres (1996) and Bechmann-Pasquinucci and Gisin (1999), respectively.

The general idea of eavesdropping on a quantum channel is as follows. When a qubit propagates from Alice to Bob, Eve can let a system of her choice, called a probe, interact with the qubit (see Fig. 28). She can freely choose the probe and its initial state, but the system must obey the rules of quantum mechanics (i.e., be described in some Hilbert space). Eve can also choose the interaction, but it should be independent of the qubit state, and she should obey the laws of quantum mechanics; i.e., her interaction must be described by a unitary operator. After the interaction a qubit has to go to Bob (in Sec. VI.H we consider lossy channels, so that Bob does not always expect a qubit, a fact that Eve can take advantage of). It makes no difference whether this qubit is the original one (possibly in a modified state). Indeed, the question does not even make sense, since a qubit is nothing but a qubit. However, in the formalism it is convenient to use the same Hilbert space for the qubit sent by Alice as for the qubit received by Bob (this is no loss of generality, since the swap operator—defined by $\psi\otimes\phi\rightarrow\phi\otimes\psi$ for all $\psi,\phi$—is unitary and could be appended to Eve's interaction).

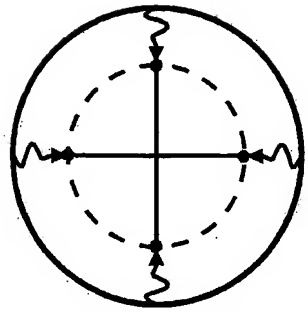

FIG. 29. Poincaré representation of BB84 states in the event of a symmetrical attack. The state received by Bob after the interaction of Eve's probe is related to the one sent by Alice by a simple shrinking factor. When the unitary operator $U$ entangles the qubit and Eve's probe, Bob's state [Eq. (46)] is mixed and is represented by a point inside the Poincaré sphere.

Let $\mathcal{H}_{Eve}$ and $\mathbb{C}^2\otimes\mathcal{H}_{Eve}$ be the Hilbert spaces of Eve's probe and of the total qubit+probe system, respectively. If $|\vec{m}\rangle$, $|0\rangle$, and $U$ denote the qubit's and the probe's initial states and the unitary interaction, respectively, then the state of the qubit received by Bob is given by the density matrix obtained by tracing out Eve's probe:

$$\rho_{Bob}(\vec{m})=\mathrm{Tr}_{\mathcal{H}_{Eve}}(U|\vec{m},0\rangle\langle\vec{m},0|U^\dagger). \tag{45}$$

The symmetry of the BB84 protocol makes it very natural to assume that Bob's state is related to Alice's $|\vec{m}\rangle$ by a simple shrinking factor[50] $\eta\in[0,1]$ (see Fig. 29):

$$\rho_{Bob}(\vec{m})=\frac{1+\eta\vec{m}\vec{\sigma}}{2}. \tag{46}$$

Eavesdropping attacks that satisfy the above condition are called *symmetric-attacks*.

Since the qubit state space is two dimensional, the unitary operator is entirely determined by its action on two states, for example, the $|\uparrow\rangle$ and $|\downarrow\rangle$ states (in this section we use spin-$\frac{1}{2}$ notation for the qubits). After the unitary interaction, it is convenient to write the states in the Schmidt form (Peres, 1997):

$$U|\uparrow,0\rangle=|\uparrow\rangle\otimes\phi_\uparrow+|\downarrow\rangle\otimes\theta_\uparrow, \tag{47}$$

$$U|\downarrow,0\rangle=|\downarrow\rangle\otimes\phi_\downarrow+|\uparrow\rangle\otimes\theta_\downarrow, \tag{48}$$

where the four states $\phi_\uparrow$, $\phi_\downarrow$, $\theta_\uparrow$, and $\theta_\downarrow$ belong to the Hilbert space of Eve's probe $\mathcal{H}_{Eve}$ and satisfy $\phi_\uparrow\perp\theta_\uparrow$ and $\phi_\downarrow\perp\theta_\downarrow$. By symmetry $|\phi_\uparrow|^2=|\phi_\downarrow|^2\equiv\mathcal{F}$ and $|\theta_\uparrow|^2=|\theta_\downarrow|^2\equiv\mathcal{D}$. Unitarity imposes $\mathcal{F}+\mathcal{D}=1$ and

$$\langle\phi_\uparrow|\theta_\downarrow\rangle+\langle\theta_\uparrow|\phi_\downarrow\rangle=0. \tag{49}$$

The $\phi$'s correspond to Eve's state when Bob receives the qubit undisturbed, while the $\theta$'s are Eve's state when the qubit is disturbed.

Let us emphasize that this is the most general unitary interaction satisfying Eq. (46). One finds that the shrinking factor is given by $\eta=\mathcal{F}-\mathcal{D}$. Accordingly, if Alice sends $|\uparrow\rangle$ and Bob measures it in the compatible basis, then $\langle\uparrow|\rho_{Bob}(\vec{m})|\uparrow\rangle=\mathcal{F}$ is the probability that Bob gets the correct result. Hence $\mathcal{F}$ is the fidelity and $\mathcal{D}$ the QBER.

Note that only four states span Eve's relevant state space. Hence Eve's effective Hilbert space is at most four dimensional, no matter how subtle she might be.[51] This greatly simplifies the analysis.

Symmetry requires that the attack on the other basis satisfy

$$U|\rightarrow,0\rangle=U\frac{|\uparrow,0\rangle+|\downarrow,0\rangle}{\sqrt{2}} \tag{50}$$

$$=\frac{1}{\sqrt{2}}(|\uparrow\rangle\otimes\phi_\uparrow+|\downarrow\rangle\otimes\theta_\uparrow \tag{51}$$

$$+|\downarrow\rangle\otimes\phi_\downarrow+|\uparrow\rangle\otimes\theta_\downarrow) \tag{52}$$

$$=|\rightarrow\rangle\otimes\phi_\rightarrow+|\leftarrow\rangle\otimes\theta_\rightarrow, \tag{53}$$

where

$$\phi_\rightarrow=\frac{1}{2}(\phi_\uparrow+\theta_\uparrow+\phi_\downarrow+\theta_\downarrow), \tag{54}$$

$$\theta_\rightarrow=\frac{1}{2}(\phi_\uparrow-\theta_\uparrow-\phi_\downarrow+\theta_\downarrow). \tag{55}$$

Similarly,

$$\phi_\leftarrow=\frac{1}{2}(\phi_\uparrow-\theta_\uparrow+\phi_\downarrow-\theta_\downarrow), \tag{56}$$

$$\theta_\leftarrow=\frac{1}{2}(\phi_\uparrow+\theta_\uparrow-\phi_\downarrow-\theta_\downarrow). \tag{57}$$

Condition (46) for the $\{|\rightarrow\rangle,|\leftarrow\rangle\}$ basis implies that $\theta_\rightarrow\perp\phi_\rightarrow$ and $\theta_\leftarrow\perp\phi_\leftarrow$. By proper choice of the phases, $\langle\phi_\uparrow|\theta_\downarrow\rangle$ can be made real. By condition (49), $\langle\theta_\uparrow|\phi_\downarrow\rangle$ is then also real. Symmetry implies that $\langle\theta_\rightarrow|\phi_\leftarrow\rangle\in\mathrm{Re}$. A straightforward computation concludes that all scalar products among Eve's states are real and that the $\phi$'s generate a subspace orthogonal to the $\theta$'s:

$$\langle\phi_\uparrow|\theta_\downarrow\rangle=\langle\phi_\downarrow|\theta_\uparrow\rangle=0. \tag{58}$$

Finally, using $|\phi_\rightarrow|^2=\mathcal{F}$, i.e., that the shrinking is the same for all states, one obtains a relation between the probe states' overlap and the fidelity:

[50] Fuchs and Peres were the first to derive the result presented in this section, using numerical optimization. Almost simultaneously, it was derived by Robert Griffiths and his student Chi-Sheng Niu under very general conditions, and by Nicolas Gisin using the symmetry argument presented here. These five authors joined forces to produce a single paper (Fuchs *et al.*, 1997). The result of this section is thus also valid without this symmetry assumption.

[51] Actually, Niu and Griffiths (1999) showed that two-dimensional probes suffice for Eve to get as much information as with the strategy presented here, though in their case the attack is not symmetric (one basis is more disturbed than the other).

$$\mathcal{F}=\frac{1+\langle\hat{\theta}_\uparrow|\hat{\theta}_\downarrow\rangle}{2-\langle\hat{\phi}_\uparrow|\hat{\phi}_\downarrow\rangle+\langle\hat{\theta}_\uparrow|\hat{\theta}_\downarrow\rangle}, \tag{59}$$

where the hats denote normalized states, e.g., $\hat{\phi}_\uparrow = \phi_\uparrow \mathcal{D}^{-1/2}$.

Consequently the entire class of symmetric individual attacks depends only on two real parameters:[52] $\cos(x) \equiv \langle\hat{\phi}_\uparrow|\hat{\phi}_\downarrow\rangle$ and $\cos(y) \equiv \langle\hat{\theta}_\uparrow|\hat{\theta}_\downarrow\rangle$.

Thanks to symmetry, it suffices to analyze this scenario for the case when Alice sends the $|\uparrow\rangle$ state and Bob measures in the $\{\uparrow,\downarrow\}$ basis (if not, Alice, Bob, and Eve disregard the data). Since Eve knows the basis, she knows that her probe is in one of the following two mixed states:

$$\rho_{Eve}(\uparrow)=\mathcal{F}P(\phi_\uparrow)+\mathcal{D}P(\theta_\uparrow), \tag{60}$$

$$\rho_{Eve}(\downarrow)=\mathcal{F}P(\phi_\downarrow)+\mathcal{D}P(\theta_\downarrow). \tag{61}$$

An optimum measurement strategy for Eve to distinguish between $\rho_{Eve}(\uparrow)$ and $\rho_{Eve}(\downarrow)$ consists in first determining whether her state is in the subspace generated by $\phi_\uparrow$ and $\phi_\downarrow$ or the one generated by $\theta_\uparrow$ and $\theta_\downarrow$. This is possible, since the two subspaces are mutually orthogonal. Eve must then distinguish between two pure states with an overlap of either $\cos x$ or $\cos y$. The first alternative occurs with probability $\mathcal{F}$, the second with probability $\mathcal{D}$. The optimal measurement distinguishing two states with overlap $\cos x$ is known to provide Eve with the correct guess with probability $[1+\sin(x)]/2$ (Peres, 1997). Eve's maximal Shannon information, attained when she performs the optimal measurements, is thus given by

$$I(\alpha,\epsilon)=\mathcal{F}\cdot\left[1-h\left(\frac{1+\sin x}{2}\right)\right] + \mathcal{D}\cdot\left[1-h\left(\frac{1+\sin y}{2}\right)\right], \tag{62}$$

where $h(p)=-p\log_2(p)-(1-p)\log_2(1-p)$. For a given error rate $\mathcal{D}$, this information is maximal when $x=y$. Consequently, for $\mathcal{D}=[1-\cos(x)]/2$, one obtains:

$$I^{\max}(\alpha,\epsilon)=1-h\left(\frac{1+\sin x}{2}\right). \tag{63}$$

This provides the explicit and analytic optimum eavesdropping strategy. For $x=0$ the QBER (i.e., $\mathcal{D}$) and the information gain are both zero. For $x=\pi/2$ the QBER is $\frac{1}{2}$ and the information gain 1. For small QBER's, the information gain grows linearly:

$$I^{\max}(\alpha,\epsilon)=\frac{2}{\ln 2}\mathcal{D}+O(\mathcal{D})^2\approx 2.9\mathcal{D}. \tag{64}$$

[52]Interestingly, when the symmetry is extended to a third maximally conjugated basis, as is natural in the six-state protocol of Sec. II.D.2, the number of parameters reduces to one. This parameter measures the relative quality of Bob's and Eve's "copy" of the qubit sent by Alice. When both copies are of equal quality, one recovers the optimal cloning presented in Sec. II.F (Bechmann-Pasquinucci and Gisin, 1999).

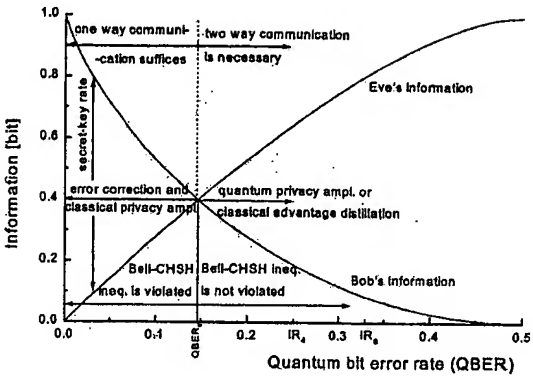


FIG. 30. Eve's and Bob's information vs the QBER, here plotted for incoherent eavesdropping on the four-state protocol. For QBER's below $QBER_0$, Bob has more information than Eve, and secret-key agreement can be achieved using classical error correction and privacy amplification, which can, in principle, be implemented using only one-way communication. The secret-key rate can be as large as the information differences. For QBER's above $QBER_0$ ($\equiv\mathcal{D}_0$), Bob has a disadvantage with respect to Eve. Nevertheless, Alice and Bob can apply quantum privacy amplification up to the QBER corresponding to the intercept-resend eavesdropping strategies ($IR_4$ and $IR_6$ for the four-state and six-state protocols, respectively). Alternatively, they can apply a classical protocol called advantage distillation, which is effective up to precisely the same maximal QBER $IR_4$ and $IR_6$. Both the quantum and the classical protocols require two-way communication. Note that for the eavesdropping strategy that will be optimal, from Eve Shannon point of view, on the four-state protocol, $QBER_0$ should correspond precisely to the noise threshold above which a Bell's inequality can no longer be violated.

Once Alice, Bob, and Eve have measured their quantum systems, they are left with classical random variables $\alpha$, $\beta$, and $\epsilon$, respectively. Secret-key agreement between Alice and Bob is then possible using only error correction and privacy amplification if and only if the Alice-Bob mutual Shannon information $I(\alpha,\beta)$ is greater than the Alice-Eve or the Bob-Eve mutual information,[53] $I(\alpha,\beta)>I(\alpha,\epsilon)$ or $I(\alpha,\beta)>I(\beta,\epsilon)$. It is thus interesting to compare Eve's maximal information [Eq. (64)] with Bob's Shannon information. The latter depends only on the error rate $\mathcal{D}$:

$$I(\alpha,\beta)=1-h(\mathcal{D}) \tag{65}$$

$$=1+\mathcal{D}\log_2(\mathcal{D})+(1-\mathcal{D})\log_2(1-\mathcal{D}). \tag{66}$$

Bob's and Eve's information are plotted in Fig. 30. As expected, for low error rates $\mathcal{D}$, Bob's information is greater. But, more errors provide Eve with more infor-

[53]Note, however, that if this condition is not satisfied, other protocols might sometimes be used; see Sec. II.C.5. These protocols are significantly less efficient and are usually not considered as part of "standard" QC. Note also that, in the scenario analyzed in this section, $I(\beta,\epsilon)=I(\alpha,\epsilon)$.

mation, while decreasing Bob's information. Hence both information curves cross at a specific error rate $\mathcal{D}_0$:

$$I(\alpha,\beta)=I^{\max}(\alpha,\epsilon)\Leftrightarrow\mathcal{D}=\mathcal{D}_0\equiv\frac{1-1/\sqrt{2}}{2}\approx 15\%. \quad (67)$$

Consequently the security criterion against individual attacks for the BB84 protocol is

$$\text{BB84 secure}\Leftrightarrow\mathcal{D}<\mathcal{D}_0\equiv\frac{1-1/\sqrt{2}}{2}. \quad (68)$$

For QBER's greater than $\mathcal{D}_0$, no (one-way communication) error correction and privacy amplification protocol can provide Alice and Bob with a secret key that is immune to any individual attacks.

Let us mention that there exists a class of more general classical protocols, called *advantage distillation* (Sec. II.C.5), which uses two-way communication. These protocols can guarantee secrecy if and only if Eve's intervention does not disentangle Alice and Bob's qubits (assuming they use the Ekert version of the BB84 protocol; Gisin and Wolf, 2000). If Eve optimizes her Shannon information as discussed in this section, this disentanglement limit corresponds to a QBER$=1-1/\sqrt{2}\approx 30\%$ (Gisin and Wolf, 1999). However, using more brutal strategies, Eve can disentangle Alice and Bob's qubits for a QBER of 25%; see Fig. 30. The latter is thus the absolute upper limit, taking into account the most general secret-key protocols. In practice, the limit (67) is more realistic, since advantage distillation algorithms are much less efficient than classical privacy amplification algorithms.

### F. Connection to Bell's inequality

There is an intriguing connection between the tight-bound [Eq. (68)] and the Clauser-Horne-Shimony-Holt (CHSH) form of Bell's inequality (Bell, 1964; Clauser *et al.*, 1969; Clauser and Shimony, 1978; Zeilinger, 1999):

$$S\equiv E(a)+E(a,b')+E(a',b)-E(a',b')\leqslant 2. \quad (69)$$

Here $E(a,b)$ is the correlation between Alice and Bob's data when measuring $\sigma_a\otimes 1$ and $1\otimes\sigma_b$, where $\sigma_a$ denotes an observable with eigenvalues $\pm 1$ parametrized by the label $a$. Recall that Bell's inequalities are necessarily satisfied by all local models but are violated by quantum mechanics.[54] To establish this connection, assume that the same quantum channel is used to test Bell's inequality. It is well known that, for error-free channels, a maximal violation by a factor $\sqrt{2}$ is achievable: $S_{\max}=2\sqrt{2}>2$. However, if the channel is imperfect, or equivalently if some perturbing Eve acts on the channel, then the quantum correlation $E(a,b|\mathcal{D})$ is reduced:

$$E(a,b|\mathcal{D})=\mathcal{F}\cdot E(a,b)-\mathcal{D}\cdot E(a,b) \quad (70)$$

$$=(1-2\mathcal{D})\cdot E(a,b), \quad (71)$$

where $E(a,b)$ denotes the correlation for the unperturbed channel. The achievable amount of violation is then reduced to $S_{\max}(\mathcal{D})=(1-2\mathcal{D})2\sqrt{2}$, and for large perturbations no violation at all can be achieved. Interestingly, the critical perturbation $\mathcal{D}$ up to which a violation can be observed is precisely the same $\mathcal{D}_0$ as the limit derived in the previous section for the security of the BB84 protocol:

$$S_{\max}(\mathcal{D})>2\Leftrightarrow\mathcal{D}<\mathcal{D}_0\equiv\frac{1-1/\sqrt{2}}{2}. \quad (72)$$

This is a surprising and appealing connection between the security of QC and tests of quantum nonlocality. One could argue that this connection is quite natural, since, if Bell's inequality were not violated, then quantum mechanics would be incomplete, and no secure communication could be based on such an incomplete theory. In some sense, Eve's information is like probabilistic local hidden variables. However, the connection between Eqs. (68) and (72) has not been generalized to other protocols. A complete picture of these connections is thus not yet available.

Let us emphasize that nonlocality plays no direct role in QC. Indeed, Alice is generally in Bob's absolute past. Nevertheless, Bell's inequality can be violated by spacelike separated events as well as by timelike separated events. However, the independence assumption necessary to derive Bell's inequality is justified by locality considerations only for spacelike separated events.

### G. Ultimate security proofs

The security proof of QC with a perfect apparatus and a noise-free channel is straightforward. However, the fact that security can still be proven for an imperfect apparatus and noisy channels is far from obvious. Clearly, something has to be assumed about the apparatus. In this section we simply make the hypothesis that they are perfect. For the channel that is not under Alice and Bob's control, however, nothing is assumed. The question is then Up to what QBER can Alice and Bob apply error correction and privacy amplification to their classical bits? In the previous sections we found that the threshold is close to a QBER of 15%, assuming individual attacks. In principle Eve could manipulate several qubits coherently. How much help to Eve this possibility provides is still unknown, though some bounds are known. In 1996, Dominic Mayers (1996b) presented the

[54] Let us stress that the CHSH-Bell's inequality is the strongest possible for two qubits. Indeed, this inequality is violated if and only if the correlation cannot be reproduced by a local hidden-variable model (Pitowski, 1989).

main ideas on how to prove security.[55] In 1998, two major papers were made public on the Los Alamos archives (Mayers, 1998, and Lo and Chau, 1999). Today, these proofs are generally considered valid, thanks to the work of—among others—Shor and Preskill (2000), Inamori *et al.* (2001), and Biham *et al.* (1999). However, it is worth noting that during the first few years after the initial disclosure of these proofs, hardly anyone in the community understood them.

Here we shall present the argument in a form quite different from the original proofs. Our presentation aims at being transparent in the sense that it rests on two theorems. The proofs of the theorems are difficult and will be omitted. However, their claims are easy to understand and rather intuitive. Once one accepts the theorems, the security proof is straightforward.

The general idea is that at some point Alice, Bob, and Eve perform measurements on their quantum systems. The outcomes provide them with classical random variables $\alpha$, $\beta$, and $\epsilon$, respectively, with $P(\alpha,\beta,\epsilon)$ the joint probability distribution. The first theorem, a standard of classical information-based cryptography, states the necessary and sufficient condition on $P(\alpha,\beta,\epsilon)$ for Alice and Bob to extract a secret key from $P(\alpha,\beta,\epsilon)$ (Csiszár and Körner, 1978). The second theorem is a clever version of Heisenberg's uncertainty relation expressed in terms of available information (Hall, 1995): it sets a bound on the sum of the information about Alice's key available to Bob and to Eve.

*Theorem 1.* For a given $P(\alpha,\beta,\epsilon)$, Alice and Bob can establish a secret key (using only error correction and classical privacy amplification) if and only if $I(\alpha,\beta) \geq I(\alpha,\epsilon)$ or $I(\alpha,\beta) \geq I(\beta,\epsilon)$, where $I(\alpha,\beta)=H(\alpha)-H(\alpha|\beta)$ denotes the mutual information and $H$ is the Shannon entropy.

*Theorem 2.* Let $E$ and $B$ be two observables in an $N$-dimensional Hilbert space. Let $\epsilon$, $\beta$, $|\epsilon\rangle$, and $|\beta\rangle$ be the corresponding eigenvalues and eigenvectors, respectively, and let $c=\max_{\epsilon,\beta}\{|\langle\epsilon|\beta\rangle|\}$. Then

$$I(\alpha,\epsilon)+I(\alpha,\beta)\leq 2\log_2(Nc), \tag{73}$$

where $I(\alpha,\epsilon)=H(\alpha)-H(\alpha|\epsilon)$ and $I(\alpha,\beta)=H(\alpha)-H(\alpha|\beta)$ are the entropy differences corresponding to the probability distribution of the eigenvalues $\alpha$ prior to and deduced from any measurement by Eve and Bob, respectively.

The first theorem states that Bob must have more information about Alice's bits than does Eve (see Fig. 31).

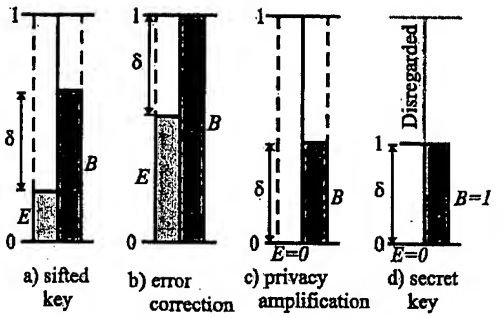


FIG. 31. Intuitive illustration of Theorem 1. The initial situation is depicted in (a). During the one-way public discussion phase of the protocol, Eve receives as much information as Bob; the initial information difference $\delta$ thus remains. After error correction, Bob's information equals 1, as illustrated in (b). After privacy amplification Eve's information is zero. In (c) Bob has replaced with random bits all bits to be disregarded. Hence the key still has its original length, but his information has decreased. Finally, in (d) removal of the random bits shortens the key to the initial information difference. Bob has full information on this final key, while Eve has none.

Since error correction and privacy amplification can be implemented using only one-way communication, Theorem 1 can be understood intuitively as follows. The initial situation is depicted in Fig. 31(a). During the public phase of the protocol, because of the one-way communication, Eve receives as much information as Bob. The initial information difference $\delta$ thus remains. After error correction, Bob's information equals 1, as illustrated in Fig. 31(b). After privacy amplification Eve's information is zero. In Fig. 31(c) Bob has replaced all bits to be disregarded by random bits. Hence the key still has its original length, but his information has decreased. Finally, upon removal of the random bits, the key is shortened to the initial information difference $\delta$; see Fig. 31(d). Bob has full information about this final key, while Eve has none.

The second theorem states that if Eve performs a measurement providing her with some information $I(\alpha,\epsilon)$, then, because of the perturbation, Bob's information is necessarily limited. Using these two theorems, the argument now runs as follows. Suppose Alice sends out a large number of qubits and that $n$ are received by Bob in the correct basis. The relevant Hilbert space's dimension is thus $N=2^n$. Let us relabel the bases used for each of the $n$ qubits such that Alice uses $n$ times the $x$ basis. Hence Bob's observable is the $n$-time tensor product $\sigma_x\otimes\cdots\otimes\sigma_x$. By symmetry, Eve's optimal information about the correct bases is precisely the same as her optimal information about the incorrect ones (Mayers, 1998). Hence one can bound her information, assuming she measures $\sigma_z\otimes\cdots\otimes\sigma_z$. Accordingly, $c=2^{-n/2}$, and Theorem 2 implies

$$I(\alpha,\epsilon)+I(\alpha,\beta)\leq 2\log_2(2^n 2^{-n/2})=n. \tag{74}$$

That is, the sum of Eve's and Bob's information per qubit is less than or equal to 1. This result is quite intuitive:

[55] One of the authors (N.G.) vividly remembers the 1996 Institute for Scientific Interchange workshop in Torino, Italy, sponsored by Elsag Bailey, where he ended his talk by stressing the importance of security proofs. Dominic Mayers stood up, gave some explanation, and wrote a formula on a transparency, claiming that this was the result of his proof. We think it is fair to say that no one in the audience understood Mayers' explanation. However, N.G. kept the transparency, and it contains the basic Eq. (75) (up to a factor of 2, which corresponds to an improvement of Mayer's result obtained in 2000 by Shor and Preskill, using ideas from Lo and Chau).

together, Eve and Bob cannot receive more information than is sent out by Alice! Next, combining the bound (74) with Theorem 1, one deduces that a secret key is achievable whenever $I(\alpha,\beta)\geq n/2$. Using $I(\alpha,\beta)=n[1-\mathcal{D}\log_2(\mathcal{D})-(1-\mathcal{D})\log_2(1-\mathcal{D})]$, one obtains the sufficient condition on the error rate $\mathcal{D}$ (i.e., the QBER):

$$\mathcal{D}\log_2(\mathcal{D})+(1-\mathcal{D})\log_2(1-\mathcal{D})\leq\frac{1}{2}, \tag{75}$$

i.e., $\mathcal{D}\leq 11\%$.

This bound, QBER$\leq$11%, is precisely that obtained in Mayers's proof (after improvement by Shor and Preskill, 2000). The above proof is, strictly speaking, only valid if the key is much longer than the number of qubits that Eve attacks coherently, so that the Shannon information we used represents averages over many independent realizations of classical random variables. In other words, assuming that Eve can coherently attack a large but finite number $n_0$ of qubits, Alice and Bob can use the above proof to secure keys much longer than $n_0$ bits. If one assumes that Eve has unlimited power and is able to attack coherently any number of qubits, then the above proof does not apply, but Mayers's proof can still be used and provides precisely the same bound.

This 11% bound for coherent attacks is clearly compatible with the 15% bound found for individual attacks. The 15% bound is also necessary, since an explicit eavesdropping strategy reaching this bound is presented in Sec. VI.E. It is not known what happens in the intermediate range 11%<QBER<15%, but the following scenario is plausible. If Eve is limited to coherent attacks on a finite number of qubits, then in the limit of arbitrarily long keys, she has a negligibly small probability that the bits combined by Alice and Bob during the error correction and privacy amplification protocols originate from qubits attacked coherently. Consequently, the 15% bound would still be valid (partial results in favor of this conjecture can be found in Cirac and Gisin, 1997 and Bechmann-Pasquinucci and Gisin, 1999). However, if Eve has unlimited power, in particular, if she can coherently attack an unlimited number of qubits, then the 11% bound might be required.

To conclude this section, let us stress that the above security proof applies equally to the six-state protocol (Sec. II.D.2). It also extends in a straightforward fashion to protocols using larger alphabets (Bechmann-Pasquinucci and Peres, 2000; Bechmann-Pasquinucci and Tittel, 2000; Bourennane, Karlsson, and Björn, 2001; Bourennane, Karlsson, Björn, Gisin, and Cerf, 2001).

### H. Photon number measurements and lossless channels

In Sec. III.A we saw that all real photon sources have a finite probability of emittting more than one photon. If all emitted photons encode the same qubit, Eve can take advantage of this. In principle, she can first measure the number of photons in each pulse without disturbing the degree of freedom encoding the qubits.[56] Such measurements are sometimes called quantum nondemolition measurements, because they do not perturb the qubit; in particular they do not destroy the photons. This is possible because Eve knows in advance that Alice sends a mixture of states with well-defined photon numbers[57] (see Sec. II.F). Next, if Eve finds more than one photon, she keeps one and sends the other(s) to Bob. In order to prevent Bob from detecting a lower qubit rate, Eve must use a channel with lower losses. Using an ideally lossless quantum channel, Eve can even, under certain conditions, keep one photon and increase the probability that pulses with more than one photon get to Bob! Finally, when Eve finds one photon, she may destroy it with some probability that she does not affect the total number of qubits received by Bob. Consequently, if the probability that a nonempty pulse has more than one photon (on Alice's side) is greater than the probability that a nonempty pulse is detected by Bob, then Eve can get full information without introducing any perturbation. This is possible only when the QC protocol is not perfectly implemented, but it is a realistic situation (Huttner *et al.*, 1995; Yuen, 1997).

Quantum nondemolition atacks have recently received a lot of attention (Brassard *et al.*, 2000; Lütkenhaus, 2000). The debate is not yet settled. We would like to argue that it might be unrealistic, or even unphysical, to assume that Eve can perform ideal quantum nondemolition attacks. Indeed, she first needs the capacity to perform quantum nondemolition photon-number measurements. Although impossible with today's technology, this is a reasonable assumption (Nogues *et al.*, 1999). Next, she should be able to keep her photon until Alice and Bob reveal the basis. In principle, this could be achieved using a lossless channel in a loop. We discuss this eventuality below. Another possibility would be for Eve to map her photon to a quantum memory. This does not exist today but might well exist in the future. Note that the quantum memory should have essentially unlimited decoherence time, since Alice and Bob could easily wait for minutes before revealing the bases.[58] Finally, Eve must access a lossless channel, or at least a channel with lower losses than that used by Alice and

[56]For polarization coding, this is quite clear, but for phase coding one may think (incorrectly) that phase and photon number are incompatible. However, the phase used for encoding is a relative phase between two modes. Whether these modes are polarization modes or correspond to different times (determined, for example, by the relative length of interferometers), does not matter.

[57]Recall that a mixture of coherent states $|e^{i\phi}\alpha\rangle$ with a random phase $\phi$, as produced by lasers when no phase reference is available, is equal to a mixture of photon number states $|n\rangle$ with Poisson statistics: $\int_0^{2\pi}|e^{i\phi}\alpha\rangle\langle e^{i\phi}\alpha|\,(d\phi/2\pi)=\sum_{n\geq 0}(\mu^n/n!)\,e^{-\mu}|n\rangle\langle n|$, where $\mu=|\alpha|^2$.

[58]The quantum part of the protocol could run continuously, storing large amounts of raw classical data, but the classical part of the protocol, which processes these raw data, could take place just seconds before the key is used.

Bob. This might be the trickiest point. Indeed, besides using a shorter channel, what can Eve do? Telecommunications fibers are already at the physical limits of what can be achieved (Thomas *et al.*, 2000). The loss is almost entirely due to Rayleigh scattering, which is unavoidable: solve the Schrödinger equation in a medium with inhomogeneities and you get scattering. When the inhomogeneities are due to the molecular stucture of the medium, it is difficult to imagine lossless fibers. The 0.18-dB/km attenuation in silica fibers at 1550 nm is a lower bound imposed by physics rather then technology.[59] Note that using air is not a viable solution, since attenuation at telecommunications wavelengths is rather high. Vacuum, the only way to avoid Rayleigh scattering, also has limitations, due to diffraction, again an unavoidable physical phenomenon. In the end, it seems that Eve has only two possibilities left. Either she uses teleportation (with extremely high success probability and fidelity) or she converts the photons to another wavelength (without perturbing the qubit). Both of these "solutions" seem unrealistic in the foreseeable future.

Consequently, when considering the type of attacks discussed in this section, it is essential to distinguish the ultimate proofs from the practical ones. Indeed, the assumptions about the defects of Alice and Bob's apparatuses must be very specific and might thus be of limited interest, while for practical considerations these assumptions must be very general and might thus be excessive.

### I. A realistic beamsplitter attack

The attack presented in the previous section takes advantage of pulses containing more than one photon. However, as discussed, it uses unrealistic assumptions. In this section, following Dusek *et al.* (2000) and Lütkenhaus (2000), we briefly comment on a realistic attack that, also exploits multiphoton pulses (for details, see Felix *et al.*, 2001, where this and other examples are presented). Assume that Eve splits all pulses in two, analyzing each half in one of the two bases, using photon counting devices able to distinguish between pulses with 0, 1, and 2 photons (see Fig. 32). In practice this could be realized using many single-photon counters in parallel. This requires nearly perfect detectors, but at least one does not need to assume technology completely out of today's realm. Whenever Eve detects two photons in the same output, she sends a photon in the corresponding state into Bob's apparatus. Since Eve's information is classical, she can overcome all the losses of the quantum channel. In all other cases, Eve sends nothing to Bob. In this way, Eve sends a fraction $(\frac{3}{8})$ of the pulses containing at least two photons to Bob. She introduces a QBER of $\frac{1}{6}$ and gets information $I(A,E)=\frac{2}{3}=4\cdot\text{QBER}$. Bob does not see any reduction in the number of detected photons, provided that the transmission coefficient of the quantum channel $t$ satisfies

$$t\leqslant\frac{3}{8}\text{Prob}(n\geqslant 2|n\geqslant 1)\approx\frac{3\mu}{16}, \tag{76}$$

where the last expression assumes Poissonian photon distribution. Accordingly, for a fixed QBER, this attack provides Eve with twice the information she would get from using the intercept-resend strategy. To counter such an attack, Alice should use a mean photon number $\mu$ such that Eve can use this attack on only a fraction of the pulses. For example, Alice could use pulses weak enough that Eve's mean information gain is identical to what she would obtain with the simple intercept-resend strategy (see Sec. II.C.3). For 10-, 14-, and 20-dB attenuation, this corresponds to $\mu=0.25, 0.1$, and 0.025, respectively.

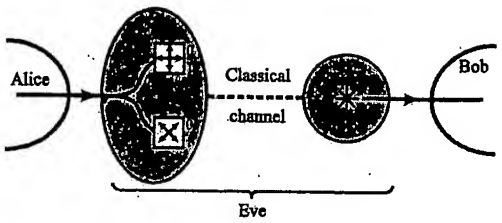


FIG. 32. Realistic beamsplitter attack. Eve stops all pulses. The two photon pulses have a 50% probability of being analyzed by the same analyzer. If this analyzer is compatible with the state prepared by Alice, then both photons are detected with the same outcome; if not, there is a 50% chance that they are detected with the same outcome. Hence there is a probability of $\frac{3}{8}$ that Eve detects both photons with the same outcome. In such a case, and only in such a case, she resends a photon to Bob. In $\frac{2}{3}$ of these cases she introduces no errors, since she has identified the correct state and gets full information; in the remaining cases she has a 50% probability of introducing an error and gains no information. The total QBER is thus $\frac{1}{6}$, and Eve's information gain is $\frac{2}{3}$.

### J. Multiphoton pulses and passive choice of states

Multiphoton pulses do not necessarily constitute a threat to key security, but they limit the key creation rate because they imply that more bits must be discarded during key distillation. This fact is based on the assumption that all photons in a pulse carry the same qubit, so that Eve does not need to copy the qubit going to Bob, but merely keeps the copy that Alice inadvertently provides. When using weak pulses, it seems unavoidable that all the photons in a pulse carry the same qubit. However, in two-photon implementations, each

[59]Photonics crystal fibers have the potential to overcome the Rayleigh scattering limit. There are two kinds of such fibers. The first kind guides light by total internal reflection, as in ordinary fibers. In these fibers most of the light also propagates in silica, and thus the loss limit is similar. In the second kind, most of the light propagates in air. Thus the theoretical loss limit is lower. However, today the losses are extremely high, in the range of hundreds of dB/km. The best reported result that we are aware of is 11 dB/km, and it was obtained with the first kind of fiber (Canning *et al.*, 2000).

photon on Alice's side independently chooses a state [in the experiments of Ribordy *et al.* (2001) and Tittel *et al.* (2000), each photon randomly chooses both its basis and its bit value; in the experiments of Naik *et al.* (2000) and Jennewein, Simon, *et al.* (2000), only the bit value choice is random]. Hence, when two photon pairs are simultaneously produced, the two twins carry independent qubits by accident. Consequently, Eve cannot take advantage of such multiphoton twin pulses. This might be one of the main advantages of two-photon schemes over the much simpler weak-pulse schemes. But the multiphoton problem is then on Bob's side, which gets a noisy signal, consisting partly of photons not in Alice's state.

### K. Trojan horse attacks

All eavesdropping strategies discussed up to this point have consisted of Eve's attempt to get a maximum information from the qubits exchanged by Alice and Bob. However, Eve can also pursue a completely different strategy: she can herself send signals that enter Alice and Bob's offices through the quantum channel. This kind of strategy is called a Trojan horse attack. For example, Eve can send light pulses into the fiber entering Alice's or Bob's apparatus and analyze the backreflected light. In this way, it is in principle possible to detect which laser just flashed, which detector just fired, or the settings of phase and polarization modulators. This cannot be prevented by simply using a shutter, since Alice and Bob must leave the "door open" for the photons to exit and enter, respectively.

In most QC setups the amount of backreflected light can be made very small, and sensing the apparatus with light pulses through the quantum channel is difficult. Nevertheless, this attack is especially threatening in the plug-and-play scheme on Alice's side (Sec. IV.C.2), since a mirror is used to send the light pulses back to Bob. Thus, in principle, Eve can send strong light pulses to Alice and sense the applied phase shift. However, by applying the phase shift only during a short time $\Delta t_{\text{phase}}$ (a few nanoseconds), Alice can oblige Eve to send the spying pulse at the same time as Bob. Remember that in the plug-and-play scheme, pulses coming from Bob are macroscopic and an attenuator at Alice's end reduces them to below the one-photon level, say, 0.1 photons per pulse. Hence, if Eve wants to get, say, one photon per pulse, she has to send ten times Bob's pulse energy. Since Alice is detecting Bob's pulses for triggering her apparatus, she must be able to detect an increase in energy of these pulses in order to reveal the presence of a spying pulse. This is a relatively easy task, provided that Eve's pulses look the same as Bob's. However, Eve could of course use another wavelength or ultrashort pulses (or very long pulses with low intensity, hence the importance of $\Delta t_{phase}$); therefore Alice must introduce an optical bandpass filter with a transmission spectrum corresponding to the sensitivity spectrum of her detector and choose a $\Delta t_{phase}$ that fits the bandwidth of her detector.

There is no doubt that Trojan horse attacks can be prevented by technical measures. However, the fact that this class of attacks exists illustrates that the security of QC can never be guaranteed by the principles of quantum mechanics only, but must necessarily rely on technical measures that are subject to discussion.[60]

### L. Real security: Technology, cost, and complexity

Despite the elegance and generality of security proofs, the ideal of a QC system whose security relies entirely on quantum principles is unrealistic. The technological implementation of abstract principles will always be questionable. It is likely that they will remain the weakest point in all systems. Moreover, one should remember the obvious relation:

$$\text{Infinite security} \Rightarrow \text{Infinite cost} \Rightarrow \text{Zero practical interest}. \quad (77)$$

On the other hand, however, one should not underestimate the following two advantages of QC. First, it is much easier to forecast progress in technology than in mathematics: the danger that QC will break down overnight is negligible, in contrast to public-key cryptosystems. Next, the security of QC depends on the technological level of the adversary *at the time of the key exchange*, in contrast to complexity-based systems whose coded message can be registered and broken thanks to future progress. The latter point is relevant for secrets whose value lasts many years.

One often points to low bit rate as one of the current limitations of QC. However, it is important to stress that QC need not be used in conjunction with one-time-pad encryption. It can also be used to provide a key for a symmetrical cipher such as AES, whose security is greatly enhanced by frequent key changes.

To conclude this section, let us briefly elaborate on the differences and similarities between technological and mathematical complexity and on their possible connections and implications. Mathematical complexity means that the number of steps needed to run complex algorithms increases exponentially as the size of the input grows linearly. Similarly, one can define the technological complexity of a quantum computer as an exponentially increasing difficulty to process coherently all the qubits necessary to run a (noncomplex) algorithm on a linearly growing number of input data. It might be interesting to consider the possibility that the relationship between these two concepts of complexity is deeper. It could be that the solution of a problem requires either a complex classical algorithm or a quantum algorithm that itself requires a complex quantum computer.[61]

---

[60] Another technological loophole, recently pointed out by Kurtsiefer *et al.* (2001), is the possible information leakage caused by light emitted by APD's during their breakdown.

[61] Penrose (1994) pushes these speculations even further, suggesting that spontaneous collapses stop quantum computers whenever they try to compute beyond a certain complexity.

## VII. CONCLUSIONS

Quantum cryptography is a fascinating illustration of the dialog between basic and applied physics. It is based on a beautiful combination of concepts from quantum physics and information theory and made possible by the tremendous progress in quantum optics and the technology of optical fibers and free-space optical communication. Its security principle relies on deep theorems in classical information theory and on a profound understanding of Heisenberg's uncertainty principle, as illustrated by Theorems 1 and 2 in Sec. VI.G (the only mathematically involved theorems in this review). Let us also emphasize the important contributions of QC to classical cryptography: privacy amplification and classical bound information (Secs. II.C.4 and II.C.5) are examples of concepts in classical information whose discovery were much inspired by QC. Moreover, the fascinating tension between quantum physics and relativity, as illustrated by Bell's inequality, is not far away, as discussed in Sec. VI.F. Now, despite significant progress in recent years, many open questions and technological challenges remain.

One technological challenge at present concerns improved detectors compatible with telecommunications fibers. Two other issues concern free-space QC and quantum repeaters. The former is currently the only way to realize QC over thousands of kilometers using the technology of the near future (see Sec. IV.E). The idea of quantum repeaters (Sec. III.E) is to encode the qubits in such a way that if the error rate is low, then errors can be detected and corrected entirely in the quantum domain. The hope is that such techniques could extend the range of quantum communication to essentially unlimited distances. Indeed, Hans Briegel, then at the University of Innsbruck, and co-workers (1998) showed that the number of additional qubits needed for quantum repeaters can be made smaller than the numbers of qubits needed to improve the fidelity of the quantum channel (Dur *et al.*, 1999). One could thus overcome the decoherence problem. However, the main practical limitation is not decoherence but loss (most photons never get to Bob, but those that do get there exhibit high fidelity).

As for open questions, let us emphasize three main concerns. First, complete and realistic analyses of the security issues are still missing. Next, figures of merit for comparing QC schemes based on different quantum systems (with different dimensions, for example) are still awaited. Finally, the delicate question of how to test the apparatuses has not yet received enough attention. Indeed, a potential customer of quantum cryptography buys confidence and secrecy, two qualities hard to quantify. Interestingly, both of these issues are connected to Bell's inequality (see Secs. VI.F and VI.B). Clearly, this connection cannot be phrased in the old context of local hidden variables, but rather in the context of the security of tomorrow's communications. Here, as in the entire field of quantum information, old concepts are renewed by looking at them from a fresh perspective: let us exploit quantum weirdness.

QC could well be the first application of quantum mechanics at the single-quantum level. Experiments have demonstrated that keys can be exchanged over distances of a few tens of kilometers at rates on the order of at least a thousand bits per second. There is no doubt that the technology can be mastered and the question is not whether QC will find commercial applications, but when. At present QC is still very limited in distance and in secret bit rate. Moreover, public-key systems dominate the market and, being pure software, are tremendously easier to manage. Every so often, we hear in the news that some classical cryptosystem has been broken. This would be impossible with properly implemented QC. But this apparent strength of QC might turn out to be its weak point: security agencies would be equally unable to break quantum cryptograms!

## ACKNOWLEDGMENTS

This work was supported by the Swiss Fonds National de la Recherche Scientifique (FNRS) and the European Union projects European Quantum Cryptography and Single-Photon Optical Technologies (EQCSPOT) and Long-Distance Photonic Quantum Communication (QUCOMM) financed by the Swiss Office Fédéral de l'Education et de la Science (OFES). The authors would also like to thank Richard Hughes for providing Fig. 8, and acknowledge Charles H. Bennett and Paul G. Kwiat for their very careful reading of the manuscript and their helpful remarks.

## REFERENCES

Ardehali, M., H. F. Chau, and H.-K. Lo, 1998, "Efficient quantum key distribution," preprint quant-ph/9803007.

Aspect, A., J. Dalibard, and G. Roger, 1982, "Experimental test of Bell's inequalities using time-varying analyzers," Phys. Rev. Lett. **49**, 1804–1807.

Bechmann-Pasquinucci, H., and N. Gisin, 1999, "Incoherent and coherent eavesdropping in the 6-state protocol of quantum cryptography," Phys. Rev. A **59**, 4238–4248.

Bechmann-Pasquinucci, H., and A. Peres, 2000, "Quantum cryptography with 3-state systems," Phys. Rev. Lett. **85**, 3313–3316.

Bechmann-Pasquinucci, H., and W. Tittel, 2000, "Quantum cryptography using larger alphabets," Phys. Rev. A **61**, 062308.

Bell, J. S., 1964, "On the problem of hidden variables in quantum mechanics," Rev. Mod. Phys. **38**, 447–452 [reprinted in Bell, J. S., 1987, *Speakable and Unspeakable in Quantum Mechanics* (Cambridge University, Cambridge, England)].

Bennett, C. H., 1992, "Quantum cryptography using any two nonorthogonal states," Phys. Rev. Lett. **68**, 3121–3124.

Bennett, C. H., F. Bessette, G. Brassard, L. Salvail, and J. Smolin, 1992, "Experimental quantum cryptography," J. Cryptology **5**, 3–28.

Bennett, C. H., and G. Brassard, 1984, in *Proceedings of the IEEE International Conference on Computers, Systems and Signal Processing*, Bangalore, India, (IEEE, New York), pp. 175–179.

Bennett, C. H., and G. Brassard, 1985, "Quantum public key distribution system," IBM Tech. Discl. Bull. **28**, 3153–3163.
Bennett, C. H., G. Brassard, C. Crépeau, R. Jozsa, A. Peres, and W. K. Wootters, 1993, "Teleporting an unknown quantum state via dual classical and Einstein-Podolsky-Rosen channels," Phys. Rev. Lett. **70**, 1895–1899.
Bennett, C. H., G. Brassard, C. Crépeau, and U. M. Maurer, 1995, "Generalized privacy amplification," IEEE Trans. Inf. Theory **41**, 1915–1923.
Bennett, C. H., G. Brassard, and A. Ekert, 1992, "Quantum cryptography," Sci. Am. **267**, 50–57.
Bennett, C. H., G. Brassard, and N. D. Mermin, 1992, "Quantum cryptography without Bell's theorem," Phys. Rev. Lett. **68**, 557–559.
Bennett, C. H., G. Brassard, and J.-M. Robert, 1988, "Privacy amplification by public discussion," SIAM J. Comput. **17**, 210–229.
Berry, M. V., 1984, "Quantal phase factors accompanying adiabatic changes," Proc. R. Soc. London, Ser. A **392**, 45–57.
Bethune, D., and W. Risk, 2000, "An autocompensating fiber-optic quantum cryptography system based on polarization splitting of light," IEEE J. Quantum Electron. **36**, 340–347.
Biham, E., M. Boyer, P. O. Boykin, T. Mor, and V. Roychowdhury, 1999, "A proof of the security of quantum key distribution," preprint quant-ph/9912053.
Biham, E., and T. Mor, 1997a, "Security of quantum cryptography against collective attacks," Phys. Rev. Lett. **78**, 2256–1159.
Biham, E., and T. Mor, 1997b, "Bounds on information and the security of quantum cryptography," Phys. Rev. Lett. **79**, 4034–4037.
Bourennane, M., F. Gibson, A. Karlsson, A. Hening, P. Jonsson, T. Tsegaye, D. Ljunggren, and E. Sundberg, 1999, "Experiments on long wavelength (1550 nm) 'plug and play' quantum cryptography system," Opt. Express **4**, 383–387.
Bourennane, M., A. Karlsson, and G. Björn, 2001, "Quantum key distribution using multilevel encoding," Phys. Rev. A **64**, 012306.
Bourennane, M., A. Karlsson, G. Björn, N. Gisin, and N. Cerf, 2001, "Quantum key distribution using multilevel encoding: security analysis," preprint quant-ph/0106049.
Bourennane, M., D. Ljunggren, A. Karlsson, P. Jonsson, A. Hening, and J. P. Ciscar, 2000, "Experimental long wavelength quantum cryptography: from single photon transmission to key extraction protocols," J. Mod. Opt. **47**, 563–579.
Braginsky, V. B., and F. Y. Khalili, 1992, *Quantum Measurement* (Cambridge University, Cambridge, England).
Brassard, G., 1988, *Modern Cryptology: A Tutorial*, Lecture Notes in Computer Science, Vol. 325 (Springer, New York).
Brassard, G., C. Crépeau, D. Mayers, and L. Salvail, 1998, in *Proceedings of Randomized Algorithms, Satellite Workshop of the 23rd International Symposium on Mathematical Foundations of Computer Science*, Brno, Czech Republic, edited by R. Freivalds (Aachen University, Aachen, Germany), pp. 13–15.
Brassard, G., N. Lütkenhaus, T. Mor, and B. C. Sanders, 2000, "Limitations on practical quantum cryptography," Phys. Rev. Lett. **85**, 1330–1333.
Brassard, G., and L. Salvail, 1994, in *Advances in Cryptology—EUROCRYPT '93 Proceedings*, Lecture Notes in Computer Science, Vol. 765, edited by T. Helleseth (Springer, New York), p. 410.
Bréguet, J., and N. Gisin, 1995, "New interferometer using a 3×3 coupler and Faraday mirrors," Opt. Lett. **20**, 1447–1449.
Bréguet, J., A. Muller, and N. Gisin, 1994, "Quantum cryptography with polarized photons in optical fibers: experimental and practical limits," J. Mod. Opt. **41**, 2405–2412.
Brendel, J., W. Dultz, and W. Martienssen, 1995, "Geometric phase in 2-photon interference experiments," Phys. Rev. A **52**, 2551–2556.
Brendel, J., N. Gisin, W. Tittel, and H. Zbinden, 1999, "Pulsed energy-time entangled twin-photon source for quantum communication," Phys. Rev. Lett. **82**, 2594–2597.
Briegel, H.-J., W. Dur, J. I. Cirac, and P. Zoller, 1998, "Quantum repeaters: the role of imperfect local operations in quantum communication," Phys. Rev. Lett. **81**, 5932–5935.
Brouri, R., A. Beveratios, J.-P. Poizat, and P. Grangier, 2000, "Photon antibunching in the fluorescence of individual colored centers in diamond," Opt. Lett. **25**, 1294–1296.
Brown, R. G. W., and M. Daniels, 1989, "Characterization of silicon avalanche photodiodes for photon correlation measurements. 3: Sub-Geiger operation," Appl. Opt. **28**, 4616–4621.
Brown, R. G. W., R. Jones, J. G. Rarity, and K. D. Ridley, 1987, "Characterization of silicon avalanche photodiodes for photon correlation measurements. 2: Active quenching," Appl. Opt. **26**, 2383–2389.
Brown, R. G. W., K. D. Ridley, and J. G. Rarity, 1986, "Characterization of silicon avalanche photodiodes for photon correlation measurements. 1: Passive quenching," Appl. Opt. **25**, 4122–4126.
Brunel, C., B. Lounis, P. Tamarat, and M. Orrit, 1999, "Triggered source of single photons based on controlled single molecule fluorescence," Phys. Rev. Lett. **83**, 2722–2725.
Bruss, D., 1998, "Optimal eavesdropping in quantum cryptography with six states," Phys. Rev. Lett. **81**, 3018–3021.
Bruss, D., A. Ekert, and C. Macchiavello, 1998, "Optimal universal quantum cloning and state estimation," Phys. Rev. Lett. **81**, 2598–2601.
Buttler, W. T., R. J. Hughes, P. G. Kwiat, S. K. Lamoreaux, G. G. Luther, G. L. Morgan, J. E. Nordholt, C. G. Peterson, and C. Simmons, 1998, "Practical free-space quantum key distribution over 1 km," Phys. Rev. Lett. **81**, 3283–3286.
Buttler, W. T., R. J. Hughes, S. K. Lamoreaux, G. L. Morgan, J. E. Nordholt, and C. G. Peterson, 2000, "Daylight quantum key distribution over 1.6 km," Phys. Rev. Lett. **84**, 5652–5655.
Bužek, V., and M. Hillery, 1996, "Quantum copying: beyond the no-cloning theorem," Phys. Rev. A **54**, 1844–1852.
Cancellieri, G., 1993, Ed., *Single-Mode Optical Fiber Measurement: Characterization and Sensing* (Artech House, Boston).
Canning, J., M. A. van Eijkelenborg, T. Ryan, M. Kristensen, and K. Lyytikainen, 2000, "Complex mode coupling within air-silica structured optical fibers and applications," Opt. Commun. **185**, 321–324.
Cirac, J. I., and N. Gisin, 1997, "Coherent eavesdropping strategies for the 4-state quantum cryptography protocol," Phys. Lett. A **229**, 1–7.
Clarke, R. B. M., A. Chefles, S. M. Barnett, and E. Riis, 2000, "Experimental demonstration of optimal unambiguous state discrimination," Phys. Rev. A **63**, 040305.
Clauser, J. F., M. A. Horne, A. Shimony, and R. A. Holt, 1969, "Proposed experiment to test local hidden variable theories," Phys. Rev. Lett. **23**, 880–884.

Clauser, J. F., and A. Shimony, 1978, "Bell's theorem: experimental tests and implications," Rep. Prog. Phys. **41**, 1881–1927.

Cova, S., M. Ghioni, A. Lacaita, C. Samori, and F. Zappa, 1996, "Avalanche photodiodes and quenching circuits for single-photon detection," Appl. Opt. **35**, 1956–1976.

Cova, S., A. Lacaita, M. Ghioni, and G. Ripamonti, 1989, "High-accuracy picosecond characterization of gain-switched laser diodes," Opt. Lett. **14**, 1341–1343.

Csiszár, I., and J. Körner, 1978, "Broadcast channels with confidential messages," IEEE Trans. Inf. Theory **IT-24**, 339–348.

De Martini, F., V. Mussi, and F. Bovino, 2000, "Schroedinger cat states and optimum universal quantum cloning by entangled parametric amplification," Opt. Commun. **179**, 581–589.

Desurvire, E., 1994, "The golden age of optical fiber amplifiers," Phys. Today **47** (1), 20–27.

Deutsch, D., 1985, "Quantum theory, the Church-Turing principle and the universal quantum computer," Proc. R. Soc. London, Ser. A **400**, 97–105.

Deutsch, D., A. Ekert, R. Jozsa, C. Macchiavello, S. Popescu, and A. Sanpera, 1996, "Quantum privacy amplification and the security of quantum cryptography over noisy channels," Phys. Rev. Lett. **77**, 2818–2821; **80**, 2022(E) (1996).

Dieks, D., 1982, "Communication by EPR devices," Phys. Lett. **92A**, 271–272.

Diffie, W., and M. E. Hellman, 1976, "New directions in cryptography," IEEE Trans. Inf. Theory **IT-22**, 644–654.

Dur, W., H.-J. Briegel, J. I. Cirac, and P. Zoller, 1999, "Quantum repeaters based on entanglement purification," Phys. Rev. A **59**, 169–181; **60**, 725(E).

Dusek, M., M. Jahma, and N. Lütkenhaus, 2000, "Unambiguous state discrimination in quantum cryptography with weak coherent states," Phys. Rev. A **62**, 022306.

Einstein, A., B. Podolsky, and N. Rosen, 1935, "Can quantum-mechanical description of physical reality be considered complete?," Phys. Rev. **47**, 777–780.

Ekert, A. K., 1991, "Quantum cryptography based on Bell's theorem," Phys. Rev. Lett. **67**, 661–663.

Ekert, A. K., 2000, "Coded secrets cracked open," Phys. World **13** (2), 39–40.

Ekert, A. K., and B. Huttner, 1994, "Eavesdropping techniques in quantum cryptosystems," J. Mod. Opt. **41**, 2455–2466.

Ekert, A. K., J. G. Rarity, P. R. Tapster, and G. M. Palma, 1992, "Practical quantum cryptography based on two-photon interferometry," Phys. Rev. Lett. **69**, 1293–1296.

Elamari, A., H. Zbinden, B. Perny, and C. Zimmer, 1998, "Statistical prediction and experimental verification of concatenations of fiber optic components with polarization dependent loss," J. Lightwave Technol. **16**, 332–339.

Enzer, D., P. Hadley, R. Hughes, G. Peterson, and P. Kwiat, 2001, private communication.

Felix, S., A. Stefanov, H. Zbinden, and N. Gisin, 2001, "Faint laser quantum key distribution: Eavesdropping exploiting multiphoton pulses," J. Mod. Opt. **48**, 2009–2021.

Fleury, L., J.-M. Segura, G. Zumofen, B. Hecht, and U. P. Wild, 2000, "Nonclassical photon statistics in single-molecule fluorescence at room temperature," Phys. Rev. Lett. **84**, 1148–1151.

Franson, J. D., 1989, "Bell inequality for position and time," Phys. Rev. Lett. **62**, 2205–2208.

Franson, J. D., 1992, "Nonlocal cancellation of dispersion," Phys. Rev. A **45**, 3126–3132.

Franson, J. D., and B. C. Jacobs, 1995, "Operational system for quantum cryptography," Electron. Lett. **31**, 232–234.

Freedmann, S. J., and J. F. Clauser, 1972, "Experimental test of local hidden variable theories," Phys. Rev. Lett. **28**, 938–941.

Fry, E. S., and R. C. Thompson, 1976, "Experimental test of local hidden variable theories," Phys. Rev. Lett. **37**, 465–468.

Fuchs, C. A., N. Gisin, R. B. Griffiths, C.-S. Niu, and A. Peres, 1997, "Optimal eavesdropping in quantum cryptography. I: Information bound and optimal strategy," Phys. Rev. A **56**, 1163–1172.

Fuchs, C. A., and A. Peres, 1996, "Quantum state disturbance vs. information gain: uncertainty relations for quantum information," Phys. Rev. A **53**, 2038–2045.

Gérard, J.-M., and B. Gayral, 1999, "Strong Purcell effect for InAs quantum boxes in three-dimensional solid-state microcavities," J. Lightwave Technol. **17**, 2089–2095.

Gérard, J.-M., B. Sermage, B. Gayral, B. Legrand, E. Costard, and V. Thierry-Mieg, 1998, "Enhanced spontaneous emission by quantum boxes in a monolithic optical microcavity," Phys. Rev. Lett. **81**, 1110–1113.

Gilbert, G., and M. Hamrick, 2000, "Practical quantum cryptography: a comprehensive analysis (part one)," internal report (MITRE, McLean, USA), preprint quant-ph/0009027.

Gisin, B., and N. Gisin, 1999, "A local hidden variable model of quantum correlation exploiting the detection loophole," Phys. Lett. A **260**, 323–327.

Gisin, N., 1998, "Quantum cloning without signaling," Phys. Lett. A **242**, 1–3.

Gisin, N., *et al.*, 1995, "Definition of polarization mode dispersion and first results of the COST 241 round-robin measurements," Pure Appl. Opt. **4**, 511–522.

Gisin, N., and S. Massar, 1997, "Optimal quantum cloning machines," Phys. Rev. Lett. **79**, 2153–2156.

Gisin, N., R. Renner, and S. Wolf, 2000, *Proceedings of the Third European Congress of Mathematics*, Barcelona (Birkhäuser, Basel) (in press).

Gisin, N., and S. Wolf, 1999, "Quantum cryptography on noisy channels: quantum versus classical key-agreement protocols," Phys. Rev. Lett. **83**, 4200–4203.

Gisin, N., and S. Wolf, 2000, *Advances in Cryptology—Proceedings of Crypto 2000*, Lecture Notes in Computer Science, Vol. 1880, edited by M. Bellare (Springer, New York), pp. 482–500.

Gisin, N., and H. Zbinden, 1999, "Bell inequality and the locality loophole: active versus passive switches," Phys. Lett. A **264**, 103–107.

Goldenberg, L., and L. Vaidman, 1995, "Quantum cryptography based on orthogonal states," Phys. Rev. Lett. **75**, 1239–1243.

Gorman, P. M., P. R. Tapster, and J. G. Rarity, 2001, "Secure free-space key exchange to 1.9 km and beyond," J. Mod. Opt. **48**, 1887–1901.

Haecker, W., O. Groezinger, and M. H. Pilkuhn, 1971, "Infrared photon counting by Ge avalanche diodes," Appl. Phys. Lett. **19**, 113–115.

Hall, M. J. W., 1995, "Information exclusion principle for complementary observables," Phys. Rev. Lett. **74**, 3307–3310.

Hariharan, P., M. Roy, P. A. Robinson, and J. W. O'Byrne, 1993, "The geometric phase observation at the single photon level," J. Mod. Opt. **40**, 871–877.

Hart, A. C., R. G. Huff, and K. L. Walker, 1994, "Method of making a fiber having low polarization mode dispersion due to a permanent spin," U.S. Patent No. 5,298,047.

Hildebrand, E., 2001, Ph.D. thesis (Johann Wolfgang Goethe-Universität, Frankfurt am Main).

Hillery, M., V. Buzek, and A. Berthiaume, 1999, "Quantum secret sharing," Phys. Rev. A **59**, 1829–1834.

Hiskett, P. A., G. S. Buller, A. Y. Loudon, J. M. Smith, I. Gontijo, A. C. Walker, P. D. Townsend, and M. J. Robertson, 2000, "Performance and design of InGaAs/InP photodiodes for single-photon counting at 1.55 $\mu$m," Appl. Opt. **39**, 6818–6829.

Hong, C. K., and L. Mandel, 1985, "Theory of parametric frequency down conversion of light," Phys. Rev. A **31**, 2409–2418.

Hong, C. K., and L. Mandel, 1986, "Experimental realization of a localized one-photon state," Phys. Rev. Lett. **56**, 58–60.

Horodecki, M., R. Horodecki, and P. Horodecki, 1996, "Separability of mixed states: necessary and sufficient conditions," Phys. Lett. A **223**, 1–8.

Hughes, R., W. Buttler, P. Kwiat, S. Lamoreaux, G. Morgan, J. Nordhold, and G. Peterson, 2000, "Free-space quantum key distribution in daylight," J. Mod. Opt. **47**, 549–562.

Hughes, R., G. G. Luther, G. L. Morgan, and C. Simmons, 1996, in *Advances in Cryptology—CRYPTO '96 Proceedings*, Lecture Notes in Computer Science, Vol. 1109, edited by N. Koblitz (Springer, New York), pp. 329–342.

Hughes, R., G. Morgan, and C. Peterson, 2000, "Quantum key distribution over a 48-km optical fiber network," J. Mod. Opt. **47**, 533–547.

Huttner, B., J. D. Gautier, A. Muller, H. Zbinden, and N. Gisin, 1996, "Unambiguous quantum measurement of nonorthogonal states," Phys. Rev. A **54**, 3783–3789.

Huttner, B., N. Imoto, and S. M. Barnett, 1996, "Short distance applications of quantum cryptography," J. Nonlinear Opt. Phys. Mater. **5**, 823–832.

Huttner, B., N. Imoto, N. Gisin, and T. Mor, 1995, "Quantum cryptography with coherent states," Phys. Rev. A **51**, 1863–1869.

Imamoglu, A., and Y. Yamamoto, 1994, "Turnstile device for heralded single photons: Coulomb blockade of electron and hole tunneling in quantum confined p-i-n heterojunctions," Phys. Rev. Lett. **72**, 210–213.

Inamori, H., L. Rallan, and V. Vedral, 2000, "Security of EPR-based quantum cryptography against incoherent symmetric attacks," preprint quant-ph/0103058.

Ingerson, T. E., R. J. Kearney, and R. L. Coulter, 1983, "Photon counting with photodiodes," Appl. Opt. **22**, 2013–2018.

Ivanovic, I. D., 1987, "How to differentiate between nonorthogonal states," Phys. Lett. A **123**, 257–259.

Jacobs, B., and J. Franson, 1996, "Quantum cryptography in free space," Opt. Lett. **21**, 1854–1856.

Jennewein, T., U. Achleitner, G. Weihs, H. Weinfurter, and A. Zeilinger, 2000, "A fast and compact quantum random number generator," Rev. Sci. Instrum. **71**, 1675–1680.

Jennewein, T., C. Simon, G. Weihs, H. Weinfurter, and A. Zeilinger, 2000, "Quantum cryptography with entangled photons," Phys. Rev. Lett. **84**, 4729–4732.

Karlsson, A., M. Bourennane, G. Ribordy, H. Zbinden, J. Brendel, J. Rarity, and P. Tapster, 1999, "A single-photon counter for long-haul telecom," IEEE Circuits Devices Mag. **15**, 34–40.

Kempe, J., C. Simon, G. Weihs, and A. Zeilinger, 2000, "Optimal photon cloning," Phys. Rev. A **62**, 032302.

Kim, J., O. Benson, H. Kan, and Y. Yamamoto, 1999, "A single-photon turnstile device," Nature (London) **397**, 500–503.

Kimble, H. J., M. Dagenais, and L. Mandel, 1977, "Photon antibunching in resonance fluorescence," Phys. Rev. Lett. **39**, 691–694.

Kitson, S. C., P. Jonsson, J. G. Rarity, and P. R. Tapster, 1998, "Intensity fluctuation spectroscopy of small numbers of dye molecules in a microcavity," Phys. Rev. A **58**, 620–627.

Kolmogorov, A. N., 1956, *Foundations of the Theory of Probability* (Chelsea, New York).

Kurtsiefer, C., S. Mayer, P. Zarda, and H. Weinfurter, 2000, "Stable solid-state source of single photons," Phys. Rev. Lett. **85**, 290–293.

Kurtsiefer, C., P. Zarda, S. Mayer, and H. Weinfurter, 2001, "The breakdown flash of Silicon Avalanche Photodiodes—backdoor for eavesdropper attacks?," J. Mod. Opt. **48**, 2039–2047.

Kwiat, P. G., A. M. Steinberg, R. Y. Chiao, P. H. Eberhard, and M. D. Petroff, 1993, "High-efficiency single-photon detectors," Phys. Rev. A **48**, R867–870.

Kwiat, P. G., E. Waks, A. G. White, I. Appelbaum, and P. H. Eberhard, 1999, "Ultrabright source of polarization-entangled photons," Phys. Rev. A **60**, R773–776.

Lacaita, A., P. A. Francese, F. Zappa, and S. Cova, 1994, "Single-photon detection beyond 1 $\mu$m: performance of commercially available germanium photodiodes," Appl. Opt. **33**, 6902–6918.

Lacaita, A., F. Zappa, S. Cova, and P. Lovati, 1996, "Single-photon detection beyond 1 $\mu$m: performance of commercially available InGaAs/InP detectors," Appl. Opt. **35**, 2986–2996.

Larchuk, T. S., M. V. Teich, and B. E. A. Saleh, 1995, "Nonlocal cancellation of dispersive broadening in Mach-Zehnder interferometers," Phys. Rev. A **52**, 4145–4154.

Levine, B. F., C. G. Bethea, and J. C. Campbell, 1985, "Room-temperature 1.3-$\mu$m optical time domain reflectometer using a photon counting InGaAs/InP avalanche detector," Appl. Phys. Lett. **45**, 333–335.

Li, M. J., and D. A. Nolan, 1998, "Fiber spin-profile designs for producing fibers with low PMD," Opt. Lett. **23**, 1659–1661.

Lo, H.-K., and H. F. Chau, 1998, "Why quantum bit commitment and ideal quantum coin tossing are impossible," Physica D **120**, 177–187.

Lo, H.-K., and H. F. Chau, 1999, "Unconditional security of quantum key distribution over arbitrary long distances," Science **283**, 2050–2056.

Lütkenhaus, N., 1996, "Security against eavesdropping in quantum cryptography," Phys. Rev. A **54**, 97–111.

Lütkenhaus, N., 2000, "Security against individual attacks for realistic quantum key distribution," Phys. Rev. A **61**, 052304.

Marand, C., and P. D. Townsend, 1995, "Quantum key distribution over distances as long as 30 km," Opt. Lett. **20**, 1695–1697.

Martinelli, M., 1989, "A universal compensator for polarization changes induced by birefringence on a retracing beam," Opt. Commun. **72**, 341–344.

Martinelli, M., 1992, "Time reversal for the polarization state in optical systems," J. Mod. Opt. **39**, 451–455.

Maurer, U. M., 1993, "Secret key agreement by public discussion from common information," IEEE Trans. Inf. Theory **39**, 733–742.

Maurer, U. M., and S. Wolf, 1999, "Unconditionally secure key agreement and intrinsic information," IEEE Trans. Inf. Theory **45**, 499–514.

Mayers, D., 1996a, "The trouble with quantum bit commitment," quant-ph/9603015.

Mayers, D., 1996b, *Advances in Cryptology—Proceedings of Crypto'96*, Lecture Notes in Computer Science, Vol. 1109, edited by N. Koblitz (Springer, New York), pp. 343–357.

Mayers, D., 1997, "Unconditionally secure Q bit commitment is impossible," Phys. Rev. Lett. **78**, 3414–3417.

Mayers, D., 1998, "Unconditional security in quantum cryptography," J. Assn. Comput. Mac. (in press).

Mayers, D., and A. Yao, 1998, *Proceedings of the 39th Annual Symposium on Foundations of Computer Science* (IEEE Computer Society, Los Alamitos, California), p. 503.

Mazurenko, Y., R. Giust, and J. P. Goedgebuer, 1997, "Spectral coding for secure optical communications using refractive index dispersion," Opt. Commun. **133**, 87–92.

Mérolla, J-M., Y. Mazurenko, J. P. Goedgebuer, and W. T. Rhodes, 1999, "Single-photon interference in sidebands of phase-modulated light for quantum cryptography," Phys. Rev. Lett. **82**, 1656–1659.

Michler, P., A. Kiraz, C. Becher, W. V. Schoenfeld, P. M. Petroff, L. Zhang, E. Hu, and A. Imamoglu, 2000, "A quantum dot single photon turnstile device," Science **290**, 2282–2285.

Milonni, P. W., and M. L. Hardies, 1982, "Photons cannot always be replicated," Phys. Lett. A **92**, 321–322.

Molotkov, S. N., 1998, "Quantum cryptography based on photon 'frequency' states: example of a possible realization," Sov. Phys. JETP **87**, 288–293.

Muller, A., J. Breguet, and N. Gisin, 1993, "Experimental demonstration of quantum cryptography using polarized photons in optical fiber over more than 1 km," Europhys. Lett. **23**, 383–388.

Muller, A., T. Herzog, B. Huttner, W. Tittel, H. Zbinden, and N. Gisin, 1997, " 'Plug and play' systems for quantum cryptography," Appl. Phys. Lett. **70**, 793–795.

Muller, A., H. Zbinden, and N. Gisin, 1995, "Underwater quantum coding," Nature (London) **378**, 449–449.

Muller, A., H. Zbinden, and N. Gisin, 1996, "Quantum cryptography over 23 km in installed under-lake telecom fibre," Europhys. Lett. **33**, 335–339.

Naik, D., C. Peterson, A. White, A. Berglund, and P. Kwiat, 2000, "Entangled state quantum cryptography: eavesdropping on the Ekert protocol," Phys. Rev. Lett. **84**, 4733–4736.

Neumann, E.-G., 1988, *Single-Mode Fibers: Fundamentals*, Springer Series in Optical Sciences, Vol. 57 (Springer, Berlin).

Niu, C. S., and R. B. Griffiths, 1999, "Two-qubit copying machine for economical quantum eavesdropping," Phys. Rev. A **60**, 2764–2776.

Nogues, G., A. Rauschenbeutel, S. Osnaghi, M. Brune, J. M. Raimond, and S. Haroche, 1999, "Seeing a single photon without destroying it," Nature (London) **400**, 239–242.

Owens, P. C. M., J. G. Rarity, P. R. Tapster, D. Knight, and P. D. Townsend, 1994, "Photon counting with passively quenched germanium avalanche," Appl. Opt. **33**, 6895–6901.

Penrose, R., 1994, *Shadows of the Mind* (Oxford University, Oxford, England).

Peres, A., 1988, "How to differentiate between two nonorthogonal states," Phys. Lett. A **128**, 19.

Peres, A., 1996, "Separability criteria for density matrices," Phys. Rev. Lett. **76**, 1413–1415.

Peres, A., 1997, *Quantum Theory: Concepts and Methods* (Kluwer Academic, Dordrecht, The Netherlands).

Phoenix, S. J. D., S. M. Barnett, P. D. Townsend, and K. J. Blow, 1995, "Multi-user quantum cryptography on optical networks," J. Mod. Opt. **6**, 1155–1163.

Piron, C., 1990, *Mécanique quantique, bases et applications* (Presses Polytechniques et Universitaires Romandes, Lausanne, Switzerland).

Pitowsky, I., 1989, Ed. *Quantum Probability—Quantum Logic*, Lecture Notes in Physics, Vol. 321 (Springer, Berlin).

Rarity, J. G., P. C. M. Owens, and P. R. Tapster, 1994, "Quantum random-number generation and key sharing," J. Mod. Opt. **41**, 2435–2444.

Rarity, J. G., and P. R. Tapster, 1988, in *Photons and Quantum Fluctuations*, edited by E. R. Pike and H. Walther (Hilger, Bristol, England), pp. 122–150.

Rarity, J. G., T. E. Wall, K. D. Ridley, P. C. M. Owens, and P. R. Tapster, 2000, "Single-photon counting for the 1300–1600-nm range by use of Peltier-cooled and passively quenched InGaAs avalanche photodiodes," Appl. Opt. **39**, 6746–6753.

Ribordy, G., J. Brendel, J. D. Gautier, N. Gisin, and H. Zbinden, 2001, "Long distance entanglement based quantum key distribution," Phys. Rev. A **63**, 012309.

Ribordy, G., J.-D. Gautier, N. Gisin, O. Guinnard, and H. Zbinden, 2000, "Fast and user-friendly quantum key distribution," J. Mod. Opt. **47**, 517–531.

Ribordy, G., J. D. Gautier, H. Zbinden, and N. Gisin, 1998, "Performance of InGaAsInP avalanche photodiodes as gated-mode photon counters," Appl. Opt. **37**, 2272–2277.

Rivest, R. L., A. Shamir, and L. M. Adleman, 1978, "A method of obtaining digital signatures and public-key cryptosystems," Commun. ACM **21**, 120–126.

Santori, C., M. Pelton, G. Solomon, Y. Dale, and Y. Yamamoto, 2000, "Triggered single photons from a quantum dot," Phys. Rev. Lett. **86**, 1502–1505.

Shannon, C. E., 1949, "Communication theory of secrecy systems," Bell Syst. Tech. J. **28**, 656–715.

Shih, Y. H., and C. O. Alley, 1988, "New type of Einstein-Podolsky-Rosen-Bohm experiment using pairs of light quanta produced by optical parametric down conversion," Phys. Rev. Lett. **61**, 2921–2924.

Shor, P. W., 1994, *Proceedings of the 35th Symposium on Foundations of Computer Science*, edited by S. Goldwasser (IEEE Computer Society, Los Alamitos, California), pp. 124–134.

Shor, P. W., and J. Preskill, 2000, "Simple proof of security of the BB84 quantum key distribution protocol," Phys. Rev. Lett. **85**, 441–444.

Simon, C., G. Weihs, and A. Zeilinger, 1999, "Quantum cloning and signaling," Acta Phys. Slov. **49**, 755–760.

Simon, C., G. Weihs, and A. Zeilinger, 2000, "Optimum quantum cloning via stimulated emission," Phys. Rev. Lett. **84**, 2993–2996.

Singh, S., 1999, *The Code Book: The Science of Secrecy from Ancient Egypt to Quantum Cryptography* (Fourth Estate, London).

Snyder, A. W., and J. D. Love, 1983, *Optical Waveguide Theory* (Chapman & Hall, London).

Spinelli, A., L. M. Davis, and H. Dauted, 1996, "Actively quenched single-photon avalanche diode for high repetition rate time-gated photon counting," Rev. Sci. Instrum. **67**, 55–61.

Stallings, W., 1999, *Cryptography and Network Security: Principles and Practices* (Prentice Hall, Upper Saddle River, New Jersey).

Stefanov, A., O. Guinnard, L. Guinnard, H. Zbinden, and N. Gisin, 2000, "Optical quantum random number generator," J. Mod. Opt. **47**, 595–598.

Steinberg, A. M., P. Kwiat, and R. Y. Chiao, 1992a, "Dispersion cancellation and high-resolution time measurements in a fourth-order optical interferometer," Phys. Rev. A **45**, 6659–6665.

Steinberg, A. M., P. Kwiat, and R. Y. Chiao, 1992b, "Dispersion cancellation in a measurement of the single-photon propagation velocity in glass," Phys. Rev. Lett. **68**, 2421–2424.

Stucki, D., G. Ribordy, A. Stefanov, H. Zbinden, J. Rarity, and T. Wall, 2001, "Photon counting for quantum key distribution with Peltier-cooled InGaAs/InP APD's," J. Mod. Opt. **48**, 1967–1981.

Sun, P. C., Y. Mazurenko, and Y. Fainman, 1995, "Long-distance frequency-division interferometer for communication and quantum cryptography," Opt. Lett. **20**, 1062–1063.

Tanzilli, S., H. De Riedmatten, W. Tittel, H. Zbinden, P. Baldi, M. De Micheli, D. B. Ostrowsky, and N. Gisin, 2001, "Highly efficient photon-pair source using a periodically poled lithium niobate waveguide," Electron. Lett. **37**, 26–28.

Tapster, P. R., J. G. Rarity, and P. C. M. Owens, 1994, "Violation of Bell's inequality over 4 km of optical fiber," Phys. Rev. Lett. **73**, 1923–1926.

Thomas, G. A., B. I. Shraiman, P. F. Glodis, and M. J. Stephen, 2000, "Towards the clarity limit in optical fiber," Nature (London) **404**, 262–264.

Tittel, W., J. Brendel, H. Zbinden, and N. Gisin, 1998, "Violation of Bell inequalities by photons more than 10 km apart," Phys. Rev. Lett. **81**, 3563–3566.

Tittel, W., J. Brendel, H. Zbinden, and N. Gisin, 1999, "Long-distance Bell-type tests using energy-time entangled photons," Phys. Rev. A **59**, 4150–4163.

Tittel, W., J. Brendel, H. Zbinden, and N. Gisin, 2000, "Quantum cryptography using entangled photons in energy-time bell states," Phys. Rev. Lett. **84**, 4737–4740.

Tittel, W., H. Zbinden, and N. Gisin, 2001, "Experimental demonstration of quantum secret sharing," Phys. Rev. A **63**, 042301.

Tomita, A., and R. Y. Chiao, 1986, "Observation of Berry's topological phase by use of an optical fiber," Phys. Rev. Lett. **57**, 937–940.

Townsend, P., 1994, "Secure key distribution system based on quantum cryptography," Electron. Lett. **30**, 809–811.

Townsend, P., 1997a, "Simultaneous quantum cryptographic key distribution and conventional data transmission over installed fibre using WDM," Electron. Lett. **33**, 188–190.

Townsend, P., 1997b, "Quantum cryptography on multiuser optical fiber networks," Nature (London) **385**, 47–49.

Townsend, P., 1998a, "Experimental investigation of the performance limits for first telecommunications-window quantum cryptography systems," IEEE Photonics Technol. Lett. **10**, 1048–1050.

Townsend, P., 1998b, "Quantum cryptography on optical fiber networks," Opt. Fiber Technol.: Mater., Devices Syst. **4**, 345–370.

Townsend, P. D., S. J. D. Phoenix, K. J. Blow, and S. M. Barnett, 1994, "Design of QC systems for passive optical networks," Electron. Lett. **30**, 1875–1876.

Townsend, P., J. G. Rarity, and P. R. Tapster, 1993a, "Single photon interference in a 10 km long optical fiber interferometer," Electron. Lett. **29**, 634–639.

Townsend, P., J. Rarity, and P. Tapster, 1993b, "Enhanced single photon fringe visibility in a 10 km-long prototype quantum cryptography channel," Electron. Lett. **29**, 1291–1293.

Vernam, G., 1926, "Cipher printing telegraph systems for secret wire and radio telegraphic communications," J. Am. Inst. Electr. Eng. **45**, 109–115.

Vinegoni, C., M. Wegmuller, and N. Gisin, 2000, "Determination of nonlinear coefficient $n^2/A_{\text{eff}}$ using a self-aligned interferometer and a Faraday mirror," Electron. Lett. **36**, 886–888.

Vinegoni, C., M. Wegmuller, B. Huttner, and N. Gisin, 2000, "Measurement of nonlinear polarization rotation in a highly birefringent optical fiber using a Faraday mirror," J. Opt. A, Pure Appl. Opt. **2**, 314–318.

Walls, D. F., and G. J. Milburn, 1995, Eds., *Quantum Optics* (Springer, Berlin).

Weihs, G., T. Jennewein, C. Simon, H. Weinfurter, and A. Zeilinger, 1998, "Violation of Bell's inequality under strict Einstein locality conditions," Phys. Rev. Lett. **81**, 5039–5043.

Wiesner, S., 1983, "Conjugate coding," SIGACT News **15**, 78–88.

Wigner, E. P., 1961, *The Logic of Personal Knowledge: Essays Presented to Michael Polanyi on his Seventieth Birthday, 11 March 1961* (Routledge & Kegan Paul, London), pp. 231–238.

Wootters, W. K., and W. H. Zurek, 1982, "A single quantum cannot be cloned," Nature (London) **299**, 802–803.

Yuen, H. P., 1997, "Quantum amplifiers, quantum duplicators and quantum cryptography," Quantum Semiclassic. Opt. **8**, 939.

Zappa, F., A. Lacaita, S. Cova, and P. Webb, 1994, "Nanosecond single-photon timing with InGaAs/InP photodiodes," Opt. Lett. **19**, 846–848.

Zbinden, H., J.-D. Gautier, N. Gisin, B. Huttner, A. Muller, and W. Tittel, 1997, "Interferometry with Faraday mirrors for quantum cryptography," Electron. Lett. **33**, 586–588.

Zeilinger, A., 1999, "Experiment and the foundations of quantum physics," Rev. Mod. Phys. **71**, S288–S297.

Zissis, G., and A. Larocca, 1978, in *Handbook of Optics*, edited by W. G. Driscoll (McGraw-Hill, New York), Sec. 3.

Żukowski, M., A. Zeilinger, M. A. Horne, and A. Ekert, 1993, " 'Event-ready-detectors' Bell experiment via entanglement swapping," Phys. Rev. Lett. **71**, 4287–4290.

Żukowski, M., A. Zeilinger, M. Horne, and H. Weinfurter, 1998, "Quest for GHZ states," Acta Phys. Pol. A **93**, 187–195.